

**New insights into the rates of soil formation and their contribution
to our understanding of soil lifespans**

Daniel Lee Evans

BSc (Hons) Physical Geography

Lancaster Environment Centre

Lancaster University

Submitted for the degree of Doctor of Philosophy

April 2020

Declaration

Except where references are made to other sources, I declare that the contents of this thesis are my own work and have not been previously submitted, in part or full, for the award of a higher degree elsewhere. Collaborations with other researchers are properly acknowledged.

Daniel Lee Evans

Lancaster University

April 2020

Statement of Authorship

This thesis has been prepared as a set of papers intended for submission to peer-reviewed journals. The papers are presented in the format intended for submission, with the exception that each paper's list of references can be found in a consolidated bibliography at the end of this thesis. All papers have multiple authors, and their contributions are detailed below. Chapters 1, 2 and 7 are introductory, review, and discussion chapters, respectively, and are not intended for submission.

Chapter 1 outlines the main research challenges and structure of this thesis, and is not intended for publication.

Chapter 2 comprises a review of the literature and is not intended for publication.

Chapter 3 is in review for *European Journal of Soil Science*

Evans, D. L., Rodés, Á. and Tye, A. M. (2020) The Sensitivity of Cosmogenic Radionuclide Analysis to Soil Bulk Density: Implications for Soil Formation Rates.

D.E. designed the research, acquired the data and conducted data analysis.

Á.R. designed the CoSOILcal model with contributions from D.E. D.E. wrote the manuscript, with contributions and revisions from Á.R. and A.T.

Chapter 4 is intended for publication in *Environmental Research Letters*.

Evans, D. L., Quinton, J. N., Davies, J. A. C., Zhao, J. and Govers, G. (2020)
Soil lifespans and how they can be extended by land management change.

*D.L.E., J.N.Q. and J.A.C.D. designed research; D.L.E. performed research;
D.L.E., J.N.Q and J.A.C.D. analysed data and D.L.E wrote the paper with
contributions from all co-authors.*

Chapter 5 is published in *SOIL*

Evans, D. L., Quinton, J. N., Tye, A. M., Rodés, Á., Davies, J. A. C., Mudd, S.
M. and Quine, T. (2020) 'Arable soil formation and erosion: a hillslope-based
cosmogenic-nuclide study in the United Kingdom', *SOIL*, 5(2), pp. 253-263.

*D.L.E., J.N.Q., A.M.T. and J.A.C.D. designed the research. D.L.E. and A.M.T.
conducted sampling. D.L.E. and Á.R. conducted laboratory work and analysed
results. D.L.E. prepared the paper with contributions from all co-authors.*

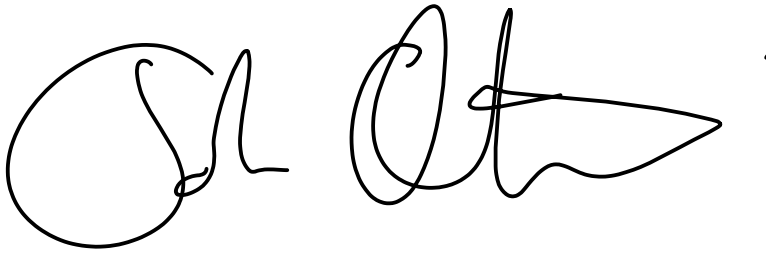
Chapter 6 is intended for publication in *Geoderma*.

Evans, D. L., Quinton, J. N., Tye, A. M., Rodés, Á., Davies, J. A. C. and Mudd,
S. M. (2020) The matrix effect: how the composition and petrographic
structure of sandstone affects rates of soil formation.

*D.L.E., J.N.Q., and A.M.T. designed the research. D.L.E. and A.M.T.
conducted sampling. D.L.E. and Á.R. conducted laboratory work and analysed
results. D.L.E. prepared the paper with contributions from all co-authors.*

Chapter 7 comprises a general discussion and conclusion, and is not
intended for publication.

I hereby agree with the above statements:

A handwritten signature in black ink, appearing to read 'John N. Quinton', with a large initial 'Q' and a stylized 'N'.

Professor John N. Quinton

Lancaster Environment Centre, Lancaster University.

A handwritten signature in black ink, appearing to read 'Jessica A. C. Davies', with a large initial 'J' and a stylized 'D'.

Professor Jessica A. C. Davies

Lancaster Environment Centre, Lancaster University.

'There is one moment at sunset in the country when the whole visible world seems to gather itself in prayer and it seems to you strange that men should move on unconscious of this with spades over their shoulders, instead of falling on their knees in the grass; for in that hush, in the benediction of seconds before the first star shines, the universe seems waiting for a revelation.'

H. V. Morton (1927)

Acknowledgements

My PhD began at about half-past seven on the morning of Friday 12th February 2016, in Room 130 at Nottingham Central Travelodge. That morning, I received the news that I had been offered a studentship. The thesis presented before you has been slowly crafted from many thousands of hours of toil and triumph since that winter's morning. It represents, for me, a formidable accomplishment, but it is by no means a personal success. I owe so much, to so many people.

First, I must underscore my considerable gratitude to my academic supervisors and collaborators: Professor John Quinton, Professor Jess Davies, Dr. Andrew Tye, and Professor Simon Mudd. Your wisdom, experience, advice, and encouragement have been a beacon of support to me over the last four years. Thank you for placing your trust in me. I have enjoyed working with you, and learning from you. Without a doubt, I am a better scientist because of you.

It was in a soils laboratory at the Royal Holloway where I first discovered the STARS CDT. I was idling away half an hour whilst a machine was running, scrolling through PhDs in soil science on my phone. When I clicked a link to the STARS website, what downloaded was nothing less than an epiphany; that uplifting feeling reserved for those rare moments in life when one learns something about one's destiny. Being a part of the STARS CDT has been a life-changing honour. I am deeply grateful for the many opportunities it has provided me to cultivate my skill set, enrich my networks, partake in knowledge exchange, and refine my career goals. Thank you Phil Haygarth,

and all those members of the consortium. I would particularly like to pay tribute to Olivia Lawrenson who, during moments of ambiguity and doubt, industriously responded to my queries and remedied my concerns.

I pen these acknowledgements in a challenging and unmatched moment of uncertainty for science. We have all endured, and will continue to endure, a lengthy period of social isolation. A scholar's work is now confined to the few cubic feet around their desk chair and computer screen. As a soil scientist, I have never felt more appreciative of the opportunities the discipline has so often provided me to leave the office. I must thank all those who permitted me access to their land, and all those who helped me extract over 1,200 soil samples, and relocate them to Lancaster. At Comer: Mike Annis, the Brockhampton National Trust Estate, and Paul McLachlan. At Hilton: Richard Wills, Mike Fullen, Andrew Black, Pedro Batista, and Miroslav Bauer. At Rufford: Tom and Kathy King, the TAG Farming Team, Tim Quine, Carl Horabin, Stephen Thorpe, Ian Longhurst, and Jonathan Riley. At Woburn: Steve McGrath, Stephen Goward, Andy Macdonald, Ian Shield, Robert Copley, John Quinton, Phil Styles and Robert Tuckwell. And let me say thanks again to Andy Tye. We journeyed many hundreds of miles together, across the country, and because of you, I am a more dexterous and capable fieldworker. (Needless to say, you have also introduced me to the virtues of the afternoon nap and the 'fieldwork pie', as I hope I have introduced you to the many merits of a Travelodge! It's *Travelodgical!*)

I must also extend my gratitude to those who have supported me in the laboratories, and with data analyses. At the CIAF laboratories in East Kilbride, thank you Allan Davidson, Derek Fabel, and Àngel Rodés. At the BGS, I'd like

to thank all those in the Core Store, Mark Kalra, and Charles Gowing. At Lancaster University, I'd like to thank Annette Ryan, John Crosse, James Heath, Catherine Wearing, Hugh Tuffen, Jackie Pates, and all those personnel who maintain the facilities both night and day! My special thanks must go to Vassil Karloukovski for his unfatiguing support and generosity of time.

I must make one final remark. Submitting my thesis represents the closing chapter in my four-year pursuit for a Doctor of Philosophy. Upon reflection, I realize I have always had *Philosophia* – a 'love for wisdom' – and it is this unremitting passion for knowledge that has partly fuelled me throughout this degree. But a love for wisdom only carries you so far, though. In times of self-doubt or rejection, when the hurdles feel too high, or when the path ahead seems unclear, one may need more than a love for a subject. Thankfully, I had more – *much* more. I had unwavering companionship and loyal support from all those in the 'Sustainable Soils' group: Pedro, Emma, Aimee, Rosanne, Bea, Hollie, Rose, Tori, Cristina, Jonathan, Roisin, Helena, Marx, Jacky, Stacia, Lael, Gabriel, and Dmitry. Likewise, I could always rely upon friends in STARS to get me laughing again at the end of a busy week: Mihai, Hannah, Emily, Lucy, Chris, Lewis, and Alex, to name only some. Often, I would need some projects away from research to recharge, and thanks to Benjamin Vis, TruLife, and the British Society of Soil Science, I always had plenty of options! Sometimes, I needed to unload on my closest friends: thank you for listening Sophie Paddock, Beckie Grimmer, Rachael Seaman, Lucinda Webb, Ben Church, Lewis Martins, 'Odd Pastonians', Emma Cooper, and Georgie Wood. And finally my greatest thanks must go to the most loyal,

dependable, and devoted family anyone could wish for: Mum and Dad (and Ruggs!) From my first steps with you under those big Norfolk skies, to our traditional walks in our beloved Dorset, it was you who brought me up to have a passion for nature, a passion for the landscape, a passion for knowledge, and a passion for life.

Abstract

Sustaining the provision of services by soils for future generations has become a critical goal for soil scientists. Preventing soil thinning and the exposure of the underlying parent material is paramount for achieving this goal. Soil thinning occurs when rates of soil erosion exceed those of soil formation. Although measuring soil erosion has received widespread attention, there has not been a commensurate effort to obtain rates of soil formation, and this undermines our capacity to determine the long-term sustainability of our soils. This thesis responds to that sizeable knowledge gap in two ways: measuring soil formation rates at sites previously subject to soil erosion monitoring, and demonstrating how rates of soil formation and erosion can be used to estimate soil lifespans.

Cosmogenic radionuclide analysis was used to measure the rates of soil formation across four UK hillslopes. These included the first measurements of their kind for arable soils, under some of the thickest soil profiles that have been subject to this technique. For the first time, the CoSOILcal model was used to account for the effect of variable soil bulk density on the attenuation of cosmic rays. A sensitivity analysis showed that accounting for these bulk density data for profiles thicker than 0.25 m brings about a significant difference in the calculated rates of soil formation. The rates obtained for the four hillslopes studied here fell within the range of those previously published for similar climates and lithologies. However, it was also found that rates were faster for lithologies with a greater porosity and a reduced matrix.

At one of the sites, rates of soil formation and erosion were used to calculate the lifespans for both the A horizon and the profile to bedrock. The shortest lifespans were found on the backslope, with the loss of the A horizon and bedrock exposure occurring in 138 and 212 years, respectively, in a worst-case scenario. Longer lifespans were observed for less erosive zones such as the toeslope where the time until bedrock exposure was more than triple that of the backslope. Similar analyses of soil lifespans were undertaken at the global scale. Combining over 10,030 plot years of erosion data from 255 sites with rates of soil formation, 93% of conventionally managed soils were found to be thinning, and 16% reported lifespans of less than 100 years. However, adopting conservation land-use and management practices were found to extend these lifespans, with over a third exceeding 10,000 years.

Contents

Declaration	1
Statement of authorship	2
Acknowledgements	6
Abstract	10
List of Figures	19
List of Tables	23
Abbreviations used	24
1 Introduction	25
1.1 Threats to soils and soil functioning	25
1.1.1 Soil thinning	26
1.1.2 Soil removal	26
1.2 Soil sustainability: two research challenges	28
1.3 Thesis structure	29
2 Literature Review	34
2.1 Soil Formation	34
2.1.1 Definitions	34
2.1.2 Measuring rates of soil formation	38

2.1.2.1 Chronosequences	38
2.1.2.2 Radioisotope dating	39
2.1.2.3 Cosmogenic radionuclide analysis	40
2.1.3 Rates of soil formation	42
2.1.4 Factors that affect the rate of soil formation	46
2.1.4.1 Autochthonous soil formation	47
2.1.4.1.1 Five factors of autochthonous soil formation	47
2.1.4.1.2 Water: the nexus between the five soil formation factors	50
2.1.4.1.3 Human activity: a sixth soil formation factor?	51
2.1.4.1.4 Self-limiting behaviour in pedogenesis	54
2.1.4.2 Allochthonous soil formation	55
2.2 Soil lifespans	60
2.2.1 Approaches to date	60
2.2.2 Applications of the soil lifespan concept	64
2.3 Soil loss tolerance	66
2.3.1 Comparing soil formation rates with rates of soil loss tolerance	66
2.3.2 Revisiting SLT and the use of soil formation rates	68
3 The Sensitivity of Cosmogenic Radionuclide Analysis to Soil	70

Bulk Density: Implications for Soil Formation Rates

3.1 Introduction	71
3.2 Materials and methods	75
3.3 Results	79
3.4 Discussion	83
3.5 Conclusions	85
4 Soil lifespans and how they can be extended by land management change	87
4.1 Introduction	88
4.2 Materials and methods	91
4.2.1 Data collation	91
4.2.2 Lifespan model	92
4.3 Baseline lifespans for bare and conventional agricultural soils	95
4.4 Extending soil lifespans by changing land use and agricultural practice	97
4.4.1 Land use change	97
4.4.2 Changing agricultural practices	99
4.4.3 Decision making at the site-scale	101
4.5 Global and regional distribution of soil lifespans	104

4.6 Site-specific variables that influence lifespans	107
4.7 Limitations and knowledge gaps	112
4.8 Conclusions	115
5 Arable soil formation and erosion: a hillslope-based cosmogenic-nuclide study in the United Kingdom	117
5.1 Introduction	118
5.2 Materials and methods	121
5.2.1 Site description	121
5.2.2 Saprolite extraction and soil sampling	123
5.2.3 Lifespan analysis at Rufford Forest Farm	127
5.3 Results and discussion	130
5.3.1 Soil formation rates	130
5.3.2 Derived soil formation rates in reference to the global inventory	135
5.3.3 Lifespan analysis at Rufford Forest Farm	138
5.4 Conclusions	141
6 The matrix effect: how the composition and petrographic structure of sandstone affects rates of soil formation	144
6.1 Introduction	145
6.2 Materials and methods	148

6.2.1 Site description	148
6.2.2 Sampling and processing soil and saprolite	157
6.3 Results and discussion	160
6.3.1 Soil profiles at Hilton and Woburn	160
6.3.2 Soil formation rates	162
6.3.3 Lithological variability: the role of the sandstone porosity and matrix	167
6.3.4 Comparison with global inventory	178
6.4 Conclusions	182
7 Discussion and conclusions	184
7.1 Introduction	184
7.2 Research challenge 1: state of the soil formation inventory	186
7.3 Research challenge 2: application of soil formation rates	190
7.4 Evaluation	192
7.4.1 Accuracy	192
7.4.2 Reliability	194
7.4.3 Validity	195
7.5 Future work	196

7.5.1 Rates of soil function formation	196
7.5.2 Lifespans after complete soil removal	197
7.5.3 Rates of soil formation for deep soils	198
7.6 Research outputs and impact statement	198
References	201
Appendices	266
A2.1 Global Inventory of Soil Formation Rates	268
A2.2 Global Inventory of Soil Loss Tolerance values	270
A3.1 Global Inventory of Soil Formation Rates used in the CoSOILcal Sensitivity Analysis	271
A3.2 Published Paper: 'Cosmogenic soil production rate calculator'	273
A3.3 Output from CoSOILcal	278
A4.1 Global Inventory of Soil Erosion Rates	282
A4.2 Soil Lifespan Analysis	289
A4.3 Definitions of Land Use and Management practices	299
A4.4 List of studies included in the Soil Lifespan Analysis	300
A5.1 Output from AMS for Rufford and Comer	316
A5.2 Soil analysis for Rufford and Comer	317

A6.1 Output from AMS for Hilton and Woburn	323
A6.2 Soil analysis for Hilton and Woburn	324
A6.3 Soil production function analysis	326
A6.4 Particle size analysis for saprolite at Hilton and Woburn	327

List of Figures

(captions are abridged)

Figure 2.1: Schematic outlining the main steps of calculating soil formation rates from cosmogenically-derived concentrations of a radionuclide.	42
Figure 2.2: Global inventory of soil formation rates against soil depth, grouped by Köppen climate type.	45
Figure 2.3: Global inventory of soil formation rates against soil depth, grouped by lithology.	46
Figure 2.4: A summary of the weathering zones within a soil profile.	49
Figure 2.5: Schematic showing both proposed exponential (a) and humped (b) relationships between soil production and mantle thickness.	55
Figure 2.6: Soil formation and erosion processes down a hillslope.	61
Figure 2.7: Critical time (T_c) required to erode a soil profile of differing initial thickness (S) for different net soil erosion rates.	64
Figure 2.8: Distribution of SLT values from a global inventory	67
Figure 2.9: Distribution of soil loss tolerance values and soil formation rates	69
Figure 3.1: Soil formation rates from the global inventory previously published (x axis) and those calculated using the CoSOILcal model (y axis).	81

Figure 3.2: Difference in the soil formation rate when the CoSOILcal was employed in comparison to the original dataset for different climatic regions (top panel) and lithologies (bottom panel).	82
Figure 4.1: Number and spatial distribution of plot years for the 255 unique locations in this study.	90
Figure 4.2: Cumulative distribution of soil lifespans and annual soil gain for bare soils (red), non-bare conventionally managed soils (blue), and conservation management (green).	96
Figure 4.3: (a) Distribution of critical (<100 years), finite (>100 years), and infinite (thickening) lifespans for bare, conventional, and conservation-based management. (b) Soil lifespans for conventional (blue) and soil conservation (green) management practices excluding those soils that are thickening. (c) Net annual soil gain following the shift from a conventional (blue) to a conservation-based (green) management regime. NG stands for 'No Gain' and denotes incidences where annual soil gain did not occur.	103
Figure 4.4: Soil lifespans for conventional (blue) and soil conservation (green) management practices under different mean annual precipitations. Boxplots represent the interquartile range of soil lifespans. Error bars refer to the 5 th and 95 th percentile soil lifespans.	109
Figure 4.5: Soil lifespans for conventional (blue) and soil conservation (green) management practices under different slopes. Boxplots represent the interquartile range of soil lifespans. Error bars refer to the	110

5th and 95th percentile soil lifespans.

Figure 4.6: Soil lifespans for conventional (blue) and soil conservation (green) management practices under different soil textures. Boxplots represent the interquartile range of soil lifespans. Error bars refer to the 5th and 95th percentile soil lifespans. 112

Figure 5.1: Locations of the study sites in this chapter (a) with elevation profiles (b) for both Comer Wood (CW; green) and Rufford Forest Farm (RFF; blue). The position of summit (triangles), shoulder (diamonds), backslope (circles), and toeslope (squares) sampling positions are indicated on each profile. Photographs of RFF (c) and CW (d) were taken by the author at the time of sampling. 123

Figure 5.2: Soil formation rates and the depths to saprolite for the four sampling positions along the catena transects at Rufford Forest Farm (blue) and Comer Woodland (green). 131

Figure 5.3: Soil formation rates against sampling depth for Rufford Forest Farm (blue) and Comer Woodland (green). 132

Figure 5.4: Soil formation rates from a globally compiled inventory (grey circles) and from this study at Rufford Forest Farm (blue triangles) and Comer Woodland (green diamonds) plotted against sampling depth. 137

Figure 5.5: First-order soil lifespans calculated at four catena positions at Rufford Forest Farm for Scenario 1 (the time until the erosion of a 30 cm A horizon) and Scenario 2 (the time until bedrock exposure). 140

Figure 6.1: Location of the study sites (a) with elevation profiles (b) for Hilton (blue) and Woburn (green). Summit (circles), shoulder (squares), backslope (triangles), and toeslope (diamonds) are indicated on each profile. Photographs of the hillslope at Hilton (c) and Woburn (d) were taken from the toeslope during the reconnaissance survey. An exposure of the fluvially-derived sandstone (interbedded with sub-rounded pebbles) close to the study slope at Hilton is shown in (e) (photograph by Miroslav Bauer, 2019). The soil profile, soil-saprolite interface, and underlying bedrock at Woburn are shown in (f). 155

Figure 6.2: Photographs of the saprolite at Hilton (a) and Woburn (b). 156

Figure 6.3: Soil formation rates against sampling depth for Hilton (blue) and Woburn (green). The error bars represent one standard deviation uncertainties. 165

Figure 6.4: Soil formation rates and the depths to saprolite for the four landscape positions at Hilton (blue) and Woburn (green). 166

Figure 6.5: Soil formation rates against sampling depth for Hilton (blue) and Woburn (green) with those previously measured at Rufford Forest Farm (brown diamonds) and Comer Wood (grey triangles). The error bars represent one standard deviation uncertainties. 175

Figure 6.6: Analysis of the relationship between sampling depth and the content of clay-sized material in the saprolite (a) and that between the content of clay-sized material in the saprolite and the soil formation rate (b) for Hilton (blue) and Woburn (green). 175

Figure 6.7: Soil formation rates from Hilton (blue) and Woburn (green), 181
together with those from Rufford Forest Farm (brown diamonds), Comer
Wood (grey triangles), and those from a globally compiled inventory of
soil formation rates on sandstone geology from Heimsath *et al.*, 1997
(orange circles), Heimsath *et al.*, 2001b (grey circles), and Wilkinson *et*
al., 2005 (purple circles).

List of Tables

(captions are abridged)

Table 2.1: Definitions of soil formation.	36
Table 2.2: Major types of allochthonous parent materials and their soil properties.	57
Table 2.3: Previous approaches to define the soil lifespan.	61
Table 4.1: Global distribution of finite, critical, and infinite lifespans for the five regions studied in this chapter.	106
Table 5.1: ¹⁰ Be concentrations and calculated maximum soil formation rates for Rufford Forest Farm (RFF) and Comer Wood (CW).	133
Table 6.1: Locational context of the Hilton and Woburn study sites.	154
Table 6.2: Properties of the sandstone and soil formation rates for each of the four sites in this paper.	176
Table 6.3: Particle size distributions for the saprolite sampled at Hilton and Woburn.	177

Abbreviations used

ALD	Active Layer Development
AMS	Accelerator Mass Spectrometry
ASL	Above Sea Level
FAO	Food and Agriculture Organization of the United Nations
IPCC	Intergovernmental Panel on Climate Change
ISRIC	International Soil Reference and Information Centre
LOI	Loss On Ignition
NIST	National Institute of Standards and Technology
SEM	Scanning Electron Microscope
SLT	Soil Loss Tolerance
USDA	United States Department of Agriculture
WCED	World Commission on Environment and Development
WRB	World Reference Base

Chapter 1: Introduction

1.1 Threats to soils and soil functioning

Soil science enters the third decade of the 21st century enjoying a disciplinary renaissance (Hartemink and McBratney, 2008). There has been increasing recognition about the unique roles that soil plays in the Earth system as a critical nexus between the lithosphere, hydrosphere, biosphere, atmosphere and anthroposphere. The inextricable dependence that humankind places on soil resources means that they are not only the venue of geomorphological processes, but responsible for addressing societal demands too, including water purification, carbon storage, nutrient cycling, gene reserve, waste bioremediation, and habitat provision (Blum, 1993; Lal, 2009; Verheijen *et al.*, 2009; Larkin, 2015; Vereecken *et al.*, 2016). Since a third of global soil resources are moderately or highly degraded, ensuring that soils meet these present-day demands has become an intensified challenge for soil scientists (Bot *et al.*, 2000). In addition, the United Nations' projection that the global population will rise to 9.7 billion by 2050 (FAO, 2015a) further exacerbates the pressures placed on soils. Ensuring that soils will continue to deliver ecosystem services for future generations against a contextual backdrop of increasing demand and uncertain environmental change has become one of the most critical items on the soil science agenda.

Resistance and adaptation to a suite of environmental and human-induced pressures are important for a soil to remain sustainable. However, there are two principal challenges that threaten soils and their functionality which are, arguably, of greater hierarchical importance: soil thinning and soil removal.

1.1.1 Soil thinning

The thickness of soil is one of the critical factors that promotes or constrains soil functionality (Patton *et al.*, 2018). Over decadal to centennial timescales, soil thickness plays an important role in the geomorphology of landscapes. For instance, previous work has shown that soil thickness is a fundamental variable in influencing the stability and drainage of hillslopes (Dietrich *et al.*, 1995). Over shorter time periods, soil thickness has been shown to affect the runoff and residence of water (Botter *et al.*, 2011). This has important implications on the storage of plant-available water, and therefore, primary productivity (Evaristo *et al.*, 2015). In addition, soil thickness significantly determines the size and the stability of the soil organic carbon reservoir. For example, the mean residence time of soil organic carbon has been shown to increase down the soil profile, with values between 2,000 and 10,000 years in soils that are deeper than 0.2 m (Fontaine *et al.*, 2007).

Such is the importance of soil thickness on a variety of ecosystem functions and geomorphological processes that soil thinning can represent a serious threat. The extent of that threat is dictated by the rate of soil thinning (the rate of net soil loss) and the original soil thickness. For example, a soil profile of 5 m thickness thinning at a rate of 2 mm y^{-1} does not pose as much of a threat than a soil of 1 m thickness thinning at a rate of 0.5 mm y^{-1} , even though the rate is four times greater.

1.1.2 Soil removal

Without amelioration, the trajectory of any thinning soil is one that ultimately leads to the exposure of the underlying parent material. In the absence of soil,

it is palpably clear that soil ecosystem services cannot be delivered. Often the complete removal of the soil cover takes place on the most erosive convexities of hillslopes. Zhang *et al.* (2008) demonstrate that the extent of bedrock exposure on an arable hillslope in the Sichuan Basin (southwestern China) is influenced, in part, by the frequency of tillage. After five tillage events, the length of bedrock exposure was 1.05 m, representing 4.8% of the total experimental area. After a further ten tillage events, the length of bedrock exposure had more than doubled to 2.2 m. Similarly, the area of exposure had increased by more than 5%.

For some soil profiles it may be difficult to ascertain the point at which the soil has been removed, and the parent material has become exposed. This may largely depend on one's definition of soil. The most recently published definition is: "the layer(s) of generally loose mineral and/or organic material that are affected by physical, chemical, and/or biological processes at or near the planetary surface and usually hold liquids, gases, and biota and support plants" (van Es, 2017, p. 21). Furthermore, it could be the case that some parent materials have the physical, chemical and biological properties necessary for basic ecosystem functions, or the capacity to be developed relatively quickly into a proto-soil. For example, a mudstone or similar soft-rock may be able to be crushed by tillage equipment in order to preserve a shallow, but otherwise cultivable regolith. However, this regolith is likely to lack the organic carbon, nutrients, and aggregate stability to sustain a crop over multiple seasons.

1.2 Soil sustainability: two research challenges

In the previous section, two principal threats to soil sustainability were presented: soil thinning and soil removal. Both of these threats manifest when soil erosion rates exceed those of soil formation.

Soil erosion has received widespread scholarly attention (Kirkby and Morgan, 1980; Hooke, 2000; Boardman and Poesen, 2006; Montgomery, 2007; Quinton *et al.*, 2010; Poesen, 2017). Many authors have attributed erosion as one of the most significant aspects of global soil degradation (Bot *et al.*, 2000; Quinton *et al.*, 2010). The anthropogenic acceleration of soil erosion, and the need for its effective attenuation on agricultural landscapes, is increasingly being discussed by governments and policy makers (IPCC, 2019). Over the last century, a range of soil conservation strategies aimed at reducing the rates of soil erosion have been deployed. These efforts have included changes to land use, such as afforestation and grassland restoration, and adaptations to agricultural practices, such as adopting conservation tillage or cover cropping (Panagos *et al.*, 2016). However, active investment around the world in quantifying and evaluating the severity of soil erosion for this objective is overshadowed because we do not know, with equivalent accuracy, the rates of soil formation.

There are arguably two research challenges associated with the study of soil formation that need to be addressed for the effective combatting of soil thinning and soil removal.

1. The first research challenge is the impoverished state of the soil formation rate inventory. The meagre dataset of soil formation rates has been noted

by soil scientists, previously. Many authors comment on how “field measurements are impossible” (Li *et al.*, 2009, p. 97), “limited data are available” (Schertz, 1983, p. 11) and how “current scientific knowledge on soil formation processes is insufficient” (Duan *et al.*, 2017a, p. 8). To some extent, this challenge has been partly tackled by the conception of new field- and laboratory-based methods to measure rates of soil formation. Despite these methodological developments, there is still a dearth of soil formation data, which contrasts with the frequent and widespread measurement of soil erosion. This compromises our ability to determine the balance between soil formation and soil erosion, and therefore whether soils are thinning or not.

2. Second, the existing soil formation rate inventory has been mostly collated by those outside soil science (Portenga and Bierman, 2011; Heimsath *et al.*, 2012) and so expectedly it has hitherto paid little contribution to the soil sustainability discourse. Instead, rates of soil formation have been obtained from uncultivated (often mountainous or ‘pristine’) sites in order to determine rates of landform and landscape evolution. One of the implications of this is that there have been few, if any, studies where rates of soil formation and soil erosion have been measured in parallel. Addressing this challenge is essential to better understand the sustainability of our global soil resources.

1.3 Thesis Structure

This thesis will respond to the research challenges presented above in the following sequence:

1. **Chapter 2:** To establish our current knowledge and understanding of soil formation, an extensive review of the literature will be conducted. It will first engage with the existing methodological approaches that soil scientists use to measure the rates of soil formation (Section 2.1.1 and 2.1.2). Next, a comprehensive global inventory of previously reported soil formation data will be presented (Section 2.1.3), followed by a discussion into the limiting factors that control the process of soil formation (Section 2.1.4). After this, the review will explore two applications of soil formation data: soil productive lifespans (Section 2.2) and soil loss tolerance (Section 2.3).

2. **Chapter 3:**

Gap: In cosmogenic radionuclide analysis, bedrock lowering rates are inferred by measuring concentrations of Beryllium-10, and using a cosmogenic depth-profile model to calculate the attenuation of cosmic rays to the bedrock. To date, this model has assumed that the bulk density of the soil overlying the bedrock is either equal to that of the bedrock or constant with depth. The failure to acknowledge variations in soil bulk density in cosmogenic radionuclide analysis means that we do not know the sensitivity of soil formation rates to this important parameter.

Research question: To what extent are cosmogenically-derived soil formation rates, measured at the soil-saprolite interface, sensitive to the overlying soil bulk density profile?

Objectives: (1) Develop a model that calculates isotopically-derived soil formation rates, considering the bulk density profile of the soil overlying the

bedrock surface; (2) Use the model developed in Objective 1 to recalculate cosmogenically-derived rates of soil formation.

Deliverables: (1) CoSOILcal model: a calculator that accounts for soil bulk density when deriving soil formation rates; (2) Sensitivity analysis of the effect of soil bulk density on cosmogenically-derived soil formation rates; (3) A revised global inventory of soil formation rates, recalculated using the CoSOILcal model.

3. Chapter 4:

Gap: Although rates of soil formation and soil erosion have been measured separately, there has been no attempt to bring these datasets together to assess global soil lifespans.

Research question: What is the distribution of soil lifespans globally and to what extent can changes in land-use or management practices extend them?

Objectives: (1) Compile a global inventory of soil erosion rates from the published literature; (2) Quantify soil lifespans for each study compiled in Objective 1; (3) Assess the extent to which land-use or management change extends soil lifespans.

Deliverables: (1) A global soil erosion dataset: 10,030 plot years of annual water erosion rates, derived from 1,103 erosion plot-based records from 240 studies, that comprise 255 unique locations across 38 countries; (2) Estimated soil lifespans for bare, conventionally-managed and conservation-managed soil.

4. **Chapter 5:**

Gap: For soils currently supporting arable agriculture, cosmogenically-derived soil formation rates and rates of soil erosion have never been empirically measured in parallel. Therefore, we are unable to accurately assess the balance between soil formation and soil erosion, and thus unable to calculate soil lifespans.

Research question: To what extent do rates of soil erosion exceed the rates of soil formation at two sites in the United Kingdom, and what are the estimated soil lifespans?

Objectives: (1) Using cosmogenic radionuclide analysis, derive rates of soil formation for two sites in the United Kingdom (one arable and one woodland); (2) Quantify soil lifespans at the arable site.

Deliverables: (1) Twelve ^{10}Be -derived soil formation rates for two catena sequences in an arable and coniferous woodland setting; (2) Estimated soil lifespans at the arable site.

5. **Chapter 6:**

Gap: Although there has been a growing awareness about the role of major bedrock types on governing rates of soil formation, there has been no cosmogenic study into the effects of the lithological variabilities of a single rock type.

Research question: To what extent does sandstone porosity govern rates of soil formation?

Objectives: (1) Using cosmogenic radionuclide analysis, derive rates of soil formation for two arable hillslopes in the United Kingdom (one fluvially-

derived sandstone and one marine-based sandstone); (2) Statistically test the difference between rates of soil formation measured from fluvially-derived sandstone and those procured from marine-based sandstone; (3) Statistically test the difference between rates of soil formation measured in this study and those from other groups of sandstone using the global soil formation rate inventory.

Deliverables: (1) Sixteen ^{10}Be -derived soil formation rates for two catena sequences in arable settings.

6. **Chapter 7:** Finally, a general discussion of this thesis' findings will be presented, including an evaluation of the work, areas for further research, and an impact statement detailing how these findings may influence society.

Chapter 2: Literature Review

2.1 Soil Formation

2.1.1 Definitions

The study of soil formation – pedogenesis – is one of the oldest scholarly pursuits within soil science (Dokuchaev, 1879). The intellectual jurisdiction for a soil formation scholar is also very wide. In consequence, multiple definitions of pedogenesis exist (Table 2.1), ranging from the accumulation and transformation of parent material, the horizonisation of soil profiles, and the factors that influence the evolution of soil properties. Not only are there multiple foci, but there is a similarly inconsistent use of terminology within the discourse. A Web of Science search (1950 – 2017) found that scholars are just as likely to use ‘Soil Formation’ ($n = 2,292$) and ‘Soil Development’ ($n = 1,947$) in their publications as ‘Pedogenesis’ ($n = 2,600$). Furthermore, ‘Soil Evolution’ ($n = 298$), ‘Soil Production’ ($n = 315$) and ‘Soil Genesis’ ($n = 466$) are also commonly used terms.

Despite the multifarious strands of soil formation work, it could be argued that there are two categories by which to organise the research. The first grouping concerns itself with the accumulation of soil mass. Examples of this work include the research into the development of residual soils from bedrock weathering (Stockmann *et al.*, 2014), or the generation of soils from parent material of allochthonous provenance, such as loess or alluvium (Catt, 2001). The second grouping focuses on the ways by which a soil profile matures from undifferentiated regolith into one with a series of distinctive horizons with distinguishing physical, chemical, and biological properties, from which

particular processes operate. Examples of this include the work carried out by Phillips (1993) who studied the “degree of pedogenic alteration and profile organisation”. A similar categorisation is observed between soil erosion and soil degradation. Whilst soil erosion is concerned with the absolute loss of soil mass from the system (often quantified in units of mass over area), soil degradation is concerned with the regressive changes to soil properties that lead to the decline of soil health and soil productivity (Lal, 2001).

The *mass* of a soil must first be present before soil profile development can take hold. At what stage does weathered rock or deposited parent material become soil is a contested question. There is also an argument that certain horizon-building and soil structure transformations are required before regolith can be recognized as soil. Nevertheless, understanding the mass losses from a soil system warrants a similar effort in quantifying the mass inputs into it. In consequence, the remainder of this section within the review will focus on soil formation as the accumulation of soil mass.

Table 2.1: Definitions of soil formation

Source	Definition
Shaw (1930)	Modification and partial destruction of the parent material by the action of water, air, temperature changes, and organic life.
Jenny (1941)	Transformation of rock into soil is designated as soil formation.
Simonson (1959)	Accumulation of parent materials and the differentiation of horizons in the profile. Of these two steps, the second is of more immediate concern to soil scientists.
Hurni (1983)	A mixture of processes which involve gains, losses, and transformations of different components, occurring at different rates in different horizons.
Catt (1991)	Changes to uppermost layers of the Earth's crust occurring beneath stable land surfaces.
Wakatsuki and Rasyidin (1992)	Rate of formation of soil materials that have the same mean composition as the mean composition of the A, B and C horizons of the soils in the area.
Phillips (1993)	Soil Development is defined here as the degree of pedogenic alteration and profile organization (where) ... development is characterized by increases in thickness and by increasing degrees of alteration of parent material.
McAuliffe (1994)	Soil horizon development.
Huggett (1998)	Product of essentially downwards acting processes that lead to two sets of interrelated layers – the A Horizons and the B Horizons, which constitute the solum.
Minasny and McBratney (1999)	Breakdown or weathering of the underlying parent materials under physical, chemical, and biological processes, which will result in the lowering of the soil-bedrock interface.
Bockheim and Gennadiyev (2000)	Soil horizons, properties, and materials.
van Breemen and Burrman (2002)	Processes responsible for the formation of major genetic horizons.
Wilkinson and Humphreys (2005)	Rate at which saprolite is altered to soil.

Wilkinson and Humphreys (2005)	Development of horizons...a continuation of mineral alteration that began during the development of saprolite.
Ewing <i>et al.</i> (2006)	A mass balance between inputs and losses over integrated timescales.
Richter <i>et al.</i> (2007a)	Transformations over time, as energy chemical elements, and water are processed.
Targulian and Krasilnikov (2007)	The result of synergetic processes of self-organization of an in situ soil system during its functioning in time and space.
Targulian and Krasilnikov (2007)	Transformation of the solid-phase lithomatrix (parent material) of the soil system into the pedomatrix (soil body, soil mantle).
Yoo and Mudd (2008)	Chemical weathering of primary materials.
Verheijen <i>et al.</i> (2009)	Natural process of soil accumulation at any location.
Duchaufour (2012)	Initially thin surface soil gradually increases in thickness and successive layers, become differentiated in terms of colour, texture and structure to form a profile.
Egli <i>et al.</i> (2014)	A net change in the mass balance of the soil compartment.
Egli <i>et al.</i> (2014)	Transformation of the parent material into soil due to chemical and physical weathering, mineral transformation, and the lowering of the bedrock (or parent materials)–soil boundary.
Stockmann <i>et al.</i> (2014)	Conversion of parent material to soil combining physical and chemical processes.
Schaetzl and Thompson (2015)	All the natural processes involved in the formation of soils, including progressive and regressive processes.
Vereecken <i>et al.</i> (2016)	The combination of physical, chemical, biological and anthropogenic processes acting on a soil parent material over periods from years to millennia.
Yu <i>et al.</i> (2017)	Biogeochemical weathering, as a combination of physical, chemical, thermal, and biological processes together causing the disintegration of rocks, an evolutionary process that does not stop with the initial formation of soil.

2.1.2 Measuring rates of soil formation

The question “how fast does soil grow?” posed by Stockmann *et al.* (2014) represents one of the many examples when soil science scholars have enquired into the rates of soil formation. Whilst Li *et al.* (2009, p. 97) suggest that “field measurements are impossible”, there are many empirical methods to quantify rates of soil formation. Three of the most practiced include chronosequences, radioisotopic dating, and cosmogenic radionuclide analysis.

2.1.2.1 Chronosequences

Chronosequences are “a group of related soils that differ from one another, primarily as a result of differences in time or soil age, as a soil-forming factor” (Schaetzl and Thompson, 2015, p. 740). This adopts the ergodic principle where soils across space have the ability to also represent soils across different time periods (Huggett, 1998). In the context of measuring the rates at which the bedrock is converted to soil, the depth and age of soil can be used to estimate rates of soil formation. There are three critical presuppositions when employing this method. The first is that *time* is the only state factor of soil formation allowed to change, whilst all other state factors – climate, organisms, relief, and parent material – remain constant. In reality, and particularly for long (decadal to centennial) periods, this is not the case because these latter factors are variable. The second issue is that the chronosequence concept assumes that the rates of soil formation are constant. However, there is evidence to suggest that soil formation rates are self-limiting, with rates declining as soil mass increases (Wilkinson and

Humphreys, 2005). This will be further explored in Section 2.1.4.1.4. The third assumption is that the age of the soil is known. Accurately dating soils is a complex objective, as this review will now explore.

2.1.2.2 Radioisotopic dating

A number of radioisotopic dating techniques have been applied to estimate the age of distinct horizons within soil profiles, each with differing degrees of accuracy and precision, and each with their own inherent uncertainties.

Radiocarbon dating is often utilized due to the fact that the radiocarbon cycle is relatively well understood (Ramsey, 2008). Radiocarbon, which is produced in the upper atmosphere, is converted to $^{14}\text{CO}_2$ and is then absorbed by plants during photosynthesis, such that it becomes incorporated as part of that plant's biomass. When the plant dies, this uptake of radiocarbon ceases, and the concentration of residual $^{14}\text{CO}_2$ in decaying leaves or seeds can be measured using Accelerator Mass Spectrometry (AMS) and used to determine the radiocarbon age (Taylor, 1987; Linick *et al.*, 1989). This provides a minimum age of the soil.

Although the use of AMS dating is fast and requires a small sample size (2 – 30 mg), allowing one to select the most pristine portion of the carbon within a sample, there is an incongruity between the radiocarbon age and calendar age. This is because radiocarbon production in the atmosphere varies over time. Furthermore, soil horizons store a wide variety of organic matter representing many different stages of decomposition and thus ages potentially ranging over millennia (Tipping *et al.*, 2010). To some extent, this can be addressed by calculating a 'mean residence time' which accounts for all humic

compounds that comprise the organic matter fraction within a sample (Paul *et al.*, 1964). However, this does not resolve the fact that some carbon particles within the soil profile may be allochthonous, and introduced to the soil profile at a later date, thus leading to the erroneous over-estimation of the radiocarbon age.

2.1.2.3 Cosmogenic radionuclide analysis

Cosmogenic radionuclide analysis was first used to constrain the rates of various geomorphic processes by Lal (1991) but the technique was adapted for pedological studies by Heimsath *et al.* (1997). Terrestrial cosmogenic radionuclides (such as ^{10}Be , ^{26}Al , and ^{36}Cl) are produced when secondary cosmic rays interact with minerals in the uppermost metres of the Earth surface (in this case, the bedrock). The concentration of these radionuclides is dependent upon both the duration of bedrock exposure to cosmic rays, and the denudation of this bedrock into weathered regolith. If the bedrock is not directly exposed (i.e.: overlain by a mantle of soil) it is also important to determine the attenuation of these cosmic rays. This is often achieved using a model conceived by Lal (1991). Many other additional considerations are often applied in this process, including the need to normalize the radionuclide production rate in accordance with the site's elevation, longitude and latitude and, furthermore, any topographic shielding that may obstruct the cosmic ray flux (Dunne *et al.*, 1999; Stone *et al.*, 2000; Balco *et al.*, 2008; Stockmann *et al.*, 2014).

The concentration of the radionuclide in a sample of soil-mantled bedrock (*a* in Figure 2.1; hereafter referred to as the 'current bedrock surface') can be

measured using Accelerator Mass Spectrometry. Given that secondary cosmic rays are attenuated as they travel through the soil profile (b in Figure 2.1), this means that less of the radionuclide is produced at depth than that which is produced at the soil surface. The soil surface in this instance represents the 'old bedrock surface' (c in Figure 2.1). In other words, this would have been the position of the bedrock surface before soil started to form. By quantifying the extent to which cosmic rays are attenuated, the measured concentration of the radionuclide at the current bedrock surface can be used to calculate that at the old bedrock surface. By knowing the annual production rate of the radionuclide, and this back-calculated concentration, the age of the soil can be estimated; that is to say, the time since the bedrock was at the Earth's surface. Finally, this age and the depth to the new bedrock surface (d in Figure 2.1, which is equal to the thickness of the soil) can be used to calculate the rate of bedrock lowering.

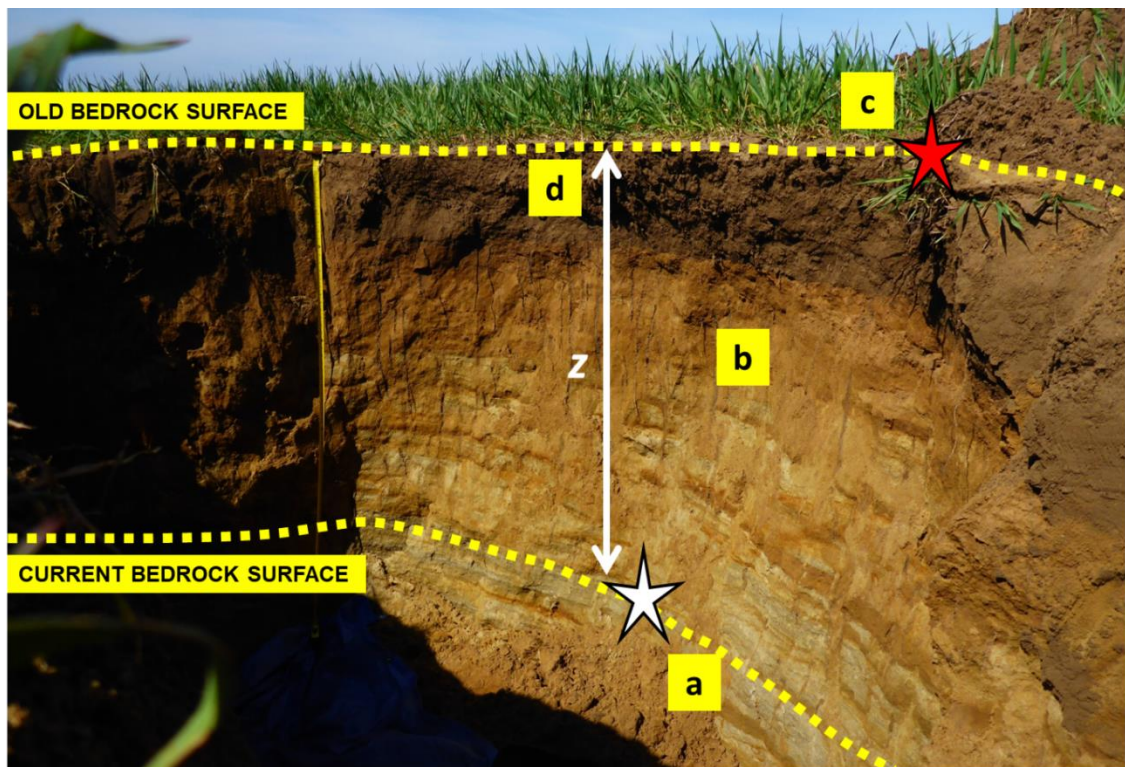


Figure 2.1: Schematic outlining the main steps of calculating soil formation rates from cosmogenically-derived concentrations of a radionuclide. Measured concentrations of a radionuclide in a sample from the current bedrock surface (a) and the attenuation of cosmic rays through the soil profile (b) are used to calculate the radionuclide concentration at the current soil surface (the old bedrock surface, c). In a final step (d), this surface concentration can be used to calculate an approximate age since the start of bedrock lowering. By dividing the age by the depth to the current bedrock surface (z), the rate of bedrock lowering (or soil formation) can be calculated. Photograph was taken by the author.

2.1.3 Rates of soil formation

Although there are multiple methods to measure the rates of soil formation, cosmogenic radionuclide analysis has become one of the most utilized, and provides the best opportunity to cross-compare rates across a wide range of environments. As a result, this review will focus on cosmogenically-derived soil formation rates.

¹⁰Be-derived rates of soil formation ($n = 243$) were amassed by combining a range of previously published studies (Dixon *et al.*, 2009; Heimsath, 2006; Heimsath *et al.*, 1997; 2000; 2001a; 2001b; 2005; 2009; 2012; Owen *et al.*, 2009; 2011; Riggins *et al.*, 2011; Small *et al.*, 1999; Wilkinson *et al.*, 2005). This inventory represents fifteen sites across four countries (Australia, USA, Chile, and the UK). As such, six different Köppen climates are represented (Aw, Bsk, Bwk, Cfa, Cfb, and Csb) as well as all three major rock types (igneous, sedimentary and metamorphic). Although Portenga and Bierman (2011) present more ¹⁰Be-derived rates of soil formation, these stem from samples extracted from bare rock terrain (outcrops, tors) and catchment deposits (stream sediments). Moreover, rates of weathering for bare bedrock surfaces have been shown not to be equal to rates of bedrock weathering at the soil-saprolite interface (Wilkinson and Humphreys, 2005).

Rates of soil formation span four orders of magnitude, ranging from 6×10^{-5} to $6 \times 10^{-1} \text{ mm y}^{-1}$ with a median of 0.021 mm y^{-1} . The fastest rates ($0.010 - 0.594 \text{ mm y}^{-1}$; median = 0.069 mm y^{-1}) are associated with Warm Summer Mediterranean (Csb) climates ($n = 103$) whilst the slowest rates ($0 - 0.005 \text{ mm y}^{-1}$; median = 0.001 mm y^{-1}) are found for Arid Cold (Bwk) climates ($n = 38$) (Figure 2.2). This is most likely due to the fact that bedrock weathering, and thus soil formation, is less effective in environments where water is limited which reduces the potential for frost shattering (Portenga and Bierman, 2011; Stockmann *et al.* 2014). Moreover, the fastest rates ($0.009 - 0.359 \text{ mm y}^{-1}$; median = 0.038 mm y^{-1}) are associated with sedimentary lithologies such as sandstones and siltstones ($n = 55$). These contrast with the slowest rates ($0 - 0.594 \text{ mm y}^{-1}$; median = 0.014 mm y^{-1}) measured from soils developing on

metamorphic lithologies, such as metasediments and gneiss ($n = 120$) (Figure 2.3). This may be explained by the fact that sedimentary rocks are inherently more porous which increases the residence time between water and rock grains, and enhances their susceptibility to weathering (Morel *et al.*, 2003; Palumbo *et al.*, 2009).

It is possible that the rates of soil formation presented here are overestimates. Given that these soil formation rates all stem from cosmogenic radionuclide analysis, this inventory is biased towards relatively shallow soils where access to the soil-bedrock interface makes for easier sample acquisition. The median depth for the inventory presented here is 0.35 m (range: 0.025 – 3.2 m) whilst only 6% of the inventory (five studies) report formation rates for soils deeper than a meter ($n = 15$). It is widely acknowledged that rates of soil formation exponentially decrease as soil thickens (Wilkinson and Humphreys, 2005). In this inventory, soils deeper than 1.5 m have a median formation rate of 0.013 mm y^{-1} ($n = 7$), nearly half that of the overall median reported for the total inventory.

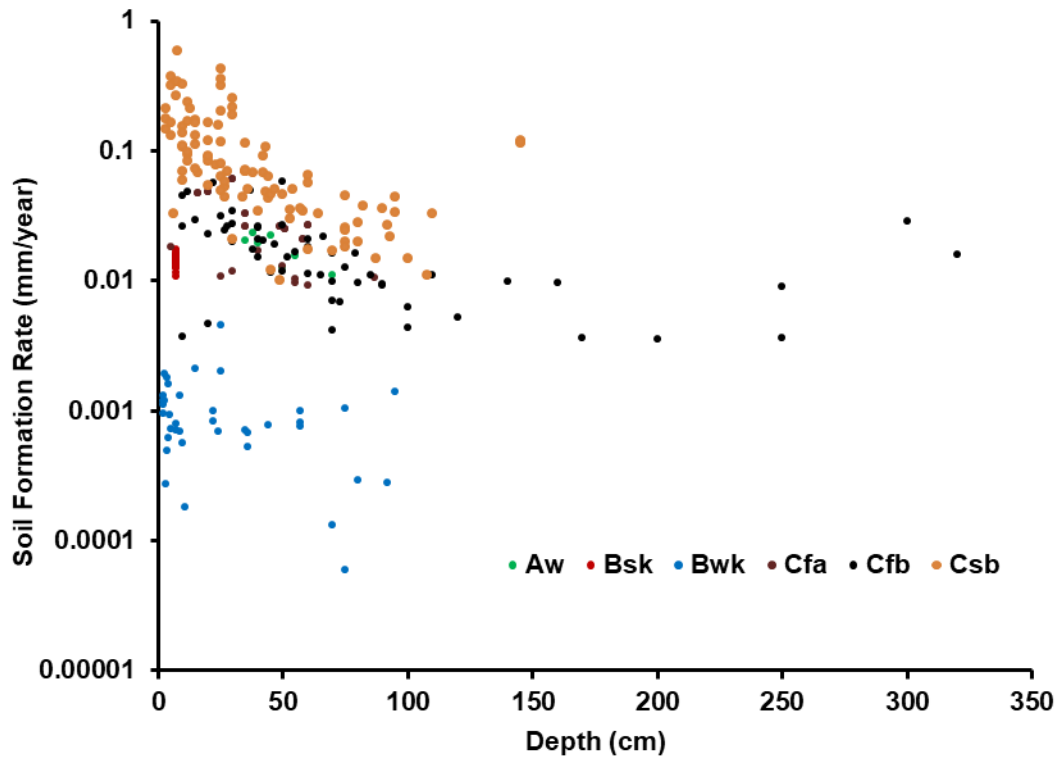


Figure 2.2: Global inventory of soil formation rates against soil depth, grouped by Köppen climate type ($n = 243$). Aw = tropical wet-dry; Bsk = cold semi-arid; Bwk = cold desert; Cfa = humid subtropical; Cfb = temperate oceanic; Csb = warm summer Mediterranean. For full dataset, see Appendix 2.1.

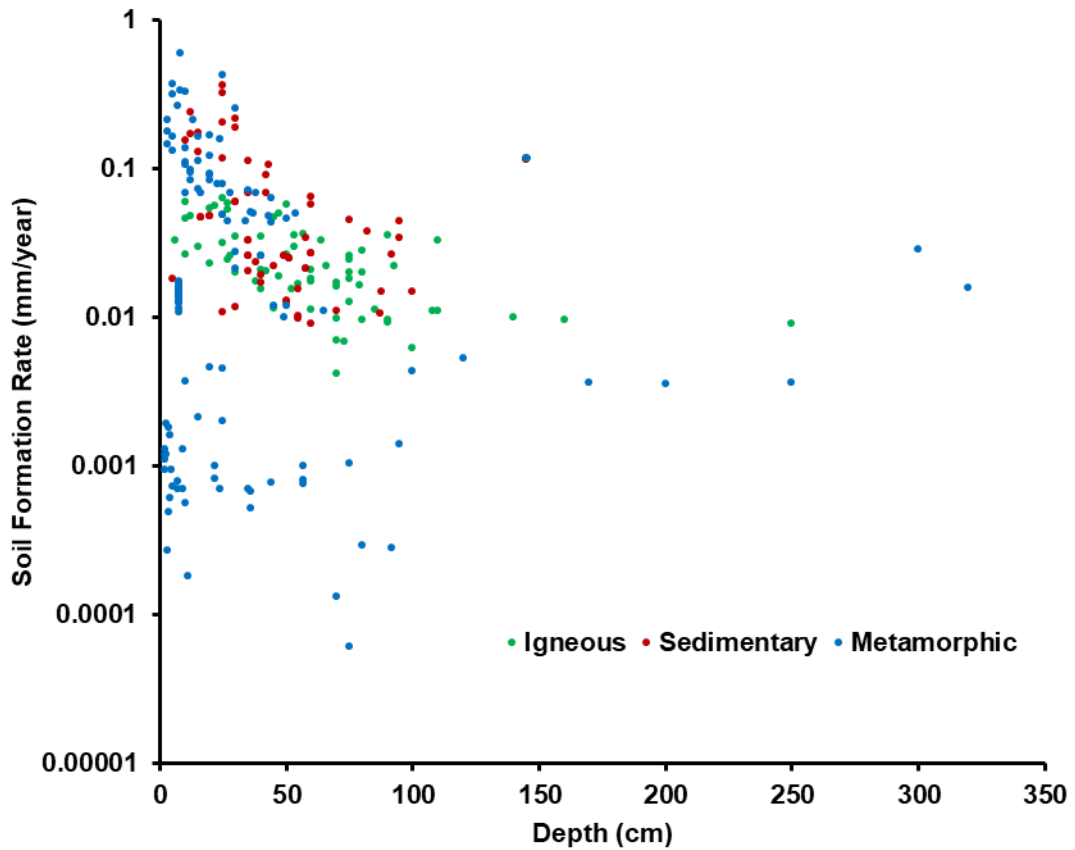


Figure 2.3: Global inventory of soil formation rates against soil depth, grouped by lithology ($n = 243$). For full dataset, see Appendix 2.1.

2.1.4 Factors that affect the rate of soil formation

As previously shown in Table 2.1, there are a range of definitions that have been applied to describe ‘soil formation’. Many of these refer to the breakdown and transformation of the underlying bedrock, and the subsequent weathering processes that convert saprolite into soil (Shaw, 1930; Jenny, 1941; Minasny and McBratney, 1999; Wilkinson and Humphreys, 2005; Egli *et al.*, 2014; Yu *et al.*, 2017). The residual soils which form in this way will be referred to as autochthonous soils, and discussed in Section 2.1.4.1. However, in some instances, soils either partially or solely form from the deposition of parent

material transported from another location. These are hereafter referred to as allochthonous soils, and discussed in Section 2.1.4.2.

2.1.4.1 Autochthonous soil formation

2.1.4.1.1 Five factors of autochthonous soil formation

At the bedrock, soil formation occurs at the nexus of geochemical and physical weathering (Brunsden, 1979; Gabet *et al.*, 2003). Much of the scholarship in this area has been delivered by the Critical Zone community (Brantley *et al.*, 2017) interested in the processes and mechanisms that occur over relatively long timescales (millennia) and at depth below the soil profile. Recent work has elucidated our knowledge and understanding of the incipient stages of soil formation. It has been demonstrated that fractures in bedrock, even micro-fractures <1 μm wide (Graham *et al.*, 2010), enable the transmission of meteoric water, enriched with dissolved oxygen and organic acids, which promotes mineral dissolution and weathering-induced fracturing (Navarre-Sitchler *et al.*, 2015; Banwart *et al.*, 2019). Further work by the Critical Zone community has been called for to further explore the evolution of pore-scale changes which occur in rock during incipient weathering since these represent the very beginning of the soil formation process (Navarre-Sitchler *et al.*, 2015). The Critical Zone community has also invested a large research effort to studying the biotic mechanisms that contribute towards the weathering of parent material, following the creation of this initial porosity. For example, Brantley *et al.* (2017) show that trees both 'build' the critical zone, by micromechanically fracturing the rock mass, thereby promoting further weathering, and 'plumb it', by influencing the fluxes, pathways, and chemistry

of water (see also Zwieniecki and Newton, 1994; Pate *et al.*, 1998). In addition, the roles played by microbiota (e.g., fungi and bacteria) have also been examined. Taylor *et al.* (2009) present a sequence of plant- and fungi-induced weathering mechanisms, demonstrating that mycorrhizal fungi in particular have the propensity to colonise mineral grains between roots, affect the solution pH (Bago *et al.*, 1996), and secrete low molecular organic compounds that can accelerate mineral dissolution (Ochs, 1996; Schmalenberger *et al.*, 2015).

Critical Zone examinations of incipient weathering in the parent material underlying soils have demonstrated that, much like the horizons observable in soil, the weathering profile can be similarly delineated in terms of the extent to which the parent material has been weathered. Figure 2.4 presents a conceptual diagram to illustrate this. Fresh, unweathered bedrock at the base is overlain by a layer of isovolumetrically weathered bedrock referred to as *saprolite* (Stolt and Baker, 1994) or *saprock* (Anand and Paine, 2002).

Saprolite is chemically altered bedrock which maintains the fabric of the underlying fresh bedrock. This layer may exhibit fractures and support biotic weathering processes such as root expansion, mineral acquisition, or the release of organic acids (Brantley *et al.*, 2017). One of the more challenging delineations to make is that of the transition between saprolite and soil, and workers in this area have often used the term 'transition zone' to underscore the diffuse nature of this boundary (Stolt *et al.*, 1991). Lebedeva and Brantley (2017) expand on this idea by dividing a column of weathered bedrock into a series of blocks to explore the contribution of joint fractures in the weathering process.

Sowers, 1963	Deere and Patton, 1971	Ruhe, 1975	Martin, 1977	Jones, 1985	Pavich, 1986
Upper zone	A horizon	Solum	Residual soil	Decomposed	Soil
Intermediate zone	B horizon			Decomposed soil	Massive
	Saprolite	Oxidized and leached zone	Saprolite	Saprolite	
Partially weathered zone	Transition zone	Oxidized and unleached zone	Disintegrated rock	Slightly weathered	Weathered rock
	Partly weathered			Active weathering	
Unweathered bedrock					

Acworth, 1987	Stolt <i>et al.</i> , 1992	Tandarich <i>et al.</i> 1994	Ollier and Pain, 1996	Huggett, 2003	Brantley <i>et al.</i> , 2017
A horizon B horizon	Soil	Pedologic	Solum	Mobile zone	Mobile soil or colluvium
Upper saprolite	Transition zone	Pedologic and geologic		Rounded corestones	
Mid saprolite	Saprolite	Geologic structure	Angular corestones in saprolite	Saprolite	Weathered immobile material
Lower saprolite	Partially weathered rock	Transition zone		Saprock	
Saprolite transition		Unaltered, unoxidized			
Unweathered bedrock					

Figure 2.4: A summary of the weathering zones within a soil profile

Whilst Critical Zone scientists continue to explore the incipient fracturing and weathering mechanisms occurring in bedrock, soil scientists have focused on the extrinsic and intrinsic factors that may perpetuate that weathering. Early work (Dokuchaev, 1879; Glinka, 1914; Jenny, 1941) identified an array of independent extrinsic factors: climate, organisms, parent material, relief, and time. What was not manifestly explored at this time was the dynamic hierarchy of these factors. For instance, climate and organisms represent external factors that actively promote or retard soil development (Hasenmueller *et al.*, 2017; Anderson *et al.*, 2018). In contrast, relief is a passive variable that can indirectly influence soil formation through affecting these external factors, such as controlling the thermal and water regime of the developing soil, and thus its biota (Yair, 1990). Likewise, the parent material can be considered as a

passive state factor: a substrate from which the developing soil inherits many significant genetic properties, such as texture and mineralogy (Kirkby, 2018). Time, itself, is not an independent state factor (Mudd and Yoo, 2010). Time is a unit of measurement over which soils form. Soils do not form directly because of time.

2.1.4.1.2 Water: the nexus between the five soil formation factors

Fundamental for chemical weathering, and somewhat significant for mechanical weathering, is the presence of water (Pelletier and Baker, 2011). Work has been conducted to examine how the state factors listed above encourage or otherwise impede the contact time between water and the bedrock-soil interface (Heimsath and Burke, 2013). For example, Pope *et al.* (1995) suggests that climate influences soil formation rates, citing a linear relationship between precipitation and the magnitude of weathering. However, an increase in precipitation is not always analogous to an increase in subsurface water contact and water residence time at the bedrock. It is possible that increased precipitation results in greater rainsplash and surface crusting, thus progressively impeding the infiltration of water to the bedrock (Assouline, 2004). In addition, increased precipitation may stimulate greater biomass production, although this will also depend on other environmental factors (such as temperature) that govern vegetation development (Nearing *et al.*, 2004). If greater biomass is stimulated, the proportion of the precipitation that can infiltrate through the soil to the bedrock may be species-dependent. Plants with a high leaf area index – one of the major determinants of water flux from plants (Wang *et al.*, 2017a) – may increase transpiration and reduce

the transmission of water to the bedrock. However, some plants may have specific root traits (such as wider diameters) that create macropores and promote preferential flow (Gould *et al.*, 2016). The relief of the site also determines the flow and residence time of water at the bedrock with steeper slopes promoting overland flow and consequently reducing water contact time in subsurface horizons (Burke *et al.*, 2007).

Other workers have focussed on the biochemistry of water and how that contributes or retards the lowering of the bedrock weathering front (Wright, 1988). For example, Huang *et al.* (2013) demonstrate a positive relationship between acid precipitation and local bedrock weathering rates. However, the relative hierarchical importance of water chemistry to other limiting factors (water quantity and water residence time) has not been established. Since many of the state factors of soil formation are considered in isolation (Drever, 1994; Dixon *et al.*, 2009), more research is needed to consider the roles and feedback mechanisms that exist between multiple state factors. In addition, another major gap in our understanding is the effect of human activity on rates of soil formation.

2.1.4.1.3 Human activity: a sixth soil formation factor?

Anthropic influence on pedogenesis is not entirely a fresh idea given that early work (Jenny, 1941) considered the organism state factor to encompass the role of humans. Despite this, some workers have recently concluded that “soil formation (is) affected little by human activities” (Verheijen *et al.*, 2009, p. 33). Ultimately, the degree to which humankind influences the rates of soil formation is likely to be context specific. Some scholars have concluded that,

in some contexts, the role of humans represents more than that originally conceived for the state factor of organisms (Richter, 2007a).

One of the ways that humans may bear an influence on soil formation is through crop cultivation. In shallow soils, roots have the capacity to bio-mechanically induce bedrock weathering (Dietrich *et al.*, 1995). This represents a direct influence of crop cultivation on pedogenesis. For deeper soils, root growth may assume a more indirect role in influencing bedrock weathering (Dixon *et al.*, 2009; Rautaray, 2011; Jin *et al.*, 2013). Deep-rooted crops, such as the forage radish (*Raphanus sativus* L. 'Diachon'), have roots that can alleviate compaction, and have been used to condition soils prior to the cultivation of high value crops. For example, Williams and Weil (2004) observed soybean roots (*Glycine Max* (L.) Merr.) growing through plough pans using channels created by decomposing forage radish.

One of the key characteristics of 'primer' or 'bio-tillage' crops, like the forage radish, is the large rooting diameter. Roots with larger diameters have been shown to increase hydraulic conductivity (Gould *et al.*, 2016). This would theoretically permit more water to reach deeper zones of the profile, potentially augmenting the contact time between the water and the bedrock (Gabet *et al.*, 2003). It is also likely that root-developing processes (such as root diameter expansion) contribute to an increase in hydraulic conductivity. As root diameter enlarges, the radial pressures exerted on to the soil increase (Mizra *et al.*, 1986). In the rhizosphere, and in proximal bulk soil, these pressures can induce macroporosity and micro-fissure formation within the soil, reducing bulk densities in this zone (Yanusa and Newton, 2003; Bodner *et al.*, 2014).

Crop cultivation also changes the biochemistry of the soil, which in turn, influences the chemical weathering potential in the bedrock (Drever, 1994; Riebe *et al.*, 2004). For example, White and Blum (1995) find that root exudates accelerate silicate hydrolysis. As explained above, the ratio between soil depth and rooting depth will determine the potential significance of root exudates to bedrock weathering. On a shallow soil, where roots may grow into the bedrock horizon, these exudates may significantly enhance chemical weathering processes (Puente *et al.*, 2004). For a soil of a thickness greater than root length, the mobilisation of these exudates to the bedrock zone will rely on the water flux of the soil. This re-engages the earlier discussion about how plant roots may induce macroporosity and assist with eluviation and percolation processes.

In addition to crop cultivation, land preparation methods may also affect soil formation. One study on a regosol in southwest China suggests that soil formation rates on conventionally tilled cropland are greater than that within forestland and grassland with rates of 3005, 2457 and 2036 t km⁻² y⁻¹ respectively (He *et al.*, 2009 *citing* Liu *et al.*, 2009). However, these rates were determined in a controlled experimental set-up whereby soils from each land use were first removed from the bedrock, and replaced on top of a nylon fabric with a pore diameter of 0.15 mm. The soil was later removed again to expose the bedrock, and the weathered bedrock was collected, dried, and measured (Liu *et al.*, 2009). Critically, this study was not able to qualify whether the accelerated soil formation rates in tilled soils were due to the tillage operations *per se*, or the roots of the crops involved (especially the tuberous roots of *Ipomoea batatas* Lam.). Alternatively, the authors suggest that accelerated

pedogenesis could have been induced by acidification from fertilizer application.

2.1.4.1.4 Self-limiting behaviour in pedogenesis

A noteworthy development in pedogenesis studies is the awareness of the self-limiting behaviour demonstrated in the soil formation process (Muhs, 1984). This discussion is less focussed on the external factors that govern bedrock weathering and, instead, more concerned with the ways by which soil formation stimulates a negative feedback loop (Schaetzl and Thompson, 2005). Moreover, as the soil thickens, the soil formation rate decreases. Whilst this relationship has been widely accepted (Wilkinson and Humphreys, 2005) there is debate about the specific nature of the decline in soil formation. Many workers (Wilkinson *et al.*, 2005; Gabet and Mudd, 2010) have advocated an 'exponential decay function' (Figure 2.5; curve *a*) by suggesting that an increasing soil thickness insulates the bedrock from the external influences of climate, organisms and relief. Moreover, Minasny and McBratney (1999) observe that a thickening soil insulates the bedrock from the diurnal temperature variations which are ultimately responsible for freeze-thaw weathering. Similarly, thicker soils are more likely to buffer the underlying bedrock from water contact and chemical weathering processes such as hydrolysis (Wilkinson and Humphreys, 2005).

Disputing this hypothesis are advocates for an alternative, humped production function (Figure 2.5; curve *b*) which suggests there is a threshold mantle thickness under which water residence times are not conducive for maximum weathering rates. Heimsath *et al.* (2009) find that a shallow mantle of 0.35 m

brings about peak soil formation rates. Above this threshold thickness, the soils increasingly act as insulating buffers, as discussed above. Indeed, the humped production function should be considered as a development of the original exponential decay function, although they are often treated as juxtaposing theories in the literature (Norton *et al.*, 2014).

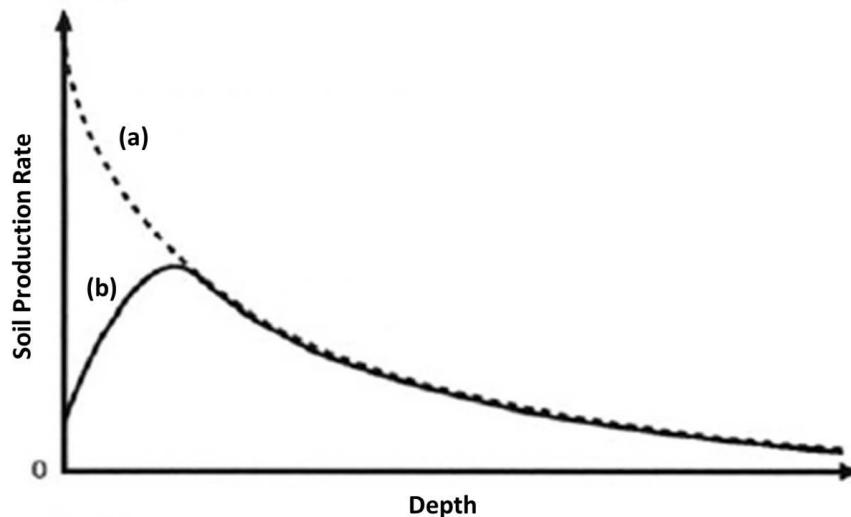


Figure 2.5: Schematic showing both proposed exponential (a) and humped (b) relationships between soil production and mantle thickness (Adapted from Wilkinson and Humphreys, 2005).

It has been demonstrated that soil thickness is a paramount variable in the soil formation process (Heimsath and Burke, 2013). Burke *et al.* (2007, p. 859) suggest that bedrock weathering “may depend simply on the vertical distance from the ground surface to the soil base”. However, the thickness of soil does not fully explain the roles that soils play in regulating pedogenesis. This is clearly demonstrated in Figures 2.2 and 2.3 where, for a given soil thickness, there is a wide range of soil formation rates.

2.1.4.2 Allochthonous soil formation

Hitherto, we have considered autochthonous soil formation: processes acting on a pre-existing body of parent material (Simonson, 1959). This neglects the soils that form in aggrading landscapes. In this context, soils are in part, or sometimes wholly, constituted from the accumulation of allochthonous parent material, transported from another location (Hunt, 1972). There are multiple examples of these; the major types are itemized in Table 2.2.

Understanding the fundamental controls on the up-building of these soils requires a different approach than the traditional five factors of soil formation, previously outlined. Here, the accumulation of parent material is influenced by an array of geomorphological – rather than pedological – phenomena. For instance, the deposition of alluvium may be controlled by river discharge, just as the deposition of loess may be governed by wind speed. Nevertheless, there are some commonalities among different types of transport sediment. First, the sediment must become entrained, which is often a function of its texture and the velocity of the transporting medium (Schaetzl and Thompson, 2015). Second, the transported sediment must at some point be deposited, and this often relies on the force of gravity overcoming the capacity of the transporting medium to sustain material transport.

Table 2.2: Major types of allochthonous parent materials and their soil properties

Environment	Parent material	Characteristic soil properties
Channelized water	Alluvium	Finer soil textures at the top of soil profiles indicate larger particles were deposited first, followed by progressively finer materials (Baker <i>et al.</i> , 1991).
Lacustrine	Proglacial lakes	Well preserved stratification of clay- and silt-rich sediments (James, 1988).
	Glacial varves	Annual couplets of fine dark clay (comminuted organic matter) with lighter silt horizons (Schaetzl <i>et al.</i> , 2000).
	Marls	Carbonate-rich forms of organic-limnic sediment (Chambers, 1999).
	Playas	Soils are often saline (Peterson, 1980).
Coastal	Barrier islands, beaches and bars	Sandy soils, sometimes rich in sulphur and pyrite, developing into acid sulphate soils (Fanning and Fanning, 1989).
	Deltas	Sandy and clayey soils, finer-textured further away from delta head (Wang <i>et al.</i> , 2017b).
Aeolian	Dunes	Yellow, thin coatings of oxidised iron and clay; well-sorted medium and fine, quartz rich sands; often negligible clay fraction (Muhs and Wolfe, 1999).
	Loess	Silt-loam and silty clay loams; porous; highly erodible; often high pH, weathering is not advanced (Lu and An, 1998).
Volcanic	Tephra	Minimal weathering; dominated by amorphous materials; low bulk densities; high macroporosity; high available water (McDaniel <i>et al.</i> , 2011).

Glacial	Till	Unsorted; very clay-rich to coarse sandy textures; basal till is dense, superglacial till is porous (Applegarth and Dahms, 2011).
	Outwash sediment	Sandy and gravelly; small volume of clay; formation of E horizons and clay lamellae (Cooper and Crellin, 1996).
Gravity	Colluvium	Range in texture, depending on the source; some pre-existing weathered material; breakdown of aggregates (Goswami <i>et al.</i> , 1996).

One of the anthropic contributions to allochthonous soil formation is the addition of mineral and organic material to the surface of the soil profile (Pape, 1970; Conry, 1971, 1972; Davidson and Simpson, 1984; Kosse, 1990; Bockheim and Gennadiyev, 2000; Dudal, 2004; Davidson *et al.*, 2006). There is a long history to this, often evidenced in Plaggen Anthrosols where the uppermost part of the soil profile is characterized by a dark, and often anthropogenic, horizon formed after long-term manuring (Denevan and Turner, 1974; Blume and Leinweber, 2004; Giani *et al.*, 2014; Schaetzl and Thompson, 2015). In northeast Scotland, the addition of turves, dung, midden material, calcareous sand, and seaweed, or a combination thereof, contributed towards a gradual increase in the depth of the solum (Davidson and Simpson, 1984) with accumulation rates believed to reach 1.9 cm y^{-1} giving rise to farm mounds of up to 4.3 m in thickness (Davidson *et al.*, 1986). In the St. Kilda archipelago in Scotland, high rates of historic manure addition over-deepened soils to depths of 1.5 m (Hornung, 1974). In the Netherlands, a lower accretion rate of 1.3 mm y^{-1} is cited by de Bakker (1979) but it is

important to note that this is still two orders of magnitude greater than the natural rates of soil formation from bedrock weathering.

Inspired by the pluggen agriculture are a number of strategies in operation today that return waste streams to soils (Read *et al.*, 1997). For instance, in Vietnam, a programme of toilet building in the 1950s led to the construction of thousands of concrete chambers in which to dry-process excrement for use as an agricultural fertiliser (Richardson, 2012). Similarly, in China, approximately 90% of agricultural produce is fertilised through human effluent (Black and Fawcett, 2008).

As well as these examples of untreated effluent, other techniques involve ecological sanitation, which removes the pathogens from by-products through dry-composting or the use of biogas, before agricultural application. One of these is vermicomposting, which has proven to be an effective treatment of faecal matter (Buzie, 2010). This refers to the decomposition of organic materials using the combined action of earthworms and micro-organisms (Shalabi, 2006; Buzie, 2010; Fatura *et al.*, 2010). Whilst micro-organisms are responsible for the biochemical breakdown of organic matter, earthworms are able to physically bioturbate the material into finer-particles (casts and fibres) than would otherwise occur in their absence (Aira *et al.*, 2002).

This review has discussed a range of methodologies employed to measure rates of soil formation and has presented a global inventory of the data that currently exist. Furthermore, it has also explored the multifarious environmental and internal factors that influence the process of both autochthonous and allochthonous soil formation. In accordance with those

that argue that theoretical concepts within soil science should contribute towards issues of soil security and soil sustainability, this review will now turn to explore how our knowledge and understanding of soil formation can contribute towards two areas of soil conservation research: the soil lifespan and soil loss tolerance.

2.2 Soil lifespans

2.2.1 Approaches to date

If soil erosion rates exceed those of soil formation (Figure 2.6), soil profiles thin. The trajectory of any thinning soil is one that, left uninterrupted, will lead to the removal of the soil cover and the exposure of the underlying bedrock, thus threatening the long term sustainability of the soil resource (Amundson, 2015). The soil lifespan is “the length of time, under a given management regime, that a soil can be expected to fulfil the ecosystem services”.

Expressing the sustainability of soil in units of time has been attempted in the past (see Table 2.3). For instance, Stocking and Pain (1983) calculate the lifespan of a soil based on the length of time it can remain productive at a given erosion rate. Although this fails to account for any mass input to the soil system (such as that from bedrock weathering), this is later addressed by Elwell and Stocking (1984). The soil life in this revised model is constrained by the minimum depth required for a particular crop to grow. However, this ignores the possibility that soils under such depths may still be able to contribute towards other ecosystem services, such as the filtering of water or the sequestration of carbon. To avoid prioritizing one function over another, some authors have quantified soil lifespans by simplifying the model. For

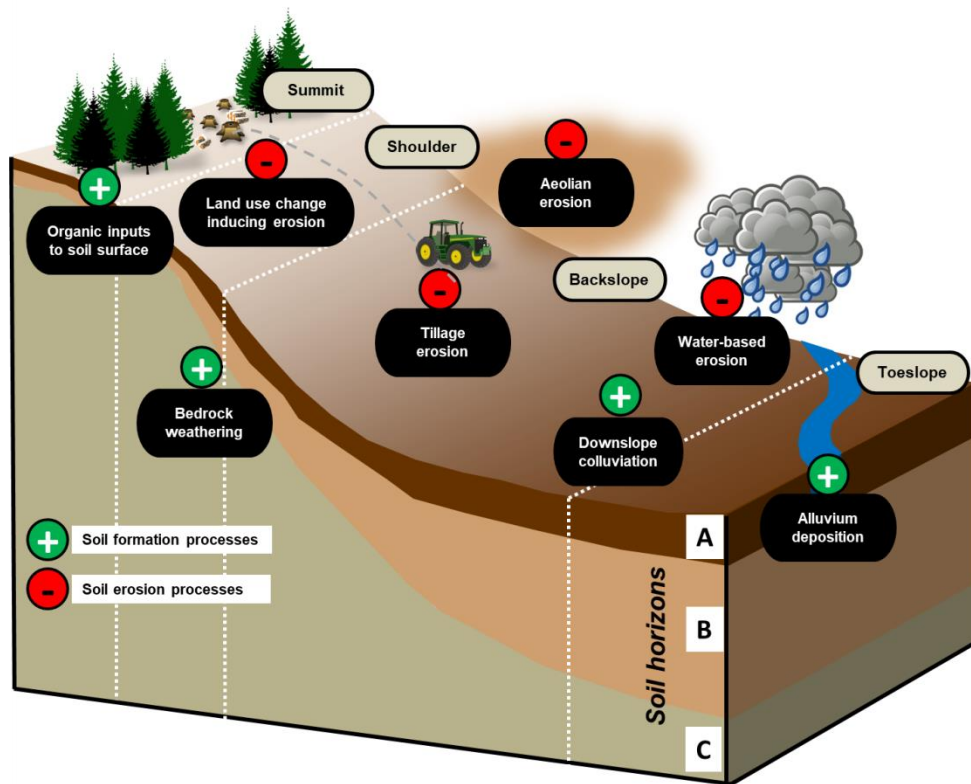


Figure 2.6: Soil formation and erosion processes down a hillslope

Table 2.3: Previous approaches to define the soil lifespan.

Source	Equation Name	Equation	Definition of Terms
Stocking and Pain (1983)	Soil Lifespan	$L = \frac{(D_z - D_o)M}{(Z - Z_f)}$	D_z is initial depth (m), D_o is minimum depth required to support production (m), M is bulk density, Z is mean annual rate of soil erosion (t/ha) and Z_f is soil loss tolerance (t/ha)
Elwell and Stocking (1984)	Soil Life	$L_f = \frac{(D_e - D_o)M}{(Z - Z_f)}$	D_e is depth of available productive soil (m), D_o is minimum depth required for particular crop (m), M is bulk density, Z is predicted rate of soil loss (t/ha/yr) and Z_f is estimated rate of soil formation ($t\ ha^{-1}\ y^{-1}$)
Montgomery (2007)	Critical Time	$T_c = \frac{S}{(E - P)}$	S is initial soil thickness (m), E is soil erosion rate ($mm\ y^{-1}$) and P is soil production rate ($mm\ y^{-1}$)
Sparovek and Schnug (2001)	Lifetime	$LT = \frac{SD - SD_{min}}{\frac{SL}{D_s} + SF}$	SD is present soil depth (m), SD_{min} is minimum soil depth (0.2 m), SL is soil erosion (+soil loss - soil deposition, $kg\ m^{-2}\ y^{-1}$), D_s is bulk density ($1200\ kg\ m^{-3}$), SF is soil formation ($0.0002\ m\ y^{-1}$; $-0.24\ kg\ m^{-2}\ y^{-1}$)
Medeiros et al. (2016)	Soil Lifetime Index	$SLti = \frac{P_{net}}{h_L}$	P_{net} is net solum depth (mm) and h_L is net soil loss rate ($mm\ y^{-1}$)

example, Medeiros et al. (2016) simply divide the solum thickness by the net soil loss rate, applying the model to assess the sustainability of soil in the São Paulo state of Brazil. However, the soil renewal rate used to determine net soil loss was assumed to be 0.2 mm y^{-1} across the state, citing Friend (1992) who did not directly measure soil formation.

Although the literature base developing the concept of the soil lifespan is meagre, it is clear from Table 2.3 that two types of lifespan may be considered. First, a 'lifespan to bedrock' can be calculated to forecast the duration until the bedrock, or parent material, is exposed (Montgomery, 2007; Medeiros *et al.*, 2016; Figure 2.7). However, Bakker *et al.* (2004, p. 58) assert "the point of zero yield may often be reached before the soil is completely removed". Therefore, a second 'truncated lifespan' can be calculated to forecast the length of time before a soil thins beyond a defined threshold depth, under which the soil is believed to be of inadequate quality to deliver one or more of the ecosystem services. This is arguably a more complex calculation than the 'lifespan to bedrock' since the degree to which a soil may provide ecosystem services is dependent both upon a range of spatially and temporally variable soil properties, and the ecosystem service under study.

Setting a threshold depth for the 'truncated lifespan' may be assisted by identifying any regressors or limiting factors down the soil profile (Bakker *et al.*, 2004). This often involves the need to undertake test soil pit inspections or, for some structural properties, the use of dynamic cone penetrometers or ground penetrating radar (Raper *et al.*, 1990). For example, some root growth hindrances may be incurred by the presence of a plough pan but there could also be other, or indeed more, restrictions such as the deterioration of soil

structure, water holding capacity, or the presence of a pebble/gravel bed (Passioura, 1991). Equally, a threshold depth of nutrient deficiency may exist within the profile, potentially by the upward transport and progressive accumulation of clay particles into the A horizon which nutrients absorb to, rendering them inaccessible (Rhoton and Lindbo, 1997). Another limiting factor that occurs at depth is soil acidity. Soil acidity can hinder plant production because of the low content of base cations that affects root growth and the absorption of water (Tang *et al.*, 1999). Whilst surface liming has been shown to improve topsoil acidity, it is generally less effective in improving subsoils (Caires *et al.*, 2008). Therefore, it is likely that a threshold between lime-improved soil at the surface and less-improved and/or untreated subsoil may truncate primary production, and therefore, the soil lifespan.

There has been some attempt in the past to experimentally ascertain how and where in the soil profile these restrictions may occur. Desurfacing investigations, where the soil is removed at incremental depths to emulate high magnitude erosion processes has been conducted (Malhi *et al.*, 1994; Larney *et al.*, 1995; Tanaka, 1995). For example, Gollany *et al.* (1992) performed a desurfacing investigation over a five year period on a Typic Argustoll at three depths (0, 0.3 and 0.45 m). The thinner Ap horizons overlying substantially more clayey Bw and Bt horizons introduced clay into the Ap horizon, which deteriorated structure, and reduced water holding capacity. However, Gollany *et al.* (1992) suggest that these desurfacing experiments often exaggerate the reality of natural soil erosion which typically allow for the mixing and incorporation of subsurface horizons into the top horizon.

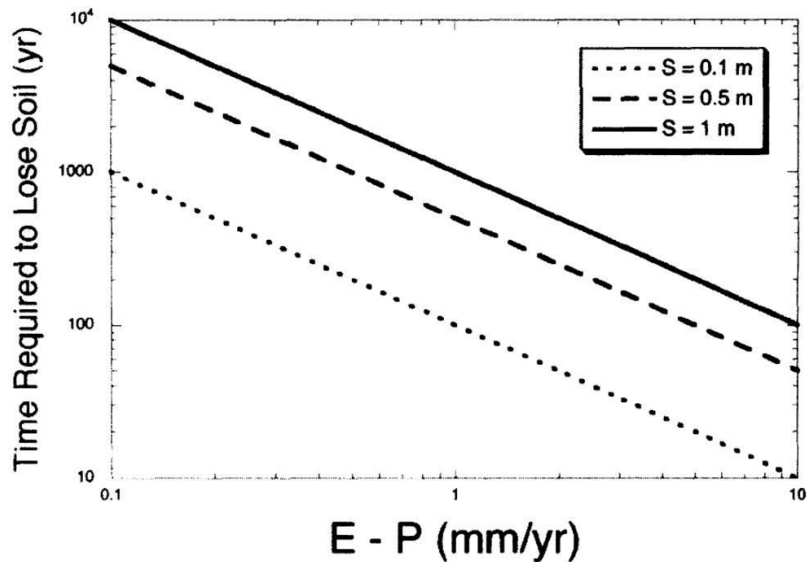


Figure 2.7: Critical time (T_c) required to erode a soil profile of differing initial thickness (S) for different net soil erosion rates (Adapted from: Montgomery, 2007).

2.2.2 Applications of the soil lifespan concept

To date, soil conservation management has been reported in terms of the units of soil protected ('erosion has been reduced by x tonnes per hectare') or enhancements to ecosystem services ('yields have increased by x %'). These do not explicitly address how soil conservation management enhances soil *sustainability*, a concept that demands a forward-looking perspective. After all, sustainability is defined as the "ability to meet the needs of the present without compromising the ability of *future* generations to meet their own needs" (WCED, 1987, my emphasis). The soil lifespan concept provides a direct forecast: an assessment as to the length of time, under a given land management regime, that a soil can be expected to deliver ecosystem services.

To directly evaluate the effectiveness of a range of erosion amelioration techniques to address the long-term sustainability of the soil, lifespans can be calculated (before and after their implementation). If the latter lifespan is greater, the conservation technique has extended the soil lifespan. The benefit of this method is the fact that a range of soil erosion amelioration techniques can be assessed using a standardized unit which is directly comparable. This can be shown with the use of an example.

Consider two soils (soil A and soil B), both of which have been subject to two different types of soil erosion amelioration; soil A has been subject to zero tillage whilst soil B has been subject to contour cultivation. If, for both soils, rates of erosion have been reduced from 12 mm y^{-1} to 1 mm y^{-1} , this would suggest that these strategies have had an equal effect. However, these results have not expressed how soil sustainability has been enhanced, neither have they considered rates of soil formation, nor the depth of the soil profile. It could be the case that soils A and B represent different positions down a hillslope where soil depths, and thus soil formation rates, may be spatially variable. Soil A forms at 0.9 mm y^{-1} and has a depth of 0.5 m, whilst soil B forms at 0.5 mm y^{-1} and has a depth of 2.0 m. The pre- and post-management lifespans to bedrock can then be calculated: 45 years and 5,000 years for soil A, and 174 years and 4,000 years for soil B, respectively. Although soil B has a greater post-management lifespan, this is due to the soil profile being four times as deep. Erosion amelioration on soil A has, in fact, achieved the greatest extension of the lifespan: 4,955 years, in comparison with 3,826 years for the amelioration on soil B.

The soil lifespan concept can be used to evaluate a range of different soil conservation practices. Some measures may reduce the net erosion rate and extend the soil lifespan. In these cases, erosion rates may still be finite; that is to say, net erosion rates remain positive, and soil profiles still thin, albeit at a retarded rate. Some measures may zero net erosion rates, extending lifespans indefinitely. This would bring about no long-term change in the thickness of the soil profile. The most effective soil conservation measures are those that yield negative net erosion rates (soil erosion rates fall below those of soil formation) leading to an aggrading soil profile.

2.3 Soil loss tolerance

2.3.1 Comparing soil formation rates with rates of soil loss tolerance

Soil formation rates are also used to derive rates of soil loss tolerance (SLT, hereafter). The premise of this concept is to curtail rates of erosion to those of soil formation so that the soil can sustain crop productivity, economically, and indefinitely (Di Stefano and Ferro, 2016).

This review conducted a Web of Science search using the phrase 'soil loss tolerance' (Appendix 2.2). Out of the 101 studies compiled, 58 reported SLT values, representing 18 countries (Figure 2.8). For 51 of these, the SLT values were presented as a range (for example, $0.5 - 1.5 \text{ t h}^{-1} \text{ y}^{-1}$). In these instances, a median SLT value can be calculated. This dataset comprised 17 of the 26 World Reference Base soil orders (IUSS Working Group WRB, 2015) and included all soil textures apart from 'sandy clay', 'sandy clay loam' and 'silty clay'.



Figure 2.8: Distribution of SLT values from a global inventory ($n = 58$). For full dataset, see Appendix 2.2.

Early work to derive SLT values was limited by a lack of evidence and understanding of soil formation rates. Those that were calculated often led to claims that they represented “a scientific weakness” (Di Stefano and Ferro, 2016, p. 128), which were “rooted in erroneous beliefs” (Johnson, 1987, p. 160) and based on “a matter of guesswork” (Stocking, 1978, p. 307). In the inventory compiled by this review’s Web of Science search, 19 out of the 58 studies used soil formation data to calculate SLT. However, it is also the case that the soil formation rates used were based on a small number of historic studies, comprising non-isotopic data. Although cosmogenic radionuclide methods represent a relatively recent advancement in soil science, these SLT values made use of soil formation data derived more than a century ago. For example, more than 40% of the SLT values made use of soil formation rates that can be traced back to a 1909 White House address by the geologist T. S.

Chamberlin (Chamberlin, 1909). Many also used the methodology from Barth (1961) measuring the volume of mobile geochemical elements in runoff as a proxy for bedrock weathering, but fail to account for any atmospheric inputs, thus reducing the validity of the data (Alexander, 1988a; Velbel, 1989). Others have cited rates of building disintegration, such as the weathering of the Great Pyramid of Egypt, to represent the rates of soil formation (Barton, 1916 *cited in* Lal, 1998).

2.3.2 Revisiting SLT and the use of soil formation rates

Given that cosmogenic radionuclide analysis now allows the long-term rates of soil formation to be constrained with greater accuracy (Heimsath *et al.*, 1997; Wilkinson *et al.*, 2005), it is possible to bring these data together with our current estimates of SLT. This exercise is key to our understanding of the long-term sustainability of soils and whether our current metrics of tolerance are sufficient.

Analysing this review's inventory of SLT as outlined in the previous section, rates of soil loss tolerance range from 0.002 to 3.64 mm y⁻¹ with the median being 0.49 mm y⁻¹ (Figure 2.9). Whilst more than two thirds of these data fall within the range of soil formation, 97% of the data are greater than the median soil formation rate with 95% being more than twice this. Only two of the 66 inventoried SLT values fall below the median rate of soil formation.

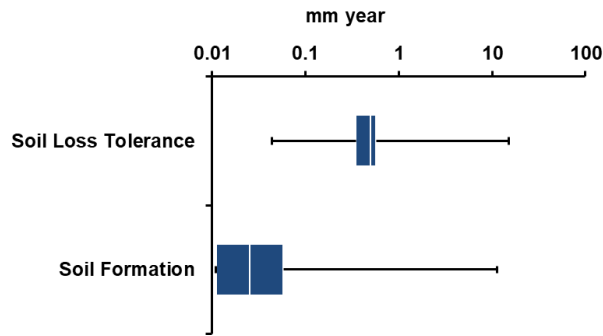


Figure 2.9: Distribution of soil loss tolerance values ($n = 58$) and soil formation rates ($n = 243$). Full data for soil formation can be seen in Appendix 2.1; for SLT, see Appendix 2.2. White lines within bars represent the median; boxplots represent interquartile ranges; error bars represent the 5th and 95th percentiles.

The incongruence between rates of SLT and soil formation has also led to erosion being inaccurately described on many erosion forecast maps. For instance, labels such as “tiny” and “minimal” erosion are used to represent rates of erosion that are an order of magnitude greater than soil formation (Hua *et al.*, 2012; Zhu, 2015). Similarly, Weltz *et al.* (2014) indicate that a rate of 0.15 mm y^{-1} is “sustainable” despite it being six times faster than the median rate of soil renewal.

As demand on global soil resources grows, it is vital that soil loss tolerance is founded on a reliable and valid evidence base. To this end, more isotopic measurements to quantify the rates of soil formation are needed, particularly for soils of depths $>1 \text{ m}$ and for climates and lithologies hitherto unvisited. As part of this effort, rates of soil formation must also account for both the long-term rates of bedrock surface lowering, but also the short-term rates of soil up-building at the surface from colluvial, aeolian, alluvial, and glacial deposition. This requires greater synergy between soil scientists and other Earth Science disciplines.

Chapter 3: The Sensitivity of Cosmogenic Radionuclide Analysis to Soil Bulk Density: Implications for Soil Formation Rates

D. L. Evans, Á. Rodés, and A. M. Tye

This chapter has been submitted as a paper, and is in review in the *European Journal of Soil Science*.

Abstract

Improving our knowledge of soil formation is critical so that we can better understand the first-order controls on soil thickness and more effectively inform land management decisions. Cosmogenic radionuclide analysis has afforded soil scientists the opportunity to more accurately constrain the rates at which soils form from bedrock. In such analysis, the concentration of an isotope, such as Beryllium-10, is measured from a sample of bedrock. Since this concentration is partly governed by the lowering of the bedrock-soil interface, a cosmogenic depth-profile model can be fitted to infer the bedrock and surface lowering rates compatible with the measured concentrations. Given that the bedrock-soil interface is shielded by soil, the cosmic rays responsible for the in-situ production of the radionuclide are attenuated, with attenuation rates dependent on the density profile of this soil. Many studies have assumed that soil bulk density is either equal to that of the bedrock or constant with depth. The failure to acknowledge the variations in soil bulk density means that cosmogenically-derived soil formation rates previously published may be under- or over-estimates. Here, we deploy a new model

called 'CoSOILcal' to a global compilation of cosmogenic analyses of soil formation and, by making use of estimated bulk density profiles, re-calculate rates of soil formation to assess the sensitivity to this important parameter. We found that where a soil mantle > 0.25 m overlies the soil-bedrock interface, accounting for the soil bulk density profile brings about a significantly slower rate of soil formation than that previously published. Moreover, the impact of using bulk density profiles on cosmogenically-derived soil formation rates increases as soil thickens. These findings call into question the accuracy of our existing soil formation knowledge, and we suggest that future cosmogenic radionuclide analysis must consider the bulk density profile of the overlying soil.

3.1 Introduction

How, where and why do soils form? These questions represent some of the oldest scholarly enquiries within soil science (Dokuchaev, 1879). Being able to identify the processes of, and the factors that influence, soil formation can help to inform our understanding of the soil system: its processes and functions, and the delivery of multiple ecosystem services. Given the diverse range of environments in which soils form, the sub-discipline of pedogenesis has a wide focus. An inexhaustive list of the types of enquiries undertaken by soil formation scholars includes: the study of the accumulation and transformation of parent material (Jenny, 1941; Simonson, 1959; Hurni, 1983; Minasny and McBratney, 1999), the horizonisation of soil profiles (McAuliffe, 1994; Bockheim and Gennadiyev, 2000; Wilkinson and Humphreys, 2005), and the factors that influence the evolution of soil properties (Richter *et al.*, 2007a; Schaetzl and Thompson, 2015; Vereecken *et al.*, 2016). For the

purposes of this chapter, we define 'soil formation' here and hereafter as the process by which bedrock material converts into soil (Targulian and Krasilnikov, 2007; Egli *et al.*, 2014).

One of the most important questions asked by soil scientists is: how fast does soil form? (Stockmann *et al.*, 2014). Knowledge of the first-order balance between rates of soil formation and erosion is integral if we are to ensure the long-term sustainability of global soil resources (Montgomery, 2007). Whilst measuring soil erosion is a long-established practice within soil science (Quinton *et al.*, 2010; Poesen, 2017), quantifying the rates that soils form from bedrock has received less widespread attention (Schertz, 1983; Duan *et al.*, 2017a). Only within the past twenty to thirty years have technological advancements and interdisciplinary liaisons allowed soil scientists to more precisely constrain the rates at which soils form from bedrock (Heimsath *et al.*, 1997; Román-Sánchez *et al.*, 2019a,b). By conducting analyses across a range of climatological and lithological contexts, it has also become possible to assess the extent to which the state factors of soil formation – climate, organisms, relief, parent material, and time (Jenny, 1941) – influence these soil formation rates (Stockmann *et al.*, 2014).

The development of cosmogenic radionuclide analysis has demonstrated that soil thickness exerts a significant internal control on these state factors, and by extension, soil formation rates (Larsen *et al.*, 2014). Many authors have observed that soil thickening leads to an exponential decline in soil formation rates (Wilkinson and Humphreys, 2005). Thicker soil more effectively insulates the parent material against temperature and precipitation variations that drive weathering processes (Minasny and McBratney, 1999; Heimsath *et al.*, 2009).

However, soil formation rates are not solely determined by this relationship with soil thickness. Moreover, Yu *et al.* (2017) show that rates of bedrock weathering are instead constrained by the transmission of water and solutes down the soil profile. A major determinant in the dynamics of this process is the bulk density of the soil, with greater bulk densities limiting the volume of water and solutes, and slowing their infiltration to the bedrock (Gabet *et al.*, 2006).

Despite the fact that soil bulk density influences soil formation (Price and Velbel, 2003; Neely *et al.*, 2019), precise density profiles are usually not integrated in the cosmogenic nuclide's production models. The cosmogenic nuclide concentrations in bedrock samples under the soil are fundamentally dependent upon two factors. One of these is the duration that the bedrock has been exposed to cosmic rays, as the cosmic bombardment of the minerals in the uppermost metres of bedrock produce these nuclides. Therefore, longer exposure times give rise to greater cosmogenic nuclide concentrations. The second factor is the evolution of the effective depth (lithostatic pressure) to the bedrock with time, which can be numerically related to the rate at which the bedrock weathers into soil (Lal, 1991; Stockmann *et al.*, 2014). Given that the bedrock weathering rate is the desired dependent variable, concentrations of the radionuclide – N in Eq. (1) – can be measured using Accelerator Mass Spectrometry and interpolated to solve for bedrock weathering rates (ϵ).

$$N = \sum_{i=sp, \mu_f, \mu^-} \frac{P_i(\theta) \cdot e^{-z\rho/\Lambda_i}}{\lambda + \epsilon\rho/\Lambda_i} \quad (1)$$

where: P_i are the annual production rates of the radionuclide by spallation, fast muons and stopping muons (sp , μ_f and μ^-) at a surface with slope θ ; z is the

sample depth; ρ is the mean density of material overlying the sample; λ is the decay constant of the radionuclide and Λ_i are the mean attenuation lengths of the cosmic radiations (Lal, 1991).

Cosmic rays are attenuated when they pass through the soil to reach the underlying bedrock. Accounting for the factors that drive this attenuation is critical so that accurate bedrock weathering rates can be determined. Two terms in Eq. (1) directly address this attenuation: the depth of the sample and the density of the overburden material (in this case, the soil) (Balco *et al.*, 2008). Many studies (Heimsath *et al.*, 1997; Owen *et al.*, 2011; Riggins *et al.*, 2011) have assumed that the density of the soil is either equal to the bedrock density, or is constant with depth (but see Larsen *et al.*, 2014). This fails to acknowledge the heterogeneities of the soil profile and, in particular, the spatial variation in bulk density (Evans *et al.*, 2019). As a result, all previous cosmogenic radionuclide analyses estimating soil formation rates for bedrock overlain by soil that have not measured and/or accounted for the variation in the soil density, may have yielded data which are under- or over-estimates.

Here, we amass an inventory of cosmogenically-derived soil formation rates previously reported for bedrock overlain by soil, where spatial changes in soil bulk density have hitherto not been employed. Employing the CoSOILcal programme, the first of its kind that considers overburden density (Rodés and Evans, 2019), our aim is to assess the sensitivity of these soil formation rates when bulk density data are accounted for.

3.2 Materials and methods

^{10}Be -derived rates of soil formation ($n = 264$) were amassed by compiling studies where *in-situ* ^{10}Be has been measured under soil profiles (Heimsath, 2006; Heimsath *et al.*, 1997; 1999; 2000; 2001a; 2001b; 2005; 2009; 2012; Wilkinson *et al.*, 2005; Dixon *et al.*, 2009; Owen *et al.*, 2011; Riggins *et al.*, 2011). More studies exist (e.g.: Portenga and Bierman, 2011) but these measure soil formation from samples extracted from bare rock (outcrops, tors) and catchment deposits (stream sediments), and as such were not appropriate for the aims here.

From each of the shortlisted studies, raw data were extracted including sample latitude, longitude, and elevation, ^{10}Be concentration, the concentration uncertainty, and the soil formation rate. The density assumed by the authors (which was generally either bedrock density or average soil density) was also recorded. Although the production rate of ^{10}Be is influenced by topographic obstructions, this can be addressed by calculating a shielding factor. This represents the ratio of the ^{10}Be production rate at the obstructed site to that at a site where the surface is flat and the horizon is clear (Balco *et al.*, 2008). These shielding factors were recorded from each study. Some studies did not report data for all of the above criteria. As a result, the inventory was truncated so as to only analyse entries with a complete dataset. This resulted in the removal of 101 entries, permitting 163 for analysis.

The resulting inventory of soil formation rates used in this analysis were collated from twelve studies, representing ten unique locations across Australia, USA, Chile, and the UK, five different climates (according to the

Köppen classification system) and all three major rock types ($n = 163$; see Appendix 3.1 for the full dataset). The median depth for the inventory was 0.35 m, with 72% between 0 – 0.5 m, 25% between 0.5 – 1.0 m, and 12% > 1.0 m.

The variations in the bulk density of the soil above the bedrock were not provided in any of the inventoried studies or their accompanying supplementary information files. Therefore, in the absence of these bulk density data, fine earth bulk densities were estimated for five depths (0, 50, 100, 150, and 200 cm) down the soil profile at each site using the International Soil Reference Information Centre (ISRIC) Global Soil Information System 'SoilGrids' (250 m resolution; June 2016 update; see Hengl *et al.*, 2017). We acknowledge the fact that the ISRIC 250 m raster was not intended for this type of site-specific analysis; a better approach would be to measure the bulk densities down the soil profiles at each site studied in the inventory. However, in the absence of bulk densities measured at the site-scale, we use the ISRIC data here solely as a means by which to demonstrate the sensitivity of soil formation rates to bulk density.

For this sensitivity analysis, we employed the CoSOILcal model (Rodés and Evans, 2019; see Appendix 3.2) first applied in Evans *et al.* (2019). The main objective of the CoSOILcal model is to calculate a 'best fit' bedrock lowering rate and its associated uncertainty at a site with known latitude, longitude, elevation, and shielding using measured concentrations of *in-situ* cosmogenic radionuclides (and their uncertainties) at or below the bedrock-soil interface of known depth, taking into account the overlying soil bulk density (Eq. 2).

First, an array of modelled bulk densities are generated and logarithmically distributed between 1 cm and 100 m, including those which are measured 'in the field' (z,x). Densities shallower and deeper than those measured are extrapolated using the shallowest and deepest measurement, respectively. The remaining densities to be calculated are those that lie in between each measured density; these are linearly interpolated from the nearest neighbours. Second, an array of erosion rates (ϵ) are generated and logarithmically distributed between 1 cm y^{-1} and 100 m My^{-1} .

Next, the surface production rates (P) of the radionuclide are calculated, based on the inputted latitude, longitude, and elevation data, as well as the apparent attenuation lengths of fast ($\Lambda_{\mu f}$) and stopping muons ($\Lambda_{\mu -}$) under the soil surface. The model then uses these surface production rate and attenuation data, as well as the generated bulk density profile (z,x) and the array of erosion rates (ϵ), to calculate the concentrations of the cosmogenic isotope at several depths (z_s) down the soil profile for a given landscape age. The landscape age here refers to the known age of the landscape and is inputted by the user. Time (t) is discretized in an array of 100 values logarithmically distributed between 100 years and the landscape age. For each of these 100 time steps, the model calculates an effective depth (x) by an interpolation of $z_s + \epsilon \cdot t$ down the profile. The concentration of the cosmogenic isotope that accumulates during each time step is then calculated using the following equation:

$$N = \sum_{i=sp,\mu f,\mu -} \frac{P_i(\theta) \cdot e^{-\frac{x}{\Lambda_i}}}{\lambda + \frac{\epsilon \rho}{\Lambda_i}} \left(1 - e^{-t \left(\lambda + \frac{\epsilon \rho}{\Lambda_i}\right)}\right) \quad (2)$$

where N is the cosmogenic isotope concentration accumulated during Δt time step at the effective depth x ; ε is the bedrock weathering rate, P are the annual production rates of the radionuclide by spallation, fast muons and stopping muons (sp , μ_f and μ_s) at a surface with slope Θ ; λ is the decay constant of the radionuclide; Λ are the mean attenuation lengths of the cosmic radiations and ρ is the density of overburden material for the time frame $t - \Delta t$ to t .

All of the modelled concentrations for the 100 time steps are then summed:

$$C = \sum_{t=0}^T N \cdot e^{-\lambda \cdot t} \quad (3)$$

where T is the landscape age.

Since isotope concentrations are measured using Accelerator Mass Spectrometry, bedrock weathering rates (ε) can be found by the simple interpolation of N . 'Best fit' bedrock weathering rates can be computed by first calculating the deviation(s) of these modelled isotope concentrations (C) from those which were measured using Accelerator Mass Spectroscopy:

$$s = \sum \frac{C-M}{\sigma_M} \quad (4)$$

where C is the modelled isotope concentration, M is the measured isotope concentration, and σ_M is the uncertainty of the measured concentrations.

Chi-square values are then computed as the sum of the squared deviations. Where chi-squared values are smaller than the minimum chi-squared value plus the number of samples, the modelled bedrock weathering rates are

considered to fit the data within a one-sigma confidence level. Further details about the model can be found in Rodés and Evans (2019; see Appendix 3.2).

This model was run for each entry within the soil formation rate inventory ($n = 163$). Soil formation rates from both the original inventory and those re-calculated using the CoSOILcal model were not normally distributed (the Anderson Darling Test statistics were -5.1 and -12.2, respectively; $p > 0.05$ for both tests), so the Mann Whitney U Test (a non-parametric statistical test for difference) was run. All statistical analyses were completed at 95% significance on a standard Excel workbook.

3.3 Results

Before the CoSOILcal model was applied, rates of soil formation as previously published spanned five orders of magnitude, ranging from 6×10^{-5} to 6×10^{-1} mm y^{-1} with a median of 0.03 mm y^{-1} . Climatologically, the fastest rates ($0.01 - 0.59 \text{ mm y}^{-1}$; median = 0.07 mm y^{-1}) were associated with Warm Summer Mediterranean (Csb) climates ($n = 80$) whilst the slowest rates ($0 - 0.01 \text{ mm y}^{-1}$; median = 0.001 mm y^{-1}) were found for Arid Cold (Bwk) climates ($n = 25$).

With regards to the effects of lithology, the fastest rates ($0 - 0.59 \text{ mm y}^{-1}$; median = 0.05 mm y^{-1}) were associated with metamorphic lithologies such as metasediments and gneiss ($n = 70$). These contrast with the slowest rates ($0.01 - 0.06 \text{ mm y}^{-1}$; median = 0.03 mm y^{-1}) measured from soils developing on igneous lithologies, such as granites and granodiorites ($n = 49$).

Employing the CoSOILcal model, the median rate of soil formation for the total inventory increased by 16% to 0.034 mm y^{-1} (range: $0.001 - 0.47 \text{ mm y}^{-1}$) (Figure 3.1). However, this was not found to be statistically significant ($p >$

0.05). Moreover, 68% of the inventory reported instances where soil formation rates decreased after the adoption of the CoSOILcal model. Within this subset, the mean reduction in soil formation rates was 0.02 mm y^{-1} (range: $0 - 0.21 \text{ mm y}^{-1}$). In just under a third of instances, soil formation rates increased after applying CoSOILcal, with the mean increase for this subset being 0.03 mm y^{-1} (range: $0.001 - 0.22 \text{ mm y}^{-1}$). With respect to the effect of climate, the fastest rates were still associated with Warm Summer Mediterranean (Csb) contexts and, although the median had decreased by 0.02 mm y^{-1} in comparison to the original data, this was not found to be statistically significant ($p > 0.05$). On the contrary, the CoSOILcal output showed that the slowest rates were not associated with Arid Cold (Bwk) conditions, as was the case previously, but with Humid Subtropical (Cfa) climates ($n = 26$) (Figure 3.2; top panel). The median soil formation rate for the Humid Subtropical subset was 0.02 mm y^{-1} , representing a decrease of 0.006 mm y^{-1} in comparison to the original data, which was not statistically significant ($p > 0.05$). For Arid Cold climates, the CoSOILcal output reported an increase of 0.04 mm y^{-1} in the median soil formation rate, which was statistically significant ($p < 0.05$).

The CoSOILcal output had less of an impact on the lithological influence on soil formation (Figure 3.2; bottom panel). The fastest rates were again associated with metamorphic lithologies. For this subset, the median soil formation rate had increased by 0.01 mm y^{-1} but this was not found to be significant ($p > 0.05$). Likewise, the slowest rates were associated with igneous lithologies. For this subset, the CoSOILcal output reported a small decrease of 0.002 mm y^{-1} in the median soil formation rate, which again was not found to be significant ($p > 0.05$).

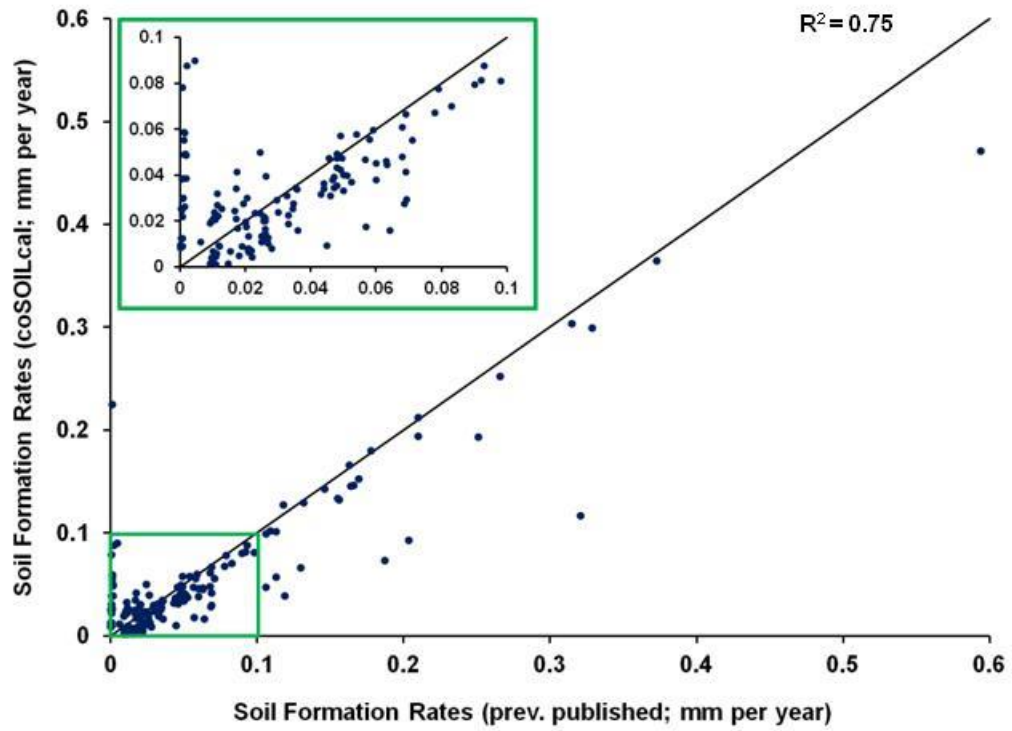


Figure 3.1: Soil formation rates from the global inventory previously published (x axis) and those calculated using the CoSOILcal model (y axis). The diagonal line represents $y = x$. The inset shows a zoomed projection of rates between 0 and 0.1 mm y^{-1} . Full dataset can be found in Appendix 3.3.

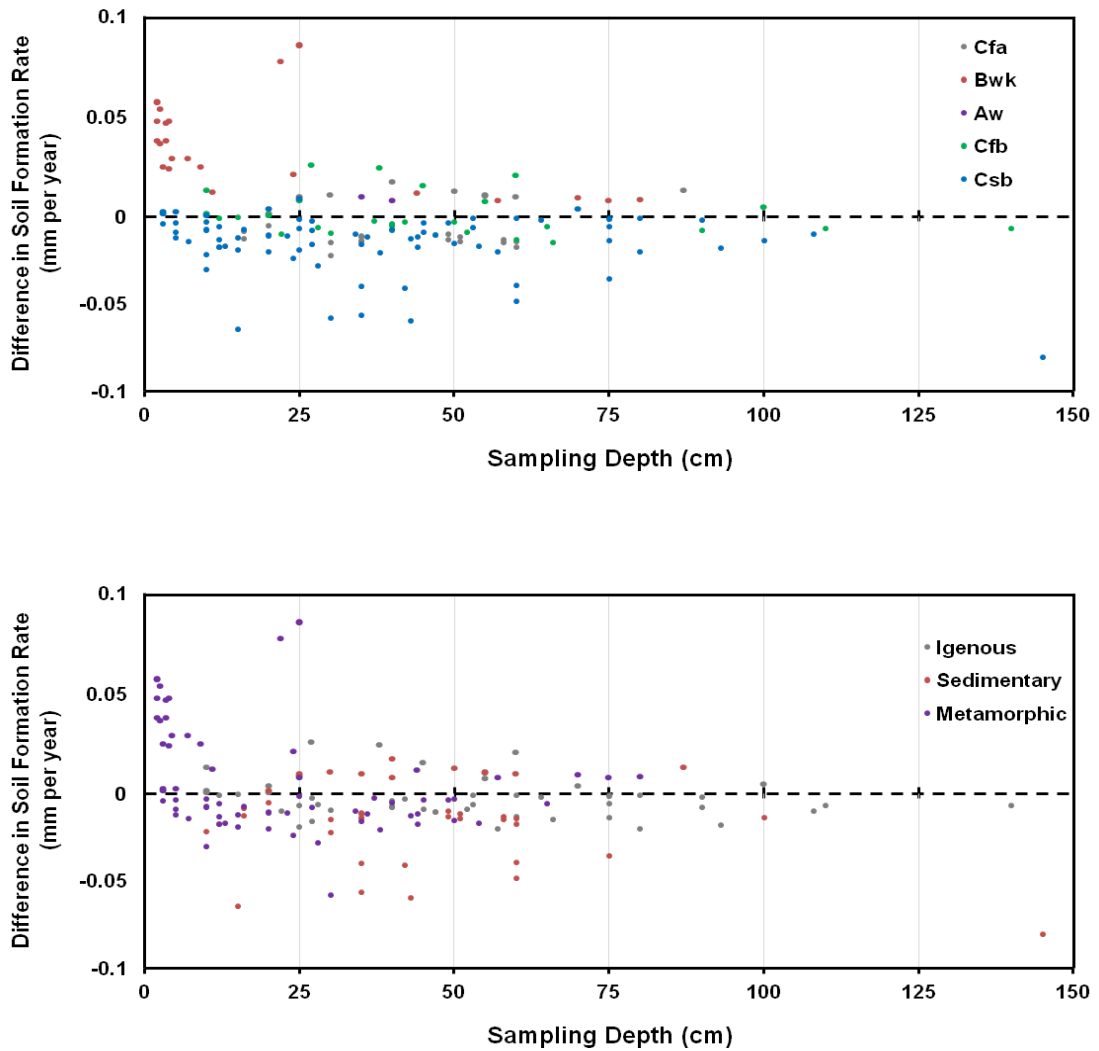


Figure 3.2: Difference in the soil formation rate when the CoSOILcal was employed in comparison to the original dataset ($n = 163$) for different climatic regions (*top panel*) and lithologies (*bottom panel*). Full dataset can be found in Appendix 3.3.

3.4 Discussion

The lack of a significant difference between soil formation rates prior to the application of CoSOILcal and those after the model was run may be explained by soil thickness. Moreover, the basis of the CoSOILcal model is that more of the heterogeneity in the density of the soil overlying the bedrock is accounted for. It is therefore reasonable to hypothesise that there is a threshold soil thickness under which the employment of these density data do not bring about a significant difference to soil formation rates. This was tested using the global inventory collated for this chapter. It was found that the CoSOILcal model brought about a statistically significant difference in soil formation rates for soils > 0.25 m ($p < 0.05$). For those soils within the inventory > 0.25 m ($n = 95$), the median soil formation rate derived using the CoSOILcal model was 1.2 times slower than the median of the rates previously published.

Furthermore, as soil thickness increased, the difference between the CoSOILcal median and that of the original inventory also increased. For instance, for soils > 0.4 m ($n = 64$) and > 0.5 m ($n = 46$) in thickness, the medians calculated using CoSOILcal were 1.3 and 1.7 times slower than those previously published, respectively.

Given that over half of the soil formation rates in this study's inventory are attributed to soils which are > 0.25 m ($n = 95$), of which 48% of these are > 0.5 m ($n = 46$), it calls into question the accuracy of these data. Moreover, it suggests that for these deeper soils, cosmogenically-derived soil formation rates may be slower than we have previously estimated. This may have wider implications on some of the land management decisions that have been based around these rates. For example, soil formation rates have been

previously used to derive rates of soil loss tolerance. Although there are multiple methods of calculating soil loss tolerance values, one of those that has been popularly used is based on the premise that rates of soil erosion should be curtailed to those of soil formation (Di Stefano and Ferro, 2016). A review of the soil formation rates used hitherto to calculate soil loss tolerance values is beyond the scope of this study. However, our findings suggest that if the soil formation rates used stem from studies where the soil depth exceeded 0.25 m, the soil loss tolerance values may have been over estimated.

To address the potential inaccuracies of the existing soil formation rate data, the CoSOILcal model can be applied *post hoc* so that the measurement of radionuclide concentrations does not have to be repeated. However, this would require bulk density values being measured from the positions where sampling for cosmogenic radionuclide analysis took place. To ensure that these re-calculated rates are as accurate as possible, we argue that the approach taken here (that is, the use of the ISRIC 250 m raster for soil bulk density) should not be used to make these corrections. The use of the ISRIC data here was solely to demonstrate the sensitivity of soil formation rates to bulk density. Nevertheless, following the preliminary analyses presented here, a global effort is now required to revisit our network of soil formation studies, and recalculate rates using soil bulk density data measured at the site-scale.

Furthermore, we argue that future attempts to derive soil formation rates using cosmogenic radionuclide analysis should encompass the measurement of bulk density down the soil profile and the use of these data in the CoSOILcal model when calculating bedrock lowering rates. Accurately quantifying soil formation rates is essential given that these are often used to guide policy

decisions on soil conservation and erosion mitigation (Montgomery, 2007; Verheijen *et al.*, 2009).

Although we have focused this work on the implications of bulk density on soil formation rates, it is also important to acknowledge that these findings are equally impactful beyond soil science. Cosmogenic radionuclide analysis has been used to derive rates of bedrock weathering for a range of geomorphological discourses and Earth System models (Cockburn and Summerfield, 2004). These include calculating the long-term rates of landscape evolution (Heimsath *et al.*, 1997) and quantifying the mobilisation of bedrock-derived petrogenic carbon (Hemingway *et al.*, 2018). The bulk density profiles of the unconsolidated material overlying the bedrock in these studies will have a similar effect on attenuating cosmic rays and should be accounted for. As a result, we argue that both our findings and the CoSOILcal model represent a significant contribution to multiple communities across Earth Sciences.

3.5 Conclusions

We have demonstrated that applying higher resolution estimates of soil bulk density when using cosmogenic radionuclide analysis to calculate rates of soil formation is essential. Applying the CoSOILcal model to a global inventory of previously published analyses, we found that soil formation rates, modelled from measured concentrations of Beryllium-10 in the bedrock, were significantly different when high resolution bulk density data for soils > 0.25 m in thickness were applied. Furthermore, the impact of soil bulk density on cosmogenically derived rates increases with soil thickness. These findings

highlight important implications for the community using cosmogenic radionuclide analysis both within and beyond soil science. Not only does our existing soil formation rate inventory require re-visiting, future work that uses cosmogenic radionuclide analysis to derive soil formation rates should account for the bulk densities down the soil profile, and employ the CoSOILcal model to calculate the rates of bedrock lowering. This is especially important given that soil formation rates have been, and continue to be, employed when constructing land management policies and decisions.

Further papers arising from the work presented in this chapter:

Rodés, A. and Evans, D. L. (2019) 'Cosmogenic soil production rate calculator', *MethodsX*, 7, pp. 1-5.

This can be found in Appendix 3.2.

Chapter 4: Soil lifespans and how they can be extended by land management change

D. L. Evans, J. N. Quinton, J.A.C. Davies, J. Zhao and G. Govers

This chapter is intended for publication in *Environmental Research Letters*.

Abstract

Human-induced soil erosion is a serious threat to global sustainability, endangering global food security, driving land use change and biodiversity loss, and degrading other vital ecosystem services. We amassed a global inventory of soil erosion rates consisting of 10,030 plot years of data from 255 sites under conventional agriculture and soil conservation management. Utilising existing soil formation data to estimate soil sustainability expressed as a lifespan, here defined as the time taken for a topsoil of 30 cm to be eroded, we show that over a quarter of conventionally managed soils in the dataset exhibit lifespans of <200 years, with 16% <100 years. Conservation measures substantially extend lifespan estimates, and in many cases promote soil thickening, with 39% of soils under conservation measures exhibiting lifespans exceeding 10,000 years. However, the efficacy of conservation measures is influenced by site- and region-specific variables such as climate, slope, and soil texture. Finally, we show that short soil lifespans of <100 years are widespread globally, including in some of the wealthiest nations. These findings highlight the pervasiveness, magnitude, and in some cases the immediacy of the threat posed by soil erosion to near-term soil sustainability. Yet, this work also demonstrates that we have a toolbox of conservation methods that have potential to ameliorate this issue, and their implementation

can help ensure that the world's soils continue to provide for us for generations to come.

4.1 Introduction

Soils have underpinned the health and longevity of every society. They are a critical global resource, providing the basis of food production, a store and filter for our water resources, the largest organic carbon store, and a platform for development (Blum, 2005). Pressures on the soil resource grow as food demands rise and land degradation increases. To date, 36% of the world's cultivable land has been farmed (FAO, 2015) and in many areas of the world conventional plough-based agriculture is accelerating local soil degradation (Montgomery, 2007). The United Nations' Food and Agriculture Organisation (FAO) estimates that 66% of the world's soils suffer from some form of degradation (Bot *et al.*, 2000), with soil erosion estimated at between 25 and 40 Pg y⁻¹ globally (Quinton *et al.*, 2010).

Rates of human-induced soil erosion are estimated to outpace soil formation rates by more than an order of magnitude (Montgomery, 2007). The consequential trajectory of soil thinning is one that, left uninterrupted, leads to the removal of the soil cover and the exposure of the underlying parent material. Given that the thickness of the pedosphere is a first-order control on soil functioning, with thicker soils having a greater capacity for water, carbon, and nutrient storage (Power *et al.*, 1980), the continued thinning of near non-renewable soil profiles, and the associated consequences on their productivity and health, is one of the most significant threats to soil sustainability (FAO, 2015; UNCCD, 2017). Understanding the timeline for soil ecosystem services

to be severely degraded by complete loss of topsoil is of considerable importance for policy makers, land managers, and society as a whole.

Yet, we have not quantified the longevity of our remaining soil resource. Media reports (e.g. Arsenault, 2014; Wong, 2019) have repeatedly stated that there are as little as 60 years of topsoil left, but there appears to be no scientific basis for these claims. Here, we provide the first scientifically robust, globally relevant estimate of soil lifespans and the degree to which changes in land use or management can extend them. We define a first-order upper physical limit on the productive lifespan of soils as the time it would take for the uppermost 0.3 m of soil to erode, assuming current rates of soil erosion and soil formation remain constant. We then employ this definition with a global dataset (10,030 plot years of annual water erosion rates, derived from 1,103 erosion plot-based records from 240 studies, that comprise 255 unique locations across 38 countries; Fig. 4.1) to quantify typical soil productive lifespans and examine the extent to which land use change and management practices can extend the timescales over which soils remain productive. This is a critical step in motivating and informing land management decisions that secure and sustain food, water, and climate services from soils.



Figure 4.1: Number and spatial distribution of plot years for the 255 unique locations in this study. Full dataset can be found in Appendix 4.1.

4.2 Materials and methods

4.2.1 Data collation

A compilation of 4,285 plot-based gross erosion rates representing 10,030 plot years, were amassed from 240 studies, comprising 255 unique locations across 38 countries (Fig. 4.1; sources are listed in Appendix 4.1). These data were initially obtained from a Web of Science search, using the search term “Soil Erosion”. Compiled studies were then scanned, with modelling-based studies and those that did not measure erosion rates empirically being discarded. In addition, studies which reported singular erosion events or those failing to report a year’s worth of erosion data (or a mean annual erosion rate) were discarded. To avoid biasing the analysis towards studies with long timeseries or many replicates, we averaged plot replicates and multi-year studies such that all data points represent one erosion rate for each treatment at a single location. Throughout this chapter, we use n to denote the number of these gross erosion rates, and PY to denote the number of plot years.

The data were assigned into three categories with respect to land management: bare, non-bare conventional agriculture, and conservation-based agriculture. The bare soils dataset was from soils that are kept free of vegetation on experimental plots ($n = 62$; $PY = 470$). These are often used to gauge erosion in a worst-case scenario. Whilst instances of constantly bare soil are only likely to occur periodically (e.g. prior to crop emergence), the use of bare soil data provides a worst-case baseline against which conventional agriculture and soil conservation practices can be assessed. The non-bare conventional agriculture dataset includes observations from plots undergoing non-conservation agricultural practices including downslope cultivation, non-

terraced cropland, and conventional tillage ($n = 320$; $PY = 4,816$). The conservation-based agriculture dataset comprises an array of plots that have been subject to soil conservation techniques, such as land-use change and modifications to agricultural practices ($n = 721$; $PY = 4,744$).

Gross erosion rates in the study's native units were compiled along with details of the respective management or soil conservation practice. Additional information about the study site was noted, including: soil type (FAO), textural data, mean annual precipitation, slope, and location co-ordinates. Bulk density was recorded if such information was provided; otherwise, the lower and upper values from bulk density ranges were calculated utilising accepted standards for each soil texture (US Department of Agriculture, 2018).

Cultivation notes, including ploughing depth, mulching technique, and crop species were recorded wherever applicable. The dataset includes soils from 14 of the 26 soil orders as recognized by the World Reference Base. All soil textures apart from 'Silt' and 'Sandy Clay' soils are represented within this inventory, with the modal texture being 'Silt Loam' ($n = 182$; $PY = 1,865$); a comprehensive breakdown of textural data can be found in Appendix 4.1.

4.2.2 Lifespan model

To permit a valid comparison between the rates of gross erosion and those of soil formation, all erosion data were converted from their native units to mm y^{-1} . This involved a two-step approach whereby data in native units were first converted into $\text{t ha}^{-1} \text{y}^{-1}$ and then, with the bulk density estimate, into mm y^{-1} , following previous approaches (Montgomery, 2007). Bulk densities were either taken directly from original papers or, in the case of these data being absent,

a lower and upper bulk density were estimated based on accepted standards (US Department of Agriculture, 2018). A lower and an upper gross erosion rate were thus calculated.

A previously compiled global dataset ($n = 264$) of soil formation rates were used in this study (Evans *et al.*, 2019; see Appendix 2.1). This dataset comprises ^{10}Be -derived rates of soil formation measured at ten unique locations across Australia, USA, Chile, and the UK, representing five different climates (according to the Köppen classification system) and all three major rock types (igneous, sedimentary, and metamorphic) (Heimsath, 2006; Heimsath *et al.*, 1997; 1999; 2000; 2001a; 2001b; 2005; 2012; Wilkinson *et al.*, 2005; Dixon *et al.*, 2009; Owen *et al.*, 2011; Riggins *et al.*, 2011; Evans *et al.*, 2019). The mean soil formation rate was $0.053 \pm 0.005 \text{ mm y}^{-1}$. The 25th and 75th percentiles of this dataset (0.011 and 0.059 mm y^{-1} , respectively) were employed into the lifespan model (Appendix 4.2).

Where gross erosion rates exceed those of soil formation, soil profiles thin and over time, assuming these rates remain constant, the soil profile will eventually erode beyond a critical depth required for the delivery of ecosystem services. The length of time until such a threshold thickness is crossed is referred to as the soil lifespan. Various iterations of the soil lifespan model exist within the literature (Stocking and Pain, 1983; Elwell and Stocking, 1984; Sparovek and Schnug, 2001; Montgomery, 2007; Medeiros *et al.*, 2016). In principle, the three inputs of these lifespan models consistently include: gross annual soil formation rate, gross annual soil erosion rate, and soil thickness or soil depth. Often gross formation and gross erosion rates are used to produce a net annual erosion or net annual loss rate (E).

Soil thickness invariably refers to the whole solum but has been truncated in previous models to calculate lifespans at the horizon scale, rather than for the whole profile. In this study, we employed a truncated soil thickness (D) of 0.3 m and used this consistently throughout. We argue that the surface horizons of the soil are critical for ecosystem service delivery as they are enriched with nutrients and organic matter, and critical for plant growth. In line with the FAO Harmonised World Soil Database, the World Reference Base Soil Classification and by the IPCC (IPCC, 2006; Nachtergaele *et al.*, 2008; FAO, 2014) we set the critical functional topsoil depth as 0.3 m. We chose a single topsoil depth as few of the plots where the erosion rates were measured had detailed soil descriptions. Global spatially explicit estimates of soil depth exist, such as the International Soil Reference Information Centre (ISRIC) Global Soil Information System 'SoilGrids', however, the representativeness of these data products for the individual sites is unknown (Hengl *et al.*, 2017; Shangguan *et al.*, 2017).

Lifespans (L) were calculated for bare, non-bare conventional, and conservation-based land use regimes using Eq. 1 (Appendix 4.2):

$$L = \frac{D}{E-F} \quad (1)$$

where D is depth (mm) (set at 3000 mm); E is the gross annual soil erosion rate (mm y^{-1}), and F is the gross annual soil formation rate (mm y^{-1}).

For each form of land use, calculated lifespans were pooled, and an Anderson Darling test for normality was conducted. Each sub-dataset was found to be non-parametric so the median was employed as a measure of central tendency, rather than the mean. To demonstrate the scatter of the lifespan

data for each category, both the interquartile range and the 5th and 95th percentiles were calculated.

Where gross erosion rates fall below those of soil formation, the lifespan calculated in the way expressed thus far becomes defunct. As such, the soil profile has crossed a lifespan threshold, from being a once-thinning soil to a now-thickening soil. In these instances, the net annual soil gain was calculated using the gross soil erosion and formation rates.

4.3 Baseline lifespans for bare and conventional agricultural soils

Here we consider soils that are devoid of vegetation (bare) and under conventional cropping (e.g.: inversion tillage, seedbed preparation followed by cereal or vegetable cropping), representing the worst-case and business-as-usual scenarios, respectively. The cumulative distribution of the estimated soil lifespans is illustrated in Figure 4.2. For plots kept bare, 34% of the dataset reported lifespans of <100 years ($n = 60$; $PY = 447$), and the median lifespan was 333 years. For bare thickening soils ($n = 2$; $PY = 23$), the mean annual estimated soil gain was $0.03 \pm 0.003 \text{ mm y}^{-1}$. For soils from non-bare, conventionally managed plots, 16% of the dataset ($n = 298$; $PY = 4,737$) reported lifespans of <100 years, with a median of 491 years for thinning soils, and the mean annual estimated soil gain was $0.03 \pm 0.001 \text{ mm y}^{-1}$ for thickening soils ($n = 22$; $PY = 79$).

Our analysis forms the first quantitative estimate of the baseline lifespans of soils. It demonstrates the magnitude of the threat that soil thinning can place on relatively near-term soil sustainability, and identifies the urgent need to ameliorate soil erosion. Whilst these conclusions are alarming, it should be

noted that these baseline lifespans were spread across five orders of magnitude, and were heavily dependent on the management in operation and the local environmental conditions at the site-scale. This suggests that the popular quote that there are 60 years of global topsoil left (e.g. Arsenault, 2014; Wong, 2019), and particularly the citation of a single figure, does not effectively acknowledge the range of baseline lifespans that exist under a number of different land management practices.

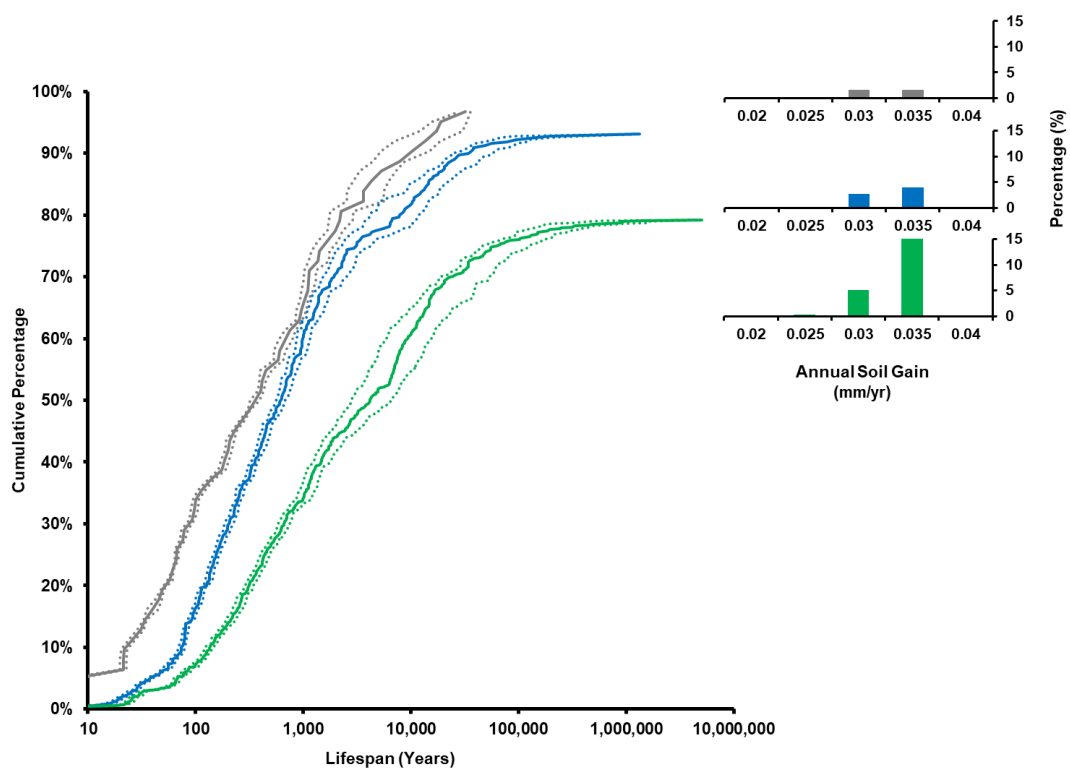


Figure 4.2: Cumulative distribution of soil lifespans ($n = 929$; $PY = 9,168$ for thinning and $n = 174$; $PY = 862$ for thickening soils) and annual soil gain for bare soils (grey), non-bare conventionally managed soils (blue), and conservation management (green). Percentages are normalized based on the total sample (finite and indefinite lifespans). Bold lines on the cumulative distribution chart represent median lifespans; dotted lines represent upper and lower bounds of lifespans when uncertainties in soil formation and soil erosion data are taken into account (see *Materials and Methods*). Full dataset can be found in Appendix 4.2.

4.4 Extending soil lifespans by changing land use and agricultural practice

The lifespans of soils under conservation management, including changes to both land use and agricultural practice, were estimated using measured erosion rates ($n = 721$; $PY = 4,744$) drawn from 201 plot-based studies. Gross soil erosion rates were lower than soil formation in 21% of cases ($n = 150$; $PY = 760$), leading to a net annual soil gain (Figure 4.2). Compared with the bare and conventionally managed plots, the conservation management plots were more than twice as likely to be thickening rather than thinning.

Pooling all data for plots managed with conservation practices, 7% of lifespans were <100 years. This represents a reduction of more than half in the proportion of lifespans <100 years compared with the conventionally managed plots in the dataset (Figure 4.2). The distribution of lifespans for the plots under conservation management was shifted towards longer lifespans when compared to conventionally managed soils. For conservation managed soils, 48% of the estimated lifespans exceeded 5,000 years compared to 23% for conventional agriculture, and 39% exceeded 10,000 years compared to 18% for conventionally managed soils.

4.4.1 Land use change

Afforesting both bare soil and cropland soil was one of the most effective land use changes for extending the soil lifespan (Figure 4.3). The shortest lifespan in the afforestation dataset was 420 years, compared to 16 years for cropland soils. In 50% of cases, gross erosion rates in forests fell below those of soil formation, promoting soil thickening ($0.032 \pm 0.001 \text{ mm y}^{-1}$). This proportion of

thickening soils was fifteen times that for bare plots, and six times that for cropland plots.

These findings concur with similar work that has concluded that croplands erode, on average, more than an order of magnitude faster than forest soils (Zhao *et al.*, 2016). One of the principal ways that forests ameliorate soil erosion is to intercept rainfall and reduce the volume of concentrated flow on the forest floor (Jirasuktaveekul *et al.*, 1998; Reubens *et al.*, 2007; Shinohara *et al.*, 2019). As forests mature, and their above-ground biomass increases, the potential for this interception and consequent erosion reduction increases. However, the management of the understorey to promote ground cover is important since where it has been removed the size and kinetic energy of raindrops can result in soil detachment (Shinohara *et al.*, 2019).

Similarly effective in lengthening soil lifespans was the shift from bare soil and cropland to grassland. For plots with bare soils converted to grassland, we found that 2% of lifespans were <100 years, a 17-fold reduction in the proportion <100 year lifespans found for plots kept bare. Converting cropland to grassland led to a seven-fold reduction in lifespans of <100 years. In 37% of cases, gross soil erosion rates fell below those of soil formation, promoting soil thickening ($0.032 \pm 0.001 \text{ mm y}^{-1}$). This represents an 11-fold increase in the occurrence of thickening soils compared to bare soils, and a four-fold increase compared to cropland soils.

The effectiveness of grassland systems for ameliorating soil erosion is widely established. Many authors have cited dense above-ground biomass and fine root architecture as two particular traits that can contribute to dissipating the

energy of drop impact and overland flow (De Baets *et al.*, 2006; Reubens *et al.*, 2007). It has been suggested that grasslands subject to grazing pressures may be less able to reduce erosion, either because of stock-induced compaction, which reduces the soil's hydraulic conductivity, or the removal of above-ground biomass, which increases vulnerability to soil detachment and promotes overland flow generation (Evans *et al.*, 2017). To overcome grazing pressures, rangeland scientists have focused their restoration efforts on defining sustainable stocking rates, improving shepherding, resting pastures, and excluding grazing from the worst affected areas.

4.4.2 Changing agricultural practices

Conversion of cropland to forest and grassland may be effective in extending the soil lifespan but it requires a change in land use. Without reducing the area of land designated for agriculture, we found that cover cropping previously bare soils was an effective method of extending lifespans. No plot in the cover-crop dataset had lifespans of <100 years, in contrast with the 34% of bare plots and the 16% of non-bare, conventionally managed plots which did. In a quarter of cases, gross soil erosion rates fell below those of soil formation, promoting an estimated net annual soil gain of $0.031 \pm 0.001 \text{ mm y}^{-1}$. These results accord with previous work showing the importance of cover cropping in reducing erosion (Nyakatawa *et al.*, 2001; Verstraeten *et al.*, 2002; Gyssels *et al.*, 2005). Not only does the above-ground biomass act as a buffer against potential rainsplash detachment, but cover cropping is also likely to improve soil structure, increase infiltration rates, and slow overland flow, further reducing water erosion (Smith *et al.*, 1987).

Whilst cover cropping is one of the most effective agricultural practices for lengthening soil lifespans, a suite of additional practices both prior to and during the cropping season can extend these further. The shift towards conservation-based tillage practices has previously been found to reduce soil loss (Sharratt *et al.*, 2006). In our dataset the shift from conventional tillage to conservation tillage led to a two-fold reduction in the proportion of cases with critically short lifespans (<100 years). Similarly, we found the shift from conventional tillage to zero tillage also lengthened soil lifespans.

In terms of cultivation direction, we found that the shift from downslope to contour cultivation brought about an extension of the soil lifespan, with 7% of these having lifespans of <100 years compared to 37% for up-and-downslope cultivation. For 6% of the contour cultivation dataset, soil thickening led to an estimated net annual soil gain of $0.032 \pm 0.001 \text{ mm y}^{-1}$; a two-fold increase in the cases of soil thickening compared to soils cultivated downslope. On particularly steep gradients, contour cultivation may not be practical, and the most effective conservation-based management strategy may be terracing. For terraced soils, 2% of the dataset reported lifespans of <100 years, which compared to downslope cultivation represents a 23-fold reduction in critical lifespans. However, terraces can lead to a reduction in the crop production area (Herweg and Ludi, 1999), although some have argued that the risers are potentially cultivable (Sahoo *et al.*, 2015). The ultimate performance of terrace systems as a soil conservation strategy is fundamentally dependent on the maintenance of the terraces. A review of over 60 studies into terrace abandonment showed that even though terrace abandonment can give rise to an increase in scrub cover, it is often not expansive enough to protect soils

from extensive surface and sub-surface erosional processes, and ultimately terrace collapse (Arnáez *et al.*, 2015).

4.4.3 Decision making at the site-scale

The decision about which conservation practice is most likely to be more effective in sustaining soils at a given location is dependent on an array of social, economic and site-specific factors. For example, land use change to either forest or grassland may not be appropriate if agricultural activity is displaced to more erosive locations. The selection of specific agricultural practices is also likely to be partly determined by the social context, as well as the financial and resource capability of the land manager in question. Issues such as the duration of land tenancies and the existing policies, incentives, and advisory services provided at a regional and national level will influence the adoption of soil conservation approaches. Furthermore, the land use changes and agricultural practices presented in this chapter vary in their 'establishment time': the time for a selected conservation management regime to be set up, launched, and become effective. For soils with critical lifespans, and especially the 25 instances in our dataset where lifespans are shorter than 25 years, it could be argued that the most effective management decision is to adopt a strategy with a short establishment time. In this context, conversion to grass, cover cropping, and/or contour cultivation may be most appropriate, as the establishment time for these strategies is in the order of months to a year. By contrast, the planting of trees to convert cropland to forest may require less preparatory time, but there is a lag time for forests to mature. Previous studies have found that effective soil conservation in forests is only ensured when vegetation cover reaches a minimum coverage of 50%,

and the litter layer achieves a thickness of 0.8 cm (Wu *et al.*, 1994; Béliveau *et al.*, 2017). An immature forest is therefore unlikely to be as effective in extending soil lifespans as one where the canopy and litter are more established.

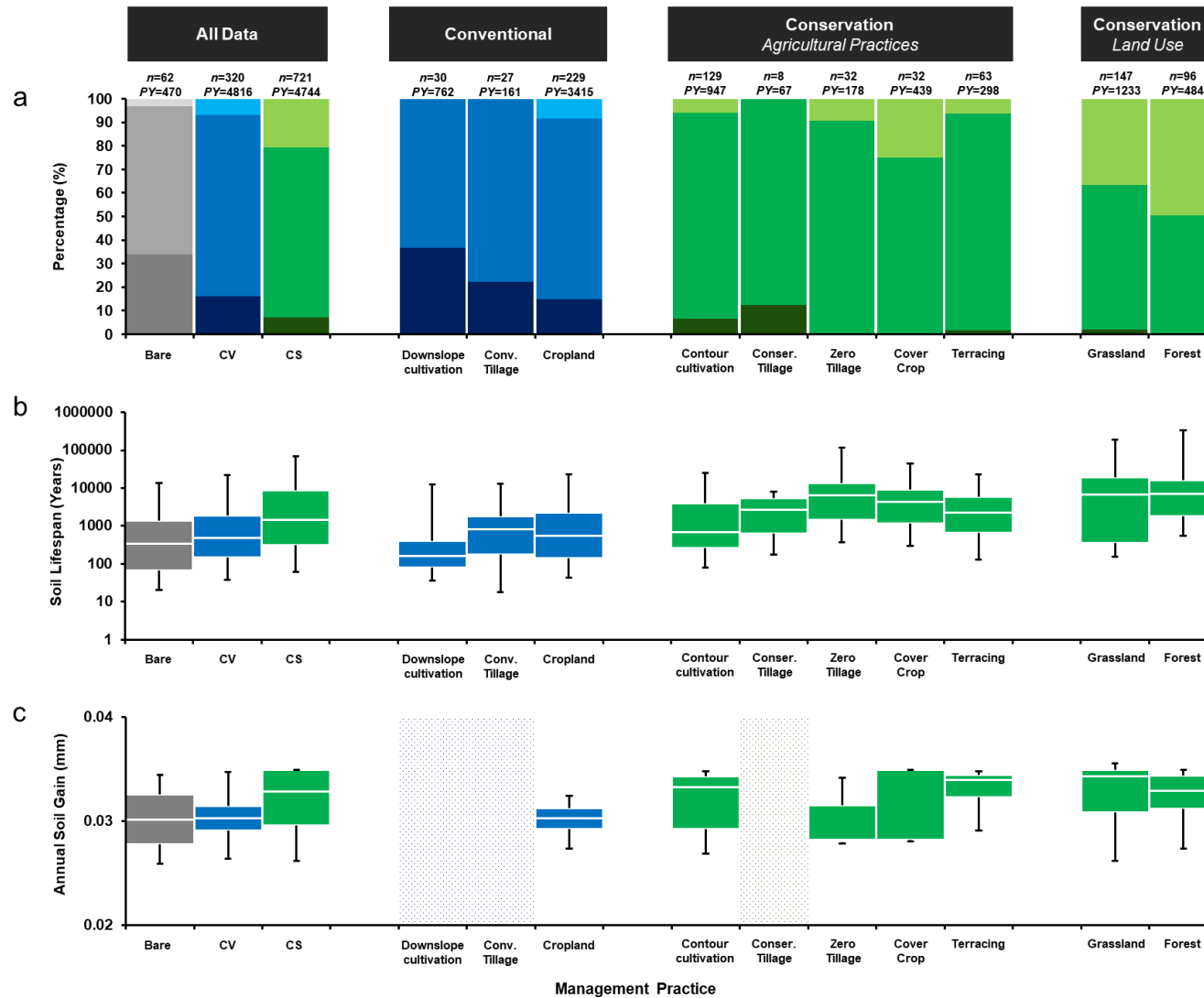


Figure 4.3: (a) Distribution of critical (<100 years; lowermost bars), finite (>100 years; middle bars), and infinite (thickening; uppermost bars) lifespans for bare, conventional, and conservation-based management ($n = 1,103$; $PY = 10,030$). (b) Soil lifespans for conventional (blue) and soil conservation (green) management practices ($n = 929$; $PY = 9,168$), excluding those soils that are thickening. (c) Net annual soil gain for conventional (blue) and conservation-based (green) management practices ($n = 174$; $PY = 862$). Dotted bars denote incidences where either annual soil gain did not occur or there were not enough data. Boxplots represent the interquartile range; error bars refer to the 5th and 95th percentiles, within each management shift category. A description of management practices can be found in Appendix 4.3. Full dataset can be found in Appendix 4.2.

4.5 Global and regional distribution of soil lifespans

The effects of soil conservation management, either through implementing shifts in land use or changes in agricultural practices, are also influenced by factors operating at local and regional scales. The 261 unique locations in this study were grouped into five regions: North America ($n = 217$; $PY = 2,487$); South America ($n = 201$; $PY = 3,221$); sub-Saharan Africa ($n = 105$; $PY = 1,219$), Europe and the Middle East ($n = 107$; $PY = 963$); and Asia and Australia ($n = 473$; $PY = 2,140$).

Pooling conventional and conservation-based data, sub-Saharan Africa, Asia and Australia and North America had the greatest proportions of data reporting thinning soils (95%, 88% and 83%, respectively), with North America having the greatest proportion of critical lifespans (18%) (Table 4.1). These contrast with South America where 73% of the dataset reported thinning soils, with 12% of lifespans being critical. Although 78% of the Europe and the Middle East dataset reported thinning soils, only 5% of these were critical.

Comparing conventionally managed soils with those under conservation management for each region, we found that the shift towards conservation practices nearly always reduced the proportion of cases with critical lifespans. The largest reduction was found in the sub-Saharan Africa region, where there was a 14-fold reduction in cases with lifespans of <100 years. We found that shifting from conventional to conservation management in this region led to an increase in the occurrence of thickening soils.

Our regional analysis indicates three important findings. First, whilst previous authors have identified hotspots of soil erosion, we show that every region has

soils that have critical lifespans. Many of the wealthiest countries, as defined by gross domestic product (World Bank, 2019), report some lifespans shorter than 100 years. Second, soil lifespans can be significantly extended even in regions prone to some of the shortest lifespans, such as sub-Saharan Africa. The soil conservation practices attributed to reducing gross soil erosion rates, and thereby extending lifespans in this region, included the conversion of cropland to grassland and forest (15% of the data), contouring (16%) and terracing (21%). The same practices in Asia and Australia had a similar effect of reducing the proportion of lifespans shorter than 100 years from 13% to 2%. The third main finding is that there are some conservation measures that are less effective in reducing gross erosion, emphasising the importance of additional region- and site-specific factors. Contour cultivation in Lacrosse, USA, implementing contour ridges in Tanzania, and practising conservation tillage in Hailun Heilongjiang, China are three examples where the implementation of conservation management did not enhance the soils' sustainability, with lifespans shorter than 100 years in all three cases.

Table 4.1 | Global distribution of finite, critical, and infinite lifespans for the five regions studied in this chapter.

	All Data		Finite Lifespans				Critical Lifespans			Infinite Lifespans			
	<i>n</i>	<i>PY</i>	<i>n</i>	<i>PY</i>	% of region	Median lifespan (years)	<i>n</i>	<i>PY</i>	% of region	<i>N</i>	<i>PY</i>	% of region	Mean soil gain (mm y ⁻¹)
North America	217	2,487	181	2,346	83	583	39	755	18	36	141	17	0.033
South America	201	3,221	147	3,019	73	7,101	24	134	12	54	203	27	0.031
sub-Saharan Africa	105	1,219	100	1,198	95	671	17	212	16	5	21	5	0.035
Europe and Middle East	107	963	83	689	78	6,270	5	24	5	24	274	22	0.032
Asia and Australia	473	2,140	418	1,917	88	1,397	40	162	9	55	223	11	0.031

^a Comprises bare, non-bare conventional, and conservation land use management.

^b Full data can be found in Appendix 4.2.

4.6 Site-specific variables that influence lifespans

Underpinning the variability in the efficacy of soil conservation management across different regions are local, site-specific variables including climatic, topographic and pedological factors. Our data suggest that precipitation has a substantial influence on governing soil lifespans (Figure 4.4). The data were grouped into four classes of mean annual precipitation (MAP, hereafter): 0 to 500 mm y^{-1} ($n = 70$; $PY = 400$); 501 to 1,000 mm y^{-1} ($n = 335$; $PY = 2,549$); 1,001 to 1,500 mm y^{-1} ($n = 255$; $PY = 3,576$); and 1,501 to 2,000 mm y^{-1} ($n = 110$; $PY = 708$). For conventionally managed soils subject to MAP between 0 and 500 mm y^{-1} , 92% of observations reported thinning soils whilst the remaining 8% reported soil thickening. This increased to 96% and 4%, respectively, for soils subject to MAP of between 500 and 1,000 mm y^{-1} . One explanation for this is that the erosion associated with those soils subject to MAP less than 500 mm y^{-1} is water-limited. As MAP increases to between 500 and 1,000 mm y^{-1} , the potential for erosion intensifies and, in consequence, the proportion of thinning soils also swells. However, soils subject to MAP greater than 1,500 mm y^{-1} reported a reduction in observations of thinning soils and a commensurate increase in the occurrence of soil thickening. For instance, comparing the 500 to 1,000 mm y^{-1} class with the 1,500 to 2,000 mm y^{-1} class, the proportion of instances of thinning soils decreased by 30% and there was a eight-fold increase in the proportion of cases of thickening soils. A similar pattern is observed for critical lifespans. Soils subject to MAP of between 500 and 1,000 mm y^{-1} reported the greatest proportion (17%) of critical lifespans whilst this proportion more than halved for the 1,500 to 2,000 mm y^{-1} class. The reduction in soil thinning for soils subject to MAP less than

1,000 mm y⁻¹ can potentially be explained by the fact that the increase in precipitation gives rise to increased biomass production, leading to the protection of the soil surface from rain drops, slowing of overland flow, and in some cases, the enhancement of infiltration (Nearing *et al.*, 2004).

For soils subject to conservation management, the patterns described above are similar, albeit less pronounced. Between the 0 to 500 mm y⁻¹ and 500 to 1,000 mm y⁻¹ classes, there was a 2% increase in the proportion of thinning soils. Although this proportion then decreased for conventionally managed soils subject to MAP greater than 1,000 mm y⁻¹, this was not observed for soils managed with conservation practices. Instead, the instances of soil thinning increased by a further 1% for soils subject to MAP of between 1,000 and 1,500 mm y⁻¹. However, between the 1,000 to 1,500 mm y⁻¹ and the 1,500 to 2,000 mm y⁻¹ classes, observations of soil thinning decreased by 2%. With regards to critical lifespans, there was a steady increase in the proportion of soils reporting critical lifespans for each successive MAP class, from 2% for the 0 to 500 mm y⁻¹ class, to 10% for the 1,500 to 2,000 mm y⁻¹ class. Whilst MAP may explain some of the variation in soil lifespans, it is also important to acknowledge that it is one of the many measures of precipitation that influence soil loss (Doetterl *et al.*, 2012; Ballabio *et al.*, 2017).

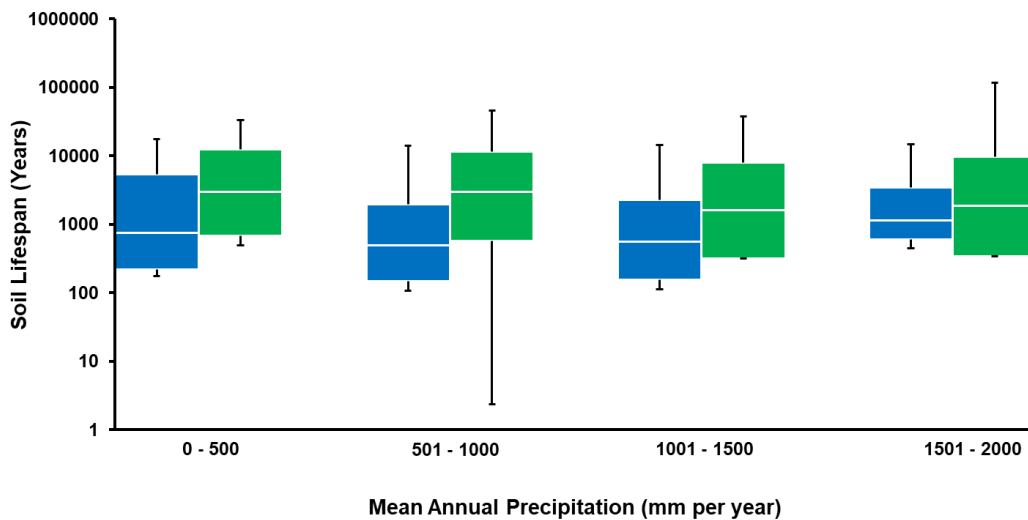


Figure 4.4: Soil lifespans for conventional (blue) and soil conservation (green) management practices under different mean annual precipitations. Boxplots represent the interquartile range of soil lifespans. Error bars refer to the 5th and 95th percentile soil lifespans.

The slope or gradient of a soil surface is another factor controlling soil loss, and driving the variability in the efficacy of soil conservation strategies (Figure 4.5). The data were grouped into three slope classes with a similar number of data points: 0 to 5% ($n = 264$; $PY = 4,099$); 6 to 10% ($n = 103$; $PY = 1,581$) and 11 to 20% ($n = 144$; $PY = 1,539$). For soils subject to conventional management, the proportion of instances of soil thinning was higher in the 6 to 10% class (100%) compared to the 0 to 5% class (92%). Between the 0 to 5% and 6 to 10% class, there is also a corresponding increase in the proportion of cases with critical lifespans from 4 to 43%, respectively. Counterintuitively, a reduction in the instances of soil thinning and the proportion of cases with critical lifespans was observed for slopes between 11 and 20%. Between the 6 to 10% and 11 to 20% slope classes, there was a 8% decrease in the instances of soil thinning, and a 14% reduction in the proportion of cases with critical lifespans. This could be explained by the fact that nearly two-thirds of the soils within the 11 to 20% class were in crop, compared to just over a third

for the 6 to 10% class. In this instance, the crops may have diminished the potential for soil erosion that would otherwise have been expected for a steep slope class. For soils subject to conservation management, the proportion of instances of soil thinning increased by 3% between the 0 to 5% and 6 to 10% slope classes. In contrast, the proportion of critical lifespans decreased between these two bins. Furthermore, the efficacy of conservation management increased as slope increased. Shifting from conventional to conservation management brought about a 20% increase in the proportion of cases with thickening soils on slopes of 0 to 5%, and a 26% increase for slopes of 6 to 10%.

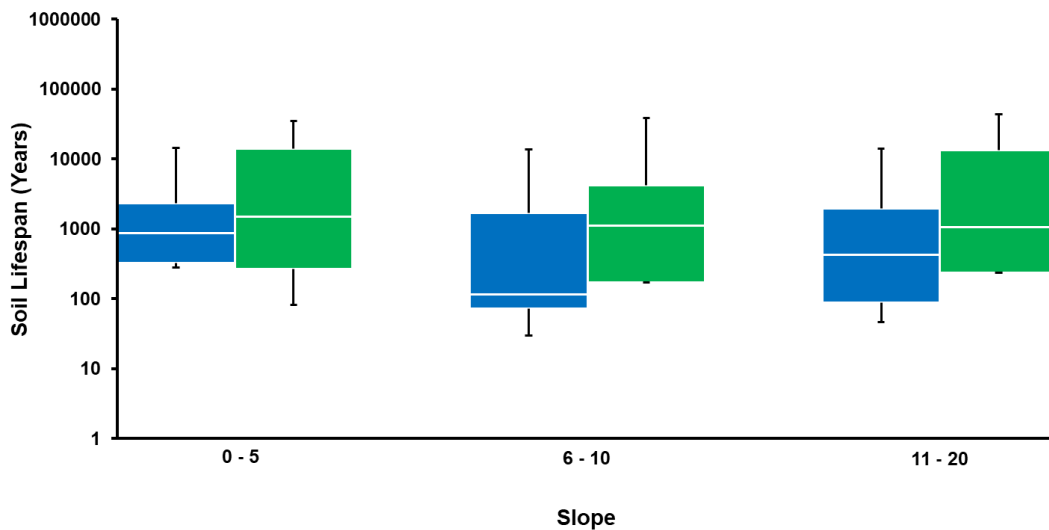


Figure 4.5: Soil lifespans for conventional (blue) and soil conservation (green) management practices under different slopes. Boxplots represent the interquartile range of soil lifespans. Error bars refer to the 5th and 95th percentile soil lifespans.

Soil texture forms a third driving variable that influences soil lifespans and the extent to which management strategies may extend them (Figure 4.6). This study's dataset of conventional- and conservation-based management comprised all soil textures apart from silt and sandy clay textured soils, with the modal texture being silty loam ($n = 182$; $PY = 1,865$). For all of the observed soil textures apart from silty clay and loamy sand, conservation-based practices reduced the proportion of the dataset reporting thinning soils, with the greatest reduction observed for silty clay loam soils. Furthermore, conservation management increased the proportion of thickening soils and reduced the proportion of critical lifespans. Compared to conventional management, conservation management was most effective at increasing the instances of soil thickening on silty loam soils (an 11-fold increase) followed by loam soils (a three-fold increase). With regards to reducing the proportion of critical lifespans, we found no instances of critical lifespans for silty clay and silty clay loam soils when subject to conventional management. Loamy sand soils reported the largest proportion of critical lifespans under conventional management, but also the greatest reduction of the proportion of critical lifespans when conservation-based practices were employed.

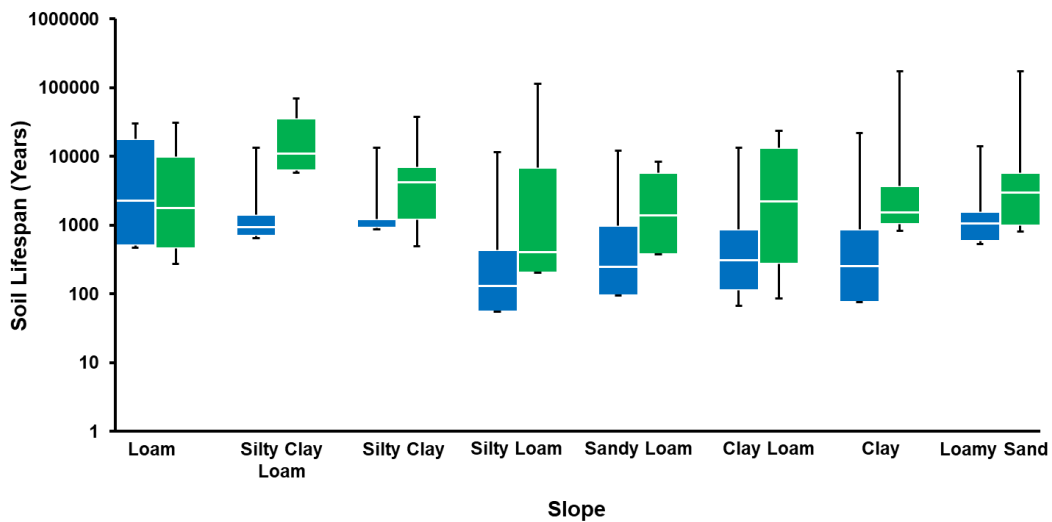


Figure 4.6: Soil lifespans for conventional (blue) and soil conservation (green) management practices under different soil textures. Boxplots represent the interquartile range of soil lifespans. Error bars refer to the 5th and 95th percentile soil lifespans.

4.7 Limitations and knowledge gaps

In setting out these first-order soil lifespans, and discussing the controlling variables, we acknowledge a range of assumptions. The lifespans calculated here are based on a single proxy (net erosion), which is just one form of degradation that threatens the sustainability of soils around the world. There are a range of retrogressive processes that can degrade soils in shorter time frames (Heimsath *et al.*, 2009). For example, soil compaction can bring about adverse effects on the physical, chemical and biological properties of soils, without a loss of soil thickness (Batey, 2009). However, the balance between soil formation and soil erosion provides a good first-order estimate of the lifespan: it is the maximum estimate of the lifespan assuming that if any soil is present, it is functioning. The soil formation and erosion rate (and, therefore, the net annual soil loss and gain) were assumed to remain constant over time. This does not account for the year-to-year fluctuations observed in long-term

soil erosion studies (Martínez-Casasnovas *et al.*, 2002), nor the potential increase in bedrock weathering rates as the overlying soil mantle progressively thins (Heimsath *et al.*, 1997). In addition, the bedrock-derived soil formation rates neither account for allochthonous additions (aeolian and alluvial deposits) nor the thickening of an organic layer on the mineral soil surface, observed as a product of some management practices, such as conservation tillage (Sharratt *et al.*, 2006). In addition, we selected a critical soil depth of 0.3 m, but in reality, depending on the soil and the environment, the critical soil depth threshold may be lower or higher than this. Furthermore, we do not account for any adaption of the subsoil: if surface erosion rates are sufficiently low, the underlying subsoil (if it exists) could be transformed, chemically and biologically, into topsoil (Bakker *et al.*, 2004). Such a transformation of subsoil into topsoil would constitute a form of soil formation which our calculation does not account for. In these instances, the lifespans calculated here would represent underestimates.

Assumptions were also made in the collation of input data used in the lifespan calculation. First, the lifespans presented here have been calculated from erosion rates measured at the plot scale, which are not wholly representative of the erosional processes observed at the landscape scale, such as gully erosion (Takken *et al.*, 1999; Cerdan *et al.*, 2010). Depending on how different plot-scale and landscape-scale erosional processes operate, the lifespans may be either overestimates or underestimates. Although the compiled data were processed through a series of quality checks often employed in similar inventory studies (Cerdan *et al.*, 2010), it should be acknowledged that the data collated here were derived from erosion plot experiments which can be

biased towards sites of high erodibility, and therefore it could be argued that the lifespans calculated here are also biased. To establish whether this bias is substantial requires a greater number of erosion investigations conducted on soils under a representative range of agricultural conditions. We also acknowledge that the erosion rates included in this analysis are solely those of water-based soil redistribution. Whilst the influence of tillage regime on water-based erosion rates has been included in our analysis, quantifying the redistribution of soil by tillage has not, although soil redistribution by tillage represents a significant mechanism for translocating soil in agricultural landscapes (St. Gerontidis *et al.*, 2001). Therefore, it is likely that estimates of lifespans are overestimated for soils on slope convexities where tillage reduces soil depth, and underestimated on slope concavities where tillage leads to soil accumulation (Van Oost, 2006).

Finally, one of the greatest limitations is the imbalance between the number of observations in the soil erosion dataset and those within the inventory of soil formation. There has been very little investment within Soil Science in the derivation of soil formation rates globally (Portenga and Bierman, 2011; Stockmann *et al.*, 2014). A Web of Science search shows that the percentage increase in publications for the search term “soil erosion and degradation” between 1950 and 2016 is more than two orders of magnitude compared to that for the search term “soil formation”. We therefore encourage a fresh movement of cross-community collaboration whereby critical zone scientists, geologists, and soil conservationists work together to expand the knowledge on the rates of the soil formation process.

4.8 Conclusions

In this chapter, we have presented the first broad quantitative estimates of the lifespans of soils and the degree to which these may be extended by land management change. By compiling globally distributed soil erosion and soil formation rate data and applying the soil lifespan concept, we can contribute the following conclusions.

First, an assessment of baseline (current) soil lifespans using soil loss rates measured from non-bare soils under conventional management systems suggest that, under a worst-case scenario, 93% are thinning with 16% having exceptionally short (0-100 years) lifespans. At these sites, soil erosion is a significant threat to the soil's capacity to grow food, support ecosystems, store and regulate water, cycle carbon and nutrients and thus the overall functioning of the soil system. It has been acknowledged that there are factors that govern the sustainability of soil resources, other than the net soil loss rate. However, given that the presence and thickness of soils are first order controls on soil functioning, the topsoil depth change calculations presented here are potentially representative of the maximum soil lifespans expected.

Second, we have shown that shifts both in land use and land management practices can meaningfully extend the soil lifespan and, in many cases, promote the onset of soil thickening. Only 7% of the conservation plot dataset had critical lifespans, with 48% of the estimated lifespans exceeding 5,000 years and 39% exceeding 10,000 years. The conversion of bare cropland to forest or grassland is most effective in achieving both of these outcomes, closely followed by cover cropping. However, given the need to meet the

growing demand for food, arguably cover cropping is the more attractive option for extending lifespans. A suite of additional strategies to extend soil lifespans and promote annual soil gain include shifts towards contour cultivation and terracing. In all of these extensions, the primary result is to lengthen the duration of time before soil profiles reach critical thickness, below which they cannot fulfil valuable ecosystem services. However, both the extension of soil lifespans and the promotion of soil thickening has secondary implications, namely to increase the potential for water, carbon, and nutrient storage, and thereby rendering conditions which could enhance yields.

Third, we have shown that there is a wide distribution of soil lifespans globally, encompassing five orders of magnitude, and partly reflective of an extensive variation in the underlying driving variables such as climate, slope, and soil texture which can influence the efficacy of soil management changes.

However, soils with human-scale lifespans shorter than 100 years are present in all of the observed regions, including many of the wealthiest nations. This clearly demonstrates that the thinning of soil is one of the most critical threats to soil sustainability globally, and that urgent action worldwide by policy makers, land managers and society is imperative to prevent the collapse of soil ecosystem service provision.

Acknowledgements:

We wish to thank all those who assisted us in our efforts to compile the dataset, particularly Khasijah Binti Muhamad, Calvin Rose, Bofu Yu, and Mark Nearing. The statistical advice of Professor Murray Lark and Dr. Victoria Janes-Bassett is also gratefully acknowledged.

Chapter 5: Arable soil formation and erosion: a hillslope-based cosmogenic-nuclide study in the United Kingdom

D. L. Evans, J. N. Quinton, A. M. Tye, Á. Rodés, J.A.C. Davies, S. M. Mudd and T. A. Quine

This chapter has been published in *SOIL* (Evans *et al.*, 2019).

Abstract

Arable soils are critical resources that support multiple ecosystem services. They are frequently threatened, however, by accelerated erosion. Subsequently, policy to ensure their long-term security is an urgent societal priority. Although their long-term security relies upon a balance between the rates of soil loss and formation, there have been few investigations of the formation rates of soils supporting arable agriculture. This chapter addresses this knowledge gap by presenting the first isotopically constrained soil formation rates for an arable (Nottinghamshire, UK) and coniferous woodland hillslope (Shropshire, UK). Rates ranged from 0.026 to 0.096 mm y⁻¹ across the two sites. These rates fell within the range of previously published rates for soils in temperate climates and on sandstone lithologies, but significantly differed from those measured in the only other UK-based study. We suggest this is due to the parent material at our sites being more susceptible to weathering. Furthermore, soil formation rates were found to be greatest for aeolian-derived sandstone when compared with fluvially derived lithology, raising questions about the extent to which the petrographic composition of the parent material governs rates of soil formation. On the hillslope currently supporting arable agriculture, we utilized cosmogenically derived rates of soil

formation and erosion in a first-order lifespan model and found, in a worst-case scenario, that the backslope A horizon could be eroded in 138 years, with bedrock exposure occurring in 212 years under the current management regime. These findings represent the first quantitative estimate of cultivated soil lifespans in the UK.

5.1 Introduction

Soil erosion is a significant threat to society (Pimentel *et al.*, 1995; UNCCD, 2017). Whilst uncultivated soils may develop steady-state thicknesses, where erosion and formation are in dynamic equilibrium (Phillips, 2010), human-induced erosion has led to soil thinning across many landscapes (Montgomery, 2007). Soil erosion, left unchecked, can ultimately lead to the removal of the soil cover and the exposure of the underlying parent material (Amundson *et al.*, 2015). The development of soil conservation strategies has long been an active field for research and practice (Panagos *et al.*, 2016; Govers *et al.*, 2017). Given any long-term strategy to preserve soil resources relies upon a balance between the rates of soil loss and soil renewal (Hancock *et al.*, 2015), the measurement of soil formation is a fundamental component in these conservation efforts.

The mechanisms associated with soil formation have been studied for over a century, with a focus on the development of soil horizons and the evolution of soil properties (Dokuchaev, 1879; Jenny, 1941; Bryan and Teakle, 1949; Tugel *et al.*, 2005). Efforts to quantify the rates at which soils form from parent materials have included studying how soil properties change across chronosequences (Turner *et al.*, 2018), developing chemical weathering

models (Burke *et al.*, 2007) and, in particular, employing terrestrial cosmogenic radionuclide analyses (Heimsath *et al.*, 1997). In the latter, the concentrations of radioactive isotopes in the bedrock, which are partly dependent upon the rate at which bedrock transforms into soil, are measured and assumed to equal the rates of soil formation.

Despite the recent advancements in cosmogenic radionuclide analysis, their application in soil science has, arguably, not been fully realized. Moreover, there are three research challenges that may explain this. First, there is a dearth of soil formation rate data. Whilst there have been many attempts at calculating a global average soil formation rate from collating multiple inventories (Alexander, 1988a; Montgomery, 2007; Stockmann *et al.*, 2014; Minasny *et al.*, 2015), these datasets often omit more than 100 countries, particularly in Africa and Europe, presenting a clear rationale for more studies to take place in these areas of the world. Second, over 80 % of the soil formation rate inventory, comprising data from Montgomery (2007), Portenga and Bierman (2011) and Stockmann *et al.* (2014), is attributed to samples taken from outcrops and stream sediments procured from drainage basins. Moreover, only 252 ^{10}Be -derived rates from this inventory of 1850 stem from samples extracted from underneath the soil mantle. In addition, the majority of these stem from mountain regions and deserts (Heimsath *et al.*, 1997; Wilkinson *et al.*, 2005; Zhao *et al.*, 2018; Struck *et al.*, 2018). This is partly because the observation and estimation of bedrock weathering rates is most commonly carried out by the geomorphological community, principally to identify the mechanisms behind long-term landscape evolution (Heimsath, 2006; Heimsath and Burke, 2013; Ackerer *et al.*, 2016; Zhao *et al.*, 2018). As

a result, there has been no investment in deriving rates of soil formation for soils that support arable agriculture (Heimsath, 2014), despite these soils being identified as a societal priority (FAO, 2015). Such soils are critical to the delivery of multiple ecosystem services and, for many countries, are one of the most critical resources in ensuring the health of the society and sustained economic growth. They are also often intensely managed, and thus the loci for accelerated erosion (Quinton *et al.*, 2010; Borrelli *et al.*, 2017). However, in the absence of soil formation rate data, the magnitude of the threat erosion places on the sustainability of soils and arable production is unknown, amounting to a critical knowledge gap. Third, although the distributions of inventoried soil erosion and formation rates are often presented together to demonstrate the severity of soil erosion (Montgomery, 2007; Minasny *et al.*, 2015), the spread of globally compiled data is such that it cannot offer a useful forecast of the sustainability of soil at a site scale. Both distributions are platykurtic, and there is substantial overlap in these rates: 0–28.8 mm y⁻¹ for soil formation (Minasny *et al.*, 2015) and 0–52.9 mm y⁻¹ for soil erosion (Montgomery, 2007). For a greater understanding into the sustainability of soil resources at the local scale, we argue that soil scientists should undertake empirical measurements of both soil formation and erosion in parallel.

In this UK-based study, we present ¹⁰Be-derived soil formation rates for two catena sequences in an arable and coniferous woodland setting. The former are the first of their kind globally, and the latter are the first of their kind in Europe. We place our results in the context of the rates previously derived in similar climatic and petrographic settings around the world. Finally, using

previously measured soil erosion rates at the arable site, we calculate first-order soil lifespans to infer the long-term sustainability of the soil resource.

5.2 Materials and methods

5.2.1 Site description

This study measures soil formation down two catena sequences (Figure 5.1). The first is an arable hillslope at Rufford Forest Farm (RFF), east of Mansfield in Nottinghamshire, UK (53°7'13.43" N, 1°4'39.61" W). The second is a woodland hillslope in Comer Wood (CW), north of Quatford in Shropshire, UK (52°30'30.43" N, 2°22'45.68" W). RFF was selected as it is the site of previous tillage and water-based erosion studies (Quine and Walling, 1991; Walling and Quine, 1991; Govers *et al.*, 1996). Electing CW as a sister site is justified based on its similarities in parent geology, macroclimate, and soil physical properties with RFF as detailed below. A Trimble S6 Total Station was used to measure the relative elevation and slope of the catenas at both sites (Fig. 5.1b).

A reconnaissance study of the parent materials and their feasibility for cosmogenic radionuclide analysis was undertaken in spring 2017. Both sites are underlain by Triassic sandstone. At RFF, the Sherwood Sandstone (Chester formation; Olenekian, 247–251 Ma) is described as pinkish to red, medium to coarse grained, pebbly, cross-bedded, and friable. In CW, the New Red Sandstone (Bridgnorth formation; Cisuralian, 273–299 Ma) is described as brick-red, medium grained, cross-bedded, and aeolian based. Both RFF and CW are south-facing slopes, and sit in a temperate oceanic climate (Cfb), between 96–99 and 50–71 m a.s.l., respectively. The mean annual

precipitation and temperature is 709 mm and 9.8 °C at RFF, and 668 mm and 9.9 °C at CW, respectively (Met Office, 2018).

Both sites are positioned beyond the areal limits of the Late Devensian ice sheet, but studies conducted on similar formations of Triassic Sherwood Sandstone nearby suggest that the weathering of the parent material was partly induced by freeze–thaw processes associated with periglacial active layer development possibly during this period (Tye *et al.*, 2012). Although proglacial glaciogenic deposits have been found in the vicinity of CW, the prevalence of similar deposits on the study hillslope has not been studied. However, unpublished work conducted by the authors suggests that the upper (3–5 m) of the lithosphere at both sites was subject to high-magnitude sediment transport at least 200,000 BP or before, potentially during the Anglian glaciation (~450,000 BP). The complex land use and vegetation change in the Sherwood Sandstone outcrop, within which RFF is based, has been extensively studied and mapped by Tye *et al.* (2013). Following the onset of the Holocene, the area has been dominated by a complex sequence of land use change including broadleaf woodland (6000–2000 BCE), heathland (43–409 CE) and landscaped heathland for hunting (1600 CE). From at least 1855 CE, RFF has been under an arable regime, and in the last 12 years, the dominant crops have been winter wheat and rye. CW is understood to have been an open field until 1903–1926, and then heathland until 1954. Between 1954 and the present day, however, the site has been continuously occupied by a coniferous forest (Mike Annis, personal communication, 8 October 2018).

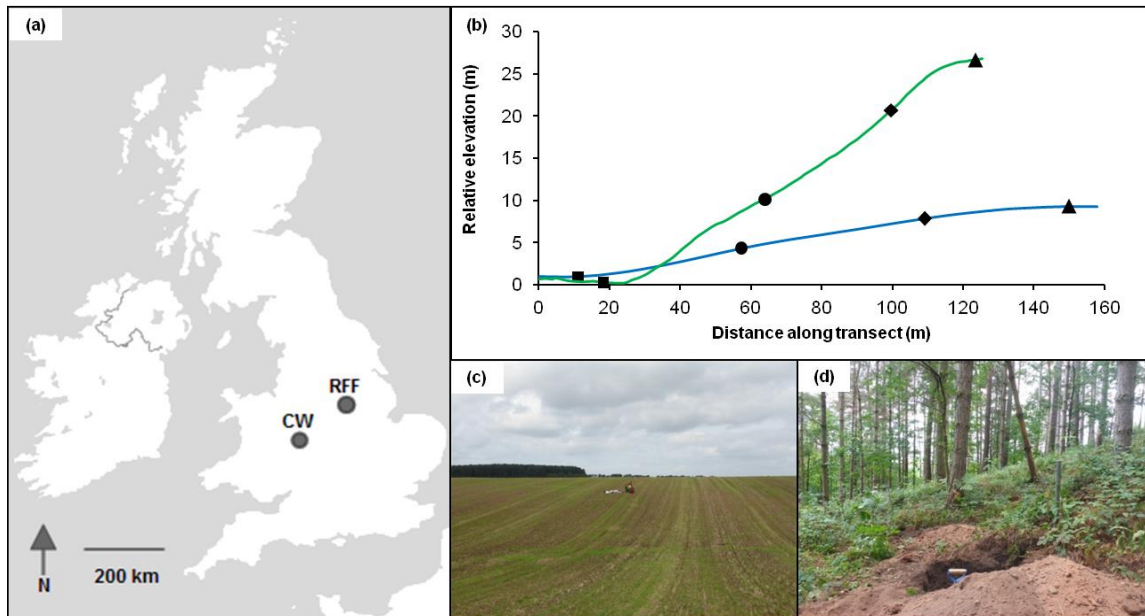


Figure 5.1: Locations of the study sites in this chapter (a) with elevation profiles (b) for both Comer Wood (CW; green) and Rufford Forest Farm (RFF; blue). The position of summit (triangles), shoulder (diamonds), backslope (circles) and toeslope (squares) sampling positions are indicated on each profile. Photographs of RFF (c) and CW (d) were taken by the author at the time of sampling.

5.2.2 Saprolite extraction and soil sampling

Four positions (summit, shoulder, backslope and toeslope) along a catena transect were selected for depth-to-bedrock surveys and saprolite extraction. First, a dynamic cone penetrometer was used to estimate the depth of the soil–saprolite interface. At RFF, a percussion drilling rig then proceeded to extract a series of vertical undisturbed core samples of the soil and saprolite. Cores were later halved lengthways, and by observing the changes in the consolidation and physical integrity of the extracted material (i.e. whether it remained intact when removed from the core), together with the penetration resistance data acquired in the field, the soil–saprolite interface was

demarcated. Two samples of saprolite (5 cm thickness) were then subsampled for cosmogenic radionuclide analysis: one at this interface and one from 50 cm below. In CW, following the use of the dynamic cone penetrometer to locate suitable sites, a soil pit was manually dug vertically at each of the four sampling locations. Observing the changes in the consolidation and physical integrity of the material down the profile wall, together with the penetration resistance data, the soil–saprolite interface was ascertained. A sample of saprolite (5 cm thickness) was then extracted from this interface for cosmogenic isotope analysis.

The bombardment of quartz minerals in the uppermost metres of bedrock with cosmic rays leads to the production of ^{10}Be . Assuming the intensity of these cosmic rays and the in situ weathering of bedrock (ϵ) is constant, the concentration of ^{10}Be (N) in a sample of bedrock, as shown in Eq. (1), is dependent upon the balance of two factors: the time that the bedrock has been exposed to cosmic rays with longer durations leading to greater concentrations, and the weathering of this bedrock into mobile regolith (soil) with greater rates of bedrock weathering leading to smaller concentrations (Lal, 1991; Stockmann *et al.*, 2014). We assume here that the production of ^{10}Be and the erosion of the bedrock is at an equilibrium:

$$N = \sum_{i=sp,\mu f,\mu-} \frac{P_i(\theta) \cdot e^{-\frac{x}{\Lambda_i}}}{\lambda + \frac{\epsilon \rho}{\Lambda_i}} \left(1 - e^{-t \left(\lambda + \frac{\epsilon \rho}{\Lambda_i} \right)} \right) \quad (1)$$

where: P are the annual production rates of ^{10}Be by spallation, fast muons and stopping muons (sp , μf and $\mu-$) at a surface with slope Θ ; x is the mass sample depth ($\rho \cdot z$); ρ is the density of overburden material; z is the depth of

the sample; t is the age of the bedrock surface (the age when the original surface was generated); λ is the decay constant of ^{10}Be with λ equalling $\ln 2 / ^{10}\text{Be}$ half-life; and Λ are the mean attenuation of cosmic radiations (Lal, 1991). t is usually considered infinite. At RFF, we took two samples from the same depth profile at each catena position to test if the data support these assumptions. RFF data are compatible with landscape ages >200 ka.

Production rates, decay constants, and attenuation lengths were calculated using field data and the CRONUS-Earth online calculator v2.3 Matlab code for the St scheme (Balco, 2008). As N can be measured using Accelerator Mass Spectrometry (AMS), Eq. (1) can be solved for ε by simple interpolation of N .

A total of twelve samples of saprolite (eight from RFF and four from CW) were prepared for AMS at the Cosmogenic Isotope Analysis Facility, East Kilbride, Scotland. This comprised of mineral separation, quartz cleaning, and procedures leading to the preparation of BeO sample cathodes (Kohl and Nishiizumi, 1992; Fifield, 2010; Corbett *et al.*, 2016). The AMS measurements were carried out at the SUERC AMS laboratory (Xu *et al.*, 2010). ^{10}Be concentrations are based on 2.79×10^{-11} $^{10}\text{Be}/^9\text{Be}$ ratio for the NIST Standard Reference Material 4325. The processed blank ratio ranged between 6 and 13% of the sample $^{10}\text{Be}/^9\text{Be}$ ratios. The uncertainty of this correction is included in the stated standard uncertainties. Concentrations of ^{10}Be were subsequently determined, following Balco (2006) (see Appendix 5.1).

Previous work (e.g. Heimsath *et al.*, 1997) has assumed that the bulk density of the soil above the bedrock surface is either equal to that of the bedrock, or constant with depth. For this chapter, we developed a model called 'CoSOILcal' to calculate soil formation rates using empirically measured bulk

density data from each catena position at both RFF and CW (Rodés and Evans, 2019). The local annual production rate of ^{10}Be at each study site must also account for any obstructions that reduce the cosmic ray flux to the parent material (Phillips *et al.*, 2016). For an obstruction to cause this reduction, it is required to be several metres thick which equates, in practice, to topographic features at the scale of tens of meters or greater. The shielding factor, therefore, is a ratio of the ^{10}Be production rate at the obstructed site to that at an identical site but with a flat surface and a clear horizon (Balco *et al.*, 2008). To calculate both shielding factors and subsequently normalize local ^{10}Be production rates, site elevation, latitude, and longitude were inputted into the CRONUS-Earth Matlab code v2.3 using Lal/Stone (St) scaling (Balco *et al.*, 2008).

Soil samples were sub-sampled every 5 cm from each core at RFF and on each profile wall at CW. All samples were then oven dried overnight (105°C for 12 hours), grounded with a pestle and mortar, and sieved to discard the >2 mm fraction before being subject to particle size analysis and loss on ignition (LOI). Particle size analysis was conducted using a Beckman Coulter Laser Diffraction Particle Sizing Analyser LS 13 320 (pump speed: 70 %; sonication: 10 seconds; run-length: 30 seconds). For LOI, 5 g of each sample was placed in a Carbolite furnace CWF 1300 (550°C for 12 hours). Full data from these analyses can be found in Appendix 5.2.

The soils at RFF are classified as Arenosols (IUSS Working Group WRB, 2015) with weak horizonisation. An Ap loamy-sand horizon (82% sand, 16% silt, 2% clay) thickens from 30 to 75 cm and increases in LOI content from 3.65 to 3.91% from summit to toeslope, respectively. Despite being subject to

arable practices for over 150 years, the presence of a 30 cm Ap horizon may be explained in part by the incorporation of mineral matter with the remaining organic material after harvest, although further isotopic work is required to verify this for RFF. This Ap horizon is underlain by a 5 cm fluvial pebble-bed, typical of the Bunter pebble-beds found in the vicinity (Ambrose *et al.*, 2014). An undifferentiated, weakly-consolidated subsoil steadily grades into saprolitic, moderately-consolidated sandstone.

The soils at CW are classified as Arenosols (IUSS Working Group WRB, 2015). Similar to RFF, there is little evidence for horizonisation down the profile at CW. A thin (<5 cm) litter-fermentation-humus layer overlays an undifferentiated, weakly-consolidated, sandy subsoil (94% sand, 5% silt, 1% clay) and grades into moderately-consolidated saprolitic sandstone. The sandy composition of these soils suggests that proglacial outwash deposits have not contributed to the soils of the study sites and that, instead, the soils are largely residual.

5.2.3 Lifespan analysis at Rufford Forest Farm

To provide an insight into the sustainability of the soil profiles at RFF under arable agriculture, in terms of the balance of erosion and formation, a first-order lifespan model was employed. Calculating the sustainability of a net-eroding soil in first-order terms has been attempted in the past (Elwell and Stocking, 1984; Sparovek and Schnug, 2001; Montgomery, 2007; Medeiros *et al.* 2016). Early models (Stocking and Pain, 1983), however, did not account for mass inputs into the soil system, such as that derived from bedrock weathering. In this study, this omission was addressed by using soil formation

rates empirically measured at RFF. Furthermore, in previous models, the solum thickness used to calculate the soil lifespan is not universally consistent. Some authors constrain the lifespan by the minimum depth required for primary production (Stocking and Pain, 1983; Elwell and Stocking, 1984).

Notwithstanding the fact that this soil threshold depth will, in part, be crop-dependent, soils that fall below this threshold may still be able to fulfil some of the ecosystem services, such as the sequestration of carbon. To address this here, two lifespan (L) scenarios were calculated, both of which are based on the continuation of contemporary arable agriculture. The first referred to the expected lifespan of the current A horizon ($D = 30$ cm across the catena). At the toeslope, an additional lifespan was calculated to account for the greater depth (75 cm) of the A horizon. Here, we did not account for any transformation of subsoil into topsoil, which could occur if erosion rates are sufficiently low, nor did we account for any allochthonous inputs to the profile such as aeolian additions and organic amendments. The second estimated the time until the underlying parent material is exposed. Here, the observed depth to the soil-saprolite interface at each catena position was employed.

Both lifespan scenarios were calculated for summit, shoulder, backslope, and toeslope catena positions. Three different erosion rates (E) were applied.

First, a mean annual erosion rate of 1.19 mm y^{-1} was used based on ^{137}Cs -based data ($n = 103$) measured by Quine and Walling (1991) at RFF. This mean value represents all erosion processes, including water-based and tillage-based erosion. Two additional lifespans were calculated using rates from the 5th and 95th percentiles of this dataset (0.19 mm y^{-1} and 2.2 mm y^{-1} ,

respectively). It should be acknowledged here that the rates of soil formation represent timescales four orders of magnitude greater than those of soil erosion. However, if lifespans are to provide an insight into the sustainability of the soil profiles at RFF, the soil erosion rates must represent those from contemporary arable agriculture.

The soil formation rates, as empirically measured in this chapter, were then plotted to derive the soil production function P ; Eq. (2):

$$P = W e^{\left(\frac{-h}{\gamma}\right)} \quad (2)$$

where W is the production rate at zero soil thickness (h) and γ is a parameter that determines the thickness of soil when soil formation decreases by $1/e$.

The data for both the production rate (P) and the thickness of the soil (h) were used to calculate W and gamma using least squares regression. In this study, γ was calculated as being 2.26 m, which is substantially greater than that previously reported (e.g. Heimsath *et al.*, 1997). It was therefore concluded that soil formation rates at RFF are relatively insensitive to changes in soil thickness. As a result, constant soil formation rates (F) for each catena position, together with two additional rates representing upper and lower standard deviations, were used to calculate soil lifespans. Furthermore, the expected increase in soil formation rates as a result of soil thinning were captured within these upper and lower uncertainties. Soil lifespans were thus calculated using Eq. (3):

$$L = \frac{D}{E-F} \quad (3)$$

where D is depth in mm, E is gross annual soil erosion rate in mm y^{-1} and F is gross annual soil formation rate in mm y^{-1} .

5.3 Results and discussion

5.3.1 Soil formation rates

Soil formation rates calculated from measured ^{10}Be concentrations at RFF range from 0.026 mm y^{-1} to 0.084 mm y^{-1} , with the mean soil formation rate being $0.048 \pm 0.008 \text{ mm y}^{-1}$ (Table 5.1). At CW, soil formation rates range from 0.053 mm y^{-1} to 0.096 mm y^{-1} , with the mean soil formation rate being $0.070 \pm 0.010 \text{ mm y}^{-1}$, which is 0.022 mm y^{-1} greater than that at RFF. These rates indicate declining soil formation rates with increasing soil thickness (Figures 5.2 and 5.3). In accordance with geomorphological theory (Conacher and Dalrymple, 1977; King *et al.*, 1983; Pennock, 2003; Schaetzl, 2013), soils are thinner on the slope convexities and the steepest gradients where surface erosion is considered most prevalent. In contrast, soil thicknesses are greater at the summit where surface erosion has been less extensive, and the toeslope zone where sediment has been deposited. In RFF, the fastest soil formation rates were found on the backslope where soils are thinnest. These results are consistent with many theorized mechanisms that demonstrate how parent material overlain by shallower soils is more affected by diurnal thermal stresses, contact with water, and physical disturbance, which can together proliferate physical and chemical weathering processes, and thus the conversion of saprolite into soil. Conversely, it was found the slowest formation rates were associated with the deepest soils at the summit where the increasing thickness of the soil mantle buffers the parent material from any subaerial factors that may otherwise proliferate weathering (Carson and Kirby,

1972; Cox *et al.*, 1980; Dietrich *et al.*, 1995; Minasny and McBratney, 1999; Wilkinson and Humphreys, 2005). At CW, the difference in soil thickness between eroding and non-eroding zones is less pronounced. On the shoulder and backslope positions, where soils are thinnest, the soil formation rates were 0.03 mm y^{-1} faster than summit and toeslope positions.

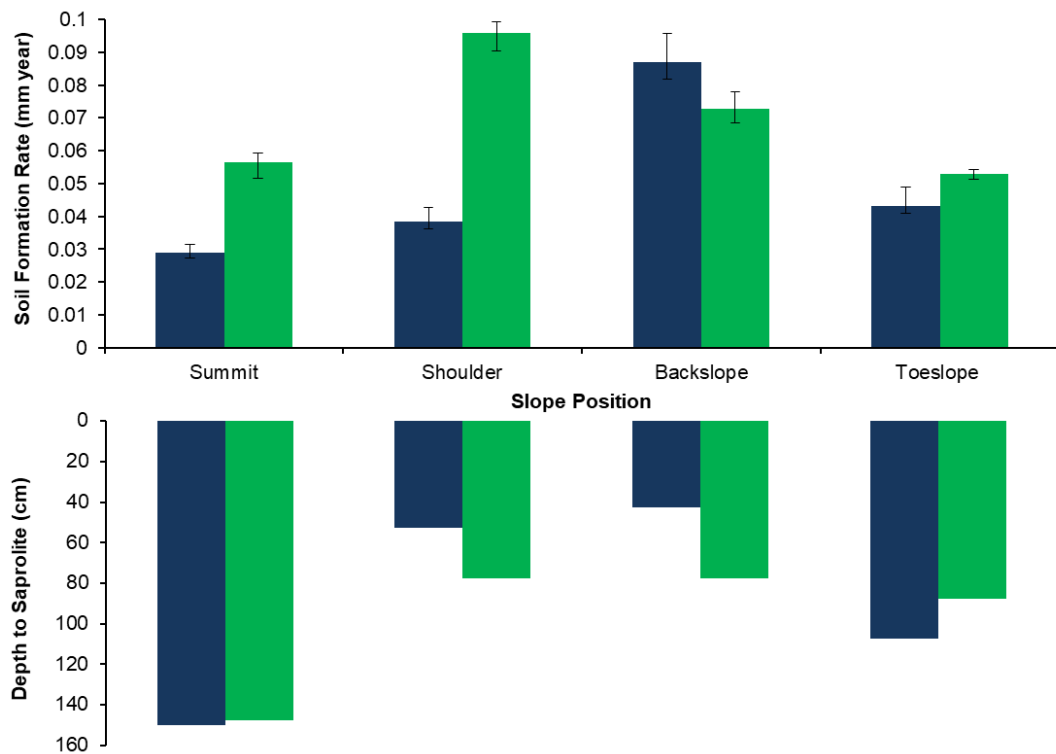


Figure 5.2: Soil formation rates and the depths to saprolite for the four sampling positions along the catena transects at Rufford Forest Farm (blue; $n = 4$) and Comer Woodland (green; $n = 4$). The error bars represent one sigma uncertainties. At RFF, two ^{10}Be concentrations down the same depth profile have been used in the CoSOILcal model to derive a 'best fit' soil formation rate. Depth here refers to that for the midpoint (between the top and bottom) of the sample.

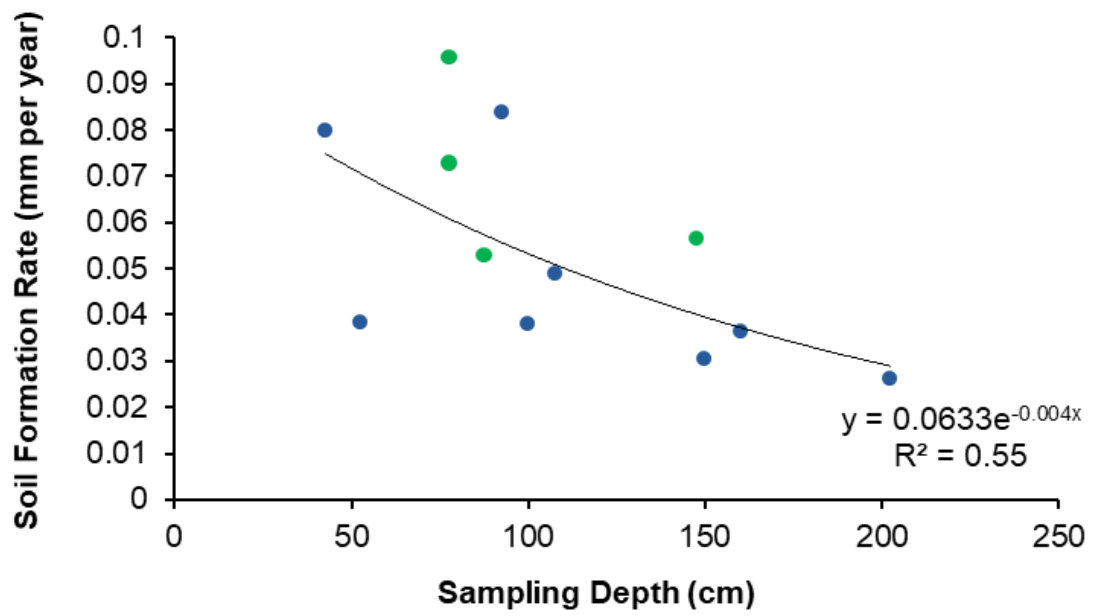


Figure 5.3: Soil formation rates against sampling depth for Rufford Forest Farm (blue; $n = 8$) and Comer Woodland (green; $n = 4$). Depth here refers to that for the midpoint (between the top and bottom) of the sample.

Table 5.1: ^{10}Be concentrations and calculated maximum soil formation rates for Rufford Forest Farm (RFF) and Comer Wood (CW)

Site	Catena Position	Elevation (m)	Horizon Position	Depth (cm)	^{10}Be atoms (atoms/g) ($\times 10^4$)	Uncertainty of ^{10}Be atoms (atoms/g) ($\times 10^4$)	^{10}Be production rate at surface ($\text{g}^{-1} \text{year}^{-1}$)	Soil Formation Rates, (Best Fit) (mm ka^{-1})	Uncertainty (mm ka^{-1})
RFF	Summit	98.7	A	150	3.5	0.2	4.63	30	29 - 33
RFF	Summit	98.7	B	203	2.3	0.2	4.63	26	24 - 28
RFF	Shoulder	99.3	A	53	5.4	0.2	4.63	38	36 - 41
RFF	Shoulder	99.3	B	100	3.0	0.2	4.63	38	36 - 40
RFF	Backslope	97.9	A	43	4.6	0.2	4.63	80	77 - 83
RFF	Backslope	97.9	B	93	2.9	0.2	4.63	84	77 - 88
RFF	Toeslope	95.7	A	108	3.3	0.2	4.62	49	46 - 53
RFF	Toeslope	95.7	B	160	2.5	0.2	4.62	36	34 - 39
CW	Summit	70.6	A	148	2.5	0.2	4.49	57	52 - 59
CW	Shoulder	65.3	A	78	2.5	0.1	4.46	96	90 - 99
CW	Backslope	58.9	A	78	3.1	0.2	4.42	73	69 - 78
CW	Toeslope	50.1	A	88	4.1	0.2	4.39	53	51 - 54

Horizon Position 'A' denotes the sample was taken at the soil-saprolite interface. Horizon Position 'B' denotes an additional sample was taken ~50cm below the interface from the same depth profile. The depth here refers to that for the midpoint (between the top and bottom) of the sample. The shielding correction was calculated as 1.0 (to 1 d.p) for all samples and ^{10}Be production rates are corrected for elevation and location (see Appendix 5.1). ^{10}Be concentrations are in the form of ^{10}Be atoms per gram of quartz, following convention. All uncertainties are one standard deviation, based on uncertainties in the measurement of ^{10}Be concentrations (Rodés et al., 2011).

Comparing data between RFF and CW demonstrates that there are other factors besides soil thickness that govern soil formation rates. For example, at the shoulder the soil thickness at CW is greater by 25 cm than that at RFF which would suggest slower formation rates. Instead soil formation rates are faster by 0.038 mm y^{-1} at CW. One possible explanation is the petrographic composition of the parent material, and the susceptibility of that parent material to weathering. Whilst both RFF and CW are underlain by sandstone, the bedrock at RFF is fluvially-derived whereas that at CW is aeolian-derived. Petrological studies on fluvially-derived sandstone report a greater concentration of cementing clays in the matrix material which ultimately reduces the porosity and decreases its susceptibility to particle detachment, leading to slower soil formation rates (Wakatsuki *et al.*, 2005; Mareschal *et al.*, 2015).

In studies where cosmogenic methodologies have not been applied, it has been found that land use regime can promote or retard rates of bedrock weathering. Humphreys (1994) found that root channels and mesofaunal pedotubes in both the topsoil and subsoil can enhance the surface to bedrock hydrological connectivity. Similarly, Dong *et al.* (2019) demonstrated how an interconnected network of ecohydrologic interactions controls the supply and transport of acid to the bedrock. When a greater proportion of root mass was distributed in the uppermost horizons of the soil profile, CO_2 was predominantly emitted as gas whereas when roots were distributed in the subsoil, more CO_2 moved downwards to increase acid production, and enhance chemical weathering. Other work has sought to identify the mechanisms that affect the thermal regime of soil profiles, and the

consequential impacts on the weathering susceptibility of the parent material (Ahnert, 1967; Minasny and McBratney, 1999). At CW, the roots are deeper than those found observed at RFF and this is likely to proliferate weathering processes. However, given the fact that the ^{10}Be derived soil formation rates are millennial scale averages, it is unlikely that relatively recent (decadal-centennial) variances in the site's land use regime would be captured in the isotopic data (Darvill, 2013).

5.3.2 Derived soil formation rates in reference to the global inventory

Figure 5.4 compares soil formation rates for the study sites to an inventory of soil formation rates extracted from the published literature ($n = 252$; Figure 5.4a; Appendix 2.1). The median soil formation rate in this study (0.051 mm y^{-1}) is 0.028 mm y^{-1} faster than that of the mantled inventory, a statistically significant difference (U test; $P < 0.05$). However, this global inventory comprises studies conducted on a range of geologies and climates, which are both influences on bedrock weathering rates.

Isolating the data from temperate climates ($n = 187$; Figure 5.4b) presents a median soil formation rate of 0.035 mm y^{-1} , which is 0.016 mm y^{-1} slower than that measured for RFF and CW, although there is no statistically significant difference between those data and those we have measured at the UK study sites presented in this chapter (U test; $P > 0.05$). It is likely that the inventory's median soil formation rate for temperate climates is slower as 44% of the temperate-based data has been collected from regions that have lower mean annual precipitation than RFF and CW, which can lead to less weathering

activity in the parent material (Heimsath *et al.*, 2001a; Heimsath *et al.*, 2005; Dixon *et al.*, 2009; Heimsath *et al.*, 2012).

Isolating the sandstone-derived data from the inventory ($n = 57$; Figure 5.4c) presents a median soil formation rate of 0.045 mm y^{-1} , which is 0.006 mm y^{-1} slower than that measured for RFF and CW, although there is no statistically significant difference (U test; $P > 0.05$). Although the sandstone-derived data were derived from the global soil-mantled database, all data stem from sites in temperate climates, which reduces the influence that climate may have otherwise had in this analysis on lithology. We suggest that faster formation rates at RFF and CW may be explained by the fact that the specific varieties of sandstone at these study sites are generally more susceptible to weathering than those within the sandstone-based inventory, of which the dominant form is the greywacke, characterised by a hard, fine-grained, argillaceous matrix, with greater resistance to weathering (Cummins *et al.*, 1962). Although there has been substantial work on the susceptibilities of major geological rock types to weathering (Stockmann *et al.*, 2014; Wilson *et al.*, 2017), we do not know of any study which seeks to identify whether the susceptibility of specific varieties of sandstone has an influence on soil formation rates.

The only other study to measure soil formation rates in the UK is that of Riggins *et al.* (2011) where rates were derived for Bodmin Moor, Cornwall ($n = 5$; Figure 5.4d). In that study, the median soil formation rate was 0.015 mm y^{-1} , which is 0.036 mm y^{-1} slower than that for RFF and CW, and statistically significant (U test; $P < 0.05$), despite the fact that Bodmin Moor receives about 300 mm more precipitation per year than the sites in this study, which should

increase soil formation rates (Riggins *et al.*, 2011). This is explained by the parent material at Bodmin Moor (coarse-grained granite) being generally less prone to weathering than the varieties of sandstone evident at RFF and CW (Portenga and Bierman, 2011).

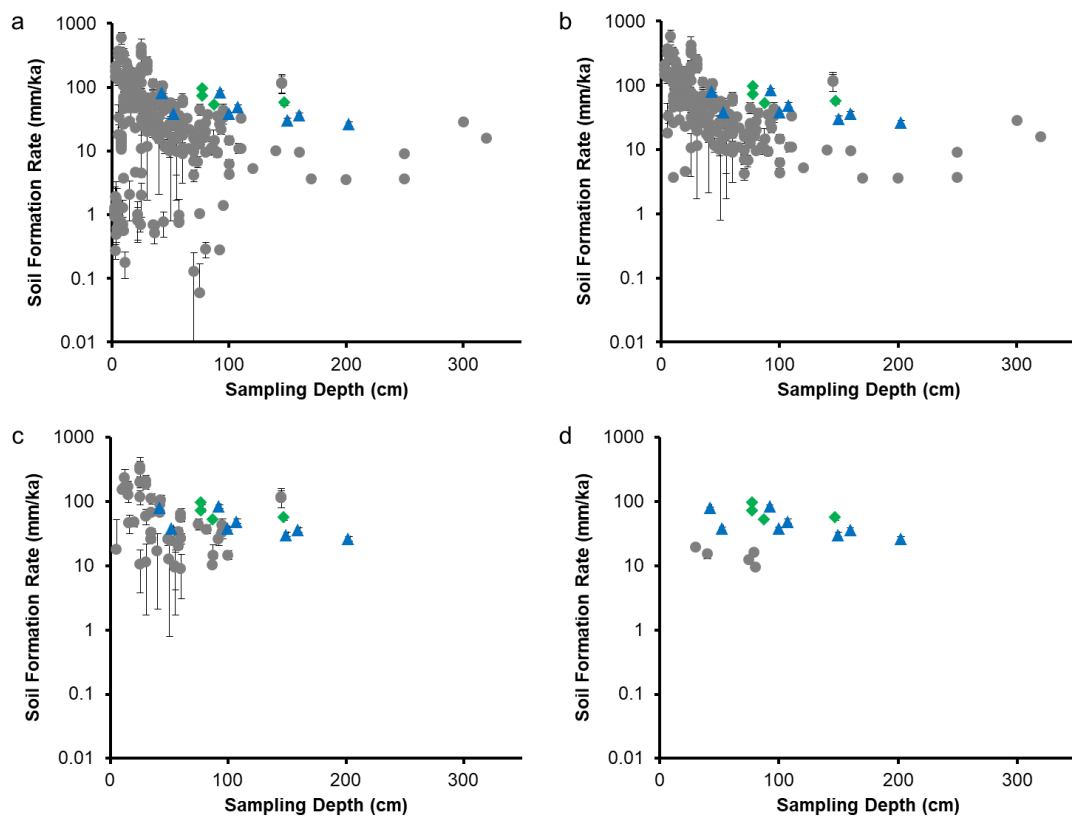


Figure 5.4: Soil formation rates from a globally compiled inventory (grey circles) and from this study at Rufford Forest Farm (blue triangles) and Comer Woodland (green diamonds) plotted against sampling depth. The depth here refers to that for the midpoint (between the top and bottom) of the sample. Rates in grey are from (a) the total mantled inventory ($n = 252$); (b) studies from temperate climates ($n = 187$); (c) studies on sandstone geology ($n = 57$); and (d) the UK, exclusively from Riggins *et al.* (2011) ($n = 5$). Error bars indicate the standard error.

5.3.3 Lifespan analysis at Rufford Forest Farm

Based on a mean annual erosion rate of 1.19 mm y^{-1} under arable agriculture, the lifespans of the A horizon across the catena at RFF range between 258 – 272 years (Figure 5.5). This range expands to 138 – 3,000 years when the 5th and 95th percentile soil erosion rates are applied. However, further examination of the A horizon from cores extracted down the catena suggest that the toeslope is in a phase of aggradation rather than thinning. This is supported by the fact that the depth of the Ap horizon at the toeslope is 75 cm, whereas it is 30 cm on all other observed landscape positions. Moreover, comprised within the upper stratigraphy of the soil profile down the catena is the Bunter Pebble Bed which can be found at approximately 30 cm on summit, shoulder, and backslope positions, but 70 cm at the toeslope. The depth to which this pebble bed occurs at the toeslope suggests that either colluviation has occurred, or is still occurring. In a scenario where colluviation is no longer active, the lifespan of this 75 cm A horizon is finite, and ranges from 347 – 5,245 years, but lifespans here could be longer or indefinite if colluviation continues. This demonstrates the difficulty of calculating lifespans using soil formation rates derived from bedrock alone, and not from other system inflows of soil mass such as that from colluviation and soil carbon additions.

Soil lifespans indicating the time until the exposure of the parent material span between 407 – 1,334 years. The range of these lifespans can be explained by the fact that unlike scenario one, where a constant A horizon thickness of 30 cm was applied across the catena, the soil thickness applied here is the depth to the soil-saprolite interface measured at each catena position (see Table

5.1). Applying upper and lower confidence intervals in the soil formation term, and the 5th and 95th percentiles in the soil erosion term further widens the breadth of lifespans to 212 – 9,688 years. The shortest lifespans are found on the backslope where bedrock exposure is expected to occur between 212 – 4,500 years. In contrast, the greatest lifespans are found at the summit where soil thickness is 155 cm (713 – 9,688 years). Although soil formation rates are greater at the toeslope, the depth to bedrock is 40 cm greater at the summit and, as a result, longer durations are required for bedrock to become exposed at this position. The soil detached and transported from the backslope is expected, in part, to continue to be a contributory source of the colluvium observed at the toeslope. Although the growth of soil profiles due to colluvium is not considered in the lifespan equation, it suggests that lifespans at the toeslope may either be longer than the calculated maximum of 8,042 years or indefinite.

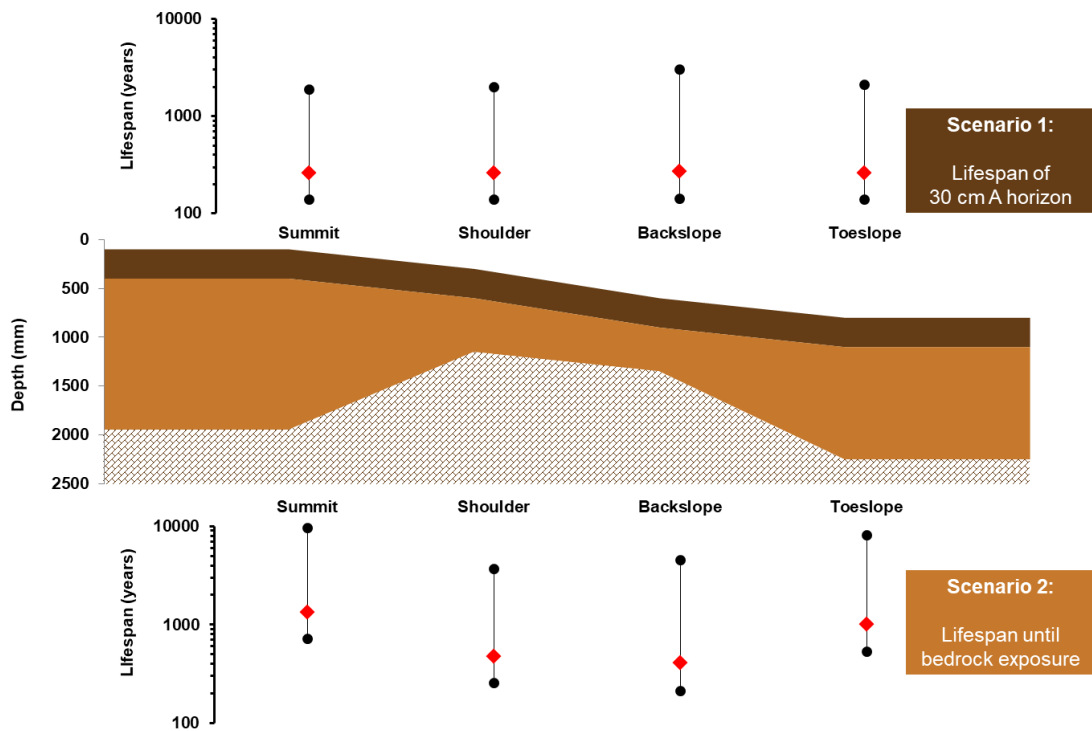


Figure 5.5: First-order soil lifespans calculated at four catena positions at Rufford Forest Farm for Scenario 1 (the time until the erosion of a 30 cm A horizon) and Scenario 2 (the time until bedrock exposure). The centre diagram indicates the thickness of the A horizon (dark brown), the subsoil (light brown) and the depth to the soil-saprolite interface (bricks). Red diamonds denote lifespans calculated using a mean annual soil erosion rate of 1.19 mm y^{-1} from Quine and Walling (1991) and soil formation rates from this study. Black dots denote the minimum and maximum lifespans calculated using the 5th and 95th percentile of the soil erosion dataset and the one sigma uncertainties in the soil formation dataset.

The first-order lifespans presented here are based on a number of assumptions. Notwithstanding the fact that the land management regime may change within the cited time spans altering the protection the soils receive from wind and water, the erosion rates employed neither reflect the increase in the erodibility of subsoil horizons, characterised by a relatively weaker soil structure (Tanner *et al.*, 2018), nor the potential role that the Bunter Pebble Bed may play in armouring the soil surface in the future. Moreover, they do not reflect the expected shift in erosivity, commensurate with more intense

precipitation events (Burt *et al.*, 2015). Acknowledging these factors, the lifespans presented here are likely to be overestimated. However, the fate of eroded soil upslope may contribute to the up-building of soil profiles in downslope concavities, extending the lifespans in the colluvial zone. In this respect the lifespans presented here, particularly those for the toeslope, are likely to be underestimated.

5.4 Conclusions

We have presented the first isotopically-derived rates of soil formation for soils currently supporting arable agriculture. Rates derived for two UK catena sequences using cosmogenic radionuclide analysis range from 0.026 mm y^{-1} to 0.084 mm y^{-1} , with mean rates being $0.048 \pm 0.008 \text{ mm y}^{-1}$ and $0.070 \pm 0.010 \text{ mm y}^{-1}$ for Rufford Forest Farm and Comer Wood, respectively. By combining soil formation rates from Rufford Forest Farm with soil erosion rates derived from a prior isotopic study in a first-order lifespan model, we estimate that in a worst-case scenario the soil that currently comprises the A horizon on the backslope may be eroded in 138 years, and bedrock exposure may occur in 212 years. Assessing gross soil erosion with measured rates of soil formation is important because soils that support arable agriculture are under threat from accelerated soil erosion. We have therefore shown that both the derivation and application of soil formation rates must become a fundamental component in future discussions of soil sustainability.

This work also represents the second of all isotopic studies of soil formation in the UK, and therefore a significant contribution to our knowledge of pedogenesis. Soil formation rates were found to fall within the range of those

previously published for soils in temperate climates and on sandstone lithologies, but were found to be significantly greater than those measured previously at Bodmin Moor. This is explained by the fact that the parent material at Bodmin Moor is a coarse-grained granite, and therefore less susceptible to weathering than the sandstone materials underlying Rufford Forest Farm and Comer Wood. Such petrographic controls may also explain the greater rates of soil formation at Comer Wood where the sandstone matrix is largely devoid of the cementing agents present at Rufford Forest Farm and, therefore, more susceptible to particle detachment during physical and chemical weathering. Given that petrographic variability has not been thoroughly investigated in pedogenesis work, greater investment is warranted to better understand how the geochemical composition of the parent material governs the rates of soil formation.

Acknowledgements

The authors wish to thank Mr Annis (National Trust) for permission to carry out fieldwork on Comer Wood, and Mr and Mrs King (TAG Farming) for permission to carry out fieldwork on Rufford Forest Farm. We thank Vassil Karloukovski for assistance in surveying, and Andrew Binley, Paul McLachlan, Jonathan Riley, Carl Horabin, and the BGS Dando Drilling Rig Team for the acquisition of samples. We also wish to thank Allan Davidson, Ángel Rodés, Derek Fabel at the NERC Cosmogenic Isotope Analysis Facility for preparing samples for AMS, and their subsequent assistance in data analysis. We thank Tim Quine for sharing multiple datasets from fieldwork conducted at Rufford Forest Farm. Finally, we wish to thank the anonymous referees and Dan Morgan for their very constructive feedback on the manuscript. This work was

partly supported by BBSRC and NERC through a Soils Training and Research Studentships (STARS) (Grant number: NE/M009106/1) and partly by a NERC research grant (Grant number: CIAF 9179/1017).

Chapter 6: The matrix effect: how the composition and petrographic structure of sandstone affects rates of soil formation

D. L. Evans, J. N. Quinton, A. M. Tye, Á. Rodés, J.A.C. Davies, and S. M. Mudd

This chapter is intended for publication in *Geoderma*.

Abstract

Soils deliver multiple ecosystem services and their long-term sustainability is fundamentally controlled by the rates at which they form and erode. Our knowledge and understanding of soil formation is not commensurate with that of soil erosion, in part due to the difficulty of measuring the former. However, developments in cosmogenic radionuclide accumulation models have enabled soil scientists to more accurately constrain the rates at which soils form from bedrock. To date, all three major rock types – igneous, sedimentary and metamorphic lithologies – have been examined in such work. Soil formation rates have been measured and compared between these rock types, but the impact of rock characteristics, such as rock matrix mineralogy and porosity on soil formation rates, have seldom been explored. In this UK-based study, we addressed this knowledge gap by using cosmogenic radionuclide analysis to investigate whether the lithological variability of sandstone governs pedogenesis. Soil formation rates were measured down two arable hillslopes at Woburn and Hilton, which are underlain by different types of arenite sandstone. These rates ranged from 0.031 to 0.193 mm y⁻¹. Rates were faster

at Woburn, and we suggest that this is due to the fact that the Woburn sandstone formation is relatively porous and less cemented than that at Hilton. Similarly, rates at Woburn and Hilton were found to be faster than those measured at two other sandstone-based sites in the UK, and with those compiled in a global inventory of cosmogenic studies on sandstone-based soils. We suggest that the matrix-abundant, less porous wackes that have been studied previously may slow the transmission and storage of water in the sandstone, and reduce the rates of bedrock weathering.

6.1 Introduction

Soils are critical global resources. They are key to our food, water and energy security, mitigating and adapting to climate change, the safeguarding of biodiversity, and the protection of human health (Blum, 2005; McBratney *et al.*, 2014; Adhikari and Hartemink, 2016). Conserving soils so that that we meet present-day demands, and those of future generations, is therefore a societal priority (Pimentel *et al.*, 1995). This is especially important in the context of the rising demands from a growing population and widespread soil degradation (Quinton *et al.*, 2010; FAO, 2015; Baude *et al.*, 2019).

A fundamental component of our efforts to ensure the long-term sustainability of the soil resource is a better understanding of the controls on soil thickness. The thickness of a soil is fundamentally determined by the balance between the rates of soil erosion and those of soil formation. Where rates of soil erosion exceed those of soil formation, the soil profile thins and, as a result, the capacity of the soil to store water, carbon and nutrients is reduced. Efforts to ameliorate soil erosion have been, and continue to be, prominent in soil

science (Panagos *et al.*, 2015). However, significant knowledge gaps remain in our understanding of the rates of soil formation.

The factors that govern soil formation were conceived in the initial development of soil science (Dokuchaev, 1879; Jenny, 1941; Simonson, 1997). The five factors, namely *Climate, Organisms, Relief, Parent Material* and *Time* have since been employed as a framework upon which to base further enquiry into the controls of pedogenesis. Although much of this work is theoretical, there has been a greater effort to empirically measure the rates of soil formation in recent decades (Stockmann *et al.*, 2014). In particular, the innovation and application of terrestrial cosmogenic radionuclide analysis in a range of landscapes (Heimsath *et al.*, 1997; Minasny *et al.*, 2015) has improved the precision of soil formation rates. Some authors have compiled global datasets inventorying cosmogenically-derived rates of soil formation in order to investigate the relationship between climate and pedogenesis (Montgomery, 2007; Portenga and Bierman, 2011). However, decadal to centennial fluctuations in regional and global climatic regimes are unlikely to be detected by cosmogenic radionuclide analysis which determine long-term soil formation rates over 1-100 kyr timescales (Cockburn and Summerfield, 2004).

A more apposite use of terrestrial radionuclide data is to study the control of lithology on soil formation rates, but such work to date has only focussed on comparisons between major rock types such as igneous, sedimentary and metamorphic (Stockmann *et al.*, 2014). One of the largest global meta-data analyses of soil formation rates conducted by Portenga and Bierman (2011) specifically omits soil-mantled bedrock, and instead focuses on bedrock

outcrops and basin sediments. Nevertheless, the authors found that sedimentary lithologies weather faster than igneous and metamorphic lithologies. This finding is also supported by Morel *et al.* (2003) in a study comparing soil formation rates from sedimentary (sandstone river bedload) and igneous (granite river bedload) lithologies, and Palumbo *et al.* (2009) in a similar study between sedimentary (Cretaceous stream sediments) and metamorphic (low grade metamorphosed Palaeozoic rocks) lithologies. However, rocks have an array of physical and geochemical properties, all of which may play different roles in influencing soil formation rates. By studying soil formation across the three major rock types, which are lithologically dissimilar in multiple properties, it is difficult to identify whether there is one lithological property that has a more noteworthy role in pedogenesis. One of the solutions to this is to measure and compare soil formation rates on variations of one lithology, thus limiting the number of lithological properties that may potentially differ.

To the best of our knowledge, few studies have assessed the variability of soil formation rates across one lithology. Gontier *et al.* (2015) used U- and Th-series nuclides to demonstrate that differences in the grain size of granites do not significantly affect the rates of soil formation. This is contrary to the work of Wakatsuki *et al.* (2005) who showed that soil formation rates in coarser grained granites were significantly faster than those of finer grained granites. The authors proposed that coarser grained minerals in granite have a smaller specific surface area, meaning a smaller volume of water is necessary for weathering than that required by finer grained minerals.

However, rates of soil formation may be regulated by other lithological properties that control the supply and transfer of water through the rock. Porosity, defined as the ratio of the aggregate volume of pores to the total volume of the rock (Goudie *et al.*, 1994), and the size and distribution of rock pores are, in turn, governed both by the composition and arrangement of rock grains, and the presence, volume and composition of the interstitial matrix are likely to be important. Furthermore, the properties of this matrix can change over time. For example, soluble cements, such as calcite, dolomite and gypsum, are dissolved (Burley and Kantorowicz, 1986) leaving a non-soluble, clay-rich matrix (Tye *et al.*, 2012). No studies have explored the roles played by rock porosity and the interstitial matrix on influencing rates of soil formation, representing a significant knowledge gap.

In this study, we use cosmogenic radionuclide analysis for the first time to investigate the extent to which the lithological variability of sandstone governs rates of soil formation. We present ^{10}Be -derived soil formation rates for two arable hillslopes in the UK, underlain by a fluvial- and a marine-derived sandstone. Furthermore, we place these rates in the context of those previously measured at two other sandstone-based sites in the UK, and with those measured in similar climatic settings around the world.

6.2 Materials and methods:

6.2.1 Site description

Two catena sequences were selected in Autumn 2018 (Table 6.1; Figure 6.1). The first site is a south-west facing hillslope at the Hilton Experimental Site (hereafter, Hilton), situated west of Wolverhampton, in Shropshire

(52°33'16.34" N, 2°19'43.17" W). This is a long-term study site established in 1976, predominantly to facilitate empirical measurements of soil erosion, but it has been employed in a range of multidisciplinary studies (Reed, 1979; Fullen, 1985, 1992). The second site is a south-facing hillslope at Woburn Experimental Farm (hereafter, Woburn), situated east of Milton Keynes in Bedfordshire (52°0'50.73" N, 0°35'5.63" W). Woburn was established in 1876 partly as an expansion on to the nearby, long-term experimental farms at Rothamsted (Catt *et al.*, 1975). Hilton and Woburn sit in a temperate oceanic climate (Cfb) between 58 – 64 m a.s.l and 97 – 109 m a.s.l., respectively. The mean annual precipitation and temperature is 751 mm and 9.8°C at Hilton, and 657.4 mm and 9.9°C at Woburn.

At Hilton, the Sherwood Sandstone Group (Helsby sandstone formation) has been described as reddish brown, well-cemented, sometimes pebbly, fine to medium grained, sub-angular to sub-rounded and locally micaceous (Bloomfield *et al.*, 2006). The reddish brown colour has been previously described as that of hematite veneers coating the grains (Strong, 1993). Studies on the interstitial matrix of the Helsby sandstone formation have observed zones of calcite and non-ferroan dolomite cement in some closed or restricted pore spaces, as well as cementation by evaporitic cements such as gypsum, anhydrite, and halite (Strong, 1993; Bloomfield *et al.*, 2006). This cementation most likely represents one of the first stages of the paragenetic sequence in the Helsby sandstone. Evaporitic cements would have been subsequently dissolved, leaving remnants of calcite and non-ferroan dolomites, which are observable today. Studies have also observed evidence of ferroan dolomite, detrital mica, and authigenic illite and kaolinite clay

cements in the matrix, representing later stages in the paragenetic sequence. These cements may account for between 30 – 50% of the rock's volume (Burley, 1984; Strong, 1993). This has the effect of reducing porosities to 15% in places.

The provenance of the Helsby Sandstone formation is debated in the literature. Bloomfield *et al.* (2006) suggest that the formation is predominately fluvial due to the presence of scoured channel bases and rounded mud-clasts. However, these rounded clasts may be the product of reworked aeolian deposits (Mountney and Thompson, 2002). Observations made by the authors suggest that the sandstone at Hilton is predominantly of fluvial origin based on the presence and abundance of sub-rounded to rounded pebbles within the sandstone matrix (Figure 6.2). What is more widely accepted is the fact that the Helsby sandstone formation developed during the Triassic period, when sediments were laid down in desert basins, in dry ($\sim <300 \text{ mm y}^{-1}$ annual precipitation) and hot conditions (Benton *et al.*, 2002). Moreover, previous research has demonstrated that the diagenetic features exhibited in the Sherwood Sandstone group are similar to those in sandstones that form today in the Sonoran Desert (Walker *et al.*, 1978).

At Woburn, the Lower Greensand Group (Woburn sandstone formation) has been described as fine to coarse grained, friable rounded quartzose sand (94%) with subsidiary alkali feldspar (2%), glauconite (2%), and muscovite (< 1%) (Catt *et al.*, 1975). In contrast to the Helsby sandstone formation, the sandstone at Woburn is nearly matrix-free and uncemented, and the interstices exhibit negligible (0.1%) clay content (Catt *et al.*, 1975; Palmer and Barton, 1987). The porosity has been previously reported as 35% with little

evidence found of porosity reduction based on the small proportion of ductile clasts and the moderate sorting (Palmer and Barton, 1987). A detailed mineralogical analysis of the Lower Greensand Group at Woburn is provided by Catt *et al.* (1975) and further assessments of the parent material at nearby sites can be found in Rastall (1919). Extensive analysis suggests that the provenance of the Lower Greensand at Woburn is marine-based (Stead and Evers, 2017). Although there is much dispute in the literature about the mechanisms of its formation, many scholars believe that the Woburn sandstone developed from an offshore tidal sand wave deposit in shallow water conditions (Stride, 1982; Evers, 1991; Owen, 1992). This marine-based sandstone cut into the Late Jurassic mudstones between the late Aptian and early Albian (126 – 100 Ma) during the Cretaceous period (Catt *et al.*, 1975). It is likely that the provenance of the sandstones at Hilton and Woburn partly explains some of the differences observed in the volume and composition of their matrix material. In a similar petrographic comparison on upper Palaeozoic sandstones, Obrist-Farner and Yang (2011) found that fluvially-derived sandstones were more enriched with calcite cements than deltaic sandstones. As a result, the fluvially-derived sandstones exhibited very low porosities (2.5%) compared with the deltaic sandstones (21%). The difference in these porosities (18.5%) is similar to that between Hilton and Woburn (Table 6.1). Similarly, Khalifa and Morad (2012) discuss the differences in cementation between fluvial and tidal Cretaceous sandstones. They suggest that the presence of interstitial detrital clays in fluvial sandstones (as is also observed at Hilton) is due to the infiltration of water rich in suspended mud, which is transferred into the interstices of alluvium; a process also observed

by Moraes and De Ros (1990) and Strong (1993). Although this may explain the presence of detrital clays in the sandstone at Hilton, this does not necessarily explain the *absence* of cementation in the sandstone at Woburn. Moreover, Palmer and Barton (1987) highlight that the lack of cementation at Woburn contrasts distinctively from other marine-based sandstone formations, which are comparatively more lithified, and exhibit a greater volume of authigenic clays (Milodowski and Wilmot, 1985). One possible explanation to account for the lack of lithification at Woburn is that the depth of burial was relatively shallow (approximately 300 m) when compared with other marine-based sandstones. The consequence of a shallow burial is that there was less diagenetic change (e.g.: porosity reduction) than would typically occur in more deeply buried sandstones.

Both sites are positioned within the Anglian glaciation (~450,000 BP). Although both sites are located beyond the areal extent of the Late Devensian ice sheet (~ 20,000 BP) (Eyles *et al.*, 1994; Gibbard and Clark, 2011), evidence suggests that periglacial conditions are likely to have dominated at these latitudes during this period (Watson and Morgan, 1977; Tye *et al.*, 2012). Hilton is positioned beyond the areal extent of the British-Irish ice sheet at the Last Glacial Maximum (LGM; ~21,000 BP) (Gibbard and Clark, 2011). However, there is some debate as to whether this area was covered, if only partly, during the earlier stages of the Devensian glaciation (Bowen *et al.*, 2002; Evans *et al.*, 2005). The site sits within the 'Wolverhampton Line' (Shotton, 1967) which represents the terminal position of the Irish Sea Glaciation and nearby the site are a number of drift and till deposits (Hollis and Reed, 1981). The area is likely to have been dominated by broadleaf

woodland between 6000 and 2000 BC, and heathland until the late 19th century. By 1883, Hilton was under agriculture, and this was most likely to have been pastoral (Fullen, 2020).

At Woburn, the study site and surrounding area was blanketed in boulder clay after the retreat of the Anglian glaciation. This was subsequently eroded, leaving a thin decalcified remnant of this clay incorporated into the Lower Greensand through processes of cryoturbation (Catt *et al.*, 1975). Particle size analysis conducted by the authors suggests that this boulder clay has not been incorporated into the soils at the study site; a finding similarly observed by Catt *et al.* (1975). The site would have been dominated by periglacial conditions during the Late Devensian (Gibbard and Clark, 2011). Johnston (1977) suggest that forests were cleared in the Middle to Late Bronze Age (~3000 years ago), when the soils were first cultivated.

Table 6.1: Locational context of the Hilton and Woburn study sites.

		Hilton	Woburn
Locational context	UK county	Shropshire	Bedfordshire
	GPS co-ordinates	52°33'16.34" N, 2°19'43.17" W	52°0'50.73" N, 0°35'5.63" W
	Aspect	South-west	South
	Elevation (m a.s.l)	58-64	97-109
	MAP (mm)	751	657
	MAT (-C)	9.8	9.9
Lithology	Parent material	Helsby Formation, Sherwood Sandstone	Woburn Formation, Lower Greensand
	Provenance	Fluvial/aeolian	Marine
	Matrix composition	Detrital mica, precipitated illite-smectite, and authigenic clays.	Nearly matrix-free and uncemented. Negligible clay content (0.1%).
	Porosity (%)	~ 6 – 27	~ 35
Glacial history	Anglian	Glaciated	Glaciated
	Last Glacial Maximum	Periglacial conditions	Periglacial conditions
Land-use history	Forest clearance	2000 BC	1000 BC
	Cultivation	Pastoral farming from 1883	From approx. 1000 BC
	Current land-use	Grass/shrub cover	Winter cereals

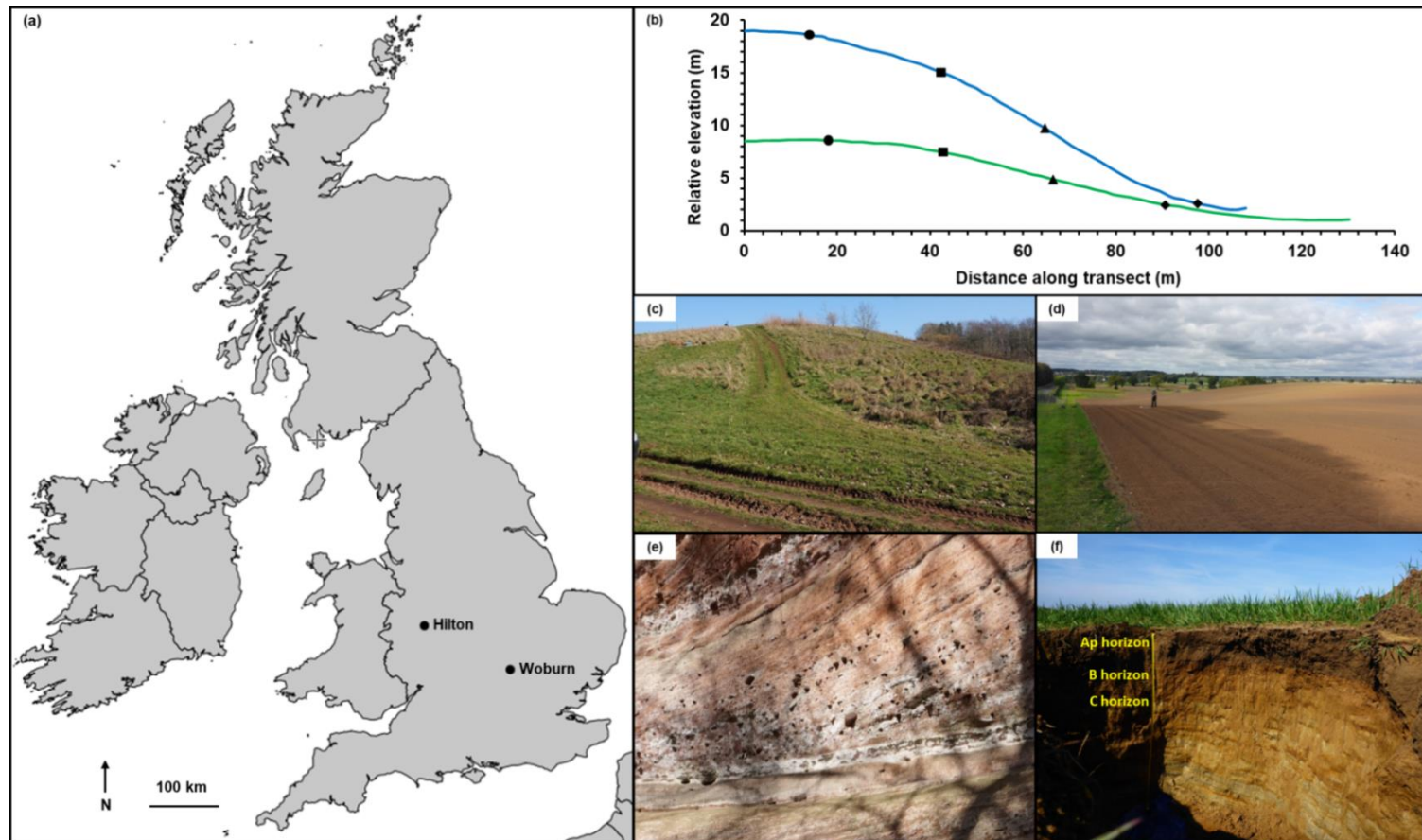


Figure 6.1: Location of the study sites (a) with elevation profiles (b) for Hilton (blue) and Woburn (green). Summit (circles), shoulder (squares), backslope (triangles), and toeslope (diamonds) are indicated on each profile. Photographs of the hillslope at Hilton (c) and Woburn (d) were taken from the toeslope during the reconnaissance survey. An exposure of the fluvially-derived sandstone (interbedded with sub-rounded pebbles) close to the study slope at Hilton is shown in (e) (photograph by Miroslav Bauer, 2019). The soil profile, soil-saprolite interface, and underlying bedrock at Woburn are shown in (f).

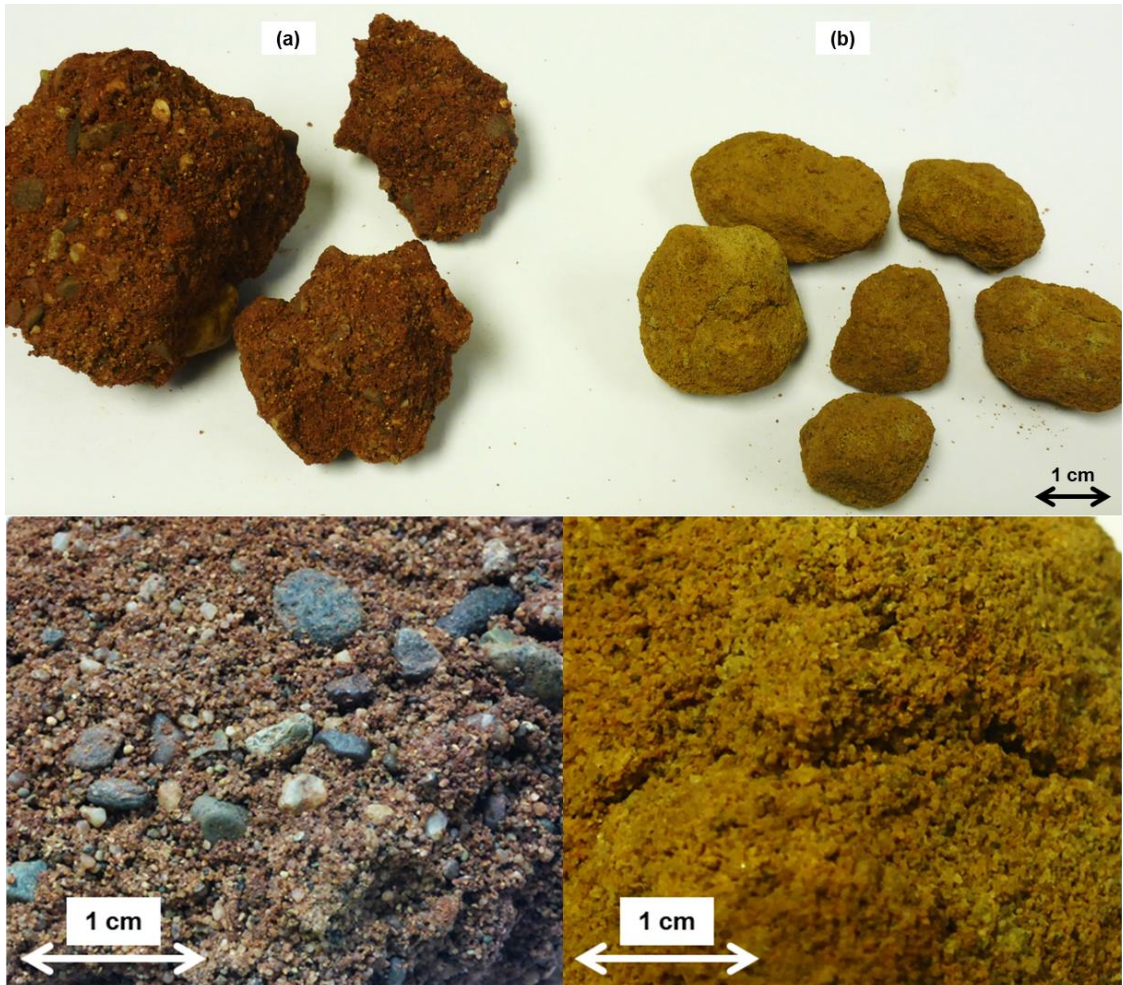


Figure 6.2: Photographs of the saprolite at Hilton (a) and Woburn (b).

6.2.2 Sampling and processing soil and saprolite

Summit, shoulder, backslope, and toeslope positions on both catenas were selected for depth to bedrock surveys, as well as soil and saprolite extraction. At each position, a dynamic cone penetrometer was employed to ascertain the approximate depth of the soil-saprolite interface before a soil pit was dug vertically to this zone. Variations in the consolidation of the profile wall were observed by extracting small cores down the profile and noting the extent to which the material remained intact. These observations were then compared with the penetration resistance data to confirm the depth of the soil-saprolite interface. Samples of saprolite of between 5 and 10 cm thickness were extracted from each interface for cosmogenic radionuclide analysis. A further sample was then extracted approximately 30 cm below this interface.

Beryllium-10 is produced when quartz grains within the uppermost metres of bedrock are bombarded with cosmic rays. In cosmogenic radionuclide analysis, the intensity of these cosmic rays and the weathering of the bedrock (ϵ) are assumed to be constant. Thus, the concentration of ^{10}Be (N) in a sample of bedrock is dependent upon the time that the bedrock has been exposed to cosmic rays, and the rate at which bedrock weathers into mobile regolith (soil). Short exposure times and fast rates of bedrock weathering both lead to lower concentrations of ^{10}Be , and vice versa (Lal, 1991; Stockmann *et al.*, 2014). We assume here that ^{10}Be production and bedrock denudation is at equilibrium.

$$N = \sum_{i=sp, \mu_f, \mu} \frac{P_i(\theta) \cdot e^{-\frac{x}{\Lambda_i}}}{\lambda + \frac{\epsilon \rho}{\Lambda_i}} (1 - e^{-t(\lambda + \frac{\epsilon \rho}{\Lambda_i})}) \quad (1)$$

where: P are the annual production rates of ^{10}Be by spallation, fast muons and stopping muons (denoted by subscripts sp, μf and $\mu\text{-}$) at a surface with slope Θ ; x is the mass sample depth ($\rho \cdot z$); ρ is the density of overburden material; z is the depth of the sample; t is the age of the bedrock surface (the age when the original surface was generated); λ is the decay constant of ^{10}Be with λ equalling $\ln 2 / ^{10}\text{Be}$ half-life; and Λ are the mean attenuation thicknesses of cosmic radiation for different production pathways (Lal, 1991). Here, we considered t as infinite to calculate the apparent weathering rate ϵ , assuming that the age of the landscape is old enough for the ^{10}Be depth-profile to be in equilibrium. By studying two samples down the same depth profile, we tested whether the data met this assumption. By measuring N using Accelerator Mass Spectrometry (AMS), Eq. (1) was solved for ϵ by simple interpolation of N .

A total of sixteen samples of saprolite (eight from Hilton and eight from Woburn) were prepared for AMS at the Cosmogenic Isotope Analysis Facility, East Kilbride, Scotland. After mineral separation, quartz cleaning, and procedures leading to the preparation of BeO sample cathodes (Kohl and Nishiizumi, 1992; Fifield, 1999; Corbett *et al.*, 2016), AMS measurements were carried out at the SUERC AMS laboratory (Xu *et al.*, 2010) (see Appendix 6.1). ^{10}Be concentrations were based on 2.79×10^{-11} $^{10}\text{Be}/^9\text{Be}$ ratio for the NIST Standard Reference Material 4325. The processed blank ratio ranged between 5 and 24% of the sample $^{10}\text{Be}/^9\text{Be}$ ratios. The uncertainty of this correction is included in the stated standard uncertainties.

As first demonstrated in Evans *et al.* (2019), the interpolation of N to solve for ϵ must account for the variability in the density of the soil above the point of sampling because the overburden density exerts an influence on the attenuation of cosmic rays down the profile. The CoSOILcal model (Rodés and Evans, 2019) was applied in this study to calculate soil formation rates using empirically measured soil bulk densities from each catena position, at both sites. In addition, the annual production rate of ^{10}Be was calculated, accounting for obstructions that would reduce the cosmic ray flux to the parent material (Phillips *et al.*, 2016; Evans *et al.*, 2019). These local ^{10}Be production rates were normalized by inputting site elevation, latitude and longitude data into the CRONUS-Earth Matlab code v2.3 using Lal/Stone (St) scaling (Balco *et al.*, 2008). Version 2.3 incorporates new reference production rates derived from Borchers *et al.* (2016).

The calculated soil formation rates were plotted to derive the soil production function (P):

$$P = W e^{\left(\frac{-h}{\gamma}\right)} \quad (2)$$

where W is the soil formation rate at zero soil thickness (h) and γ determines the soil thickness when soil formation is reduced by $1/e$. Both W and γ were calculated using least-squares regression.

Soil samples were extracted every 10 cm from the profile wall of each catena position at both sites. These samples were then oven dried at 105°C for twelve hours, grounded with a pestle and mortar, and sieved to remove the > 2 mm fraction. Using these samples, stone-corrected bulk density measurements were calculated. A Beckman Coulter Laser Diffraction Particle

Sizing Analyser LS 13 320 was employed for particle size analysis (pump speed: 70%; sonication: 10 seconds; run length: 60 seconds). Soil carbon was determined from separate 5 g sub-samples using mass loss following heating at 550°C for twelve hours in a Carbolite furnace (CWF 1300) (see Appendix 6.2).

6.3 Results and discussion

6.3.1 Soil profiles at Hilton and Woburn

At Woburn, the soils are classified as Arenosols (IUSS Working Group WRB, 2015). Both the topsoil and subsoil at each hillslope position have a coarse sand texture, with the mean particle size distribution being 83% sand, 10% silt and 7% clay, which was consistent down the soil profile. At the summit, an Ap horizon of 30 cm thickness, with a mean bulk density of 1.2 g cm³, overlies an iron pan between 30 and 70 cm. This was a hardpan horizon, principally cemented by iron oxides, which did not disaggregate when subject to manual pressure in the field. The consequential greater density of this iron pan (1.6 g cm³), and the effect on the attenuation of cosmic rays, is accounted for. The CoSOILcal model, employed in this study to calculate soil formation rates from measured ¹⁰Be concentrations, considers the density profile of the soil overlying the soil-saprolite interface (Rodés and Evans, 2019). At the bottom of this iron pan is the soil-saprolite interface, under which lies moderately consolidated, cross-bedded saprolitic sandstone with a mean bulk density of 1.5 g cm³. The LOI content decreases from 2.49% in the Ap horizon to 1.53% in the underlying subsoil to a depth of 100 cm. The iron pan observed at the summit is not present down the soil profiles at the other hillslope positions surveyed. At the shoulder and backslope, the thickness and mean bulk

density of the Ap horizon is 27 cm (1.4 g cm^3) and 30 cm (1.5 g cm^3), respectively, and both are underlain by an undifferentiated subsoil, extending down to 40 cm at the shoulder (incidentally, the shallowest soil down the catena) and 66 cm at the backslope. The mean bulk density for both the shoulder and backslope B horizons is 1.5 g cm^3 . The LOI content at the shoulder and backslope also demonstrates similar trends to the summit, with the Ap horizon having a LOI content between 2.06 and 2.21% which decreases to 0.8 and 1.04% in the B horizon. At the toeslope, there are two distinct A₁ and A₂ horizons; an A₁ mantle extending from the surface down to 35 cm (with a mean bulk density of 1.3 g cm^3) burying an A₂ horizon that extends down to 50 cm (with a mean bulk density of 1.6 g cm^3). The B horizon is similar to that observed at the shoulder and summit, with a density of 1.5 g cm^3 , except for the fact that this horizon extends to 170 cm, making this profile the thickest. The toeslope also has the greatest LOI content, with 2.85% in the A₁ horizon, 2.05% in the A₂ horizon, and 1.21% in the B horizon. The presence of an A_p horizon at each catena position may be explained in part by the mixing of mineral and organic material through cultivation following the harvest, although isotopic work at Woburn is required to verify this.

At Hilton, the soils are also classified as Arenosols (IUSS Working Group WRB, 2015) and are of a coarse sand texture, with the mean particle size distribution being 80% sand, 15% silt and 5% clay. Overall, the soil profiles surveyed at Hilton show less evidence of horizonisation than those at Woburn. At the summit, the A horizon is 30 cm in thickness with a mean bulk density of 1.4 g cm^3 , below which lies a 75 cm B horizon with a mean bulk density of 1.6 g cm^3 . The soil-saprolite interface is observed at 105 cm, below which the

profile grades into saprolitic, moderately consolidated sandstone. The LOI content decreases from 4.98% in the A horizon to 0.94% in the underlying subsoil. At the shoulder, the A horizon is 10 cm thick and, in places, it is less distinct. The loose and friable nature of the soil at the surface explains its relatively low bulk density: 1 g cm^3 . The B horizon extends to 80 cm, below which the material becomes more consolidated (mean bulk density is 1.4 g cm^3) and saprolitic. Here, the A horizon has a LOI content of 4.89%. This contrasts with the B horizon where the mean LOI content is 0.96%. The thinnest soil is found at the backslope, with the soil-saprolite interface observed at 50 cm. The soil comprises a 10 cm A horizon, and like the shoulder, has a relatively low bulk density of 0.8 g cm^3 . The B horizon is 40 cm and has a mean bulk density of 1.3 g cm^3 . The LOI content of the A horizon is 4.16%. Below this, the mean LOI content falls to 2.15%. Finally, the soil at the toeslope is 100 cm thick. Although this is also the case for the summit, the toeslope profile exhibits a comparatively thicker A horizon (40 cm) suggesting that colluviation has, or is still, happening at this position. However, the presence of a grass and shrub cover at Hilton suggests that colluviation rates are currently slow, if not negligible. Despite the thicker A horizon, the mean LOI content (3.06%) is smaller than that observed for the summit, but the mean bulk density is similar (1.4 g cm^3). In the 60 cm B horizon, the mean LOI content falls to 1.49% and the mean bulk density is 1.5 g cm^3 .

6.3.2 Soil formation rates

Soil formation rates were calculated from measured ^{10}Be concentrations at Hilton and Woburn. At Hilton, these range from 0.065 to 0.193 mm y^{-1} , with

the mean soil formation rate being $0.128 \pm 0.043 \text{ mm y}^{-1}$ (Figure 6.3; see Appendix 6.1). At Woburn, soil formation rates range from 0.031 to 0.150 mm y^{-1} , with the mean being $0.100 \pm 0.051 \text{ mm y}^{-1}$, which is 0.029 mm y^{-1} slower than that at Hilton.

Down both catenas, the depths to saprolite are in accordance with geomorphological theory (Figure 6.4). At the shoulder and backslope, the soil is thinner as the steeper convexities are typically more susceptible to erosion than the shallower plateau found at the summit. At Woburn, the deposition of soil from upslope has contributed to a thickened Ap horizon at the toeslope, with the depth to saprolite being 0.7 m greater than that at the summit, and more than double that found at the shoulder and backslope. However, this extent of colluviation is not as readily observable at Hilton, with the depth to saprolite at the toeslope (1 m) approximately equal to that of the summit (1.05 m). This could be due to the fact that the hillslope has been almost constantly vegetated, thus limiting the potential for downslope soil redistribution.

Data from both sites suggest that soil formation rates are slower under thicker soil profiles (such as those observed at the summit and toeslope positions). This largely supports the conclusions previously observed for two other sites in the UK (Evans *et al.*, 2019). Under a thicker soil, the bedrock is buffered more effectively from climate fluctuations, organism activity at the surface, and other subaerial factors that may promote bedrock weathering (Minasny and McBratney, 1999; Wilkinson and Humphreys, 2005).

Given the relationship between soil thickness and rates of soil formation, it is prudent to determine the soil formation rates for a given thickness at both

sites. This is achieved by calculating the soil production function, which can indicate the soil formation rate at a set soil thickness (Appendix 6.3). At zero soil thickness, the soil formation rates at Hilton and Woburn are 0.164 mm y^{-1} and 0.229 mm y^{-1} , respectively. The soil production function can also indicate the depth scale over which soil formation decreases by $1/e$ (see Eq. 2). At Hilton, this is 3 m, which is similar to that found in Evans *et al.* (2019) but still considerably greater than that calculated in previous studies (Heimsath *et al.*, 1997; Heimsath *et al.*, 1999; Wilkinson *et al.*, 2005). At Woburn, this decay is more than half that, at 1.15 m. This demonstrates that soil formation rates are more sensitive to soil thickness at Woburn than they are at Hilton. Given this analysis, both raw measurements of soil formation, and those modelled using the soil production function, will be presented hereafter.

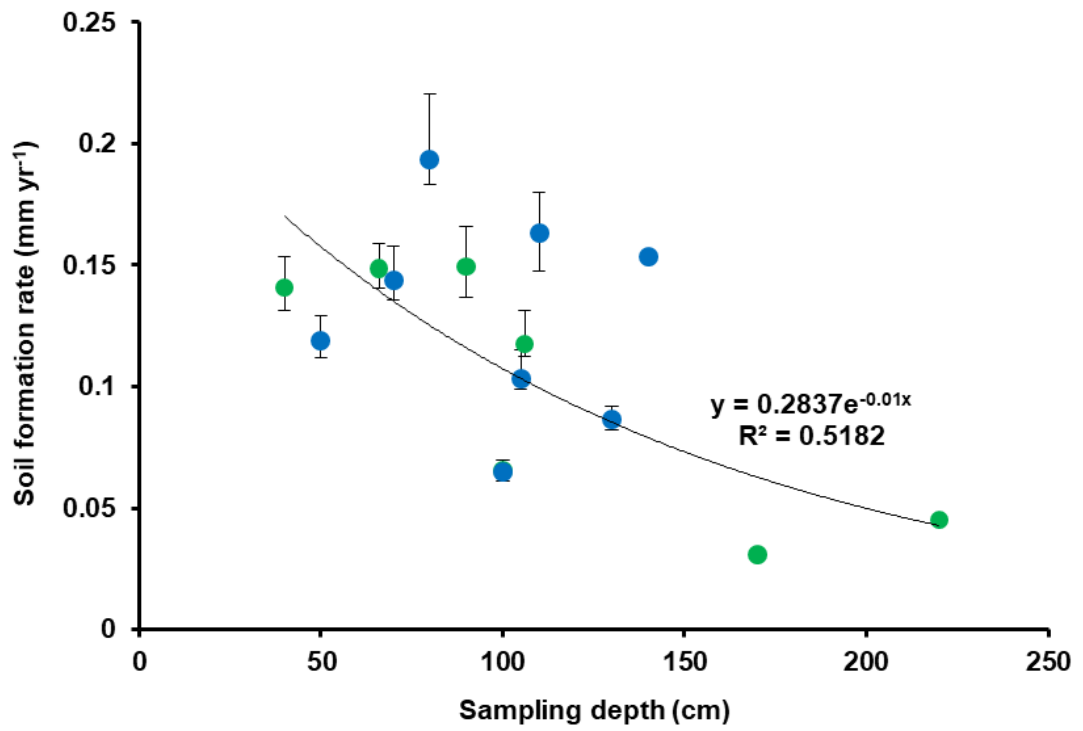


Figure 6.3: Soil formation rates against sampling depth for Hilton (blue; $n = 8$) and Woburn (green; $n = 7$). The error bars represent one standard deviation uncertainties.

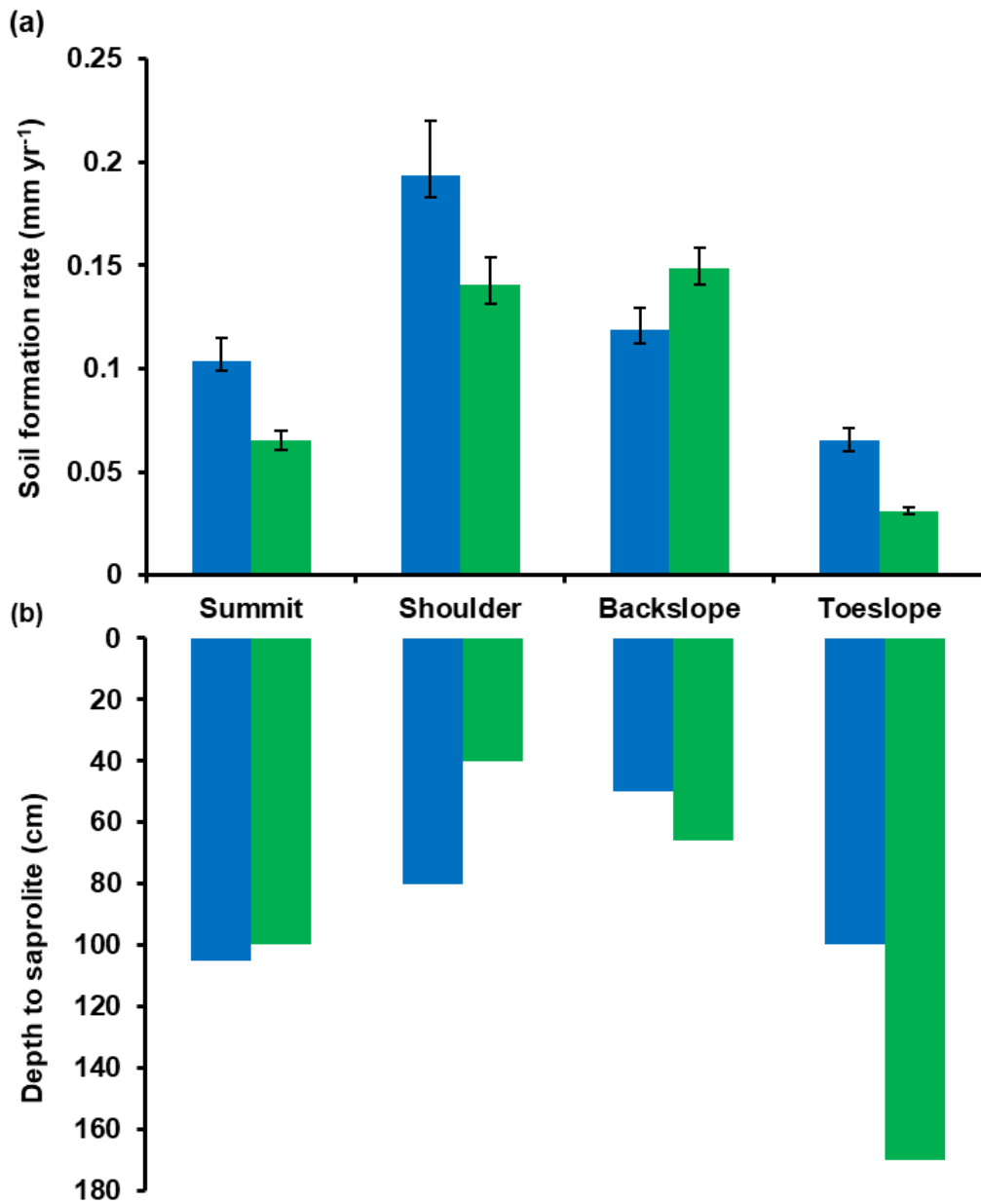


Figure 6.4: Soil formation rates and the depths to saprolite for the four landscape positions at Hilton (blue; $n = 4$) and Woburn (green; $n = 4$). The soil formation rates here represent a 'best fit' calculated using two ^{10}Be concentrations down the same depth profile. The error bars represent one standard deviation uncertainties.

6.3.3 Lithological variability: the role of the sandstone porosity and matrix

Figure 6.5 compares soil formation rates measured at Hilton and Woburn with those previously calculated for two other sandstone sites in the UK: Rufford Forest Farm, in Nottinghamshire, and Comer Woodland, in Shropshire (Evans *et al.*, 2019). Like Hilton, the soil at Rufford Forest Farm (Rufford, hereafter) has formed from the Sherwood Sandstone (Chester formation, Olenekian, 247-251 Ma) which has been described as fluvially-derived, pinkish to red, medium to coarse grained, pebbly, cross-bedded and friable (see Radley and Coram, 2016). In contrast, the soils at Comer Wood (Comer, hereafter) stem from the New Red Sandstone (Bridgnorth formation, Cisuralian, 273-299 Ma). This sandstone is of aeolian origin, and has been described as brick-red, medium grained, and cross-bedded (British Geological Survey, 2020). Further contextual details about Rufford and Comer can be found in Evans *et al.* (2019).

Figure 6.5 suggests that there are upper limits to the soil formation that can be achieved for a given soil thickness. Soil formation rates are then reduced according to other factors. Given that the data here stemmed from one climate, we suggest that this reduction can be explained by the lithological composition of the parent material. Moreover, we suggest that sandstone porosity is one of the principle factors influencing the rates of soil formation across these sites. The porosity of the saprolite will determine the extent of subsurface storage space and flow pathways for meteoric water. Saprolite with a greater porosity will have an increased water storage capacity, allowing

more mineral surfaces to be in contact not only with water, but the oxidants and acids (e.g.: fulvic, humic, oxalic, and citric acids) that can induce chemical weathering reactions (Lazo *et al.*, 2017). As chemical weathering progresses, increasing both the surface area of and overall access to these mineral surfaces, the secondary porosity of the saprolite will similarly increase (Schmidt and McDonald, 1979). This highlights a positive feedback relationship between chemical weathering (and, therefore, soil formation) and porosity (Hayes *et al.*, 2019; Lebedeva and Brantley, 2020).

Table 6.2 demonstrates the role of porosity in governing rates of soil formation. Given that soil thickness also differs between sites, and could also influence rates of soil formation, here we will focus our analysis only on the rates of soil formation calculated for zero soil thickness, using the soil production function. Soil formation at Woburn at zero soil thickness was 1.4 times faster than that at Hilton, and nearly four times faster than that at Rufford. One explanation for this is that the sandstone at Woburn has a relatively high porosity (~ 35%) in contrast to the Helsby sandstone formation at Hilton (~ 6 – 27%) and the Chester formation at Rufford (~25%) (Burley, 1984; Bloomfield *et al.*, 2006). By having a greater porosity, the sandstone at Woburn would store and transmit a greater proportion of precipitation that infiltrates down the soil profile. Greater storage of water within the Woburn sandstone would allow more mineral surfaces to be in contact with water and, in consequence, amplify chemical weathering processes. Conversely, the smaller porosities observed in the Sherwood Sandstones would imply a slower transmission of water through the rock, thus slowing down bedrock weathering.

There are multiple reasons to explain why the porosity of the saprolite at Woburn is greater than that at Hilton and Rufford. We suggest the predominant factor influencing porosity in this case is the depth of burial, and the temperatures and pressures that are associated with this. The depth of burial of the Woburn sandstone formation is relatively shallow (approximately 300 m) when compared with the Sherwood Sandstones at Hilton and Rufford (approximately 1000 m) (Burley, 1984; Palmer and Barton, 1987; Evans *et al.*, 1993). Previous work has shown that overburden compaction increases linearly with depth (Ramm, 1991). This suggests that deeper burials, such as that at Hilton, are more effective at reducing porosity since a greater overburden compaction can induce more rotation, re-orientation, and plastic deformation of ductile particles (Palmer and Barton, 1987).

In addition, the consequence of a deeper burial in the Sherwood Sandstone group would have been to increase grain-to-grain contacts within the bedrock. This ratio expresses the difference between the length of contact a grain has with its neighbouring grains, and its own individual length (Dyke and Dobereiner, 1991). Previous work elsewhere has demonstrated a strong relationship between grain contact and the strength of sandstone (Dobereiner, 1984). At Hilton and Rufford, we suggest that the greater grain-to-grain contact induced by a deeper burial may explain why these sites exhibit relatively smaller porosities than those observed at Woburn and, by extension, why soil formation rates at Hilton and Rufford are comparatively slower.

In addition to enhancing grain-to-grain contact, greater burial depths have also been shown to amplify processes of cementation within sandstones. For example, Bloch *et al.* (2002) found that greater temperatures (> 100°C)

associated with deeper burials can lead to quartz dissolution, which subsequently results in the precipitation of quartz cements. These quartz cements can bind as overgrowths to the uncoated surfaces of mineral grains within the sandstone, and strengthen their physical integrity. The additional strength provided by these overgrowths would further reduce the susceptibility of the sandstone to weathering processes. Previous work that has been undertaken on the deeply buried Sherwood Sandstones has found a pervasive presence of quartz overgrowths which, in many cases, occlude porosity (Burley, 1984). Furthermore, an increase in the grain-to-grain contact ratio in the Sherwood Sandstones would have reduced the intergranular pore volumes. A consequence of this is that a relatively smaller volume of cementing agents would have been required to cause cohesion between these mineral grains. In Hilton, Comer, and Rufford, iron oxides (mostly in the form of hematite) have often been shown to cause this intergranular welding. The formation of hematite predominantly occurred as a result of the alkaline Triassic groundwaters oxidising iron into ferric oxide. The red pigmentation exhibited in Figure 6.2a demonstrates the presence of hematite in the saprolite underlying Hilton.

By contrast, the shallow burial of the sandstone at Woburn would have resulted in a different array of diagenetic conditions. The relatively lower temperatures and pressures would have reduced quartz dissolution reactions and the subsequent precipitation of quartz overgrowths. Moreover, Palmer and Barton (1987) found a relative absence of quartz overgrowths in the Woburn sandstone in a comparison with similar lithologies, such as the Wyoming Sands. The lack of iron oxides in the sandstone at Woburn may be

a legacy of the marine conditions in which the sandstone was laid. Seawater has a relatively low concentration of iron (Bloch *et al.*, 2002) which may explain why the saprolite exhibits less evidence of hematite. Further analysis, such as the use of SEM imaging, is required to verify the relative abundance and absence of intergranular cements within the saprolite sampled at Hilton and Woburn.

During the initial formation of the Helsby and Woburn sandstone formations, the dominant environmental conditions suggest that evaporitic minerals may have composed part of the matrix material. In the case of the Helsby sandstone formation at Hilton, the climatic conditions of the Triassic period would have led to the extensive formation of evaporite minerals within the rock. In *confined* Sherwood Sandstone aquifers, to which meteoric waters have not gained access, evaporite minerals are still observable today (Burley, 1984). However, for unconfined aquifers, such as the Helsby sandstone at Hilton, isotope evidence suggests that these Triassic evaporites subsequently dissolved as a result of being flushed with cool, fresh, meteoric waters (Burley, 1984), potentially during the Pleistocene (Downing *et al.*, 1987; Tellam, 1995). Similarly, the marine provenance of the sandstone at Woburn suggests that halite, in particular, would have been abundant in the initial depositional stages; indeed, it would have likely been more abundant than that which formed at Hilton. Despite the fact that halite would have initially filled the pores in the sandstone at Woburn, this mineral is highly soluble, and would have dissolved rapidly. Milodowski and Wilmot (1985) suggest that the dissolution of evaporitic minerals at Woburn is largely responsible for the great porosities observed in the sandstones underlying this site.

Another example of a matrix mineral previously shown to give structural integrity to saprolite is clay. Heimsath and Whipple (2019) present a conceptual model that builds on earlier work which suggests that as soils develop and thicken from the underlying saprolite, soil formation rates decrease. This induces a delay in the formation of soil from saprolite (Heimsath and Whipple, 2019) and consequently leads to some clays and secondary minerals forming within it that may act to retain some structural integrity for longer. In a similar way that soil shear strength increases with greater clay content (Stark and Eid, 1994), Heimsath and Whipple (2019) suggest that the clays which begin to accumulate within the saprolite can increase its resistance to further physical weathering or disruption by helping to retain its structural integrity, thus reducing rates of soil formation. Although the authors do not present measured clay contents, they do show that the shear strength of saprolite increases as the overlying soil thickens, and propose that original clay or re-precipitated clay formation plays a large role in maintaining some structural integrity within the saprolite.

Mean particle size distributions for the saprolite sampled from Hilton and Woburn are presented in Table 6.3 (see Appendix 6.4). It shows that the proportions of clay-sized material within both sandstone formations are similar. As a result, we suggest that the importance of clay for strengthening the structural integrity of the saprolite at Hilton and Woburn is secondary to that of the depth of burial. However, there is some evidence to suggest that clay may affect soil formation rates across the two sites. Figure 6.6 shows a moderately strong negative relationship between clay content and rates of soil formation ($R^2 = 0.6$). It should also be noted that the effect of clay in

maintaining the structural integrity of saprolite may be diminished at Hilton and Woburn because these sites were subjected to periglacial processes during the Last Glacial Maximum (LGM). Moreover, the Active Layer Development (ALD), and the seasonal freeze thaw processes associated with periglacial environments, would have broken some physical bonds between particles in the saprolite (Tye *et al.*, 2012). Between the end of the LGM and the onset of deforestation, tree roots would have also played a similar role in degrading the structure of the regolith, through breaking the physical binding of the clays that act as forms of cohesive cements within the saprolite.

In some cases, analysing porosity *per se* may not be sufficient to explain the differences in rates of soil formation. For example, the rate of soil formation for zero soil thickness at Comer was about 1.3x faster than at Rufford, despite the fact that their respective sandstone porosities are similar (24 – 26%) (Allen *et al.*, 1997). Similarly, the soil formation rate for zero soil thickness at Hilton is nearly three times as fast as that at Rufford, despite the fact that both sandstone formations underlying these sites stem from the same Permo-Triassic parent rock (the Sherwood Sandstone group) and their porosities are almost identical (~ 24 – 25%). Here, we should acknowledge other hydrogeological processes and, in particular, the role of permeability: a “measure of the capacity of a rock or soil to transmit fluids” (Goudie, 1994, p. 381). This necessitates a wider understanding of bedrock features, like fractures, that may promote fluid flow (Neuman, 2005). Recent work by Critical Zone scientists has elucidated the feedback processes that may occur between bedrock weathering and the formation of fractures. Worthington *et al.* (2016) found that weathering is often focussed in the vicinity of fractures,

since fluids are concentrated along them, and this weathering could subsequently be a major factor that induces further fracturing, promoting greater permeability. Although the primary measurement of permeability was beyond the scope of this study, previous work has been published that may explain the difference in soil formation rates across sites with similar porosities. For example, faults and fractures observed in the Helsby sandstone underlying Hilton have been shown to increase its hydraulic conductivity to $> 10 \text{ m d}^{-1}$. This is in contrast to the hydraulic conductivities observed for the Chester Formation at Rufford ($0.5 - 5 \text{ m d}^{-1}$) (Allen *et al.*, 1997; Griffiths *et al.*, 2003). Given that it has been shown that weathering is often enhanced around fractures, these greater hydraulic conductivities at Hilton may, in part, be responsible for the faster soil formation rates at this site when compared to Rufford. However, further empirical evidence is required to validate this hypothesis.

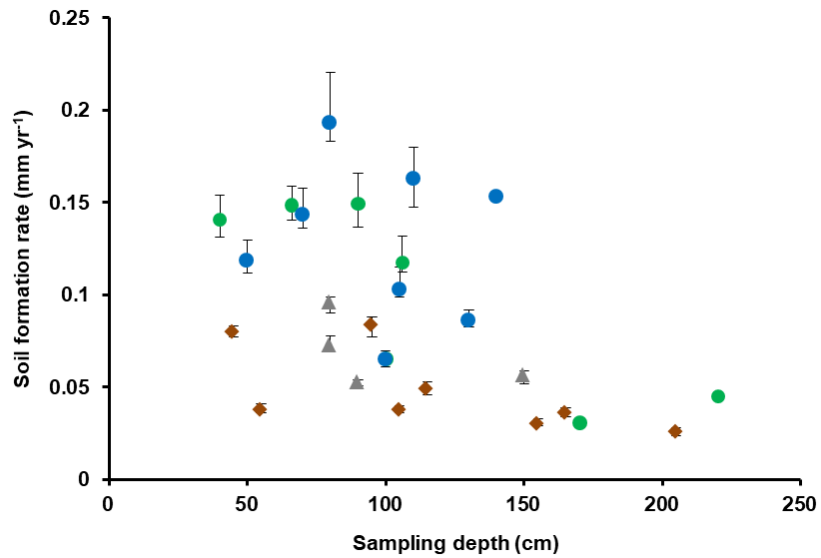


Figure 6.5: Soil formation rates against sampling depth for Hilton (blue; $n = 8$) and Woburn (green; $n = 7$) with those previously measured at Rufford Forest Farm (brown diamonds; $n = 8$) and Comer Wood (grey triangles; $n = 4$). The error bars represent one standard deviation uncertainties.

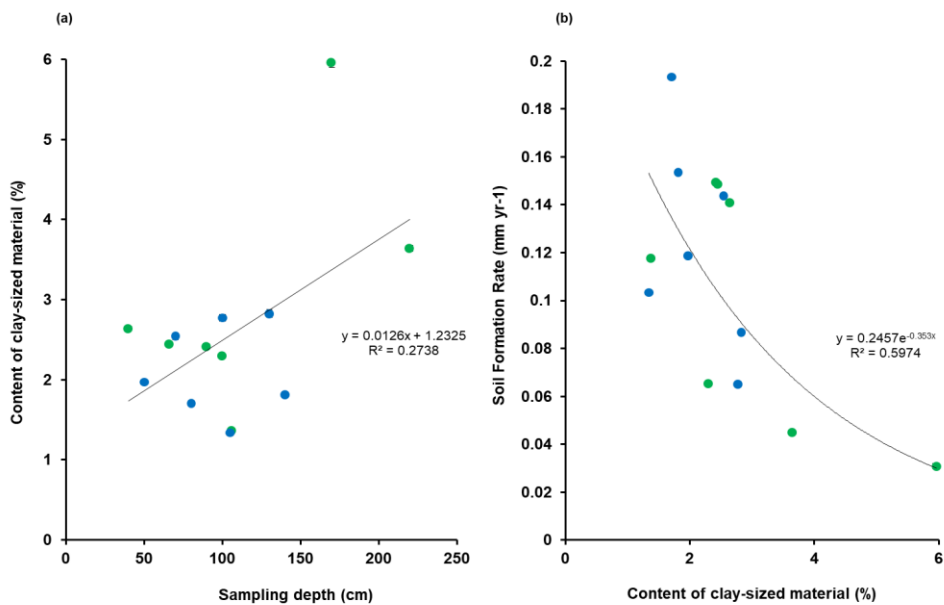


Figure 6.6: Analysis of the relationship between sampling depth and the content of clay-sized material in the saprolite (a) and that between the clay-sized material in the saprolite and the soil formation rate (b) for Hilton (blue; $n = 7$) and Woburn (green; $n = 7$).

Table 6.2: Properties of the sandstone and soil formation rates for each of the four sites in this chapter.

		Comer	Hilton	Rufford	Woburn
Sandstone formation		Bridgnorth	Helsby	Chester	Woburn
Provenance		Aeolian; Draas and linear dunes	Fluvial; channels; lateral dune and bar migration	Fluvial; Gravelly to sandy braid plains	Marine; Offshore tidal sand wave bar
Period and Age (Ma)		Cisuralian, Early Permian; 273 – 299	Anisian, Middle Triassic; 242 – 247	Olenekian, Early Triassic; 247 – 251	Aptian, Early Cretaceous; 101 – 125
Depth of Burial (m)		~ 1000	~ 1000	~ 1000	~ 300
Porosity (%)		24 - 26	6 – 27	~ 25	~ 35
Matrix composition		K-feldspars, authigenic clays, hematite, detrital rock fragments	Ferroan dolomite, hematite, detrital mica, authigenic clays	Micaceous, coarse to fine, silty matrix; pebbles/ cobbles	Alkali feldspar, glauconite, muscovite, calcite; negligible clays
Gamma value^a		1.9	3.0	2.5	1.1
Soil Formation Rate (mm y⁻¹)	<i>Mean</i>	0.046	0.128	0.037	0.100
	<i>Zero soil thickness^b</i>	0.076	0.164	0.058	0.229

^a Calculated soil thickness when soil formation is reduced by $1/e$ using the soil production function (see Eq. 2 in *Methods*).

^b Soil formation rates calculated using the soil production function (see Eq. 2 in *Methods*).

Table 6.3: Particle size distributions for the saprolite sampled at Hilton and Woburn.

		Mean Particle Size Distribution (%)	
		Hilton ($n = 7^a$)	Woburn ($n = 7^a$)
Clay		2.1*	3.0*
Silt		5.4**	6.7**
	<i>Very fine</i>	4.2	3.7
	<i>Fine</i>	24.2***	39.9***
Sand	<i>Medium</i>	47.5	41.0
	<i>Coarse</i>	15.4****	5.1****
	<i>Very coarse</i>	1.0	0.6
Median grain size^a (μm)		310	227
Mean variance (a.u.^d)		4.16	4.64
Mean skewness (a.u)		2.31	2.60

^a Mean of the sample for each site. Data for CRN2 and CRN12 are omitted from this analysis because of equipment failures during measurement.

^b Starred values denote the presence of statistically significant different (U test; $P < 0.05$).

^c Clay: $< 8 \mu\text{m}$; Silt: $8 - 63 \mu\text{m}$; Very fine sand: $63 - 100 \mu\text{m}$; Fine sand: $100 - 250 \mu\text{m}$; Medium sand: $250 - 500 \mu\text{m}$; Coarse sand: $500 - 1000 \mu\text{m}$; Very coarse sand: $1000 - 2000 \mu\text{m}$.

^d a.u = arbitrary units.

^e Full dataset can be found in Appendix 6.4.

6.3.4 Comparison with global inventory

Figure 6.7 compares soil formation rates from Hilton and Woburn with those from other sandstone-derived soils taken from the published literature ($n = 60$; Appendix 2.1). Scholars have previously shown that climate is one of the most influential factors in constraining rates of soil formation (Stockmann *et al.*, 2014). Therefore, in order to reduce the influence that climate may have on this analysis, the data that comprise this global inventory stem from temperate climates only.

The data from the global inventory demonstrate a reduction in soil formation rates as soils thicken. In accordance with previously published analyses, soil formation rates fall by more than an order of magnitude between soil thicknesses of 0 and 50 cm. Between 50 and 100 cm, this decline is less pronounced with rates oscillating between ~ 0.01 and 0.06 mm y^{-1} . Comparing the data from both this study and Evans *et al.* (2019), with those from the published inventory, presents two important findings.

First, for soils between 40 and 100 cm in thickness, soil formation rates from Hilton and Woburn are similar to those from the global inventory. The pattern is one of quasi steady-state where rates do not significantly decline with increasing soil thickness and, instead, are enveloped within a range ($\sim 0.07 - 0.19 \text{ mm y}^{-1}$). However, in the majority of instances, the rates from Hilton and Woburn are towards the upper end of, if not greater than, those previously published.

Second, for soils thicker than 100 cm, the data from Hilton and Woburn show a linear negative relationship between soil formation rates and soil thickness.

Given that there is only one rate presented for soils thicker than 100 cm from the global inventory, the data from Hilton and Woburn, together with those from Rufford and Comer, represent an important contribution to our knowledge of soil formation for deeper soils.

The soil formation rates calculated using the soil production function also show that Hilton and Woburn are toward the upper end of, if not greater than, the range of those previously published. At Hilton and Woburn, the rates at zero soil thickness are 0.229 mm y^{-1} and 0.164 mm y^{-1} , respectively. These contrast by more than an order of magnitude with those from both Heimsath *et al.* (1997) and Wilkinson *et al.* (2005), where soil formation rates at zero soil thickness were 0.068 mm y^{-1} and 0.02 mm y^{-1} , respectively.

One explanation for why soil formation rates at Hilton and Woburn are towards the upper end of, if not greater than, those previously published could be because of the volume and composition of the sandstone matrix. Many of the sandstones previously studied are classified as 'wackes' (using the Pettijohn *et al.*, 1987 scheme) due to the fact that 15% of their rock volume is matrix material. This contrasts with the arenite sandstones found at Hilton and Woburn, where the matrix material comprises less than 15% of the total rock volume. By supporting a denser matrix, the rock inherently has a lower porosity, which can reduce the rates of weathering and soil formation processes.

For example, Wilkinson *et al.* (2005) conducted work on the Blue Mountains in Australia, where the climate is described as mild temperate. The parent material was a moderately to strongly lithified Triassic sandstone, dominated

by cobbles of ferruginous sandstone that are resistant to weathering, which were neither observed at Hilton nor Woburn. At 50 cm, the soil formation rate on the Blue Mountains was nine times slower than that at Hilton for the same soil thickness. We believe that the bands of relatively resistant sandstone, cemented by an iron-enriched matrix, are in part responsible for the slower soil formation rates measured on the Blue Mountains. Similarly, Heimsath *et al.* (2001b) measured soil formation at Coos Bay, located along the Oregon coast range, in the USA. The soils are underlain by an Eocene arkosic wacke: a sandstone with a matrix comprising more than 15% by volume, and more than 25% feldspar. At 100 cm, the soil formation rate at Coos Bay was 0.014 mm y⁻¹, five times slower than that at Woburn, where the absence of this matrix promotes the transmission of water and weathering processes (Cummins, 1962).

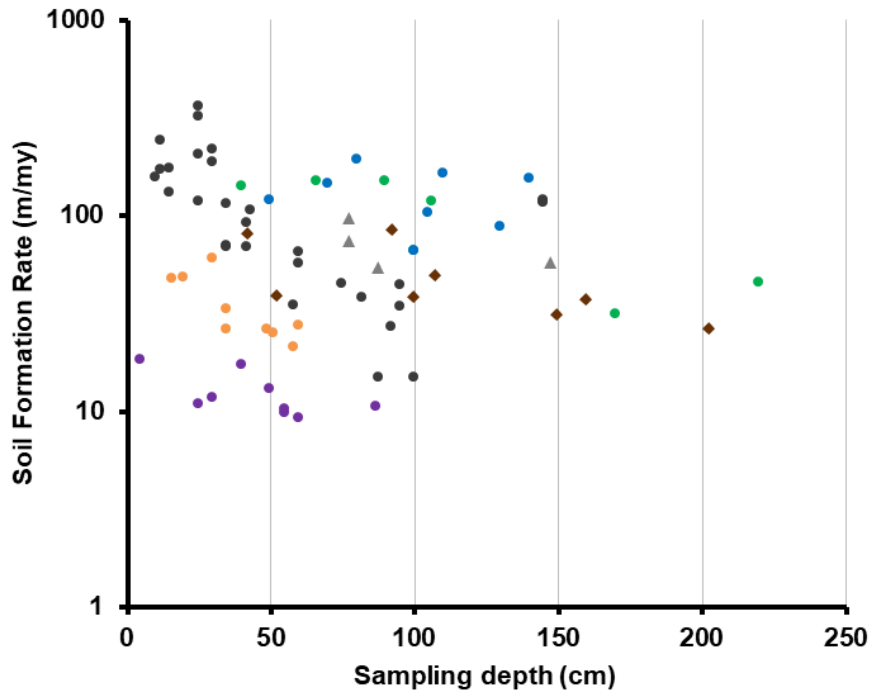


Figure 6.7: Soil formation rates from Hilton (blue; $n = 8$) and Woburn (green; $n = 7$), together with those from Rufford Forest Farm (brown diamonds; $n = 8$), Comer Wood (grey triangles; $n = 4$), and those from a globally compiled inventory of soil formation rates on sandstone geology from Heimsath *et al.*, 1997 (orange circles; $n = 9$), Heimsath *et al.*, 2001b (grey circles; $n = 30$), and Wilkinson *et al.*, 2005 (purple circles; $n = 9$).

6.4 Conclusions

In this study, we have investigated the extent to which the lithological variability of sandstone governs rates of soil formation. Cosmogenically-derived rates of soil formation for two UK hillslopes range from 0.031 – 0.193 mm y⁻¹, with the means being 0.128 ±0.043 mm y⁻¹ and 0.100 ±0.051 mm y⁻¹ for Hilton and Woburn, respectively. In addition to being only the second study in the UK to measure soil formation for soils currently supporting arable agriculture, the sandstone-derived soils studied here represent some of the deepest profiles that have been subject to cosmogenic radionuclide analysis.

We found that soil formation rates at Woburn are faster than those measured at Hilton, and suggest here that this may be substantially governed by the lithological variabilities exhibited between the two sandstone formations. The sandstone at Woburn has a greater porosity than that at Hilton, enabling more mineral surfaces to be in contact with water, and this leads to faster rates of bedrock weathering. This smaller porosity at Hilton is partly brought about by increased grain-to-grain contact, as a direct result of a greater depth of burial. The greater temperatures and pressures associated with a deeper burial would have additionally led to the cohesion of mineral grains by intergranular cements. One of the effects of these cementing agents is to slow down the transmission of water through the bedrock and reduce rates of chemical weathering.

Similarly, the rates from the arenite sandstones of Hilton and Woburn are, in some cases, up to nine times faster than those previously obtained by scholars working on wackes. Here, we suggest that these matrix-abundant

wackes reduce the transmission of water and slow down the processes of bedrock weathering. These findings highlight the need for a more precise insight into the mineralogy and petrology of the parent material when interpreting rates of soil formation.

Our work has opened a new research gap for soil formation scholars. This community has hitherto measured soil formation rates and compared them across major rock types (igneous, sedimentary, and metamorphic). An area that has not enjoyed equal investment is an exploration into the role of the mineralogical and petrographic variations within a single rock group in governing rates of soil formation. Having shown here the breadth of soil formation rates across different types of sandstone, more work is required to study other sedimentary units and, indeed, different types of igneous and metamorphic lithologies, too.

Acknowledgements

The authors wish to thank Steve McGrath, Stephen Goward, Andy Macdonald, Ian Shield and Robert Copley for permission to carry out fieldwork at Woburn Experimental Farm, and Mike Fullen, Andrew Black and Richard Wills for permission to sample at Hilton Experimental Site. We thank Phil Styles and Robert Tuckwell for fieldwork assistance at Woburn, and likewise, Pedro Velloso Gomes Batista and Miroslav Bauer for their support at Hilton. We also wish to thank Allan Davidson, Ángel Rodés, and Derek Fabel at the NERC Cosmogenic Isotope Analysis Facility for preparing samples for AMS, and their subsequent assistance in data analysis.

Chapter 7: Discussion and conclusions

7.1 Introduction

This thesis began by recognising the disciplinary renaissance occurring in soil science. Over recent decades, soil science has strengthened its liaisons with neighbouring disciplines, and forged new interdisciplinary alliances with emerging fields (Brevik *et al.*, 2015). As a result of this cross-fertilization, soil resources are more regularly discussed across a wide range of terrestrial science. Moreover, soil is now acknowledged as an important nexus in environmental systems, bridging discourses which were hitherto discrete, and highlighting opportunities for wider interdisciplinarity.

It is exactly a century since the publication of *The World's Food Resources* (von Engel, 1920) in which the author proposes solutions to expand the food supply for a climbing world population, but fails to acknowledge the role of soils. A century on, the services provided by soils are ubiquitous, and the need to conserve them is manifest. Soils have been identified as essential resources with which to combat global sustainability issues, including many of the United Nations' Sustainability Development Goals (e.g.: zero hunger, good health and wellbeing, clean water and sanitation, responsible consumption and production, and life on land).

However, addressing these challenges is more difficult when soils face a number of threats. Whilst soils have been enlisted to tackle climate change, they are also vulnerable to its impacts. Warming-induced changes in the temperature and moisture regimes of soils can increase their decomposition,

and accelerate processes such as erosion and desertification (FAO, 2015).

Finding ways to improve a soil's resistance and resilience to global environmental change, and restoring degraded soils, is therefore paramount.

However, there is arguably a superior priority for soil scientists. The chapters comprising this treatise are hinged on one fundamental principle: the processes, functions, health, productivity, resistance, and recovery of any soil can neither exist nor endure without the presence of the soil material (Power *et al.*, 1980). Thus, one of the chief duties for soil scientists must be to prevent the thinning and loss of soil profiles. In the broadest sense, this call for action heeds and advocates the large body of work already established around soil conservation, and the combatting of soil erosion (Poesen, 2017).

Yet, these efforts have ignored a sizeable knowledge gap. Whilst soil erosion has been measured, monitored, and modelled, we have not made a commensurate effort to obtain the rates of soil formation. In consequence, we have a very sparse knowledge base upon which to consider the future sustainability of global soil resources, and their long-term delivery of ecosystem services. Responding to these knowledge gaps, this thesis has made two contributions to the discourse on soil sustainability. First, it has responded to the impoverished state of the soil formation inventory by empirically measuring rates of soil formation, and furthering our understanding about the factors which govern this process. Second, it has compared soil formation rates with those of soil erosion to forecast soil lifespans. In so doing, it has demonstrated that soil formation rates can be used to help soil scientists quantify the sustainability of these resources. Both of these were set out as

'research challenges' in Chapter 1, and these will now be explored further in this general discussion.

7.2 Research challenge 1: state of the soil formation inventory

Cosmogenically-derived rates of soil formation were presented in Chapter 2. These data represent the soil formation that occurs at the soil-saprolite interface, rather than the weathering that takes place on bare bedrock surfaces, such as outcrops and tors. This inventory – thirteen studies conducted across four countries – represents a research effort spanning fifteen years (1997 to 2012). However, a Web of Science search found that over 1,217 studies were published on the topic of “soil formation” during that time-frame. This suggests that deriving rates of soil formation *per se* was not one of the major foci for this sub-discipline of soil science during this period.

There are still many contexts in which soil formation has not been measured. For example, polar regions have been the subject of relatively little pedogenesis work, despite the fact that these areas are increasingly experiencing large-scale environmental change, such as thawing permafrost and accelerated deglaciation (Liu *et al.*, 2016). Similarly, very little work to derive rates of soil formation has been conducted in monsoonal climates, even though the heavy rainfall associated with summer monsoons may promote bedrock weathering (Shao and Yang, 2012).

This leads to an important question for discussion. Should future efforts to measure rates of soil formation be concentrated in locations that have been hitherto neglected in order to expand the geographical spread of our

knowledge, or focussed more on understanding the fundamental controls that govern soil formation?

In this thesis, both of these foci have arguably been demonstrated. With regards to expanding the geographical spread of our knowledge on soil formation, Chapter 5 presented 12 cosmogenically-derived rates measured across an arable and woodland site in the UK. The former represented the first of their kind globally, since previous work had instead focused on uncultivated 'pristine' soils. Likewise, the rates derived for the woodland site represented the first of their kind in Europe. The rates obtained were found to fall within the range of those previously published for temperate climates, and on sandstone lithologies. Furthermore, this study was only the second of its kind to take place in the UK after Riggins *et al.* (2011). The rates here were significantly greater than those previously obtained for the igneous lithologies on Bodmin Moor, representing an important contribution to our knowledge about soil formation in the UK. Similarly, Chapter 6 presented a further 15 rates for arable and grassland soils in the UK. One of the main findings to stem from this chapter was that rates of soil formation significantly differed from those previously presented in Chapter 5. The variability in soil formation rates demonstrated in these two chapters suggests that further work is necessary to ascertain the full range of soil formation across a wider range of environmental contexts in the UK.

The second proposition presented above was to focus less on the geographical spread of our pedogenesis knowledge, and to instead explore the fundamental mechanisms that govern the process of soil formation. It could be argued that these foci are not mutually exclusive. After all, some of

these controlling variables may be best investigated by measuring soil formation across a range of locations and environmental contexts. For example, a global transect could be established to assess how extreme temperatures and precipitation regimes affect bedrock weathering rates, and this may consequently focus research on new locations and environments. This was the case for the work presented in this thesis. As well as being novel in its selection of field sites, Chapters 5 and 6 made two additional contributions to our knowledge on the factors that govern soil formation.

First, Chapters 5 and 6 presented rates of soil formation for relatively thick (>1 m) soils. Before this work, the median thickness in the soil formation rate inventory was 0.35 m, with only 6% of the dataset reporting rates for soils deeper than a metre. For sandstone lithologies in temperate climates, there was only one rate presented for soils deeper than a metre. Therefore, the soils studied in this thesis represent some of the thickest profiles that have been subject to cosmogenic radionuclide analysis. To better understand the relationship between rates of soil formation and soil thickness, more work needs to be carried out on thick (>1 m) soils.

Second, Chapter 6 presented further insights into the extent to which the lithological variability of sandstone governs rates of soil formation. Moreover, the rates obtained for the arenite sandstones in this study were shown, in some cases, to be up to nine times faster than those previously measured by scholars working on wackes. These findings suggest that the abundance of matrix in wackes reduces the transmission of water into the rock, slowing the process of bedrock weathering. Meanwhile, comparatively matrix-free arenite sandstones promote the transmission and storage of water, and enable more

contact between water and mineral particles, thus speeding up weathering processes.

In summary, this thesis has widened the geographical spread of our knowledge on soil formation, whilst simultaneously investigating some of the intrinsic mechanisms that control the process of bedrock weathering. It could be suggested that more rates are still required, but this thesis has also argued that accuracy should not be substituted for quantity. For example, in Chapter 3, a new model called CoSOILcal was presented. The major contribution here was the opportunity, for the first time, to take into account the overlying soil bulk density when calculating a 'best fit' bedrock lowering rate using measured concentrations of *in-situ* radionuclides from samples taken at or below the bedrock-soil interface. The model was employed in a sensitivity analysis on previously published bedrock concentrations of Beryllium-10. This was to assess the extent to which high-resolution bulk density data for the overlying soil in each case (previously ignored in the original studies) would bring about significantly different rates of soil formation. It was found that for soils thicker than 0.25 m, these bulk density data brought about a significant difference in this way. Whilst measuring rates of soil formation using cosmogenic radionuclide analysis should continue to be a priority for soil scientists, care should be taken to ensure that the rates obtained are as accurate as possible. This thesis suggests that accounting for soil bulk density in future isotopic work should be an essential aspect of this quality assurance.

7.3 Research challenge 2: application of soil formation rates

The second research challenge outlined in Chapter 1 considered the application of soil formation rates. To date, soil formation rates have been most commonly measured by communities from outside soil science (e.g.: Heimsath *et al.*, 1997). Thus, these data have been principally used to address research agenda with little, if any, relation to soil (e.g.: to identify long-term landscape evolution mechanisms). By contrast, soil formation data have provided comparatively little contribution to the discourse of soil sustainability. Although statements regarding the imbalance between soil formation and soil erosion continue to be made by soil scientists, seldom are these statements supported by empirical measurements. Instead, soil formation rates are often estimated by referring to other studies, some of which stem from contexts dissimilar in climate and lithology. Notwithstanding the need for more data, soil scientists should also explore and develop ways to apply the rates already obtained.

In Chapter 2, two potential applications for soil formation data were discussed: the estimation of soil lifespans, and the establishment of soil loss tolerance (SLT) values. Both of these have enjoyed varying degrees of engagement by soil scientists, particularly the latter (Di Stefano and Ferro, 2016). In the case of soil loss tolerance, the general principle that rates of soil erosion should fall below those of soil formation is widely accepted. However, the analysis presented in Chapter 2 shows that less than half of the studies that have calculated SLT values have employed soil formation data. In the case of soil lifespans, the development of these models has been iterative and mostly conceptual (i.e.: soil formation rates have seldom been measured for soil

lifespan calculations; rather, they have been estimated using data obtained by studies from dissimilar contexts).

Soil lifespans have been explored progressively throughout this thesis. In Chapter 4, the first scientifically robust, globally relevant, quantitative estimates of soil lifespans were presented. This work brought about two major findings. First, 93% of non-bare soils subject to conventional land management practices (e.g.: conventional ploughing, cultivation up-and-downslope, etc.) were shown to be thinning, with 16% of the dataset reporting lifespans of less than 100 years. Second, shifts in the way land is used and managed can extend these lifespans and, in many cases, promote soil thickening. For soils managed with conservation-based practices (e.g.: minimal tillage, contour cultivation, etc.), over a third of the lifespans in the dataset exceeded 10,000 years.

The work presented in Chapter 5 further developed the soil lifespan concept. At Rufford Forest Farm, soil lifespans were calculated for both the A horizon and the whole solum. Measuring rates of soil formation and erosion, and estimating soil lifespans at four different catena positions, enabled an assessment into the variability of soil lifespans at the field-scale. The shortest lifespans were found on the backslope (212 years, in a worst-case scenario), whereas the longest lifespans were found at the summit (713 years, in a worst-case scenario).

Together, the findings of Chapters 4 and 5 contest the popular claims that there are 60 years of global topsoil left (Arsenault, 2014; Wong, 2019). On the contrary, the global soil lifespans analysed in Chapter 4, and the localised

lifespans estimated for Rufford Forest Farm in Chapter 5, span five orders of magnitude. This thesis has demonstrated that land-use and management practices can influence the long-term sustainability of soil profiles, as indeed can soil depth. There is arguably much more work to be done to substantiate these findings, particularly in terms of addressing the many limitations of the soil lifespan model. Nonetheless, the analyses presented in this thesis represent the first evidence-based assessments of soil lifespans, and shows that claims citing 'single-figure' lifespan estimates do not realistically reflect the variability in the sustainability of our soil resources.

7.4 Evaluation

This section of the closing discussion will provide a general evaluation of the work completed for this thesis. It will focus, in turn, on three aspects: accuracy, reliability, and validity, and will largely discuss these with respect to Chapters 4, 5, and 6. For specific and more detailed evaluative comments, please refer to the discussions contained within each chapter.

7.4.1 Accuracy

Every attempt has been made to ensure that the findings of this thesis are as accurate as possible. However, some of the methodologies employed here are inherently limited in this regard. One of the often-cited advantages of cosmogenic radionuclide analysis is that it can be used to measure soil formation rates over long time scales, averaging out any short-term or high frequency perturbations (Cockburn and Summerfield, 2004). In Chapter 6, this was particularly advantageous; the aim here was to measure soil formation rates from multiple sites across the UK in order to better understand the

effects of lithology. Although each site is subject to a specific microclimate (e.g.: Hilton receives approximately 90 mm more precipitation annually than Woburn), these disparities would not have been detected by cosmogenic radionuclide analysis, and thus would not have impacted the examination of the lithological controls. However, if the research objective was to determine the effect of arable practices on soil formation rates, cosmogenic radionuclide analysis would no longer be a suitable method (i.e.: arable practices would not have been implemented over timescales long enough for their effects on soil formation to be detectable by this technique). Yet, other methods have demonstrated that arable practices can influence rates of soil formation over short-term (monthly to annual) timescales (Gabet *et al.*, 2003). Therefore, it is likely that the rates presented for the arable sites studied in Chapters 5 and 6 are less accurate because they do not account for short-term changes in land management. By extension, this affects the lifespan analysis for the soils at Rufford Forest Farm. In the event that the land management practices in operation at this site have increased rates of soil formation (e.g.: seasonal ploughing has increased the infiltration of water to the soil-saprolite interface), the lifespans currently estimated in Chapter 5 may have been underestimated. Conversely, if these practices have slowed the rates of soil formation (e.g.: reducing the transmission of water to the saprolite through compacting surface horizons), it is likely that the lifespans have been overestimated. To address this, cosmogenic radionuclide analysis should be used in tandem with other methods, particularly those that are able to ascertain the effects of relatively short-term land management operations on the rates of bedrock weathering.

The lifespan analysis presented for Rufford Forest Farm is also affected, in turn, by the accuracy of the erosion data applied in the lifespan model. In this case, the data stemmed from a ^{137}Cs -based study conducted by Quine and Walling (1991) and represented all erosion processes in operation at the site since approximately 1956. If annual rates of soil erosion have increased or decreased since the early 1990s, it is possible that the lifespans outlined in this thesis have been either under- or over-estimated. This point can also be extended to the global lifespan analysis presented in Chapter 4. The erosion data used here stemmed from over 240 studies, each of which may have adopted different techniques to measure rates of erosion. To some extent this was mitigated by discarding modelling-based studies, those that did not empirically measure erosion, and those that failed to report a year's worth of data. However, to ensure greater accuracy in the estimated lifespans, a standard procedure to measure soil formation would need to have been applied universally and consistently.

7.4.2 Reliability

A second consideration in this evaluation is the reliability of the data obtained. One of the negative implications of employing cosmogenic radionuclide analysis to measure soil formation rates is that it is an expensive technique (approx. £1,580 per sample, compared with approx. £315 per sample for radiocarbon dating). It also necessitates a relatively lengthy period of sample preparation and processing time (approx. 8 months, compared with approx. 4 months for radiocarbon dating). As a result, it is more challenging within a concretized budget of time and money to achieve the degree of sample replication that may be possible for other analyses within soil science.

Justifying the way that cosmogenic radionuclide analysis was employed in this thesis required balancing the benefits of spatial coverage in measuring soil formation (i.e.: across different catena positions) with the need to perform replicates. In Chapters 5 and 6, replication was only partly achieved by measuring ^{10}Be concentrations from two samples down the same depth profile. For greater reliability, and to avoid pseudo-replication, multiple transects down multiple hillslopes should have been studied.

7.4.3 Validity

Whilst the measurement of soil formation at four sites across the UK represent an important contribution to our knowledge base, the sites studied in Chapters 5 and 6 are not representative of all environmental (e.g.: climatic and lithological) contexts that characterise the UK. In part, the sites were selected based on their suitability for cosmogenic radionuclide analysis and, in particular, the presence and abundance of quartz minerals $>250\ \mu\text{m}$ within the parent material. Given that sandstone often satisfies these criteria, this biases the work towards sandstone-derived soils. As a result, the findings presented in this thesis cannot validly represent the spread of soil formation rates expected across the UK. In order to determine the likely range of soil formation rates across the country, studies covering a wider array of climates and lithologies in the UK need to be undertaken. In addition, this may require alternative radionuclides (such as ^{36}Cl) being used instead of ^{10}Be . The use of ^{36}Cl to measure the rates of weathering on carbonate-based bedrock has been demonstrated previously (Moore and Granger, 2019).

Similarly, this also implies that the soil lifespans presented for Rufford Forest Farm cannot be used to represent the sustainability of all or other soils across the UK. Rufford Forest Farm was selected in part based on the fact that it is known to have a high erosion risk. As a result, the lifespans calculated for the soils at this site may be shorter than the UK mean. To achieve a more comprehensive insight into the lifespans of UK-based soils, it is essential that soils within a broader array of environmental and land management contexts are studied. By extension, this may also require more empirical work focused on measuring soil erosion across a representative range of environmental conditions in the UK. The findings of Benaud (2017) suggest that the UK has a rich history of soil erosion research, but that work to date has been biased towards localities with a known susceptibility for soil erosion. Going forwards, it is essential that empirical measurements of soil erosion adopt an unbiased sampling design. This is essential if the uncertainties in erosion models are to be suitably quantified (Batista *et al.*, 2019).

7.5 Future work

In addition to improving the accuracy, reliability, and validity outlined in Section 7.4, there are three avenues of further research that could stem from the work presented in this thesis.

7.5.1 Rates of soil *function* formation

The rates of soil formation determined here represent the first stage of the soil formation process: the conversion from bedrock to saprolite. Critically, they cannot provide an insight into the rates at which this saprolite is converted into a functioning soil (i.e.: one that is able to maintain a host of soil ecosystem

services such as crop production, purifying water, and sequestering carbon). Further work is required to better understand the 'lag-time' – to borrow a term from hydrology – between the production of saprolite and the beginning of soil functioning, and the factors that may influence this. A useful starting point for such work may include isotopically dating low (near-bedrock) soil horizons and comparing these dates with the maximum ages derived from cosmogenic radionuclide analysis.

7.5.2 Lifespans after complete soil removal

In this thesis, maximum soil lifespans were determined based on an estimated period of time until bedrock exposure. However, this assumption disregards the possibility that the underlying saprolite may be able to perform some, if not all, of the ecosystem services provided by soils. The saprolite is one of the least studied zones of the soil profile, with the majority of the work to date feeding geomorphological and geological discourses, rather than the dialogues on soil sustainability and soil ecosystem services. Therefore, large gaps exist in our knowledge and understanding of the potential roles of saprolite for ecosystem functioning. Further work to address these gaps is essential if maximum soil lifespans are to be representative. This work may involve expanding our knowledge about the physical, chemical, and biological properties of saprolite underlying soils, and the extent to which these properties contribute towards the provision of ecosystem services. In addition, additional work may adopt the five factors of soil formation as a conceptual framework with which to study the factors that govern the functional capacity of the saprolite horizon.

7.5.3 Rates of soil formation for deep soils

A third package of work could further explore the factors that constrain the rates at which soils form at the bedrock. One of the major contributions of this thesis has been the focus on obtaining soil formation rates for relatively thick (>1 m) soils. Furthermore, the data presented here can help soil scientists better understand the relationship between soil thickness and rates of soil formation. Despite this, the relative dearth of soil formation data for soils thicker than 1 m still represents a sizeable knowledge gap, and one requiring more nuanced attention by soil scientists. However, considering cosmogenic radionuclides attenuate with depth (Gosse and Phillips, 2001), clearly this technique may need to be supported by other methods for significantly thick (>3 m) soils.

7.6 Research outputs and impact statement

The final task of this evaluation is to discuss the outputs and impact of this work, both those which have already been generated, and the potential for additional outputs and impacts going forwards.

At the time of submitting this thesis, the work contained herein has led to three major forms of research output. First, this thesis has led to the publication of two peer-reviewed articles in international, peer-reviewed journals (Evans *et al.* 2019; Rodés and Evans, 2019) and a number of conference papers. It has also facilitated the development of the CoSOILcal model (see Chapter 3) which has the potential to contribute towards cosmogenic radionuclide studies both within and beyond the discipline of soil science. The second major research output has been the publication of two outreach articles for *The*

Conversation and Air Water Environment International (Evans, 2020a,b).

These have allowed for the distillation and communication of some of the broader messages emanating from this thesis to audiences beyond the academy. Accompanying these engagement articles is a third research output: the production of a six minute film, focussing on the soil lifespan (STARS, 2018).

The work presented in this thesis has the potential to generate additional impacts. One of these is on land policy. There have been many governmental and non-governmental reports published recently which assert claims about the lifespans of UK soils, without supporting these claims with appropriate evidence. For example, the Environmental Agency's 2019 'State of the Environment' report suggests that some parts of the country "could be only 30 to 60 years away from the fundamental eradication of soil fertility" (Environmental Agency, 2019, p. 5). Although this statement made reference to an academic paper, the paper in question focussed its analysis solely on the degradation of peat (Matysek *et al.*, 2019). Similarly, Secretary of State Michael Gove has previously stated that "we may be 30, 50, 60 harvests away from the fundamental eradication of [soil] fertility in parts of the country" (Soil Association, 2017). Statements of this nature also continue to be made in both Houses of Parliament, yet are seldom evidenced (Sinclair, 2017; Featherstone, 2018; Whitty, 2019).

The lifespans presented in this thesis, particularly those from the global analysis conducted in Chapter 4, could be used, in part, to support future claims, but also to identify 'lifespan hotspots'. These hotspots would indicate areas with critical soil lifespans which are arguably most in need of urgent soil

conservation policy. Furthermore, the conclusions of Chapter 4 that discuss techniques to extend soil lifespans could be used to inform future policy, both within the UK and abroad. By implementing evidence-based measures for soil conservation, and thereby extending soil lifespans, soils will be better placed to sustain their provision of ecosystem services. Achieving this goal will bring wide-reaching impacts across present-day society, and for future generations.

References:

- Aboim, M. C. R., Coutinho, H. L. C., Peixoto, R. S., Barbosa, J. C. and Rosado, A. S. (2008) 'Soil bacterial community structure and soil quality in a slash-and-burn cultivation system in Southeastern Brazil', *Applied Soil Ecology*, 38, pp. 100-108.
- Abu Hammad, A. (2011) 'Watershed erosion risk assessment and management utilizing revised universal soil loss equation-geographic information systems in the Mediterranean environments', *Water and Environment Journal*, 25(2), pp. 149-162.
- Ackerer, J., Chabaux, F., Van der Woerd, J., Viville, D., Pelt, E., Kali, E., Lerouge, C., Ackerer, P., di Chiara Roupert, R. and Négrel, P. (2016) 'Regolith evolution on the millennial timescale from combined U-Th-Ra isotopes and in situ cosmogenic ¹⁰Be analysis in a weathering profile (Strengbach catchment, France)', *Earth and Planetary Science Letters*, 453, pp. 33–43.
- Acworth, R. I. (1987) 'The development of crystalline of basement aquifers in a tropical environment', *Quarterly Journal of Engineering Geology and Hydrogeology*, 20, pp. 265-272. doi: 10.1144/GSL.QJEG.1987.020.04.02
- Adamovič, J., Mikuláš, R., Schweigstilllová, J. and Böhmová, V. (2011) 'Porosity changes induced by salt weathering of sandstones, Bohemian Cretaceous Basin, Czech Republic', *Acta Geodynamica et Geomaterialia*, 8(1), pp. 29-45.
- Adhikari, K. and Hartemink, A. E. (2016) 'Linking soils to ecosystem services – A global review', *Geoderma*, 262, pp. 101-111.

- Ahnert, F. (1967) 'The role of the equilibrium concept in the interpretation of landforms of fluvial erosion and deposition', in Macar, P. (ed.) *L'évolution des versants*. Liege: Universite de Liege, pp. 23–41.
- Aira, M., Monroy, F., Domínguez, J. and Mato, S. (2002) 'How earthworm density affects microbial biomass and activity in pig manure', *European Journal of Soil Biology*, 38(1), pp. 7-10.
- Alexander, E. B. (1988a) 'Rates of Soil Formation: Implications for Soil-Loss Tolerance', *Soil Science*, 145(1), pp. 37-45.
- Alexander, E. B. (1988b) 'Strategies for determining soil-loss tolerance', *Environmental Management*, 12(6), pp. 791-796.
- Alexander, E. B. (1989) 'Rates of soil formation - implications for soil-loss tolerance - response', *Soil Science*, 148(1), pp. 75-76.
- Allen, D. J., Brewerton, L. J., Coleby, L. M., Gibbs, B. R., Lewis, M. A., MacDonald, A. M., Wagstaff, S. J. and Williams, A. T. (1997) *The physical properties of major aquifers in England and Wales*. Keyworth, Nottingham: British Geological Survey. Available at: <http://nora.nerc.ac.uk/id/eprint/13137/> (Accessed: 11 January 2020).
- Ambrose, K., Hough, E. and Smith, N. J. P. (2014) *Lithostratigraphy of the Sherwood Sandstone Group of England, Wales and south-west Scotland*. Available at: <http://nora.nerc.ac.uk/id/eprint/507530> (Accessed: 30 September 2018).
- Amundson, R., Berhe, A. A., Hopmans, J. W., Olson, C., Sztein, A. E. and Sparks, D. L. (2015) 'Soil and human security in the 21st century', *Science*, 348(6235), doi: 10.1126/science.1261071

Anache, J. A. A., Wendland, E. C., Oliveira, P. T. S., Flanagan, D. C. and Nearing, M. A. (2017) 'Runoff and soil erosion plot-scale studies under natural rainfall: a meta-analysis of the Brazilian experience', *Catena*, 152, pp. 29-39.

Anand, R. R. and Paine, M. (2002) 'Regolith geology of the Yilgarn Craton, Western Australia: Implications for exploration', *Australian Journal of Earth Sciences*, 49(1), pp. 3-162. doi: 10.1046/j.1440-0952.2002.00912.x

Anderson, R. S., Rajaram, H. and Anderson, S. P. (2018) 'Climate driven coevolution of weathering profiles and hillslope topography generates dramatic differences in critical zone architecture', *Hydrological Processes*, 33(1), pp. 4-19.

Andrews, S. S., Karlen, D. I., Cambardella, C. A., Andrews, S. S., Karlen, D. I. and Cambardella, C. A. (2004) 'The soil management assessment framework: a quantitative soil quality evaluation method', *Soil Science Society of America Journal*, 68(6), pp. 1945-1962.

Angima, S. D., Stott, D. E., O'Neill, M. K., Ong, C. K. and Weesies, G. A. (2003) 'Soil erosion prediction using RUSLE for central Kenyan highland conditions', *Agriculture Ecosystems and Environment*, 97(1), pp. 295-308.

Applegarth, M. T. and Dahms, D. E. (2001) 'Soil catenas of calcareous tills, Whiskey Basin, Wyoming, USA', *Catena*, 42, pp. 17-38.

Arnáez, J., Lana-Renault, N., Lasanta, T., Ruiz-Flaño, P. and Castroviejo, J. (2015) 'Effects of farming terraces on hydrological and geomorphological processes: a review', *Catena*, 128, pp. 122-134.

Arsenault, C. (2014) *Only 60 Years of Farming Left If Soil Degradation Continues* [Press release]. 5 December. Available at:

<https://www.scientificamerican.com/article/only-60-years-of-farming-left-if-soil-degradation-continues/> (Accessed: 16 June 2018).

Assouline, S. (2004) 'Rainfall-Induced Soil Surface Sealing', *Vadose Zone Journal*, 3(2), pp. 570-591.

Auerswald, K. (1987) 'Estimating soil depth and soil loss tolerances for the classification units of the German soil productivity maps', *Journal of Agronomy and Crop Science-Zeitschrift Fur Acker Und Pflanzenbau*, 158(2), pp. 132-139.

Avanzi, J. C., Silva, M. L. N., Curi, N., Norton, L. D., Beskow, S. and Martins, S. G. (2013) 'Spatial distribution of water erosion risk in a watershed with eucalyptus and atlantic forest', *Ciencia E Agrotecnologia*, 37(5), pp. 427-434.

Bagarello, V., Di Stefano, C., Ferro, V., and Pampalone, V. (2015) 'Establishing a soil loss threshold for limiting rilling', *Journal of Hydrologic Engineering*, 20(6), doi: 10.1061/(ASCE)HE.1943-5584.0001056.

Bago, B., Vierheilig, H., Piché, Y. and Azcón-Aguilar, C. (1996) 'Nitrate depletion and pH changes induced by the extraradical mycelium of the arbuscular mycorrhizal fungus *Glomus intraradices* grown in monoxenic culture', *New Phytologist*, 133, pp. 273-280. doi: 10.1111/j.1469-8137.1996.tb01894.x

Baja, S., Chapman, D. M. and Dragovich, D. (2002) 'A conceptual model for defining and assessing land management units using a fuzzy modelling approach in GIS environment', *Environmental Management*, 29(5), pp. 647-661.

Baker, R. G., Schwert, D. P., Bettis, E. A. III. and Chumbley, C. A. (1991) 'Mid-Wisconsinan stratigraphy and paleoenvironments at the St. Charles site in south-central Iowa', *GSA Bulletin*, 103, pp. 210-220.

Bakker, M. M., Govers, G. and Rounsevell, M. D. A. (2004) 'The crop productivity-erosion relationship: an analysis based on experimental work', *Catena*, 57, pp. 55-76.

Balco, G. (2006) *Converting Al and Be isotope ratio measurements to nuclide concentrations in quartz*. Available at:

http://hess.ess.washington.edu/math/docs/common/ams_data_reduction/

(Accessed: 30 September 2018).

Balco, G., Stone, J. O., Lifton, N. A. and Dunai, T. J. (2008) 'A complete and easily accessible means of calculating surface exposure ages or erosion rates from ^{10}Be and ^{26}Al measurements', *Quaternary Geochronology*, 3, pp. 174-195.

Ballabio, C., Borrelli, P., Spinoni, J., Meusburger, K., Michaelides, S., Beguería, S., Klik, A., Petan, S., Janeček, M., Olsen, P., Aalto, J., Lakatos, M., Rymaszewicz, A., Dumitrescu, A., Tadić, M. P., Diodato, N., Kostalova, J., Rousseva, S.,

Banasik, K., Alewell, C. and Panagos, P (2017) 'Mapping monthly rainfall erosivity in Europe', *Science of the Total Environment*, 579, pp. 1298-1315.

Banin, A. (2005) 'The Enigma of the Martian Soil', *Planetary Science*, 309(5736), pp. 888-890.

Banwart, S. A., Nikolaidis, N. P., Zhu, Y. G., Peacock, C. L. and Sparks, D. L.

(2019) 'Soil functions: connecting Earth's Critical Zone', *Annual Review of Earth and Planetary Sciences*, 47, pp. 333-359. doi: 10.1146/annurev-earth-063016-020544

Barth, F. W. (1961) 'Abundance of the elements, areal averages and geochemical cycles', *Geochimica et Cosmochimica Acta*, 23, pp. 1-8.

- Barton, D. C. (1916) 'Notes on the disintegration of granite in Egypt', *Journal of Geology*, 24, pp. 382-393.
- Batey, T. (2009) 'Soil compaction and soil management- a review', *Soil Use and Management*, 25(4), pp. 335-345.
- Batista, P. V. G., Davies, J., Silva, M. L. N. and Quinton, J. N. (2019) 'On the evaluation of soil erosion models: Are we doing enough?' *Earth-Science Reviews*, 197, doi: <https://doi.org/10.1016/j.earscirev.2019.102898>
- Baude, M., Meyer, B. C. and Schindewolf, M. (2019) 'Land use change in an agricultural landscape causing degradation of soil based ecosystem services', *Science of the Total Environment*, 659, pp. 1526-1536.
- Beach, T. and Gersmehl, P. (1993) 'Soil-erosion, T-values, and sustainability - a review and exercise', *Journal of Geography*, 92(1), pp. 16-22.
- Béliveau, A., Lucotte, M., Davidson, R., Paquet, S., Mertens, F., Passos, C. J. and Romana, C. A. (2017) 'Reduction of soil erosion and mercury losses in agroforestry systems compared to forests and cultivated fields in the Brazilian Amazon', *Journal of Environmental Management*, 203, pp. 522-532.
- Bell, F. G. (1978) 'Petrographical factors relating to porosity and permeability in the Fell Sandstone', *Quaternary Journal of Engineering Geology and Hydrogeology*, 11, pp. 113-126.
- Benaud, P. E. (2017) *Exploring the multiple techniques available for developing an understanding of soil erosion in the UK*. PhD thesis. Available at: <https://ore.exeter.ac.uk/repository/handle/10871/32939> (Accessed: 13 April 2020).

Benton, M. J., Cook, E. and Turner, P. (2002) *Permian and Triassic Red Beds and the Penarth Group of Great Britain*. Peterborough: Joint Nature Conservation Committee.

Bhattacharyya, P., Bhatt, V. K. and Mandal, D. (2008) 'Soil loss tolerance limits for planning of soil conservation measures in Shivalik-Himalayan region of India', *Catena*, 73(1), pp. 117-125.

Bhattacharyya, P., Mandal, D., Bhatt, V. K. and Yadav, R. P. (2011) 'A quantitative methodology for estimating soil loss tolerance limits for three states of northern India', *Journal of Sustainable Agriculture*, 35(3), pp. 276-292.

Biswas, H., Raizada, A., Mandal, D., Kumar, S., Srinivas, S. and Mishra, P. K. (2015) 'Identification of areas vulnerable to soil erosion risk in India using GIS methods', *Solid Earth*, 6(4), pp. 1247-1257.

Black, M. and Fawcett, B. (2008) *The Last Taboo: Opening the Door on the Global Sanitation Crisis*. London: Earthscan.

Bloch, S., Lander, R. H. and Bonnell, L. (2002) 'Anomalously high porosity and permeability in deeply buried sandstone reservoirs: Origin and predictability', *American Association of Petroleum Geologists Bulletin*, 86(2), pp. 301-328.

Bloomfield, J. P., Moreau, M. F. and Newell, A. J. (2006) 'Characterization of permeability distribution in six lithofacies from the Helsby and Wilmslow sandstone formations of the Cheshire Basin, UK', in Barker, R. D. and Tellam, J. H. (eds) *Fluid Flow and Solute Movement in Sandstones: The Onshore UK Permo-Triassic Red Bed Sequence*. London: Geological Society, pp. 83-101.

Blum, W. E. H. (1993) 'Soil Protection Concept of The Council of Europe and Integrated Soil Research', in Eijsackers, H. J. P. and Hamers, T. (eds) *Integrated*

Soil and Sediment Research: A Basis for Proper Protection. Netherlands: Springer, pp. 37-47.

Blum, W. E. H. (2005) 'Functions of Soil for Society and the Environment', *Reviews in Environmental Science and BioTechnology*, 4, pp. 75-79.

Blume, H. P. and Leinweber, P. (2004) 'Plaggen Soils: landscape history, properties, and classification', *Journal of Plant Nutrition and Soil Science*, 167, pp. 319-327.

Boardman, J. and Poesen, J. (2006) *Soil Erosion in Europe*. Chichester: John Wiley and Sons Ltd.

Bockheim, J. G. and Gennadiyev, A. N. (2000) 'The role of soil-forming processes in the definition of taxa in Soil Taxonomy and the World Soil Reference Base', *Geoderma*, 95, pp. 53-72.

Bodner, G., Leitner, D. and Kaul, H. P. (2014) 'Coarse and fine root plants affect pore size distributions differently', *Plant and Soil*, 380, pp. 133-151.

Borchers, B., Marrero, S., Balco, G., Caffee, M., Goehring, B., Lifton, N., Nishiizumi, K., Phillips, F., Schaefer, J. and Stone, J. (2016) 'Geological calibration of spallation production rates in the CRONUS-Earth project', *Quaternary Geochronology*, 31, pp. 188-198.

Borrelli, P., Robinson, D. A., Fleischer, L. R., Lugato, E., Ballabio, C., Alewell, C., Meusburger, K., Modugno, S., Schütt, B., Ferro, V., Bagarello, V., Van Oost, K., Montanarella, L. and Panagos, P. (2017) 'An assessment of the global impact of 21st century land use change on soil erosion', *Nature Communications*, 8, pp. 1–13. doi: 10.1038/s41467-017-02142-7

Bot, A. J., Nachtergaele, F. O. and Young, A. (2000) *Land Resource Potential and Constraints at Regional and Country Levels: World Soil Resources Report 90*. Rome: Land and Water Development Division.

Botter, G., Bertuzzo, E. and Rinaldo, A. (2011) 'Catchment residence and travel time distributions: the master equation', *Geophysical Research Letters*, 38, p. L11403.

Bowen, D. Q., Phillips, F. M., McCabe, A. M., Knutz, P. C. and Sykes, G. A. (2002) 'New data for the Last Glacial Maximum in Great Britain and Ireland', *Quaternary Science Reviews*, 21, pp. 89-101.

Brantley, S. L., Eissenstat, D. M., Marshall, J. A., Godsey, S. E., Balogh-Brunstad, Z., Karwan, D. L., Papuga, S. A., Roering, J., Dawson, T. E., Evaristo, J., Chadwick, O., McDonnell, J. J. and Weathers, K. C. (2017) 'Reviews and synthesis: on the roles trees play in building and plumbing the critical zone', *Biogeosciences*, 14, pp. 5115-5142. doi: 10.5194/bg-14-5115-2017

Brevik, E. C., Cerdà, A., Mataix-Solera, J., Pereg, L., Quinton, J. N. and Van Oost, K. (2015) 'The interdisciplinary nature of SOIL', *SOIL*, 1(1), pp. 117-129.

Brimhall, G. H. and Dietrich, W. E. (1987) 'Constitutive mass balance relations between chemical composition, volume, density, porosity, and strain in metasomatic hydrochemical systems: Results on weathering and pedogenesis', *Geochimica et Cosmochimica Acta*, 51, p. 567487.

British Geological Survey (2020) *The BGS Lexicon of Named Rock Units – Bridgnorth Sandstone Formation*. Available at: <https://www.bgs.ac.uk/lexicon/lexicon.cfm?pub=BRI> (Accessed: 7 February 2020).

Brunsdon, D. (1979) 'Weathering', in Embleton, C. and Thornes, J. (eds) *Process in Geomorphology*. London: Edward Arnold, pp. 73-130.

Bryan, W. H. and Teakle, L. J. H. (1949) 'Pedogenic Inertia: a Concept in Soil Science', *Nature*, 164, p. 969.

Bryant, K. J., Atwood, J. D., Lacewell, R. D., Lansford, V. D., McCarl, B. A. and Dyke, P. T. (1993) 'Farm-level impacts of the coastal zone management act proposed erosion regulations', *Journal of Soil and Water Conservation*, 48(5), pp. 466-470.

Buck, S. G. (1985) 'Sand-flow cross strata in tidal sands of the Lower Greensand (Early Cretaceous), Southern England', *Journal of Sedimentary Petrology*, 55(6), pp. 895-906.

Burger, J. A. and Kelting, D. L. (1999) 'Using soil quality indicators to assess forest stand management', *Forest Ecology and Management*, 122, pp. 155-166.

Burke, B. C., Heimsath, A. M. and White, A. F. (2007) 'Coupling chemical weathering with soil production across soil-mantled landscapes', *Earth Surface Processes and Landforms*, 32(6), pp. 853-873.

Burley, S. D. (1984) 'Patterns of diagenesis in the Sherwood Sandstone Group (Triassic), United Kingdom', *Clay Minerals*, 19, pp. 403-440.

Burley, S. D. and Kantorowicz, J. D. (1986) 'Thin section and S.E.M. textural criteria for the recognition of cement-dissolution porosity in sandstones', *Sedimentology*, 33(4), pp. 587-604.

Burt, T., Boardman, J., Foster, I. and Howden, N. (2015) 'More rain, less soil: long-term changes in rainfall intensity with climate change', *Earth Surface Processes and Landforms*, 41, pp. 563–566.

Buzie, C. (2010) *Development of a Continuous Flow Vermicomposting Urine Diversion Toilet for On-site Application*. PhD thesis. Hamburg University of Technology. Available at: <https://www.susana.org/en/knowledge-hub/resources-and-publications/library/details/1333> (Accessed: 3 March 2020).

Caires, E. F., Pereira Filho, P. R. S., Filho, R. Z. and Feldhaus, I. C. (2008) 'Soil acidity and aluminium toxicity as affected by surface liming and cover oat residues under a no-till system', *Soil Use and Management*, 24(3), pp. 302-309.

Calvo, J. P., Blanc-Valleron, M. M., Rodríguez-Arandía, J. P., Rouchy, J. M. and Sanz, M. E. (1995) 'Authigenic clay minerals in continental evaporitic environments', in Thiry, M. and Simon-Coinçon, R. (eds) *Palaeoweathering, Palaeosurfaces and Related Continental Deposits*. Oxford: Blackwell Science Ltd, pp. 129-151.

Campos, M. C. C., Marques, J., Martins, M. V., Pereira, G. T., De Souza, Z. M. and Barbieri, D. M. (2008) 'Spatial variation of the soil loss for erosion in different geomorphic surfaces', *Ciencia Rural*, 38(9), pp. 2485-2492.

Carozzi, A. V. (1993) *Sedimentary Petrography*. New Jersey: PTR Prentice Hall.

Carré, F., McBratney, A. B., Mayr, T. and Montanarella, L. (2007) 'Digital Soil Assessments: Beyond DSM', *Geoderma*, 142, pp. 69-79.

Carson, M. A. and Kirkby, M. J. (1972) *Hillslope form and process*. Cambridge: Cambridge University Press.

Casali, J., Gimenez, R., De Santisteban, L., Alvarez-Mozos, J., Mena, J. and De Lersundi, J. D. (2009) 'Determination of long-term erosion rates in vineyards of navarre (Spain) using botanical benchmarks', *Catena*, 78(1), pp. 12-19.

Castro, L. G., Libardi, P. I. and De Jong Van Lier, Q. (2002) 'Soil water dynamics in a Brazilian infiltration terrace under different management practices', in Pagliai, M. and Jones, R. J. A. (eds) *Sustainable Land Management-Environmental Protection: A Soil Physical Approach*. Michigan: Catena, pp. 191-198.

Catt, J. A. (1991) 'Soils as indicators of Quaternary Climate Change in Mid-Latitude Regions', *Geoderma*, 51, pp. 167-187.

Catt, J. A. (2001) 'The agricultural importance of loess', *Earth Science Reviews*, 54, pp. 213-229.

Catt, J. A., King, D. W. and Weir, A. H. (1975) *The Soils of Woburn Experimental Farm I. Great Hill, Road Piece and Butt Close*. Available at: <http://www.era.rothamsted.ac.uk/eradoc/article/ResReport1974p2-5-30> (Accessed: 10 January 2020).

Cerdan, O., Govers, G., Le Bissonnais, Y., Van Oost, K., Poesen, J., Saby, J., Gobin, A., Vacca, A., Quinton, J., Auerswald, K., Klik, A., Kwaad, F. J. P. M., Raclot, D., Ionita, I., Rejman, J., Rousseva, S., Muxart, T., Roxo, M. J. and Dostal, T. (2010) 'Rates and spatial variations of soil erosion in Europe: a study based on erosion plot data', *Geomorphology*, 122, pp. 167-177.

Chamberlin, T. C. (1909) 'Soil Wastage', *Proceedings of a Conference of Governors in the White House, Washington, D. C. 1908*. U.S. Congress 60th, 2nd Session, House Document 1425, pp. 75-83.

- Chambers, F. M. (1999) 'The Quaternary history of Llangorse Lake: implications for conservation', *Aquatic Conservation: Marine and Freshwater Ecosystems*, 9(4), pp. 343-359.
- Chaves, H. M. L. (2010) 'Uncertainty in erosion prediction with USLE: impacts and mitigation', *Revista Brasileira De Ciencia Do Solo*, 34(6), pp. 2021-2029.
- Cockburn, H. A. P. and Summerfield, M. A. (2004) 'Geomorphological applications of cosmogenic isotope analysis', *Progress in Physical Geography*, 28(1), pp. 1-42.
- Cole, L. E. S., Bhagway, S. A. and Willis, K. J. (2014) 'Recovery and resilience of tropical forests after disturbance', *Nature Communications*, 5(3906), pp. 1-7.
- Conacher, A. J. and Dalrymple, J. B. (1977) 'The nine unit landsurface model: an approach to pedogeomorphic research', *Geoderma*, 18, pp. 3–154.
- Conry, M. J. (1971) 'Irish plaggen soils – their distribution, origin and properties', *Journal of Soil Science*, 22, pp. 401-416.
- Conry, M. J. (1972) 'Pedological evidence of man's role in soil profile modification in Ireland', *Geoderma*, 8, pp. 139-146.
- Conry, M. J. (1974) 'Plaggen soils. A review of man-made raised soils', *Soil and Fertilizers*, 37(11), pp. 319-326.
- Cooper, T. H. and Crellin, J. (1996) 'Lamellae morphology in a sandy outwash soil of east-central Minnesota', *Soil Survey Horizons*, 37(3), pp. 87-92.
- Corbett, L. B., Bierman, P. and Rood, D. H. (2016) 'An approach for optimizing in situ cosmogenic ¹⁰Be sample preparation', *Quaternary Geochronology*, 33, pp. 24–34.

- Cox, N. J. (1980) 'On the relationship between bedrock lowering and regolith thickness', *Earth Surface Processes and Landforms*, 5, pp. 271–274.
- Cummins, W. A. (1962) 'The Greywacke problem', *Geological Journal*, 3, pp. 51–72.
- Da Silva, M. A., Silva, M. I. N., Curi, N., Avanzi, J. C. and Leite, F. P. (2011) 'Management systems in the eucalyptus forest plantations and the soil and water losses in Vale do Rio Doce, MG state', *Ciencia Florestal*, 21(4), pp. 765-776.
- Da Silva, M. A., Silva, M. I. N., Curi, N., Oliveira, A. H., Avanzi, C. and Norton, L. D. (2014) 'Water erosion risk prediction in eucalyptus plantations', *Ciencia E Agrotecnologia*, 38(2), pp. 160-172.
- Dai, F. Q., Lv, Z. Q., Zhou, Q. G. and Liu, G. C (2013) 'GIS-based soil loss estimation with USLE for soil conservation planning in hilly areas of purplish soils', *Fresenius Environmental Bulletin*, 22(4B), pp. 1266-1273.
- Darvill, C. M. (2013) 'Cosmogenic nuclide analysis', in Clarke, L. (ed.) *Geomorphological Techniques*. London: British Society for Geomorphology, pp. 1-25.
- Davidson, D. A. and Simpson, I. A. (1984) 'The Formation of Deep Topsoils in Orkney', *Earth Surface Processes and Landforms*, 9, pp. 75-81.
- Davidson, D. A., Harkness, D. D. and Simpson, I. A. (1986) 'The formation of farm mounds on the Island and Sanday, Orkney', *Geoarchaeology*, 1(1), pp. 45-59.

Davidson, D. A., Dercon, G., Stewart, M. and Watson, F. (2006) 'The legacy of past urban waste disposal on local soils', *Journal of Archaeologist Science*, 33, pp. 778-783.

De Baets, S., Poesen, J., Gyssels, G. and Knapen, A. (2006) 'Effects of grass roots on the erodibility of top soils during concentrated flow', *Geomorphology*, 76, pp. 54-67.

de Bakker, H. (1979) *Major Soils and Soil Regions in the Netherlands*. Wageningen: Centre for Agricultural Publishing and Documentation.

Deere, D. U. and Patton, F. D. (1971) 'Slope stability in residual cities', *Fourth Pan American Conference on Soil Mechanics and Foundation Engineering*. San Juan, Puerto Rico. New York: American Society of Civil Engineers, pp. 87-170.

Delgado, F. and Lopez, R. (1998) 'Evaluation of soil degradation impact on the productivity of Venezuelan soils', in Blum, W. E. H. (ed.) *Soil Degradation caused by Industrialization and Urbanization*. Germany: Catena Verlag, pp. 133-142.

Denevan, W. M. and Turner II, B. L. (1974) 'Forms, Functions and Associations of Raised Fields in the Old World Tropics', *Journal of Tropical Geography*, 39, pp. 24-33.

De Oliveira, P. T. S., Sobrinho, T. A., Rodrigues, D. B. B. and Panachuki, E. (2011a) 'Environmental zoning applied to soil and water conservation', *Revista Brasileira De Ciencia Do Solo*, 35(5), pp. 1723-1734.

De Oliveira, P. T. S., Sobrinho, T. A., Rodrigues, D. B. B. and Panachuki, E. (2011b) 'Erosion risk mapping applied to environmental zoning', *Water Resources Management*, 25(3), pp. 1021-1036.

Di Stefano, C. and Ferro, V. (2016) 'Establishing soil loss tolerance: an overview', *Journal of Agricultural Engineering*, 47(560), pp. 127-133.

Dietrich, W. E., Reiss, R., Hsu, M. and Montgomery, D. R. (1995) 'A process-based model for colluvial soil depth and shallow landsliding using digital elevation data', *Hydrological Processes*, 9, pp. 383-400.

Dixon, J. I., Heimsath, A. M. and Amundson, R. (2009) 'The critical role of climate and saprolite weathering in landscape evolution', *Earth Surface Processes and Landforms*, 34, pp. 1507-1521.

Dobereiner, L. (1984) *Engineering Geology of Weak Sandstones*. PhD thesis.

University of London. Available at:

<https://ethos.bl.uk/OrderDetails.do?uin=uk.bl.ethos.282418> (Accessed: 12 April 2020).

Dobereiner, L. and De Freitas, M. H. (1986) 'Geotechnical properties of weak sandstones', *Géotechnique*, 36(1), pp. 79-94.

Doetterl, S., van Oost, K. and Six, J. (2012) 'Towards constraining the magnitude of global agricultural sediment and soil organic carbon fluxes', *Earth Surface Processes and Landforms*, 37, pp. 642-655.

Dokuchaev, V. V. (1879) *Mapping the Russian Soils*. Russia: Imperial University of St. Petersburg.

Dong, X., Cohen, M. J., Martin, J. B., McLaughlin, D. L., Murray, A. B., Ward, N. D., Flint, M. K., and Heffernan, J. B. (2019) Ecohydrologic processes and soil thickness feedbacks control limestone-weathering rates in a Karst landscape, *Chemical Geology*, 527, doi: doi.org/10.1016/j.chemgeo.2018.05.021

Downing, R. A., Edmunds, W. M. and Gale, I. N. (1987) 'Regional groundwater flow in sedimentary basins in the U.K.', in Goff, J. C. and Williams, B. P. J. (eds) *Fluid Flow in Sedimentary Basins and Aquifers*. London: Geological Society of London, pp. 105-125.

Drever, J. I. (1994) 'The effect of land plants on weathering rates of silicate materials', *Geochimica et Cosmochimica Acta*, 58(10), pp. 2325-2332.

Du, S., Chen, A. and Liu, G. (2013) 'Determination of purple soil loss tolerance based on soil productivity in southwest China', *Journal of Soil and Water Conservation*, 68(2), pp. 146-152.

Duan, X., Shi, X., Li, Y., Rong, L. and Fen, D. (2017a) 'A new method to calculate soil loss tolerance for sustainable soil productivity in farmland', *Agronomy for Sustainable Development*, 37(2), pp. 1-13. doi: 10.1007/s13593-016-0409-3

Duan, X. W., Xie, Y., Liu, B. Y., Liu, G., Feng, Y. J. and Gao, X. F. (2017b) 'Soil loss tolerance in the black soil region of northeast china', *Journal of Geographical Sciences*, 22(4), pp. 737-751.

Duchaufour, R. (2012) *Pedology: Pedogenesis and Classification*. London: George Allen and Unwin.

Dudal, R. (2004) 'The Sixth Factor of Soil Formation', International Conference on Soil Classification, Petrozavodsk, Russia, 3-5 August. Available at: http://proprights.org/PDFs/workshop_2011/References/BAS/Soil%20References/Human%20Created%20Soils.pdf (Accessed: 7 June 2016).

Dunne, J., Elmore, D. and Muzikar, P. (1999) 'Scaling factors for the rates of production of cosmogenic nuclides for geometric shielding and attenuation at depth on sloped surfaces', *Geomorphology*, 27, pp. 3-11.

Dyke, C. G. and Dobereiner, L. (1991) 'Evaluating the strength and deformability of sandstones', *Quaternary Journal of Engineering Geology and Hydrogeology*, 24, pp. 123-134.

Egli, M., Dahms, D. and Norton, K. (2014) 'Soil formation rates on silicate parent material in alpine environments: Different approaches- different results?', *Geoderma*, 213, pp. 320-333.

Elwell, H. A. and Stocking, M. A. (1984) 'Estimating soil life-span for conservation planning', *Tropical Agriculture*, 61(2), pp. 148-150.

Environment Agency (2019) *The state of the environment: soil*. Available at: <https://www.gov.uk/government/publications/state-of-the-environment> (Accessed: 13 April 2020).

Evans, D. J., Rees, J. G. and Holloway, S. (1993) 'The Permian to Jurassic stratigraphy and structural evolution of the central Cheshire Basin', *Journal of the Geological Society*, 150, pp. 857-870.

Evans, D. J. A., Clark, C. D. and Mitchell, W. (2005) 'The last British Ice Sheet: A review of the evidence utilised in the compilation of the Glacial Map of Britain', *Earth-Science Reviews*, 70(3), pp. 253-312.

Evans, D. L. (2020a) *Soil is our best ally in the fight against climate change – but we're fast running out of it*. Available at: <https://theconversation.com/soil-is-our-best-ally-in-the-fight-against-climate-change-but-were-fast-running-out-of-it-128166> (Accessed: 28 January 2020).

Evans, D. L. (2020b) 'Saving our Soils for Future Generations', *Air Water Environment International*, 63, pp. 13-21.

Evans, D. L., Quinton, J. N., Tye, A. M., Rodés, Á., Davies, J. A. C., Mudd, S. M. and Quine, T. (2019) 'Arable soil formation and erosion: a hillslope-based cosmogenic-nuclide study in the United Kingdom', *SOIL*, 5, pp. 253-263.

Evans, R., Collins, A. L., Zhang, Y., Foster, I. D. L., Boardman, J., Sint, H., Lee, M. R. F. and Griffith, B. A. (2017) 'A comparison of conventional and ¹³⁷Cs-based estimates of soil erosion rates on arable and grassland across lowland England and Wales', *Earth Surface Reviews*, 173, pp. 49-64.

Evaristo, J., Jasechko, S. and McDonnell, J. J. (2015) 'Global separation of plant transpiration from groundwater and streamflow', *Nature*, 525, pp. 91–94.

Ewing, S. A., Sutter, B., Owen, J., Nishiizumi, K., Sharp, W., Cliff, S. S., Perry, K., Dietrich, W., McKay, C. P. and Amundson, R. (2006) 'A threshold in soil formation at Earth's arid- hyperarid transition', *Geochimica et Cosmochimica Acta*, 70(21), pp. 5293-5322.

Eyers, J. (1991) 'The influence of tectonics on early Cretaceous sedimentation in Bedfordshire, England', *Journal of the Geological Society*, 148, pp. 405-414.

Eyles, N., McCabe, A. M. and Bowen, D. Q. (1994) 'The stratigraphic and sedimentological significance of late Devensian ice sheet surging in Holderness, Yorkshire, UK', *Quaternary Science Reviews*, 13, pp. 727-759.

Factura, H., Bettendorf, T., Buzie, C., Pieplow, H., Reckin, J. and Otterpohl, R. (2010) 'Terra Preta Sanitation: re-discovered from an ancient Amazonian civilisation – integrating sanitation, bio-waste management and agriculture', *Water Science and Technology*, 61(10), pp. 2673-2679.

Fanning, D. S. and Fanning, M.C.B. (1989) *Soil Morphology, Genesis, and Classification*. New York: Wiley.

FAO (1995) 'Planning for sustainable use of land resources: towards a new approach', in Sombroek, W. G. and Sims, D. (eds) *Land and Water Bulletin No. 2*. Rome: FAO.

FAO (2014) *World Reference Base for Soil Resources 2014: International Soil Classification System for Naming Soils and Creating Legends for Soil Maps*. Rome, Italy: FAO.

FAO (2015a) *Status of the World's Soil Resources (SWSR) Main Report*. Rome, Italy: Food and Agriculture Organisation of the United Nations and Intergovernmental Technical Panel on Soils.

FAO (2015b) *World Agriculture: towards 2015/2030 an FAO perspective*. London: Earthscan Publications Ltd.

Featherstone, L. C. (2018) 'Environment: 25-year Plan debate in Lords Chamber', *Hansard: House of Lords debates*, 29 January, 788. Available at: <https://hansard.parliament.uk/Lords/2018-01-29/debates/7EBE9106-8C42-493F-9DF2-75D6DFF6613E/Environment25-YearPlan?highlight=%2260%20years%22%20%22soil%22#contribution-5281847E-13F4-477E-88FA-561D82B4BFC3> (Accessed: 13 April 2020).

Fifield, L. K. (1999) 'Accelerator mass spectrometry and its application', *Reports on Progress in Physics*, 62, pp. 1223–1274.

Fifield, L. K., Wasson, R. J., Pillans, B. and Stone, J. O. H. (2010) 'The longevity of hillslope soil in SE and NW Australia', *Catena*, 81, pp. 32-42.

Fontaine, S., Barot, S., Barré, P., Bdioui, N., Mary, B. and Rumpel, C. (2007) 'Stability of organic carbon in deep soil layers controlled by fresh carbon supply', *Nature*, 450, pp. 277–280.

- Friend, J. A. (1992) 'Achieving soil sustainability', *Journal of Soil and Water Conservation*, 47, pp. 156-157.
- Fullen, M. A. (1985) 'Erosion of arable soils in Britain', *International Journal of Environmental Studies*, 26, pp. 55-69.
- Fullen, M. A. (1991) 'Soil organic matter and erosion processes on arable loamy sand soils in the west midlands of England', *Soil Technology*, 4(1), pp. 19-31.
- Fullen, M. A. (1992) 'Erosion rates on bare loamy sand soils in East Shropshire, UK', *Soil Use and Management*, 8, pp. 157-162.
- Fullen, M. A. (2020) Email to Dan Evans, 10 February.
- Gabet, E. J. and Mudd, S. M. (2010) 'Bedrock erosion by root fracture and tree throw: A coupled biogeomorphic model to explore the humped soil production function and the persistence of hillslope soils', *Journal of Geophysical Research*, 115, pp. 1-14. doi: 10.1029/2009JF001526
- Gabet, E. J., Reichman, O. J. and Seabloom, E. W. (2003) 'The effects of bioturbation on soil processes and sediment transport', *Annual Review of Earth and Planetary Science*, 31, pp. 249-273.
- Gabet, E. J., Eldelman, R. and Langner, H. (2006) 'Hydrological controls on chemical weathering rates at the soil-bedrock interface', *Geology*, 34(12), pp. 1065-1068.
- Gallois, R. and Owen, H. (2019) 'The stratigraphy of the Cretaceous (Albian stage) Gault and Upper Greensand formations: Dorset to Buckinghamshire and the western Weald, UK'. To be published in *Proceedings of the Geologists'*

Association [Preprint]. Available at: <https://doi.org/10.1016/j.pgeola.2019.07.005>
(Accessed: 12 April 2020).

Ghafari, H., Gorji, M., Arabkhedri, M., Roshani, G. A., Heidari, A. and Akhavan, S. (2017) 'Identification and prioritization of critical erosion areas based on onsite and offsite effects', *Catena*, 156, pp. 1-9. doi: 10.1016/j.catena.2017.03.014

Giani, L., Makowsky, L. and Mueller, K. (2014) 'Plaggic Anthrosol: Soil of the Year 2013 in Germany: An Overview on its Formation, Distribution, Classification, Soil Function and Threats', *Journal of Plant Nutrition and Soil Science*, 177, pp. 320-329.

Gibbard, P. L. and Clark, C. D. (2011) 'Pleistocene Glaciation Limits in Great Britain', in Ehlers, J., Gibbard, P. L. and Hughes, P. D. (eds) *Quaternary Glaciations –Extent and Chronology: a closer look*. Amsterdam: Elsevier, pp. 75-93.

Glinka, K. D. (1914) *Die Typen der Bodenbildung, irhe Klassifikation und Geographische Verbreitung*. Berlin: Gebruder Borntraeger.

Gogichaishvili, G. P. (2016) 'Soil erosion in river basins of Georgia', *Eurasian Soil Science*, 49(6), pp. 696-704.

Gollany, H. T., Schmacher, T. E., Lindstrom, M. J., Evenson, P. D., Lemme, G. D. (1992) 'Topsoil depth and desurfacing effects on properties and productivity of a typic Argiustoll', *Soil Science Society of America Journal*, 56, pp. 220-225.

Gontier, A., Rihs, S., Chabaux, F., Lemarchand, D., Pelt, E. and Tarpault, M. (2015) 'Lack of bedrock grain size influence on the soil production rate', *Geochimica et Cosmochimica Acta*, 166, pp. 146-164.

- Gosse, J. C. and Phillips, F. M. (2001) 'Terrestrial in situ cosmogenic nuclides: theory and application', *Quaternary Science Reviews*, 20, pp. 1475–1560.
- Goswami, A., Das, A. L., Sah, K. D. and Sarkar, D. (1996) 'Pedological studies in Great Nicobar Island', *Geographical Review of India*, 58, pp. 162-168.
- Goudie, A. S. and Viles, H. (1997) *Salt Weathering Hazards*. Chichester: Wiley and Sons.
- Goudie, A., Atkinson, B. W., Gregory, K. J., Simmons, I. G., Stoddart, D. R. and Sugden, D. (1994) *The Encyclopaedic Dictionary of Physical Geography*. Oxford: Basil Blackwell Ltd.
- Gould, I. J., Quinton, J. N., Weigelt, A., De Deyn, G. B. and Bardgett, R. D. (2016) 'Plant Diversity and root traits benefit physical properties key to soil function in grasslands', *Ecology Letters*, 19, pp. 1140-1149.
- Govers, G., Quine, T. A., Desmet, P. J. J. and Walling, D. E. (1996) 'The relative contribution of soil tillage and overland flow erosion to soil redistribution on agricultural land', *Earth Surface Processes and Landforms*, 21, pp. 929–946.
- Govers, G., Merckx, R., van Wesemael, B. and Van Oost, K. (2017) 'Soil conservation in the 21st century: why we need smart agricultural intensification', *SOIL*, 3, pp. 45–59.
- Graham, R. C., Rossi, A. M. and Hubbert, K. R. (2010) 'Rock to regolith conversion: Producing hospitable substrates for terrestrial ecosystems', *GSA Today*, 20(2), pp. 4-9. doi: 10.1130/GSAT57A.1
- Griffiths, K. J., Shand, P. and Ingram, J. (2003) *Baseline Report Series: 8. The Permo-Triassic Sandstones of Manchester and East Cheshire*. Solihull:

Environment Agency. Available at:

<https://www.bgs.ac.uk/downloads/start.cfm?id=752> (Accessed: 11 January 2020).

Grigor'ev, V. Y. (1998) 'Calculation of a criterion for minimizing soil erosion and optimizing conservation measures', *Eurasian Soil Science*, 31(4), pp. 422-428.

Guo, Z., Zobeck, T. M., Zhang, K., and Li, F. (2013) 'Estimating potential wind erosion of agricultural lands in northern China using the revised wind erosion equation and geographic information systems', *Journal of Soil and Water Conservation*, 68(1), pp. 13-21.

Gyssels, G., Poesen, J., Bochet, E. and Li, Y. (2005) 'Impact of plant roots on the resistance of soils to erosion by water: a review', *Progress in Physical Geography*, 29, pp. 189-217.

Hacisalihoglu, S., Mert, A., Negiz, M. G. and Muys, B. (2010a) 'Soil loss prediction using Universal Soil Loss Equation (USLE) simulation model in a mountainous area in Aglasun district, Turkey', *African Journal of Biotechnology*, 9(24), pp. 3589-3594.

Hacisalihoglu, S., Oktan, E., and Yucesan, Z. (2010b) 'Predicting soil erosion in oriental Spruce (*Picea orientalis* (L.) Link.) Stands in eastern Black Sea region of Turkey', *African Journal of Agricultural Research*, 5(16), pp. 2200-2214.

Hancock, G. R., Wells, T., Martinez, C. and Dever, C. (2015) 'Soil erosion and tolerable soil loss: insights into erosion rates for a well-managed grassland catchments', *Geoderma*, 237, pp. 256–265.

Hartemink, A. E. and McBratney, A. (2008) 'A soil science renaissance', *Geoderma*, 148, pp. 123-129.

Hasenmueller, E. A., Gu, X., Weitzman, J. N., Adams, T. S., Stinchcomb, G. E., Eissenstat, D. M., Drohan, P. J., Brantley, S. L. and Kaye, J. P. (2017) 'Weathering of rock to regolith: the activity of deep roots in bedrock fractures', *Geoderma*, 300, pp. 11-31.

Hayes, J. L., Riebe, C. S., Holbrook, W. S., Flinchum, B. A. and Hartsough, P. C. (2019) 'Porosity production in weathered rock: where volumetric strain dominates over chemical mass loss', *Geology*, 5, pp. 1-11. doi: 10.1126/sciadv.aao0834

He, X., Bao, Y., Nan, H., Xiong, D., Wang, L., Liu, Y. and Zhao, J. (2009) 'Tillage pedogenesis of purple soils in southwestern China', *Journal of Mountain Science*, 6(2), pp. 205-210.

Heimsath, A. M. (2006) 'Eroding the land: steady-state and stochastic rates and processes through a cosmogenic lens', *Geological Society of America*, 415, pp. 111-129.

Heimsath, A. M. (2014) 'Limits of Soil Production?', *Science*, 343, pp. 617–618.

Heimsath, A. M. and Burke, B. C. (2013) 'The impact of local geochemical variability on quantifying hillslope soil production and chemical weathering', *Geomorphology*, 200, pp. 75–88.

Heimsath, A. M. and Whipple, K. X. (2019) 'Strength matters: resisting erosion across upland landscapes', *Earth Surface Processes and Landforms*, 44, pp. 1748-1754.

Heimsath, A. M., Dietrich, W. E., Nishiizumi, K. and Finkal, R. C. (1997) 'The Soil Production Function and Landscape Equilibrium', *Nature*, 388, pp. 358-361.

- Heimsath, A. M., Dietrich, W. E., Nishiizumi, K. and Finkel, R. C. (1999) 'Cosmogenic nuclides, topography and the spatial variation of soil depth', *Geomorphology*, 27, pp. 151-171.
- Heimsath, A. M., Chappell, J., Dietrich, W. E., Nishiizumi, K. and Finkel, R. C. (2000) 'Soil production on a retreating escarpment in southeastern Australia', *Geology*, 28(3), pp. 787-790.
- Heimsath, A. M., Chappell, J., Dietrich, W. E., Nishiizumi, K. and Finkel, R. C. (2001a) 'Late Quaternary erosion in southeastern Australia: a field example using cosmogenic nuclides', *Quaternary International*, 83, pp. 169-185.
- Heimsath, A. M., Dietrich, W. E., Nishiizumi, K. and Finkel, R. C. (2001b) 'Stochastic processes of soil production and transport: erosion rates, topographic variation and cosmogenic nuclides in the Oregon Coast Range', *Earth Surface Processes and Landforms*, 26, pp. 531-532.
- Heimsath, A. M., Furbish, D. J. and Dietrich, W. E. (2005) 'The illusion of diffusion: field evidence for depth-dependent sediment transport', *Geology*, 33(12), pp. 949-952.
- Heimsath, A. M., Fink, D. and Hancock, G. R. (2009) 'The 'humped' soil production function: eroding Arnhem Land, Australia', *Earth Surface Processes and Landforms*, 34(12), pp. 1674-1684.
- Heimsath, A. M., DiBiase, R. A. and Whipple, K. X. (2012) 'Soil production limits and the transition to bedrock-dominated landscapes', *Nature Geoscience*, 5(3), pp. 210-214.

Heimsath, A. M. and Burke, B. C. (2013) 'The impact of local geochemical variability on quantifying hillslope soil production and chemical weathering', *Geomorphology*, 200, pp. 75-88.

Hemingway, J. D., Hilton, R. G., Hovius, N., Eglinton, T. I., Haghipour, N., Wacker, L., Cheh, M. and Galy, V. V. (2018) 'Microbial oxidation of lithospheric organic carbon in rapidly eroding tropical mountain soils', *Science*, 360(6385), pp. 209-212.

Hengl, T., de Jesus, J. M., Heuvelink, G. B. M., Gonzalez, M. R., Kilibarda, M., Blagotić, A., Shangguan, W., Wright, M. N., Geng, X., Bauer-Marschaling, B., Guevara, M. A., Vargas, R., MacMillan, R. A., Batjes, N. H., Leenaars, J. G. B., Ribeiro, E., Wheeler, I., Mantel, S. and Kempen, B. (2017) 'SoilGrids250m: Global gridded soil information based on machine learning', *PLOS ONE*, 12(2), pp. 1-40. doi: 10.1371/journal.pone.0169748

Herweg, K. and Ludi, E. (1999) 'The performance of selected soil and water conservation measures- case studies from Ethiopia and Eritrea', *Catena*, 36, pp. 99-114.

Hollis, J. M. and Reed, A. H. (1981) 'The Pleistocene deposits of the southern Worfe catchment', *Proceedings of the Geologists' Association*, 92, pp. 59-74.

Hooke, R. L. B. (2000) 'On the history of humans as geomorphic agents', *Geology*, 28(9), pp. 843-846.

Hornung, M. (1974) 'Soils of Hirta', in Jewell, P. A., Milner, C., Boyd, J. M. (eds) *Island Survivors: The Ecology of the Soay Sheep of St. Kilda*. London: Athlone Press, pp. 70-87.

Hua, L. Z., He, X. B., Yuan, Y. P. and Nan, H. W. (2012) 'Assessment of Runoff and Sediment Yields Using the AnnAGNPS Model in a Three-Gorge Watershed of China', *International Journal of Environmental Research and Public Health*, 9(5), pp. 1887-1907.

Huang, L., Zhang, G. and Yang, J. (2013) 'Weathering and soil formation rates based on geochemical mass balances in a small forested watershed under acid precipitation in subtropical China', *Catena*, 105, pp. 11-20.

Huggett, R. J. (1998) 'Theories of Pedogenesis and Chronosequence Studies', *Catena*, 32, pp. 155-172.

Huggett, R. J. (2003) *Fundamentals of Geomorphology*. London: Routledge.

Humphreys, G. S. (1994) 'Bioturbation, biofabrics and the biomantle: an example from the Sydney Basin', in Ringrose-Voase, A. J. and Humphreys, G. S. (eds) *Soil Micromorphology: studies in management and genesis*. Amsterdam: Elsevier, pp. 421–436.

Hunt, C. B. (1972) *Geology of Soils*. San Francisco: W. H. Freeman.

Hurni, H. (1983) 'Soil Erosion and Soil Formation in Agricultural Ecosystems Ethiopia and Northern Thailand', *Mountain Research and Development*, 3(2), pp. 131-142.

Igwe, C. A. (1999) 'Land use and soil conservation strategies for potentially highly erodible soils of central-eastern Nigeria', *Land Degradation and Development*, 10(5), pp. 425-434.

Il'ichev, B. A. (1999) 'On the reproduction of loose mantles in mountain regions (by the example of northern Caucasus)', *Eurasian Soil Science*, 32(2), pp. 157-170.

IPCC (2006) 'Cropland', in IPCC (ed.) *IPCC Guidelines for National Greenhouse Gas Inventories. Vol. 4: Agriculture, Forestry and Other Land Use*. Available at: <https://www.ipcc-nggip.iges.or.jp/public/2006gl/vol4.html> (Accessed: 19 April 2020).

IPCC (2019) *Climate Change and Land: an IPCC Special Report on climate change, desertification, land degradation, sustainable land management, food security, and greenhouse gas fluxes in terrestrial ecosystems*. Available at: <https://www.ipcc.ch/report/srccl/> (Accessed: 2 October 2019).

IUSS Working Group WRB (2015) *World Reference Base for Soil Resources 2014, update 2015 International soil classification system for naming soils and creating legends for soil maps*. World Soil Resources Reports No. 106. FAO: Rome.

James, L. A. (1988) 'Rates of organic carbon accumulation in young mineral soils near Burroughs Glacier, Glacier Bay, Alaska', *Physical Geography*, 9, pp. 50-70.

Jenny, H. (1941) *Factors of Soil Formation: A System of Quantitative Pedology*. New York: McGraw-Hill.

Jha, P., Nitant, H. C. and Mandal, D. (2009) 'Establishing permissible erosion rates for various landforms in Delhi State, India', *Land Degradation and Development*, 20(1), pp. 92-100.

Jin, K., Shen, J., Ashton, R. W., Dodd, I. C., Parry, M. A. J. and Whalley, W. R. (2013) 'How do roots elongate in a structured soil?' *Journal of Experimental Botany*, 64(15), pp. 4761-4777.

Jirasuktaveekul, W., Sritulanon, C., Rungrojwanich, M. B. and Ploicharuen, P. (1998) *Soil and Water Losses in Reforestation Intercropped with Vetiver Strips at the Ping, Wang, Yom and Nan Sub-River Basins of Northern Thailand*. Bangkok, Thailand: Royal Forest Department.

Johnson, L. C. (1987) 'Soil Loss Tolerance: Fact or Myth?' *Journal of Soil and Water Conservation*, 42(3), pp. 155-160.

Johnson, H. D. and Levell, B. K. (1995) 'Sedimentology of a transgressive, estuarine sand complex: the Lower Cretaceous Woburn Sands (Lower Greensand), southern England', in Plint, A. G. (ed.) *Sedimentary Facies Analysis*. Oxford: Blackwell Science Ltd, pp. 17-47.

Johnston, A. E. (1977) *Woburn Experimental Farm*. Harpenden: Rothamsted Research.

Jones, M. J. (1985) 'The weathered zone aquifers of the basement complex areas of Africa', *Quarterly Journal of Engineering Geology and Hydrogeology*, 18, pp. 35-46. doi: 10.1144/GSL.QJEG.1985.018.01.06

Karas, E. and Oguz, I. (2015) 'A new approach to determine land use planning and soil conservation measures based on soil erosion classification', *Carpathian Journal of Earth and Environmental Sciences*, 10(2), pp. 145-158.

Karlen, D. L. and Stott, D. E. (1994) 'A framework for evaluating physical and chemical indicators of soil quality', in Doran, J. W., Coleman, D. C., Bezdicsek, D.

F. and Stewart, B. A. (eds) *Defining Soil Quality for a Sustainable Environment*. Madison, WI: ASA, CSSA and SSSA, pp. 53-73.

Kereselidze, D. N., Matchavariani, L. G., Kalandadze, B. B. and Trapaidze, V. Z. (2013) 'Allowable soil erosion rates in Georgia', *Eurasian Soil Science*, 46(4), pp. 438-446.

Khalifa, M. and Morad, S. (2012) 'Impact of structural setting on diagenesis of fluvial and tidal sandstones: The Bahi Formation, Upper Cretaceous, NW Sirt Basin, North Central Libya', *Marine and Petroleum Geology*, 38(1), pp. 211-231.

King, G. J., Acton, D. F. and St. Arnaud, R. J. (1983) 'Soil-landscape analysis in relation to soil redistribution and mapping at a site within the Weyburn association', *Canadian Journal of Soil Science*, 63, pp. 657–670.

Kirkbride, M. P. and Reeves, A. D. (1993) 'Soil-erosion caused by low-intensity rainfall in Angus, Scotland', *Applied Geography*, 13(4), pp. 299-311.

Kirkby, M. J. (2018) 'A conceptual model for physical and chemical soil profile evolution', *Geoderma*, 331, pp. 121-130.

Kirkby, M. J. and Morgan, R. P. C. (eds) (1980) *Soil Erosion*. Chichester: John Wiley and Sons.

Kliment'ev, A. I. and Tikhonov, V. E. (2001) 'Ecohydrological analysis of soil loss tolerance in agrolandscapes', *Eurasian Soil Science*, 34(6), pp. 673-682.

Kohl, C. P. and Nishiizumi, K. (1992) 'Chemical isolation of quartz for measurement of in-situ produced cosmogenic nuclides', *Geochimica et Cosmochimica Acta*, 56, pp. 3583–3587.

- Konert, M. and Vandenberghe, J. (1997) 'Comparison of laser grain size analysis with pipette and sieve analysis: a solution for the underestimation of the clay fraction', *Sedimentology*, 44, pp. 523-535.
- Kosse, A. D. (1990) 'Diagnostic horizons in Anthrosols', in Rozanov, B. G. (ed.) *Soil Classification*. Moscow: USSR State Committee for Environmental Protection, pp. 264-273.
- Kuznetsov, M. S. and Abdulkhanova, D. R. (2013) 'Soil loss tolerance in the central chernozemic region of the European part of Russia', *Eurasian Soil Science*, 46(7), pp. 802-809.
- Lakaria, B. I., Biswas, H. and Mandal, D. (2008) 'Soil loss tolerance values for different physiographic regions of central India', *Soil Use and Management*, 24(2), pp. 192-198.
- Lakaria, B. I., Biswas, H. and Mandal, D. (2009) 'Soil loss tolerance values for different physiographic regions of central India', *Soil Use and Management*, 25(1), p. 104.
- Lal, D. (1991) 'Cosmic ray labelling of erosion surfaces: *in situ* nuclide production rates and erosion models', *Earth and Planetary Science Letters*, 104, pp. 424-439.
- Lal, R. (1998) 'Soil Erosion Impact on Agronomic Productivity and Environment Quality', *Critical Reviews in Plant Sciences*, 17(4), pp. 319-464.
- Lal, R. (2001) 'Soil degradation by erosion', *Land Degradation and Development*, 12(6), pp. 519-539.

Lal, R. (2009) 'Ten Tenets of Sustainable Soil Management', *Journal of Soil and Water Conservation*, 64(1), p. 20.

Langdale, G. W., Mills, W. C. and Thomas, A. W. (1992) 'Use of conservation tillage to retard erosive effects of large storms', *Journal of Soil and Water Conservation*, 47(3), pp. 257-260.

Larkin, R. P. (2015) 'Soil Health Paradigms and Implications for Disease Management', *Annual Review of Phytopathology*, 53, pp. 199-221.

Larney, F. J., Izaurralde, R. C., Olson, B. M., Janzen, H. H., Solberg, E. D., Nyborg, M., Lindwall, C. W. (1995) 'Soil erosion – crop productivity relationships for six Alberta soils', *Journal of Soil and Water Conservation*, 50(1), pp. 87-91.

Larsen, I. J., Almond, P. C., Eger, A., Stone, J. O., Montgomery, D. R. and Malcolm, B. (2014) 'Rapid soil production and weathering in the southern Alps, New Zealand', *Science*, 343, pp. 637-640.

Larson, W. E. and Pierce, F. J. (1994) 'The dynamics of soil quality as a measure of sustainable management', in Doran, J. W., Coleman, D. C., Bezdicek, D. F. and Stewart, B. A. (eds) *Defining Soil Quality for a Sustainable Environment*. Madison, WI: ASA, CSSA and SSSA, pp. 37-53.

Lazo, D. E., Dyer, L. G. and Alorro, R. D. (2017) 'Silicate, phosphate and carbonate mineral dissolution behaviour in the presence of organic acids: a review', *Minerals Engineering*, 100, pp. 115-123.

Lebedeva, M. I. and Brantley, S. L. (2017) 'Weathering and erosion of fractured bedrock systems', *Earth Surface Processes and Landforms*, 42(13), pp. 2090-2108. doi: 10.1002/esp.4177

- Lebedeva, M. I. and Brantley, S. L. (2020) 'Exploring an 'ideal hill': how lithology and transport mechanisms affect the possibility of a steady state during weathering and erosion', *Earth Surface Processes and Landforms*, 45(3), pp. 652-665.
- Lenka, N. K., Mandal, D. and Sudhishri, S. (2014) 'Permissible soil loss limits for different physiographic regions of west Bengal', *Current Science*, 107(4), pp. 665-670.
- Lentz, R. D. and Sojka, R. E. (1994) 'Field results using polyacrylamide to manage furrow erosion and infiltration', *Soil Science*, 158(4), pp. 274-282.
- Le Roux, J. J., Morgenthal, T. I., Malherbe, J., Pretorius, D. J. and Sumner, P. D. (2008) 'Water erosion prediction at a national scale for South Africa', *Water Sa*, 34(3), pp. 305-314.
- Li, G., Ye, S. G., Shen, Z. W., Lu, F. C. and Zhang, J. J. (2017a) 'Study on the standard of soil erosion gradation based on erosive daily rainfall', *International Conference On Energy, Environment and Materials Science*. Singapore, 28 – 30 July. Available at: <https://iopscience.iop.org/article/10.1088/1755-1315/94/1/012076/meta> (Accessed: 19 April 2020).
- Li, L., Du, S., Wu, L. and Liu, G. (2009) 'An overview of Soil Loss Tolerance', *Catena*, 78, pp. 93-99.
- Li, Y., Bai, X. Y., Wang, S. J., Qin, L. Y., Tian, Y. C. and Luo, G. J. (2017b) 'Evaluating of the spatial heterogeneity of soil loss tolerance and its effects on erosion risk in the carbonate areas of southern China', *Solid Earth*, 8(3), pp. 661-669.

- Li, Z. W., Xu, X. I., Zhang, Y. H., Wang, K. I. and Zeng, P. (2017c) 'Reconstructing recent changes in sediment yields from a typical karst watershed in southwest China', *Agriculture Ecosystems and Environment*, 269, pp. 62-70.
- Li, Z. W., Xu, X. I., Xu, C. H., Liu, M. X., Wang, K. I. and Yi, R. Z. (2019) 'Monthly sediment discharge changes and estimates in a typical karst catchment of southwest China', *Journal of Hydrology*, 555, pp. 95-107.
- Linick, T. W., Damon, P. E., Donahue, D. J. and Jull, A. J. T. (1989) 'Accelerator mass spectrometry: the new revolution in radiocarbon dating', *Quaternary International*, 1, pp. 1-6.
- Liu, G., Lan, L., Wu, L., Wang, G., Zhou, Z. and Du, S. (2009) 'Determination of Soil Loss Tolerance of an Entisol in Southwest China', *Soil Science Society of America Journal*, 73(2), pp. 412-417.
- Liu, J., Kong, W., Zhang, G., Khan, A., Guo, G., Zhu, C., Wei, X., Kang, S. and Morgan-Kiss, R. M. (2016) 'Diversity and succession of autotrophic microbial community in high-elevation soils along deglaciation chronosequence', *FEMS Microbiology Ecology*, 92(10), pp. 1-11. doi: 10.1093/femsec/fiw160
- Liu, Y. B., Chang, Q. R., Liu, J., Ju, W. M., Zhu, G. L. and Duan, Z. (2010) 'Spatial distribution of soil erosion in a black soil region of northeast China studied using remote sensing and GIS techniques', *18th International Conference On Geoinformatics*. Beijing, China, 18 – 20 June. Available at: <https://ieeexplore.ieee.org/xpl/conhome/5559273/proceeding> (Accessed: 19 April 2020).

- Lu, H. and An, Z. (1998) 'Paleoclimatic significance of grain size of loess-palaeosol deposit in Chinese Loess Plateau', *Science in China Series D: Earth Sciences*, 41, pp. 626-631.
- Malhi, S. S., Izaurralde, R. C., Nyborg, M. and Solberg, E. D. (1994) 'Influence of topsoil removal on soil fertility and barley growth', *Journal of Soil and Water Conservation*, 49(1), pp. 96-101.
- Mandal, D. and Sharda, V. N. (2011) 'Assessment of permissible soil loss in India employing a quantitative bio-physical model', *Current Science*, 100(3), pp. 383-390.
- Mandal, D. and Sharda, V. N. (2013) 'Appraisal of soil erosion risk in the eastern Himalayan region of India for soil conservation planning', *Land Degradation and Development*, 24(5), pp. 430-437.
- Mandal, D. and Tripathi, K. P. (2010) 'Soil erosion limits for Lakshadweep archipelago', *Current Science*, 96(2), pp. 276-280.
- Mandal, D., Sharda, V. N. and Tripathi, K. R. (2009) 'Relative efficacy of two biophysical approaches to assess soil loss tolerance for Doon valley soils of India', *Journal of Soil and Water Conservation*, 65(1), pp. 42-49.
- Mareschal, L., Turpault, M. P. and Ranger, J. (2015) 'Effect of granite crystal grain size on soil properties and pedogenic processes along a lithosequence', *Geoderma*, 249, pp. 12–20.
- Martin, R. E. (1977) 'Estimating Foundation Settlements in Residual Soils', *Journal of the Geotechnical Engineering Division*, 103(3), pp. 197-212.

Martin, C. K. and Cassel, D. K. (1992) 'Soil loss and silage yield for 3 tillage management-systems', *Journal of Production Agriculture*, 5(4), pp. 581-586.

Martínez-Casasnovas, J. A., Ramos, M. C. and Ribes-Dasi, M. (2002) 'Soil erosion caused by extreme rainfall events: mapping and quantification in agricultural plots from very detailed digital elevation models', *Geoderma*, 105, pp. 125-140.

Matysek, M., Leake, J., Banwart, S., Johnson, I., Page, S., Kaduk, J., Smalley, A., Cumming, A., and Zona, D. (2019) 'Impact of fertiliser, water table, and warming on celery yield and CO₂ and CH₄ emissions from fenland agricultural peat', *Science of the Total Environment*, 667, pp. 179-190.

Mbagwu, J. S. C. (1991) 'Soil-loss tolerance of some Nigerian soils in relation to profile characteristics', *Turrialba*, 41(2), pp. 223-229.

McAuliffe, J. R. (1994) 'Landscape Evolution, Soil Formation, and Ecological Patterns and Processes in Sonoran Desert Bajadas', *Ecological Monographs*, 64(2), pp. 111-148.

McBratney, A., Field, D. J. and Koch, A. (2014) 'The dimensions of soil security', *Geoderma*, 212, pp. 203-213.

McDaniel, P. A., Lowe, D. J., Arnoulds, O. and Ping, C. L. (2011) 'Andisols', in Huang, P. M., Li, Y. and Summer, M. E. (eds) *Handbook of Soil Sciences*, 2nd ed. New York: CRC Press, pp. 33-48.

Medeiros, G. O. R., Giarolla, A., Sampalo, G. and Marinho, M. A. (2016) 'Diagnosis of the Accelerated Soil Erosion in São Paulo State (Brazil) by the Soil Lifetime Index Methodology', *Revista Brasileira de Ciência do Solo*, 40, pp. 1-15.

doi: 10.1590/18069657rbcS20150498

Mellerowicz, K. T., Rees, H. W., Chow, T. I. and Ghanem, I. (1994) 'Soil conservation planning at the watershed level using the universal soil loss equation with GIS and microcomputer technologies - a case-study', *Journal of Soil and Water Conservation*, 49(2), pp. 194-200.

Mendes, H., Tavares, A. S., Dos Santos, W. J. R., Silva, M. I. N., Santos, B. R. and Mincato, R. I. (2018) 'Water erosion in Oxisols under coffee cultivation', *Revista Brasileira De Ciencia Do Solo*, 42, doi: 10.1590/18069657rbc20170093.

Met Office (2018) *HadUK-Grid gridded and regional average climate observations for the UK*. Available at:

<http://catalogue.ceda.ac.uk/uuid/4dc8450d889a491ebb20e724debe2dfb>

(Accessed: 31 August 2019).

Milodowski, A. E. and Wilmot, R. D. (1985) 'Mineralogical and petrographic studies of Jurassic and Cretaceous sediments from southern England and their relevance to radioactive waste disposal', *Mineralogical Magazine*, 49, pp. 255-263.

Minasny, B. and McBratney, A. B. (1999) 'A rudimentary mechanistic model for soil production and landscape development', *Geoderma*, 90, pp. 3-21.

Minasny, B., Finke, P., Stockmann, U., Vanwalleghem, T. and Bratney, A. B. (2015) 'Resolving the integral connection between pedogenesis and landscape evolution', *Earth Science Reviews*, 150, pp. 102–120.

Mirtskhulava, T. E. (2001) 'On the maximum soil loss tolerance', *Eurasian Soil Science*, 34(3), pp. 321-325.

Mizra, R., Dexter, A. and Alston, A. (1986) 'Maximum Axial and Radial Growth pressures of plant roots', *Plant and Soil*, 95, pp. 315-326.

Moges, D. M. and Bhat, H. G. (2017) 'Integration of geospatial technologies with RUSLE for analysis of land use/cover change impact on soil erosion: case study in Rib watershed, north-western highland Ethiopia', *Environmental Earth Sciences*, 76(22), p. 765.

Montgomery, D. R. (2007) 'Soil erosion and agricultural sustainability', *Proceedings of the National Academy of Sciences of the United States of America*, 104(33), pp. 13268-13272.

Montgomery, D. R. (2008) 'Pay dirt', *Scientific American*, 299(1), p. 76.

Moore, A. K. and Granger, D. E. (2019) 'Watershed-averaged denudation rates from cosmogenic ^{36}Cl in detrital magnetite', *Earth and Planetary Science Letters*, 527, pp. 1-10. doi: 10.1016/j.epsl.2019.115761

Moraes, M. A. S. and De Ros, L. (1990) 'Infiltrated clays in fluvial Jurassic sandstones of Recôncavo Basin, Northeastern Brazil', *Journal of Sedimentary Petrology*, 60(6), pp. 809-819.

Morel, P., van Blankenburg, F., Schaller, M., Kubik, P. W. and Hinderer, M. (2003) 'Lithology, landscape dissection and glaciation controls on catchment erosion as determined by cosmogenic nuclides in river sediment (the Wutach Gorge, Black Forest)', *Terra Nova*, 15, pp. 398-404.

Morton, H. V. (1927) *In Search of England*. London: Methuen and Co. Ltd.

Mountney, N. P. and Thompson, D. B. (2002) 'Stratigraphic evolution and preservation of aeolian dune and damp/wet interdune strata: an example from the Triassic Helsby Sandstone Formation, Cheshire Basin, UK', *Sedimentology*, 49, pp. 805-833.

- Mudd, S. M. and Yoo, K. (2010) 'Reservoir theory for studying the geochemical evolution of soils', *Journal of Geophysical Research*, 115, pp. 1-13. doi: 10.1029/2009JF001591
- Muhs, D. R. (1984) 'Intrinsic Thresholds in Soil Systems', *Physical Geography*, 5(2), pp. 99-110.
- Muhs, D. R. and Wolfe, S. A. (1999) 'Sand dunes of the northern Great Plains of Canada and the United States', *Geological Survey of Canada Bulletin*, 534, pp. 183-197.
- Nachtergaele, F., van Velthuisen, H., Verelst, L., Batjes, N., Dijkshoorn, K., van Engelen, V., Fischer, G., Jones, A., Montanarella, L., Petri, M., Prieler, S., Teixeira, E., Wiberg, D. and Shi, X. (2008) *Harmonized World Soil Database*. Available at: <http://webarchive.iiasa.ac.at/Research/LUC/External-World-soil-database/HTML/> (Accessed: 25 May 2018).
- Nannipieri, P., Ascher, J., Ceccherini, M. T., Landi, L., Pietramellara, G. and Renella, G. (2003) 'Microbial Diversity and Soil Functions', *European Journal of Soil Science*, 54, pp. 655-670.
- Navarre-Sitchler, A., Brantley, S. L. and Rother, G. (2015) 'How porosity increases during incipient weathering of crystalline silicate rocks', *Reviews in Mineralogy and Geochemistry*, 80, pp. 331-354. doi: 10.2138/rmg.2015.80.10
- Nearing, M. A., Pruski, F. F. and O'Neal, M. R. (2004) 'Expected climate change impacts on soil erosion rates: a review', *Journal of Soil and Water Conservation*, 59(1), pp. 43-50.
- Neely, A. B., DiBiase, R. A., Corbett, L. B., Bierman, P. R. and Caffee, M. W. (2019) 'Bedrock fracture density controls on hillslope erodibility in steep, rocky

landscapes with patchy soil cover, southern California, USA', *Earth and Planetary Science Letters*, 522, pp. 186-197.

Neuman, S. P. (2005) 'Trends, prospects and challenges in quantifying flow and transport through fractured rock', *Hydrogeology Journal*, 13, pp. 124-147. doi: 10.1007/s10040-004-0397-2

Newman, J. K., Kaleita, A. I. and Laflen, J. M. (2010) 'Soil erosion hazard maps for corn stover management using national resources inventory data and the water erosion prediction project', *Journal of Soil and Water Conservation*, 65(4), pp. 211-222.

Norton, K. P., Molnar, P. and Schlunegger, F. (2014) 'The role of climate-driven chemical weathering on soil production', *Geomorphology*, 204, pp. 510-517.

Nyakatawa, E. Z., Reddy, K. C. and Lemunyon, J. L. (2001) 'Predicting soil erosion in conservation tillage cotton production systems using the revised universal soil loss equation (RUSLE)', *Soil and Tillage Research*, 57, pp. 213-224.

Obrist-Farner, J. and Yang, W. (2017) 'Provenance and depositional conditions of fluvial conglomerates and sandstones and their controlling processes in a rift setting, mid-Permian lower and upper Quanzijie low order cycles, Bogda Mountains, NW China', *Journal of Asian Earth Sciences*, 138, pp. 317-340.

Ochs, M. (1996) 'Influence of humified and non-humified natural organic compounds on mineral dissolution', *Chemical Geology*, 132, pp. 119-124.

Olivetti, D., Mincato, R. I., Ayer, J. E. B., Silva, M. I. N. and Curi, N. (2015) 'Spatial and temporal modeling of water erosion in dystrophic red latosol (Oxisol)

used for farming and cattle raising activities in a sub-basin in the south of Minas Gerais', *Ciencia E Agrotecnologia*, 39(1), pp. 58-67.

Ollier, C. and Pain, C. (1996) *Regolith, Soils, and Landforms*. Chichester: John Wiley and Sons.

Opolot, E., Yu, Y. and Finke, P. (2015) 'Modeling soil genesis at pedon and landscape scales: Achievement and problems', *Quaternary International*, 376, pp. 34-46.

Owen, H. G. (1992) 'The Gault-Lower Greensand Junction Beds in the northern Weald (England) and Wissant (France), and their depositional environment', *Proceedings of the Geologists' Association*, 103, pp. 83-110.

Owen, J. J., Amundson, R., Dietrich, W. E., Nishiizumi, K., Sutter, B. and Chong, G. (2011) 'The sensitivity of hillslope bedrock erosion to precipitation', *Earth Surface Processes and Landforms*, 36(1), pp. 117-135.

Pacheco, F. A. L., Varandas, S. G. P., Fernandes, L. F. S. and Valle, R. F. (2014) 'Soil losses in rural watersheds with environmental land use conflicts', *Science of the Total Environment*, 485, pp. 110-120.

Palmer, S. N. and Barton, M. E. (1987) 'Porosity reduction, microfabric and resultant lithification in UK uncemented sands', in Marshall, J. D. (ed.) *Diagenesis of Sedimentary Sequences*. London: Geological Society, pp. 29-40.

Palumbo, L., Hetzel, R., Tao, M. and Li, X. (2009) 'Topographic and lithologic control on catchment-wide denudation rates derived from cosmogenic ^{10}Be in two mountain ranges at the margin of NE Tibet', *Geomorphology*, 117, pp. 130-142.

- Panagos, P., Borelli, P., Meusburger, K., Alewell, C., Lugato, E. and Montanarella, L. (2015) 'Estimating the soil erosion cover- management factors at the European scale', *Land Use Policy*, 48, pp. 38-50.
- Panagos, P., Imeson, A., Meusburger, K., Borrelli, P., Poesen, J. and Alewell, C. (2016) 'Soil conservation in Europe: Wish or Reality?', *Land Degradation and Development*, 27(6), pp. 1547-1551.
- Pape, J. C. (1970) 'Plaggen soils in the Netherlands', *Geoderma*, 4, pp. 229-255.
- Passioura, J. B. (1991) 'Soil structure and plant growth', *Australian Journal of Soil Research*, 29(6), pp. 717-728.
- Pate, J. S., Jeschke, D., Dawson, T. E., Raphael, C., Hartung, W. and Bowen, B. J. (1998) 'Growth and Seasonal Utilisation of Water and Nutrients by *Banksia prionotes*', *Australian Journal of Botany*, 46(4), pp. 511-532. doi: 10.1071/BT97045
- Patsukevich, Z. V., Gennadiev, A. N. and Gerasimova, M. I. (1997) 'Soil loss tolerance and self-rehabilitation of soils', *Eurasian Soil Science*, 30(5), pp. 557-563.
- Patton, N. R., Lohse, K. A., Godsey, S. E., Crosby, B. T. and Seyfried, M. S. (2018) 'Predicting soil thickness on soil mantled hillslopes', *Nature Communications*, 9(3329), pp. 1-10.
- Paul, E. A., Campbell, C. A., Rennie, D. A. and McCallum, K. J. (1964) 'Investigations of the dynamics of soil humus utilizing carbon dating techniques', *Transactions of the 8th International Congress of Soil Science*, 3, pp. 201-208.

Pavich, M. J. (1986) 'Processes and rates of saprolite production and erosion on a foliated granitic rock of the Virginia piedmont', in Colman, S. M. and Dethier, D. P. (eds) *Rates of Chemical Weathering of Rocks and Minerals*. Florida: Academic Press, pp. 551-590.

Pelletier, J. D. and Baker, V. R. (2011) 'The role of weathering in the formation of bedrock valleys on Earth and Mars: A numerical modelling investigation', *Journal of Geophysical Research*, 116, pp. 1-13. doi: 10.1029/2011JE003821

Peltre, C., Gregorich, E. G., Bruun, S., Jensen, L. S. and Magid, J. (2017) 'Repeated application of organic waste affects soil organic matter composition: evidence from thermal analysis, FTIR-PAS, amino sugars and lignin biomarkers', *Soil Biology and Biochemistry*, 104, pp. 117-127.

Peng, T. and Wang, S. J. (2012) 'Effects of land use, land cover and rainfall regimes on the surface runoff and soil loss on karst slopes in southwest China', *Catena*, 90, pp. 53-62.

Pennock, D. J. (2003) 'Terrain attributes, landform segmentation, and soil redistribution', *Soil Tillage Research*, 69, pp. 15–26.

Peterson, F. F. (1980) 'Holocene desert soil formation under sodium salt influence in a playa-margin environment', *Quaternary Reviews*, 13, pp. 172-186.

Pettijohn, F. J., Potter, P. E. and Siever, R. (1987) *Sand and Sandstone*. New York: Springer-Verlag.

Phillips, J. D. (1993) 'Progressive and Regressive Pedogenesis and Complex Soil Evolution', *Quaternary Research*, 40, pp. 169-176.

- Phillips, J. D. (2010) 'The convenient fiction of steady-state soil thickness', *Geoderma*, 156, pp. 389–398.
- Phillips, D. I., White, D. and Johnson, B. (1993) 'Implications of climate-change scenarios for soil-erosion potential in the USA', *Land Degradation and Rehabilitation*, 4(2), pp. 61-72.
- Phillips, F. M., Argento, D. C., Balco, G., Caffee, M. W., Clem, J., Dunai, T. J., Finkel, R., Goehring, B., Gosse, J. C., Hudson, A. M., Jull, A. J. T., Kelly, M. A., Kurz, M., Lal, D., Lifton, N., Marrero, S. M., Nishiizumi, K., Reedy, R. C., Schaefer, J., Stone, J. O. H., Swanson, T., and Zreda, M. G. (2016) 'The CRONUS-Earth Project: A synthesis', *Quaternary Geochronology*, 31, pp. 119–154.
- Pierce, F. J., Larson, W. E. and Dowdy, R. H. (1984) 'Soil loss tolerance - maintenance of long-term soil productivity', *Journal of Soil and Water Conservation*, 39(2), pp. 136-138.
- Pimentel, D., Harvey, C., Resosudarmo, P., Sinclair, K., Kurz, D., McNair, M., Crist, S., Shpritz, L., Fitton, L., Saffouri, R., and Blair, R. (1995) 'Environmental and Economic Costs of Soil Erosion and Conservation Benefits', *Science*, 267, pp. 1117–1123.
- Poesen, J. (2017) 'Soil erosion in the Anthropocene: research needs', *Earth Surface Processes and Landforms*, 43(1), pp. 64-84.
- Pope, G. A., Dorn, R. I. and Dixon, J. C. (1995) 'A New Conceptual Model for Understanding Geographical Variations in Weathering', *Annals of the Association of American Geographers*, 85(1), pp. 38-64.

- Portenga, E. W. and Bierman, P. R. (2011) 'Understanding Earth's eroding surface with ^{10}Be ', *GSA Today*, 21(8), pp. 4-10.
- Power, J. F., Sandoval, F. M., Ries, R. E. and Merrill, S. D. (1980) 'Effects of Topsoil and Subsoil Thickness on Soil Water Content and Crop Production on a Disturbed Soil', *Soil Science Society of America Journal*, 45, pp. 124-129.
- Pozo, M. and Calvo, J. P. (2018) 'An overview of authigenic magnesian clays', *Minerals*, 8, doi: 10.3390/min8110520
- Price, J. R. and Velbel, M. A. (2003) 'Chemical weathering indices applied to weathering profiles developed on heterogeneous felsic metamorphic parent rocks', *Chemical Geology*, 202, pp. 397-416.
- Puente, M. E., Bashan, Y., Li, C. Y. and Lebsky, V. K. (2004) 'Microbial populations and activities in the rhizoplane of rock weathering desert plants. 1. Root colonization and weathering of igneous rocks', *Plant Biology*, 6(5), pp. 629-642.
- Quine, T. A. and Walling, D. E. (1991) 'Rates of soil erosion on arable fields in Britain: quantitative data from caesium-137 measurements', *Soil Use and Management*, 7, pp. 169–176.
- Quinton, J. N. and Catt, J. A. (2004) 'The effects of minimal tillage and contour cultivation on surface runoff, soil loss and crop yield in the long-term Woburn Erosion Reference Experiment on sandy soil at Woburn, England', *Soil Use and Management*, 20(3), pp. 343-350.

Quinton, J. N., Govers, G., Van Oost, K. and Bardgett, R. D. (2010) 'The impact of agricultural soil erosion on biogeochemical cycling', *Nature Geosciences*, 3(5), pp. 311-314.

Radley, J. D. and Coram, R. A. (2016) 'The Chester Formation (Early Triassic, southern Britain): sedimentary response to extreme greenhouse climate', *Proceedings of the Geologists' Association*, 127(5), pp. 552-557.

Rodrigues, D. B. B., Sobrinho, T. A., De Oliveira, P. T. S. and Panachuki, E. (2011) 'New approach to the Brazilian model of environmental services', *Revista Brasileira De Ciencia Do Solo*, 35(3), pp. 1037-1045.

Ramm, M. (1991) 'Porosity-depth trends in reservoir sandstones: theoretical models related to Jurassic sandstones offshore Norway', *Marine and Petroleum Geology*, 9, pp. 553-567.

Ramos, M. C. and Martinez-Casasnovas, J. A. (2009) 'Impacts of annual precipitation extremes on soil and nutrient losses in vineyards of N.E. Spain', *Hydrological Processes*, 23(2), pp. 224-235.

Ramos, M. C. and Porta, J. (1997) 'Analysis of design criteria for vineyard terraces in the Mediterranean area of north east Spain', *Soil Technology*, 10(2), pp. 155-166.

Ramsey, C. B. (2008) 'Radiocarbon dating: revolutions in understanding', *Archaeometry*, 50, pp. 249-275.

Raper, R. L., Asmussen, L. E. and Powell, J. B. (1990) 'Sensing Hard Pan Depth with Ground-Penetrating Radar', *Transactions of the American Society of Agricultural and Biological Engineers*, 33(1), pp. 41-46.

- Rastall, R. H. (1919) 'The Mineral Composition of the Lower Greensand Strata of Eastern England', *Geological Magazine*, 6(5), pp. 211-220.
- Rautaray, S. K. (2011) 'Innovations in resource management for sustainable rice based farming', *African Journal of Plant Science*, 5(15), pp. 848-854.
- Read, A. D., Phillips, P. and Robinson, G. (1997) 'Landfill as a future waste management option in England: the view of landfill operators', *Resources Conservation and Recycling*, 20, pp. 183-205.
- Reed, A. H. (1979) 'Accelerated erosion of arable soils in the United Kingdom by rainfall and runoff', *Outlook on Agriculture*, 10(1), pp. 41-48.
- Reubens, B., Poesen, J., Danjon, F., Geudens, G. and Muys, B. (2007) 'The role of fine and coarse roots in shallow slope stability and soil erosion control with a focus on root system architecture: a review', *Trees*, 21, pp. 385-402.
- Rhoton, F. E. and Lindbo, D. L. (1997) 'A soil depth approach to soil quality assessment', *Journal of Soil and Water Conservation*, 52(1), pp. 66-72.
- Richardson, A. (2012) 'A New World Ordure? Thoughts on the use of Humanure in Developed Cities', *City*, 16(6), pp. 700-712.
- Richter, D. D. (2007a) 'Humanity's Transformation of Earth's Soil: Pedology's New Frontier', *Soil Science*, 172(12), pp. 957-967.
- Richter, D. D., Oh, N. H., Fimmen, R. L. and Jackson, J. A. (2007b) 'The rhizosphere and soil formation', in Cardon, Z. G. and Whitbeck, J. L. (eds) *The Rhizosphere- An Ecological Perspective*. London: Elsevier Academic Press, pp. 179-201.

- Riebe, C. S., Kirchner, J. W., Granger, D. E. and Finkel, R. C. (2001) 'Strong tectonic and weak climatic control of long-term chemical weathering rates', *Geology*, 29(6), pp. 511-514.
- Riebe, C. S., Kirchner, J. W. and Finkel, R. C. (2003) 'Long-term rates of chemical weathering and physical erosion from cosmogenic nuclides and geochemical mass balance', *Geochimica et Cosmochimica Acta*, 67(22), pp. 4411-4427.
- Riebe, C. S., Kirchner, J. W. and Finkel, R. C. (2004) 'Erosional and climatic effects on long-term chemical weathering rates in granitic landscapes spanning diverse climatic regimes', *Earth and Planetary Science Letters*, 224, pp. 547-562.
- Riggins, S. G., Anderson, R. S., Anderson, S. P. and Tye, A. M. (2011) 'Solving a conundrum of a steady-state hilltop with variable soil depths and production rates, Bodmin Moor, UK', *Geomorphology*, 128, pp. 73-84.
- Rodés, Á. and Evans, D. L. (2019) 'Cosmogenic soil production rate calculator', *MethodsX*, 7, pp. 1-5. doi: 10.1016/j.mex.2019.11.026
- Rodés, Á., Pallàs, R., Braucher, R., Moreno, X., Masana, E. and Bourlés, D. L. (2011) 'Effect of density uncertainties in cosmogenic ^{10}Be depth-profiles: Dating a cemented Pleistocene alluvial fan (Carboneras Fault, SE Iberia)', *Quaternary Geochronology*, 6, pp. 186–194.
- Román-Sánchez, A., Reimann, T., Wallinga, J. and Vanwalleggem, T. (2019a) 'Bioturbation and erosion rates along the soil-hillslope conveyor belt, part 1: insights from single-grain feldspar luminescence', *Earth Surface Processes and Landforms*, 44(10), pp. 2051-2065.

Román-Sánchez, A., Laguna, A., Reimann, T., Giráldez, J. V., Peña, A. and Vanwalleghem, T. (2019b) 'Bioturbation and erosion rates along the soil-hillslope conveyor belt, part 2: quantification using an analytical solution of the diffusion-advection equation', *Earth Surface Processes and Landforms*, 44(10), pp. 2066-2080.

Ruhe, R. V. (1975) 'Climatic geomorphology and fully developed slopes', *Catena*, 2, pp. 309-320. doi: 10.1016/S0341-8162(75)80019-1

Rusanov, A. M. (2006) 'The integrated assessment of soil erosion resistance', *Eurasian Soil Science*, 39(8), pp. 879-884.

Saad, R., Margni, M., Koellner, T., Wittstock, B. and Deschênes, L. (2011) 'Assessment of land use impacts on soil ecological functions: development of spatially differentiated characterization factors within a Canadian context', *Journal of Life Cycle Assessment*, 16, pp. 198-211.

Sahoo, D. C., Madhu, M., Muralidharan, P. and Sikka, A. K. (2015) 'Land management practices for resource conservation under vegetable cultivation in Nilgiris hills ecosystem', *Journal of Environmental Biology*, 36, pp. 1039-1044.

Sails, W. B., Larsen, R. E., Lewis, D. J., Roche, L. M., Eastburn, D. J., Hollander, A. D., Walkinshaw, M., Kaffka, S. R., Tate, K. W. and O'Geen, A. T. (2018) 'Modelled soil erosion potential is low across California's annual rangelands', *California Agriculture*, 72(3), pp. 179-191.

Schaetzl, R. J. (2013) 'Catenas and Soils', in Shroder, J. F. (ed.) *Treatise on Geomorphology*. San Diego, California: Academic Press, pp. 145–158.

Schaetzl, R. J. and Thompson, M. L. (2005) *Soils Genesis and Geomorphology*. 2nd edn. New York: Cambridge University Press.

Schaetzl, R. J. and Thompson, M. L. (2015) *Soils: Genesis and Geomorphology*. Cambridge: Cambridge University Press.

Schaetzl, R. J., Krist, F. J., Rindfleisch, P., Liebens, J. and Williams, T. (2000) 'Postglacial landscape evolution of north-eastern lower Michigan interpreted from soils and sediments', *Annals of the Association of American Geographers*, 90(3), pp. 443-466.

Schertz, D. L. (1983) 'The basis for soil loss tolerance', *Journal of Soil and Water Conservation*, 38, pp. 10-14.

Schiettecatte, W., D'hondt, L., Cornelis, W. M., Acosta, M. I., Leal, Z., Lauwers, N., Almoza, Y., Alonso, G. R., Diaz, J., Ruiz, M. and Gabriels, D. (2008) 'Influence of land use on soil erosion risk in the Cuyaguaje watershed (Cuba)', *Catena*, 74(1), pp. 1-12.

Schils, R., Kuikman, P., Liski, J., Oijen, M. V., Smith, P., Webb, J., Alm, J., Somogyi, Z., Akker, J. V. D., Billett, M., Emmett, B., Evans, C., Lindner, M., Palosuo, T., Bellamy, P., Alm, J., Jandl, R. and Hiederer, R. (2008) *Review of existing information on the interrelations between soil and climate change*. Netherlands: Wageningen UR.

Schmalenberger, A., Duran, A. L., Bray, A. W., Bridge, J., Bonneville, S., Benning, L. G., Romero-Gonzalez, M. E., Leake, J. R. and Banwart, S. A. (2015) 'Oxalate secretion by ectomycorrhizal *Paxillus involutus* is mineral-specific and controls calcium weathering from minerals', *Scientific Reports*, 5(123187), doi: 10.1038/srep12187

- Schmidt, V. and McDonald, D. A. (1979) 'The role of secondary porosity in the course of sandstone diagenesis', *The Society of Economic Paleontologists and Mineralogists Special Publication*, 26, pp. 175-207.
- Schulte, R. P. O., Bampa, F., Bardy, M., Coyle, C., Creamer, R. E., Fealy, R., Gardi, C., Ghaley, B. B., Jordan, P., Laudon, H., O'Donoghue, C., O'hUallacháin, D., O'Sullivan, L., Rutgers, M., Six, J., Toth, G. L. and Vrebos, D. (2015) 'Making the Most of Our Land: Managing Soil Functions from Local to Continental Scale', *Frontiers in Environmental Science*, 3(81), pp. 1-14.
- Shalabi, M. (2006) *Vermicomposting of faecal matter as a component of source control sanitation*. PhD Thesis. Hamburg University of Technology. Available at: <https://cuvillier.de/de/shop/publications/2148> (Accessed: 3 March 2020).
- Shand, P., Cobbing, J., Tyler-Whittle, R., Tooth, A. F. and Lancaster, A. (2003) *Baseline Report Series: 9. The Lower Greensand of southern England*. Available at: <http://nora.nerc.ac.uk/id/eprint/3574/> (Accessed: 12 April 2020).
- Shangguan, W., Hengl, T., de Jesus, J. M., Yuan, H. and Dai, Y. (2017) 'Mapping the global depth to bedrock for land surface modelling', *Journal of Advances in Modeling Earth Systems*, 9(1), pp. 65-88.
- Shao, J. and Yang, S. (2012) 'Does chemical index of alteration (CIA) reflect silicate weathering and monsoonal climate in the Changjiang River basin?', *Chinese Science Bulletin*, 57, pp. 1178-1187.
- Sharda, V. N., Mandal, D. and Ojasvi, P. R. (2013) 'Identification of soil erosion risk areas for conservation planning in different states of India', *Journal of Environmental Biology*, 34(2), pp. 219-226.

- Sharratt, B., Zhang, M. and Sparrow, S. (2006) 'Twenty years of tillage research in subarctic Alaska: 1. Impact on Soil Strength, Aggregation, Roughness and Residue Cover', *Soil and Tillage Research*, 91, pp. 75-81.
- Shaw, C. F. (1930) 'Potent Factors in Soil Formation', *Ecology*, 11(2), pp. 239-245.
- Shi, Z. H., Cai, C. F., Ding, S. W., Wang, T. W. and Chow, T. I. (2004) 'Soil conservation planning at the small watershed level using RUSLE with GIS: a case study in the Three Gorge area of China', *Catena*, 55(1), pp. 33-48.
- Shinohara, Y., Misumi, Y., Kubota, T. and Nanko, K. (2019) 'Characteristics of soil erosion in a moso-bamboo forest of western Japan: comparison with a broadleaved forest and a coniferous forest', *Catena*, 172, pp. 451-460.
- Shipitalo, M. J. and Edwards, W. M. (1998) 'Runoff and erosion control with conservation tillage and reduced-input practices on cropped watersheds', *Soil and Tillage Research*, 46(1), pp. 1-12.
- Shotton, F. W. (1967) 'Age of the Irish Sea Glaciation of the Midlands', *Nature*, 215, p. 1366.
- Shtompel, Y. A., Lisetskii, F. N., Sukhanovskii, Y. P. and Strel'nikova, A. V. (1998) 'Soil loss tolerance of brown forest soils of north-western Caucasus under intensive agriculture', *Eurasian Soil Science*, 31(2), pp. 185-190.
- Simonson, R. W. (1959) 'Outline of a generalized theory of soil genesis', *Soil Science Society of America Proceedings*, 23, pp. 152-156.
- Simonson, R. W. (1997) 'Early Teaching in USA of Dokuchaiev Factors of Soil Formation', *Soil Science Society of America Journal*, 61(1), pp. 11-16.

Sinclair, M. I. (2017) 'Plans to Improve the Natural Environment and Animal Welfare', *Hansard: House of Lords Debate*, 7 December, 787. Available at: <https://hansard.parliament.uk/Lords/2017-12-07/debates/7F8930B9-5D52-4B18-8541-F8FC80B84947/PlansToImproveTheNaturalEnvironmentAndAnimalWelfare?highlight=%2260%20years%22%20%22soil%22#contribution-FEA116EC-5EE6-497B-8651-7C54806009A4> (Accessed: 13 April 2020).

Singh, R. K., Somasundaram, J., Lakaria, B. I., Mandal, D., Sethy, B. K., Sinha, N. K. and Lal, R. (2017) 'Using credible soil loss tolerance value for conservation planning and managing diverse physiographic regions in Rajasthan', *Agricultural Research*, 6(2), pp. 169-178.

Small, E. E., Anderson, R. S., Hancock, G. S. (1999) 'Estimates of the rate of regolith production using ^{10}Be and ^{26}Al from an alpine hillslope', *Geomorphology*, 27, pp. 131-150.

Smith, M. S., Frye, W. W. and Varco, J. J. (1987) 'Legume winter cover crops', in Stewart, B. A. (ed.) *Advances in Soil Science: Vol. 7*. New York: Springer-Verlag, pp. 95-139.

Soil Association (2017) *Secretary of State Commits to Soil*. Available at: <https://www.soilassociation.org/news/2017/october/25/secretary-of-state-commits-to-soil-health/> (Accessed: 13 April 2020).

Sowers, G. F. (1963) 'Engineering properties of residual soils derived from igneous and metamorphic rocks', *Panamerican Conference on Soil Mechanics and Foundation Engineering*. Sao Paulo, Brazil, 1963, pp. 39-61.

Sparovek, G. and Schnug, E. (2001) 'Temporal Erosion-Induced Soil Degradation and Yield Loss', *Soil Science Society of America Journal*, 65, pp. 1479-1486.

Stark, T. D. and Eid, H. T. (1994) 'Drained residual strength of cohesive soils', *Journal of Geotechnical Engineering*, 120(5), pp. 856-871.

STARS (2018) *The Soil Lifespan*. Available at:

https://www.youtube.com/watch?v=XKeGv6z5a10&feature=emb_logo (Accessed: 13 April 2020).

Stead, D. and Evers, J. (2017) 'The palynology and geology of the Lower Cretaceous (Aptian-Albian) of Munday's Hill Quarry, Bedfordshire, UK', *Proceedings of the Geologists' Association*, 128(4), pp. 599-612.

St. Gerontidis, D. V., Kosmas, C., Detsis, B., Marathianou, M., Zafirious, T. and Tsara, M. (2001) 'The effect of moldboard plow on tillage erosion along a hillslope', *Journal of Soil and Water Conservation*, 56, pp. 147-151.

Stocking, M. (1978) 'A dilemma for soil conservation', *Area*, 10(4), pp. 306-308.

Stocking, M. A. and Pain, A. (1983) *Soil Life and the Minimum Soil Depth for Productive Yields: Developing a New Concept*. Norwich: University of East Anglia, School of Development Studies.

Stockmann, U., Minasny, B. and McBratney, A. B. (2014) 'How fast does soil grow?', *Geoderma*, 216, pp. 48-61.

Stolt, M. H. and Baker, J. C. (1994) 'Strategies for Studying Saprolite and Saprolite Genesis', in Cremeens, D. L., Brown, R. B. and Huddleston, J. H. (eds) *Whole Regolith Pedology*. Madison: Soil Science Society of America, pp. 1-21.

Stolt, M. H., Baker, J. C. and Simpson, T. W. (1991) 'Micromorphology of the Soil-

Saprolite Transition Zone in Hapludults of Virginia', *Soil Science Society of America Journal*, 55(4), doi: 10.2136/sssaj1991.03615995005500040029x

Stolt, M. H., Baker, J. C. and Simpson, T. W. (1992) 'Characterization and Genesis of Saprolite Derived from Gneissic Rocks of Virginia', *Soil Science Society of America Journal*, 56(2), doi:

10.2136/sssaj1992.03615995005600020030x

Stone, J. O. (2000) 'Air pressure and cosmogenic isotope production', *Journal of Geophysical Research*, 105, pp. 23753-23759.

Stride, A. H. (1982) *Offshore tidal sands: Processes and deposits*. London: Chapman and Hall.

Strong, G. E. (1993) 'Diagenesis of Triassic Sherwood Sandston Group rocks, Preston, Lancashire, UK: a possible evaporitic cement precursor to secondary porosity?', in North, C. P. and Prosser, D. J. (eds) *Characterization of Fluvial and Aeolian Reservoirs*. London: Geological Society, pp. 279-289.

Struck, M., Jansen, J. D., Fujioka, T., Codilean, A. T., Fink, D., Egholm, D. L., Fülöp, R., Wilcken, K. M. and Kotevski, S. (2018) 'Soil production and transport on postorogenic desert hillslopes quantified with ^{10}Be and ^{26}Al ', *GSA Bulletin*, 130, pp. 1017–1040.

Takken, I., Beuselinck, L., Nachtergaele, J., Govers, G., Poesen, J. and Degraer, G. (1999) 'Spatial evaluation of a physically-based distributed erosion model (LISEM)', *Catena*, 37, pp. 431-447.

Tanaka, D. L. (1995) 'Spring wheat straw production and composition as influenced by topsoil removal', *Soil Science Society of America Journal*, 59, pp. 649-654.

Tandarich, J. P., Darmody, R. G. and Follmer, L. R. (1994) 'The pedoweathering profile: a paradigm for whole regolith pedology from the glaciated midcontinental United States of America', in Cremeens, D. R. (ed.) *Whole Regolith Pedology*. Madison: Soil Science Society of America, pp. 97-117.

Tang, C., Sparling, G. P., McLay, C. D. A. and Raphael, C. (1999) 'Effect of short-term legume residue decomposition on soil acidity', *Australian Journal of Soil Research*, 37, pp. 561-573.

Tanner, S., Katra, I., Argaman, E. and Ben-Hur, M. (2018) 'Erodibility of waste (Loess) soils from construction sites under water and wind erosional forces', *Science of the Total Environment*, 616, pp. 1524–1532.

Targulian, V. O. and Krasilnikov, P. V. (2007) 'Soil system and pedogenic processes: Self-organization, time scales, and environmental significance', *Catena*, 71(3), pp. 373-381.

Tavares, A. S., Spalevic, V., Avanzi, J. C., Nogueira, D. A., Silva, M. I. N. and Mincato, R. I. (2019) 'Modelling of water erosion by the erosion potential method in a pilot sub basin in southern Minas Gerais', *Semina-Ciencias Agrarias*, 40(2), pp. 555-572.

Taylor, L. L., Leake, J. R., Quirk, J., Hardy, K., Banwart, S. A. and Beerling, D. J. (2009) 'Biological weathering and the long-term carbon cycle: integrating mycorrhizal evolution and function into the current paradigm', *Geobiology*, 7, pp. 171-191, doi: 10.1111/j.1472-4669.2009.00194.x

Taylor, R. E. (1987) *Radiocarbon Dating: An Archaeological Perspective*. New York: Academic Press.

Tellam, J. H. (1995) 'Hydrochemistry of the saline groundwaters of the lower Mersey Basin Permo-Triassic sandstone aquifer, UK', *Journal of Hydrology*, 165, pp. 45-84.

Tipping, E., Chamberlain, P. M., Bryant, C. L. and Buckingham, S. (2010) 'Soil organic matter turnover in British deciduous woodlands, quantified with radiocarbon', *Geoderma*, 155, pp. 54-59.

Trigunasih, N. M., Kusmawati, T. and Lestari, N. W. Y. (2018) 'Erosion prediction analysis and land use planning in Gunggung watershed, Bali, Indonesia', *2nd Geoplanning - International Conference On Geomatics and Planning*. Surakarta, Central Java, Indonesia, 9-10 August. Available at: <https://iopscience.iop.org/article/10.1088/1755-1315/123/1/012025> (Accessed: 19 April 2020).

Tugel, A. J., Herrick, J. E., Brown, J. R., Mausbach, M. J., Puckett, W. and Hipple, K. (2005) 'Soil change, soil survey and natural resources decision making: a blueprint for action', *Soil Science Society of America Journal*, 69, pp. 738–747.

Turner, B. L., Hayes, P. E. and Laliberté, E. (2018) 'A climosequence of chronosequences in southwestern Australia', *Eurasian Journal of Soil Science*, 69, pp. 69–86.

Tye, A. M., Kemp, S. J., Lark, R. M. and Milodowski, A. E. (2012) 'The role of peri-glacial active layer development in determining soil-regolith thickness across a Triassic sandstone outcrop in the UK', *Earth Surface Processes and Landforms*, 37, pp. 971–983.

Tye, A. M., Robinson, D. A., and Lark, R. M. (2013) 'Gradual and anthropogenic soil change for fertility and carbon on marginal sandy soils', *Geoderma*, 207, pp. 35–48.

UNCCD (2017) *Global Land Outlook*. Available at:
<https://knowledge.unccd.int/publication/full-report> (Accessed: 31 August 2019).

US Department of Agriculture (2018) *National Soil Survey Handbook Title 430-VI*. Available at:
http://www.nrcs.usda.gov/wps/portal/nrcs/detail/soils/ref/?cid=nrcs142p2_054242
(Accessed 23 April 2018).

Van Breemen, N. and Burman, P. (2002) *Soil Formation*. Netherlands: Kluwer Academic Publishers.

Van Es, H. (2017) 'A New Definition of Soil', *CSA News Magazine*, 62(10), pp. 20-21.

Van Oost, K., Govers, G., de Alba, S. and Quine, T. A. (2006) 'Tillage erosion: a review of controlling factors and implications for soil quality', *Progress in Physical Geography*, 30, pp. 443-466.

Velbel, M. A. (1989) 'Rates of soil formation - implications for soil-loss tolerance', *Soil Science*, 148(1), pp. 71-74.

Vereecken, H., Schnepf, A., Hopmans, J. W., Javaux, M., Or, D., Roose, T., Vanderborght, J., Young, M. H., Amelung, W., Aitkenhead, M., Allison, S. D., Assouline, S., Baveye, P., Berli, M., Brüggemann, N., Finke, P., Flury, M., Gaiser, T., Govers, G., Ghezzehei, T., Hallett, P., Hendricks Franssen, H. J., Heppell, J., Horn, R., Huisman, J. A., Jacques, D., Jonard, F., Kollet, S., Lafolie, F., Lamorski,

K., Leitner, D., McBratney, A., Minasny, B., Montzka, C., Nowak, W., Pachepsky, Y., Padarian, J., Romano, N., Roth, K., Rothfuss, Y., Rowe, E. C., Schwen, A., Šimůnek, J., Tiktak, A., Van Dam, J., van der Zee, S. E. A. T. M., Vogel, H. J., Vrugt, J. A., Wöhling, T. and Young, I. M. (2016) 'Modeling Soil Processes: Review, Key Challenges, and New Perspectives', *Vadose Zone Journal*, 15(5), pp. 1-57. doi: 10.2136/vzj2015.09.0131

Verheijen, F. G. A., Jones, R. J. A., Rickson, R. J. and Smith, C. J. (2009) 'Tolerable versus actual soil erosion rates in Europe', *Earth Science Reviews*, 94, pp. 23-38.

Verstraeten, G., Van Oost, K., Van Rompaey, A., Poesen, J. and Govers, G. (2002) 'Evaluating an integrated approach to catchment management to reduce soil loss and sediment pollution through modelling', *Soil Use and Management*, 18, pp. 386-394.

von Engel, O. D. (1920) 'The World's Food Resources', *Geographical Review*, 9(3), pp. 170-190.

Wakatsuki, T. and Rasyidin, A. (1992) 'Rates of weathering and soil formation', *Geoderma*, 52(3), pp. 251-263.

Wakatsuki, T., Tanaka, Y. and Matsukura, Y. (2005) 'Soil slips on weathering-limited slopes underlain by coarse-grained granite or fine-grained gneiss near Seoul, Republic of Korea', *Catena*, 60, pp. 181–203.

Walker, T. R., Waugh, B. and Crone, A. J. (1978) 'Diagenesis in first cycle desert alluvium of Cenozoic age, southwestern United States and northwestern Mexico', *Geological Society of America Bulletin*, 89, pp. 19-32.

- Walling, D. E. and Quine, T. A. (1991) 'The use of ^{137}Cs measurements to investigate soil erosion on arable fields in the UK: potential applications and limitations', *Journal of Soil Science*, 42, pp. 147–165.
- Wang, H., Sánchez-Molina, J. A., Li, M., Berenguel, M., Yang, X. T. and Bienvenido, J. F. (2017a) 'Leaf area index estimation for a greenhouse transpiration model using external climate conditions based on genetics algorithms, back-propagation neural networks and nonlinear autoregressive exogenous models', *Agricultural Water Management*, 183, pp. 107-115.
- Wang, Z., Zhao, G., Gao, M. and Chang, C. (2017b) 'Spatial variability of soil salinity in coastal saline soil at different scales in the Yellow River Delta, China', *Environmental Monitoring and Assessment*, 189(80), pp. 1-12. doi: 10.1007/s10661-017-5777-x
- Warkentin, B. P. (2001) 'The tillage effects in sustaining soil functions', *Journal of Plant Nutrition and Soil Science*, 164, pp. 345-350.
- Watson, E. and Morgan, A. (1977) 'The Periglacial Environment of Great Britain during the Devensian [and Discussion]', *Philosophical Transactions of the Royal Society of London B, Biological Sciences*, 280, pp. 183-198.
- Watters, S. E., Weltz, M. A. and Smith, E. I. (1996) 'Evaluation of a site conservation rating system in south-eastern Arizona', *Journal of Range Management*, 49(3), pp. 277-284.
- WCED (1987) *Our Common Future: Report of the World Commission on Environment and Development*. Oxford: Oxford University Press.

Weill, M. D. M. and Sparovek, G. (2008) 'Erosion study in the Ceveiro watershed (Piracicaba sp). li - interpreting soil loss tolerance using the soil useful life index methodology', *Revista Brasileira De Ciencia Do Solo*, 32(2), pp. 815-824.

Weltz, M. A., Jolley, L., Hernandez, M., Spaeth, K. E, Rossi, C., Talbot, C., Nearing, M. Stone, J., Goodrich, D., Pierson, F., Wei, H. and Morris, C. (2014) 'Estimating Conservation Needs for Rangelands using USDA National Resources Inventory Assessments', *Transactions of the ASABE*, 57(6), pp. 1559-1570.

White, A. F. and Blum, A. E. (1995) 'Effects of climate on chemical weathering in watersheds', *Geochimica et Cosmochimica*, 59(9), pp. 1729-1747.

Whitty, J. L. (2019) 'Reducing Greenhouse Gas Emissions debate in Lords Chamber', *Hansard: House of Lords debates*, 2 May, 797. Available at: <https://hansard.parliament.uk/Lords/2019-05-02/debates/E78F2663-7606-497F-95C3-7218F4F6D092/ReducingGreenhouseGasEmissions?highlight=%2260%20years%22%20%22soil%22#contribution-80234E69-78A4-4995-82F0-92CA3569D68A> (Accessed: 13 April 2020).

Wight, J. R. and Lovely, C. J. (1982) 'Application of the soil loss tolerance concept to rangelands', *Workshop on Estimating Erosion and Sediment Yield on Rangelands*. Tuscon, Arizona, 7 – 9 March. Available at: https://www.google.co.uk/url?sa=t&rct=j&q=&esrc=s&source=web&cd=2&cad=rja&uact=8&ved=2ahUKEwj8sXQ8_PoAhUWRxUIHVBgCQUQFjABegQIAxAB&url=https%3A%2F%2Fwww.tucson.ars.ag.gov%2Funit%2Fpublications%2FPDFfiles%2F408.pdf&usg=AOvVaw3x4V9NgNvs00ZF6MqNB-FL (Accessed: 19 April 2020).

Wilkinson, M. T. and Humphreys, G. S. (2005) 'Exploring pedogenesis via nuclide-based soil production rates and OSL-based bioturbation rates', *Australian Journal of Soil Research*, 43, pp. 767-779.

Wilkinson, M. T., Chappell, J., Humphreys, G. S., Fifield, K., Smith, B., Hesse, P., Heimsath, A. M. and Ehlers, T. A. (2005) 'Soil production in heath and forest, Blue Mountains, Australia: influence of lithology and palaeoclimate', *Earth Surface Processes and Landforms*, 30(8), pp. 923-934.

Williams, S. M. and Weil, R. R. (2004) 'Crop cover root channels may alleviate soil compaction effects on Soybean crop', *Soil Science Society of America Journal*, 68(4), pp. 1403-1409.

Wilson, S. G., Lambert, J., Nanzyo, M. and Dahlgren, R. A. (2017) 'Soil genesis and mineralogy across a volcanic lithosequence', *Geoderma*, 285, pp. 301–312.

Winkler, E. M. (1975) *Stone: properties, durability in Man's environment*. Wien: Springer-Verlag.

Wong, J (2019) *Are there really only 100 harvests left?* [Press release]. 11 May. Available at: <https://institutions.newscientist.com/article/mg24232291-100-the-idea-that-there-are-only-100-harvests-left-is-just-a-fantasy/> (Accessed: 27 May 2019).

Wonham, J. P. and Elliott, T. (1996) 'High-resolution sequence stratigraphy of a mid-Cretaceous estuarine complex: the Woburn Sands of the Leighton Buzzard area, southern England', in Hesselbo, S. P. and Parkinson, D. N. (eds) *Sequence Stratigraphy in British Geology*, London: Geological Society of London, pp. 41-62.

- World Bank (2019) *GDP Current US\$*. Available at:
<https://data.worldbank.org/indicator/ny.gdp.mktp.cd> (Accessed: 27 May 2019).
- Worthington, S. R. H., Davies, G. J. and Alexander Jr, E. C. (2016) 'Enhancement of bedrock permeability by weathering', *Earth-Science Reviews*, 160, pp. 188-202.
- Wright, R. F. (1988) 'Influence of Acid Rain on Weathering Rates', in Lerman, A. and Meybeck, M. (eds) *Physical and Chemical Weathering in Geochemical Cycles*. Netherlands: Springer, pp. 181-196.
- Wu, Q. X., Wang, Y. K., Han, B. and Wu, R. W. (1994) 'Forest and grassland resources and vegetation construction in the soil and water loss region of the Loess Plateau', *Research of Soil and Water Conservation*, 1, pp. 2-7.
- Xu, S., Dougans, A. B., Freeman, S., Schnabel, C. and Wilcken, K. M. (2010) 'Improved Be-10 and Al-26 AMS with a 5 MV spectrometer', *Eleventh International Conference on Accelerator Mass Spectrometry*, Rome, Italy, 14–19 September 2008, pp. 736–738.
- Yair, A. (1990) 'The role of topography and surface cover upon soil formation along hillslopes in arid climates', *Geomorphology*, 3, pp. 287-299.
- Yanusa, I. A. M. and Newton, P. J. (2003) 'Plants for amelioration of the subsoil constraints and hydrological control: the primer-plant concept', *Plant and Soil*, 257, pp. 261-281.
- Yoo, K. and Mudd, S. M. (2008) 'Discrepancy between mineral residence time and soil age: Implications for the interpretation of chemical weathering rates', *Geology*, 36(1), pp. 35-38.

- Yu, F., Faybishenko, B., Hunt, A. and Ghanbarian, B. (2017) 'A Simple Model of the Variability of Soil Depths', *Water*, 9, pp. 1-13. doi: 10.3390/w9070460
- Zhang, J. H., Nie, X. J. and Su, Z. A. (2008) 'Soil profile properties in relation to soil redistribution by intense tillage on a steep hillslope', *Soil Science Society of America Journal*, 72, pp. 1767-1773.
- Zhao, J., Van Oost, K., Chen, L. and Govers, G. (2016) 'Moderate topsoil erosion rates constrain the magnitude of the erosion-induced carbon sink and agricultural productivity losses on the Chinese Loess Plateau', *Biogeosciences*, 13, pp. 4735-4750.
- Zhao, T., Liu, W., Xu, Z., Liu, T., Xu, S., Cui, L. and Shi, C. (2018) 'Cosmogenic nuclides (^{10}Be and ^{26}Al) erosion rate constraints in the Badain Jaran Desert, northwest China: implications for surface erosion mechanisms and landform evolution', *Journal of Geosciences*, 23, pp. 1–10. doi: 10.1007/s12303-018-0010-7
- Zhu, M. Y. (2015) 'Soil Erosion Assessment using USLE in the GIS Environment: a case study in the Danjiangkou Reservoir Region, China', *Environmental Earth Sciences*, 73(12), pp. 7899-7908.
- Zuzel, J. F., Allmaras, R. R. and Greenwalt, R. N. (1993) 'Temporal distribution of runoff and soil-erosion at a site in north-eastern Oregon', *Journal of Soil and Water Conservation*, 48(4), pp. 373-378.
- Zwieniecki, M. A. and Newton, M. (1994) 'Root distribution of 12-year-old forests at rocky sites in southwestern Oregon: effects of rock physical properties', *Canadian Journal of Forest Research*, 24, pp. 1791-1796. doi: 10.1139/x94-231.

Appendices:

A2.1 Global Inventory of Soil Formation Rates	268
A2.2 Global Inventory of Soil Loss Tolerance values	270
A3.1 Global Inventory of Soil Formation Rates used in the CoSOILcal Sensitivity Analysis	271
A3.2 Published Paper: 'Cosmogenic soil production rate calculator'	273
A3.3 Output from CoSOILcal	278
A4.1 Global Inventory of Soil Erosion Rates	282
A4.2 Soil Lifespan Analysis	289
A4.3 Definitions of Land Use and Management practices	299
A4.4 List of studies included in the Soil Lifespan Analysis	300
A5.1 Output from AMS for Rufford and Comer	316
A5.2 Soil analysis for Rufford and Comer	317
A6.1 Output from AMS for Hilton and Woburn	323
A6.2 Soil analysis for Hilton and Woburn	324
A6.3 Soil production function analysis	326
A6.4 Particle size analysis for saprolite at Hilton and Woburn	327

This page has been intentionally left blank

Owen et al.	2011	Atacama Desert, Chile	Bwk	Volcanic, Plutonic and Metasedimentary (Igneous and Metamorphic)	3	1.5	233000	4540	-26.28	-70.49	670	N/A	0.00027	0.00007
Owen et al.	2011	Atacama Desert, Chile	Bwk	Volcanic, Plutonic and Metasedimentary (Igneous and Metamorphic)	4	1.5	238000	6670	-26.28	-70.49	670	N/A	0.00061	0.00016
Owen et al.	2011	Atacama Desert, Chile	Bwk	Volcanic, Plutonic and Metasedimentary (Igneous and Metamorphic)	11	1.5	389000	6610	-26.28	-70.49	670	N/A	0.00018	0.00008
Owen et al.	2011	Atacama Desert, Chile	Bwk	Volcanic, Plutonic and Metasedimentary (Igneous and Metamorphic)	44	1.5	294000	8800	-26.28	-70.49	670	N/A	0.00077	0.00033
Owen et al.	2011	Atacama Desert, Chile	Bwk	Volcanic, Plutonic and Metasedimentary (Igneous and Metamorphic)	22	1.3	22600	1150	-29.77	-71.08	377	N/A	0.001	0.0006
Owen et al.	2011	Atacama Desert, Chile	Bwk	Volcanic, Plutonic and Metasedimentary (Igneous and Metamorphic)	22	1.3	65400	2390	-29.78	-71.08	400	N/A	0.00082	0.00045
Owen et al.	2011	Atacama Desert, Chile	Bwk	Volcanic, Plutonic and Metasedimentary (Igneous and Metamorphic)	25	1.3	57100	1530	-29.78	-71.08	400	N/A	0.002	0.0011
Owen et al.	2011	Atacama Desert, Chile	Bwk	Volcanic, Plutonic and Metasedimentary (Igneous and Metamorphic)	25	1.3	55500	1390	-29.78	-71.08	400	N/A	0.0045	0.0181
Heimsath et al.	2006	Brown Mountain, Bega Basin, SE Australia	Cfb	Granite/Granodiorite (Igneous)	55	1.3	250000	20000	-36.62	149.5	970	1	0.0167	0.00299
Heimsath et al.	2006	Brown Mountain, Bega Basin, SE Australia	Cfb	Granite/Granodiorite (Igneous)	100	1.3	192000	16000	-36.62	149.5	1033	0.4	0.00623	0.00115
Heimsath et al.	2006	Snug, Bega Basin, SE Australia	Cfb	Granite/Granodiorite (Igneous)	27	1.3	100000	10000	-36.62	149.5	214	1.1	0.02451	0.0025
Heimsath et al.	2006	Snug, Bega Basin, SE Australia	Cfb	Granite/Granodiorite (Igneous)	45	1.3	160000	10000	-36.62	149.5	220	1.1	0.01143	0.00073
Heimsath et al.	2006	Snug, Bega Basin, SE Australia	Cfb	Granite/Granodiorite (Igneous)	38	1.3	120000	10000	-36.62	149.5	221	1.2	0.01727	0.00147
Heimsath et al.	2006	Snug, Bega Basin, SE Australia	Cfb	Granite/Granodiorite (Igneous)	60	1.3	130000	10000	-36.62	149.5	222	1.2	0.0113	0.00089



ELSEVIER

Contents lists available at ScienceDirect

MethodsX

journal homepage: www.elsevier.com/locate/mex

Method Article

Cosmogenic soil production rate calculator

Ángel Rodés^{a,*}, Daniel L. Evans^b^a Scottish Universities Environmental Research Centre, East Kilbride, UK^b Lancaster Environment Centre, Lancaster University, Lancaster, Lancashire, UK

A B S T R A C T

To understand the rates at which soils form from bedrock, it is important to know the rates at which the bedrock surface lowers (the apparent erosion rate, which is assumed to be constant). Previous models that calculate apparent erosion rates using measured concentrations of cosmogenic radionuclides rely on the assumption that the bulk density of the soil which forms as a product of bedrock erosion either equals that of the bedrock itself or is constant with depth down the soil profile. This assumption fails to recognise that soils have significantly lower densities that might not be constant with depth. The model presented here allows for the calculation of isotopically-derived soil production rates, considering the bulk density profile of the soil overlying the bedrock surface. This calculator, which can be run both in MATLAB[®] and GNU Octave[©], represents a novel and significant contribution to the derivation of soil production rates.

© 2019 The Authors. Published by Elsevier B.V. This is an open access article under the CC BY license (<http://creativecommons.org/licenses/by/4.0/>).

A R T I C L E I N F O

Method name: Cosmogenic soil production rate calculator (CoSOILcal)

Keywords: Cosmogenic nuclides, ¹⁰Be, ²⁶Al, ²¹Ne, ³He, ³⁶Cl, ¹⁴C, MATLAB, Octave, Soil production, Erosion rate

Article history: Received 19 July 2019; Accepted 24 November 2019; Available online 28 November 2019

Specification Table

Subject Area:	Earth and Planetary Sciences
More specific subject area:	geochemistry; geochronology; cosmogenic nuclides; ¹⁰ Be; ²⁶ Al; ²¹ Ne; ³ He; ³⁶ Cl; ¹⁴ C
Method name:	Cosmogenic soil production rate calculator (CoSOILcal)
Name and reference of original method:	Evans, D. L., Quinton, J. N., Tye, A. M., Rodés, Á., Davies, J. A. C., Mudd, S. M., and Quine, T. A. (2019) Arable soil formation and erosion: a hillslope-based cosmogenic-nuclide study in the United Kingdom, <i>SOIL</i> , 5, 253-263. https://doi.org/10.5194/soil-5-253-2019
Resource availability:	set of scripts submitted with this paper

* Corresponding author.

E-mail address: angel.rodés@glasgow.ac.uk (Á. Rodés).

1 Method details

Herewith we present a set of MATLAB[®] / GNU Octave[©] scripts and their mathematical description. These are designed to calculate the surface erosion rates using one or more measured cosmogenic concentrations at or below the surface when the bulk density profile is known. An example of this model's application is described in [4].

1.1 Input data

Site data has to be inputted in individual comma separated files (.csv) for each site. An example of input file is attached (see "input_data.csv"). The input file contains the following headers (first line) that we recommend are not changed:

- 1 **Depth:** List of depths where density was measured or where samples were collected for cosmogenic radionuclide analysis. In cm.
- 2 **Density:** Measured densities in g/cm^3
- 3 **Concentration:** Measured concentrations of *in-situ* cosmogenic ^{10}Be , ^{26}Al , ^{21}Ne , ^3He , ^{36}Cl or ^{14}C in atoms/g.
- 4 **Concentration Uncertainty:** Uncertainty of the cosmogenic isotope concentration in atoms/g.
- 5 **Isotope mass:** Atomic mass of the measured isotope: 10, 26, 21, 3, 36 or 14.
- 6 **Lat. (Degrees):** Latitude of the sampled site, to be inputted only in the second line of the csv file.
- 7 **Lon. (degrees):** Longitude of the sampled site, to be inputted only in the second line of the csv file.
- 8 **Elv. (m):** Elevation of the sampled site, to be inputted only in the second line of the csv file.
- 9 **Shielding:** Shielding factor at the surface of the sampled site, to be inputted only in the second line of the csv file.
- 10 **Landscape age (a):** Known age of the landscape in years. Input a large number (e.g. the age of the Earth: 4.54E+09) to consider steady state conditions. Only in the second line of the csv file.

Please leave the cells without data empty (i.e. do not put zeros) and place the desired csv files in the same folder as the scripts (by default in the CoSOILcal folder).

1.2 Model fit

To model the apparent erosion rates, associated uncertainty and the graphical output shown in Fig. 1, just run the script `start.m` and select the desired csv file(s) in the pop-up dialog.

2 Under the hood

The mathematical details of the calculations made in each script are described here:

2.1 `start.m`

This script generates the dialog that allows selecting the input file(s) and calls `soil_solver.m` for each dataset.

2.2 `soil_solver.m`

This is the main function. Depth (z), density (ρ) and effective mass depth (x) arrays are generated and are logarithmically distributed between 1 cm and 100 m, including all the depths that contain input data (density measurements or cosmogenic concentrations). Densities outside the measured range are extrapolated using the shallowest and deepest measurements. The rest of the densities is interpolated from the nearest neighbours, as shown in Fig. 1a. The effective mass depth (x) is

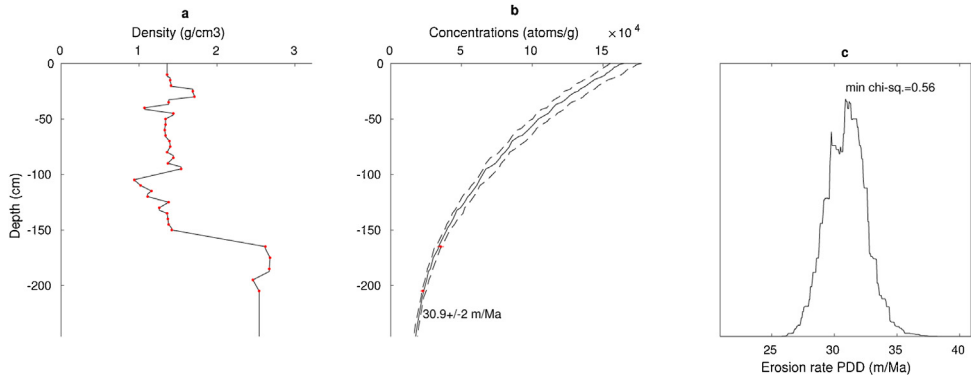


Fig. 1. Graphical abstract. The graphical output of CoSOLcal includes (a) the considered density profile (measured densities as red dots), (b) the measured cosmogenic concentrations (red) and the depth profile of modelled concentrations in black (dashed lines reflect the results within one-sigma), and (c) the probability density distribution (PDD) of the modelled erosion rates.

calculated as

$$x(z) = \sum_{z_i=0}^z \Delta z_i \cdot \rho \quad (1)$$

The surface production rates for cosmogenic isotopes are calculated using the `Production_rate.m` function, described below. Modelled cosmogenic concentrations and deviation from the data are calculated with the `model.m` and `desvmodel.m` functions, also described below.

Erosion rates (ε) are fitted iteratively by the interpolation of a variable erosion rate array, starting with erosion rates logarithmically distributed between 1 cm/a and 100 m/Ma. Best fit and one sigma upper and lower bounds are plotted in Fig. 1b.

Chi-square values (χ^2) are calculated as the sum of the squared deviations. Models with chi-squared values smaller than the minimum chi-square value plus the number of samples are considered to fit the data within one-sigma confidence level. Relative probabilities associated to the chi-squared values are calculated as $e^{(-\chi^2/2)}$. These probabilities are plotted in Fig. 1c.

2.3 `Production_rate.m`

This function calculates these surface production rates, the apparent attenuation lengths of fast and stopping muons under the surface, and the corresponding pressure for a given latitude, longitude and elevation. It uses the following code from the CRONUS calculators v.2.3 [2]: `NCEPat_2.m` and `NCEP2.mat` to calculate pressure, `antatm.m` to calculate pressure in Antarctica (if latitude < -55), `al_be_consts_v23.mat` for constants, `stone2000.m` and `PMag_Mar07.mat` for spallation production rates, and `P_mu_total.m` for muon production rates at the surface.

The inputs of this function are `site_lat`, `site_lon`, `site_elv`, `shielding` and `nuclide`, as defined in section 1.1.

Calculated ^{10}Be production rates in quartz are scaled for other isotopes based on published ratios:

- $^{26}\text{Al}/^{10}\text{Be}$ production rate ratios in quartz are taken from [2]
- $^{21}\text{Ne}/^{10}\text{Be}$ production rate ratios in quartz are taken from [1]
- $^3\text{He}/^{10}\text{Be}$ production rate ratios in pyroxenes and quartz are taken from [3]
- $^{36}\text{Cl}/^{10}\text{Be}$ production rate ratios in calcite and quartz are taken from [5]
- $^{14}\text{C}/^{10}\text{Be}$ production rate ratios in quartz are taken from [5]

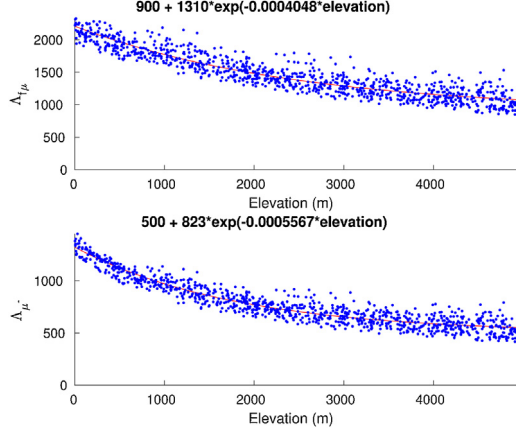


Fig. 2. Apparent muon attenuation lengths. A thousand muon-production depth profiles between 2 and 10 m around the globe were generated using `P_mu_total.m`. 100 muon production rates were calculated for each profile. Apparent muon attenuation lengths (blue dots) were calculated by fitting production rates to exponentials. The calculated relations between apparent attenuation lengths and elevation (red lines) fit the synthetic data within a 7%. This 7% uncertainty is mostly due to the variability in the depth of the randomly generated profiles.

Apparent muon attenuation lengths can be calculated by fitting muon production rates at different depths (from `P_mu_total.m`) to simple exponentials. A thousand depth profiles were randomly generated for maximum depths between 2 and 10 m around the globe. Resulting values of the apparent attenuation lengths were they fitted to altitude exponentials as shown in Fig. 2. The following approximations fit the apparent attenuation lengths within a standard deviation of 7%:

$$\Lambda_{f\mu} = 900 + 1310 * e^{-0.0004048 \cdot h} \quad (2)$$

$$\Lambda_{\mu^-} = 500 + 823 * e^{-0.0005567 \cdot h} \quad (3)$$

where $\Lambda_{f\mu}$ and Λ_{μ^-} are the attenuation lengths of fast and stopping muons in g/cm^2 respectively and h is the elevation of the site.

The outputs of this function are: Production rates, attenuation lengths and atmospheric pressure.

2.4 `model.m`

This function calculates the cosmogenic isotope concentration at several depths (z_s) considering the surface production rate data and decay rate (P , Λ , λ), a variable-density profile (z , ρ) for a landscape age and several erosion rates (ε). The time (t) is discretized in an array of 100 values logarithmically distributed between 100 years and the landform age. For each t , z_s and ε combination, a corresponding effective depth x is calculated by interpolation of $z_s + \varepsilon \cdot t$ in the variable-density profile. Then the accumulated cosmogenic concentration is calculated following:

$$C_i = \sum_{Sp, J\mu, \mu^-} \frac{P}{\lambda + \frac{\varepsilon \cdot \rho}{\Lambda}} \cdot e^{-x/\lambda} \cdot \left(1 - e^{-\Delta t \cdot (\lambda + \frac{\varepsilon \cdot \rho}{\Lambda})}\right) \quad (4)$$

where C_i is the concentration accumulated during Δt time step at the mass depth x , *epsilon* is the erosion rate of the surface and ρ is the average density at the depth $\varepsilon \cdot t$ for the time frame from $t - \Delta t$ to t .

Finally, all the calculated concentrations for the 100 time steps are summed as:

$$C = \sum_{t=0}^T C_i \cdot e^{-\lambda \cdot t} \quad (5)$$

where T is the landform age.

2.5 desvmodel.m

This function calculates the deviation of a model respect a set of cosmogenic isotope concentrations as:

$$s = \sum \frac{C - M}{\sigma_M} \quad (6)$$

where C is the model concentration, M is the measured concentration and σ_M is the uncertainty of measured concentrations. The inputs are the same as in `model.m` plus a set of sample depths, measured concentrations and their uncertainties. This function accepts erosion rates as an array of values.

Supplementary material

All scripts discussed in section 2 are included in the `CoSOILcal_v1_0.zip` file.

Acknowledgements

We wish to thank John N. Quinton for his very constructive comments on the calculator description. This work was partly supported by BBSRC and NERC through a Soils Training and Research Studentships (STARS) (Grant number: NE/M009106/1) and partly by a NERC research grant (Grant number: CIAF 9179/1017). STARS is a consortium consisting of Bangor University, British Geological Survey, Centre for Ecology and Hydrology, Cranfield University, James Hutton Institute, Lancaster University, Rothamsted Research and the University of Nottingham.

References

- [1] Greg Balco, L. David, Shuster, ^{26}Al - ^{10}Be - ^{21}Ne burial dating, *Earth and Planetary Science Letters* 286 (3-4) (2009) 570-575, doi:<http://dx.doi.org/10.1016/j.epsl.2009.07.025> ISSN 0012-821X.
- [2] Greg Balco, O. John, Stone, A. Nathaniel, Lifton, J. Tibor, Dunai, A complete and easily accessible means of calculating surface exposure ages or erosion rates from ^{10}Be and ^{26}Al measurements, *Quaternary Geochronology* 3 (3) (2008) 174-195, doi: <http://dx.doi.org/10.1016/j.quageo.2007.12.001> ISSN 1871-1014. Prospects for the New Frontiers of earth and Environmental Sciences.
- [3] P.-H. Blard, R. Braucher, J. Lavé, D. Bourlès, Cosmogenic ^{10}Be production rate calibrated against ^3He in the high tropical andes (3800-4900 m, 20-22 s), *Earth and Planetary Science Letters* 382 (2013) 140-149, doi:<http://dx.doi.org/10.1016/j.epsl.2013.09.010> ISSN 0012-821X.
- [4] D.L. Evans, J.N. Quinton, A.M. Tye, Á. Rodés, J.A.C. Davies, S.M. Mudd, T.A. Quine, Arable soil formation and erosion: a hillslope-based cosmogenic-nuclide study in the united kingdom, *SOIL* 5 (2019) 253-263, doi:<http://dx.doi.org/10.5194/soil-5-253-2019>.
- [5] B. Heisinger, E. Nolte, Cosmogenic in situ production of radionuclides: Exposure ages and erosion rates, *Nuclear Instruments and Methods in Physics Research Section B: Beam Interactions with Materials and Atoms* 172 (1) (2000) 790-795, doi: [http://dx.doi.org/10.1016/S0168-583X\(00\)00204-4](http://dx.doi.org/10.1016/S0168-583X(00)00204-4) ISSN 0168-583X. 8th International Conference on Accelerator Mass Spectrometry.

Appendix 3.3: Output from CoSOILcal

Author	Year	CoSOILcal Best fit Soil Formation Rate (mm/y)	CoSOILcal Lower Soil Formation Rate (mm/y)	CoSOILcal Upper Soil Formation Rate (mm/y)
Heimsath et al	1997	0.0344445	0.0319139	0.0366477
Heimsath et al	1997	0.0123492	0.0118929	0.0127029
Heimsath et al	1997	0.0064126	0.0058275	0.0068861
Heimsath et al	1997	0.0108542	0.0101644	0.0117319
Heimsath et al	1997	0.0380189	0.0346497	0.0411391
Heimsath et al	1997	0.0132488	0.0123541	0.0149
Heimsath et al	1997	0.043229	0.0399645	0.0463251
Heimsath et al	1997	0.0188428	0.0178019	0.0198954
Heimsath et al	1997	0.0101125	0.009172	0.0112303
Heimsath et al	2001	0.0661228	0.062652	0.0707072
Heimsath et al	2001	0.0276699	0.0261457	0.030322
Heimsath et al	2001	0.0926844	0.0843856	0.1029291
Heimsath et al	2001	0.0015018	0.0014054	0.0017066
Heimsath et al	2001	0.0386206	0.0350183	0.041842
Heimsath et al	2001	0.0094512	0.00838	0.0099941
Heimsath et al	2001	0.0175474	0.0161054	0.0188159
Heimsath et al	2001	0.0160743	0.0148456	0.017887
Heimsath et al	2001	0.0570024	0.052116	0.0618698
Heimsath et al	2001	0.126915	0.1152845	0.1392033
Heimsath et al	2001	0.0468457	0.0435498	0.0533517
Heimsath et al	2001	0.1335545	0.1229163	0.1442944
Heimsath et al	2001	0.1521347	0.1379022	0.1646957
Heimsath et al	2001	0.116523	0.1152211	0.116775
Heimsath et al	2001	0.0732656	0.067336	0.0782028
Heimsath et al	2001	0.029463	0.0279944	0.0304941
Heimsath et al	1999	0.03912	0.0369967	0.0416297
Heimsath et al	1999	0.0147547	0.0142117	0.0152755
Heimsath et al	1999	0.0080359	0.0075846	0.0088425
Heimsath et al	1999	0.0135019	0.0124509	0.0144941
Heimsath et al	1999	0.045282	0.0412345	0.0491481
Heimsath et al	1999	0.0165602	0.0150389	0.0179366
Heimsath et al	1999	0.049285	0.0464217	0.0528166
Heimsath et al	1999	0.022482	0.021275	0.0237574
Heimsath et al	1999	0.0128595	0.011301	0.013966
Heimsath et al	2000	0.0015104	0.001425	0.0015309
Heimsath et al	2000	0.0472433	0.0460147	0.0483984
Heimsath et al	2000	0.0474614	0.0463702	0.0500416
Heimsath et al	2000	0.007789	0.0075522	0.007927
Heimsath et al	2000	0.0173537	0.0164699	0.0177061
Heimsath et al	2000	0.0253422	0.0242487	0.0262487
Heimsath et al	2000	0.0201335	0.0192407	0.0204965
Heimsath et al	2000	0.0134624	0.0130719	0.0136497

Heimsath et al	2000	0.0089301	0.0087766	0.0089836
Heimsath et al	2000	0.0468102	0.0459038	0.0484013
Heimsath et al	2000	0.0067831	0.0065857	0.007036
Heimsath et al	2000	0.0292723	0.0286646	0.0293954
Heimsath et al	2000	0.0072574	0.0071461	0.0074327
Heimsath et al	2000	0.0218845	0.0203231	0.0232374
Heimsath et al	2000	0.0046552	0.0044881	0.0047214
Heimsath et al	2000	0.0039231	0.0038205	0.0041329
Heimsath et al	2000	0.0233862	0.0222091	0.0243383
Heimsath et al	2000	0.00329	0.0030328	0.0034267
Heimsath et al	2000	0.0394691	0.0385203	0.0400407
Wilkinson et al	2005	0.0343225	0.0321751	0.0379784
Wilkinson et al	2005	0.0207262	0.0191146	0.0217388
Wilkinson et al	2005	0.0201419	0.01889	0.0222189
Wilkinson et al	2005	0.0255099	0.0238573	0.0284979
Wilkinson et al	2005	0.0211961	0.0200756	0.0227563
Wilkinson et al	2005	0.0191033	0.0182189	0.0204954
Wilkinson et al	2005	0.0237065	0.022124	0.0264137
Wilkinson et al	2005	0.0223311	0.0209077	0.0242336
Heimsath et al	2001a	0.0571422	0.0551867	0.0602586
Heimsath et al	2001a	0.0473704	0.0446566	0.0493877
Heimsath et al	2001a	0.0212698	0.0203242	0.0222919
Heimsath et al	2001a	0.0091762	0.0087105	0.0097763
Heimsath et al	2001a	0.0058401	0.0052796	0.0062848
Heimsath et al	2012	0.3644489	0.3428425	0.3980215
Heimsath et al	2012	0.0478951	0.0462571	0.0488798
Heimsath et al	2012	0.1931335	0.1888329	0.2041649
Heimsath et al	2012	0.0670696	0.0643591	0.070862
Heimsath et al	2012	0.0354323	0.0341849	0.0376389
Heimsath et al	2012	0.0397249	0.0368471	0.0422005
Heimsath et al	2012	0.1454127	0.1423991	0.1525173
Heimsath et al	2012	0.1009841	0.0945149	0.1077262
Heimsath et al	2012	0.09891	0.0955295	0.1027499
Heimsath et al	2012	0.0461076	0.0448313	0.0477285
Heimsath et al	2012	0.0363102	0.0350031	0.0385704
Heimsath et al	2012	0.0341007	0.0325615	0.035636
Heimsath et al	2012	0.0796083	0.075439	0.0830504
Heimsath et al	2012	0.0315624	0.0301542	0.032373
Heimsath et al	2012	0.0332942	0.0323747	0.0347048
Heimsath et al	2012	0.0089252	0.0086083	0.0091024
Heimsath et al	2012	0.0609363	0.0590831	0.0633114
Heimsath et al	2012	0.0665062	0.0638171	0.0678462
Heimsath et al	2012	0.1014731	0.0985773	0.1037334
Heimsath et al	2012	0.0414137	0.0398238	0.042767
Heimsath et al	2012	0.0877481	0.0854575	0.0909913
Heimsath et al	2012	0.1322151	0.129427	0.1361336
Heimsath et al	2012	0.0068935	0.0066849	0.0071047
Heimsath et al	2012	0.0310176	0.0300023	0.0336467
Heimsath et al	2012	0.0553779	0.0522581	0.0589623
Heimsath et al	2012	0.3032675	0.286747	0.31386

Heimsath et al	2012	0.2522359	0.2383057	0.2672564
Heimsath et al	2012	0.1934319	0.1855379	0.1986148
Heimsath et al	2012	0.2122655	0.2024987	0.2151415
Heimsath et al	2012	0.0813444	0.0791293	0.0831829
Heimsath et al	2012	0.1289619	0.1245581	0.1366502
Heimsath et al	2012	0.1421741	0.1384237	0.1504457
Heimsath et al	2012	0.1796604	0.1698558	0.183238
Heimsath et al	2012	0.0699468	0.0674392	0.0717525
Heimsath et al	2012	0.080945	0.0790073	0.085377
Heimsath et al	2012	0.4708325	0.4299359	0.5103225
Heimsath et al	2012	0.0776666	0.0744695	0.0812793
Heimsath et al	2012	0.2992131	0.282219	0.3246379
Heimsath et al	2012	0.146171	0.1417777	0.1519706
Heimsath et al	2012	0.1654442	0.1575702	0.1706747
Dixon et al.	2009	0.044688	0.04335	0.0466653
Dixon et al.	2009	0.0368861	0.0350168	0.039814
Dixon et al.	2009	0.0275183	0.0262904	0.0284497
Dixon et al.	2009	0.0378371	0.037031	0.0382165
Dixon et al.	2009	0.023907	0.0233099	0.024392
Dixon et al.	2009	0.0201612	0.0195825	0.0211053
Dixon et al.	2009	0.0344559	0.0334865	0.034951
Dixon et al.	2009	0.0311322	0.0291466	0.0338262
Dixon et al.	2009	0.0208555	0.0204161	0.0213802
Dixon et al.	2009	0.0195536	0.0194312	0.0199833
Dixon et al.	2009	0.0233889	0.0232827	0.0239404
Dixon et al.	2009	0.0167127	0.0161728	0.017315
Dixon et al.	2009	0.0339483	0.0321477	0.0348508
Dixon et al.	2009	0.0192406	0.0186921	0.019721
Heimsath et al	2005	0.0080959	0.0075508	0.0091167
Heimsath et al	2005	0.0423369	0.0390869	0.0454519
Heimsath et al	2005	0.0577595	0.0528363	0.0627409
Heimsath et al	2005	0.0159375	0.0149023	0.0168549
Heimsath et al	2005	0.0048291	0.0045578	0.0052584
Heimsath et al	2005	0.040088	0.0365941	0.0442246
Heimsath et al	2005	0.0010995	0.00096737	0.0011582
Heimsath et al	2005	0.0042978	0.003874	0.0045519
Heimsath et al	2005	0.0597234	0.0565799	0.0633386
Heimsath et al	2005	0.0556704	0.051995	0.0597157
Heimsath et al.	2009	0.0275146	0.0254717	0.0301254
Heimsath et al.	2009	0.0301513	0.0287145	0.03166
Owen et al.	2011	0.0299641	0.0283594	0.031235
Owen et al.	2011	0.0218216	0.0214462	0.0220754
Owen et al.	2011	0.0261846	0.0257883	0.0263332
Owen et al.	2011	0.0298315	0.0297628	0.0306676
Owen et al.	2011	0.0089071	0.0083667	0.0093351
Owen et al.	2011	0.0097491	0.0091343	0.0101661
Owen et al.	2011	0.0082854	0.0081829	0.0086541
Owen et al.	2011	0.008836	0.0084464	0.009121
Owen et al.	2011	0.0551371	0.0543289	0.0577201
Owen et al.	2011	0.05856	0.0571973	0.0587952

Owen et al.	2011	0.0585334	0.0572053	0.0587727
Owen et al.	2011	0.0494247	0.048409	0.0513678
Owen et al.	2011	0.0488105	0.0471247	0.04919
Owen et al.	2011	0.0486551	0.0473162	0.051499
Owen et al.	2011	0.0386227	0.0380895	0.0404805
Owen et al.	2011	0.0383468	0.037937	0.0400115
Owen et al.	2011	0.0384589	0.0375417	0.0397933
Owen et al.	2011	0.0253186	0.0251727	0.0255286
Owen et al.	2011	0.0246999	0.0237911	0.0251978
Owen et al.	2011	0.0124621	0.0121258	0.0127983
Owen et al.	2011	0.0123654	0.0121045	0.0128776
Owen et al.	2011	0.2242985	0.2123798	0.2345693
Owen et al.	2011	0.0783399	0.0749527	0.0806167
Owen et al.	2011	0.0877764	0.0860846	0.0897007
Owen et al.	2011	0.0898516	0.0879186	0.092735
Heimsath et al.	2006	0.0242881	0.0231707	0.0271705
Heimsath et al.	2006	0.0107927	0.0100034	0.0120793
Heimsath et al.	2006	0.0500597	0.046172	0.0559453
Heimsath et al.	2006	0.026796	0.0259365	0.0291846
Heimsath et al.	2006	0.0414188	0.0386309	0.0457069
Heimsath et al.	2006	0.0321081	0.0299194	0.0349615

Table with 15 columns: ID, Author, Count, Soil Type, Status, Country, Region, Locality, Country Code, Year, Altitude, Slope, Aspect, Management, and several numerical values. The table lists various soil profiles and their characteristics across different geographical locations.

237	Jirasuktaveekul	4	No Data	Asia and Australia	Yom	Thailand	30	1156	Conventional	Crop (Teak and Vetiver)	0.017875	0.020428571	
237	Jirasuktaveekul	4	No Data	Asia and Australia	Yom	Thailand	40	1156	Conventional	Crop (Teak and Vetiver)	0.0205625	0.0235	
237	Jirasuktaveekul	4	No Data	Asia and Australia	Yom	Thailand	30	1156	Conventional	Crop (Teak)	0.0215	0.024571429	
237	Jirasuktaveekul	4	No Data	Asia and Australia	Yom	Thailand	20	1156	Conventional	Crop (Teak and Vetiver)	0.02425	0.027714286	
237	Jirasuktaveekul	4	No Data	Asia and Australia	Yom	Thailand	20	1156	Conventional	Crop (Teak)	0.0345625	0.0395	
237	Jirasuktaveekul	4	No Data	Asia and Australia	Yom	Thailand	40	1156	Conventional	Crop (Teak)	0.0365	0.04174286	
237	Jirasuktaveekul	4	No Data	Asia and Australia	Mae Taeng	Thailand	20	1053.8	Conventional	Crop (Teak and Vetiver)	0.157	0.179428571	
237	Jirasuktaveekul	4	No Data	Asia and Australia	Mae Taeng	Thailand	30	1053.8	Conventional	Crop (Teak and Vetiver)	0.282875	0.323285714	
237	Jirasuktaveekul	4	No Data	Asia and Australia	Mae Taeng	Thailand	40	1053.8	Conventional	Crop (Teak and Vetiver)	0.3275625	0.374357143	
237	Jirasuktaveekul	4	No Data	Asia and Australia	Mae Taeng	Thailand	30	1053.8	Conventional	Crop (Teak)	0.428875	0.490142857	
237	Jirasuktaveekul	4	No Data	Asia and Australia	Mae Taeng	Thailand	20	1053.8	Conventional	Crop (Teak)	0.4595	0.525142857	
237	Jirasuktaveekul	4	No Data	Asia and Australia	Mae Taeng	Thailand	40	1053.8	Conventional	Crop (Teak)	0.765625	0.875	
237	Jirasuktaveekul	4	No Data	Asia and Australia	Yom	Thailand	30	1156	Conventional	Forest	0.0154375	0.017942857	
237	Jirasuktaveekul	4	No Data	Asia and Australia	Yom	Thailand	40	1156	Conventional	Forest	0.0156875	0.017928571	
237	Jirasuktaveekul	4	No Data	Asia and Australia	Mae Taeng	Thailand	40	1053.8	Conservation	Forest	0.0845625	0.096642857	
237	Jirasuktaveekul	4	No Data	Asia and Australia	Mae Taeng	Thailand	30	1053.8	Conservation	Forest	0.0783125	0.0895	
238	Herweg and Ludi	7	Haplic Phaeozem	No Data	sub-Saharan Africa	Maybar	Ethiopia	28	1211	Conservation	Strips (Lentil)	0.05625	0.064285714
238	Herweg and Ludi	4	Haplic Luvisol	No Data	sub-Saharan Africa	Dizi	Ethiopia	18	1512	Conservation	Terracing (Stone and Soil Bunds)	0.04375	0.05
238	Herweg and Ludi	5	Vertic Luvisol	No Data	sub-Saharan Africa	Anjeni I	Ethiopia	28	1690	Conservation	Terracing (Stone and Soil Bunds)	2.375	2.714285714
238	Herweg and Ludi	5	Vertic Luvisol	No Data	sub-Saharan Africa	Anjeni I	Ethiopia	28	1690	Conservation	Terracing (Fanya Juu Graded)	2.25	2.571428571
238	Herweg and Ludi	1	Eutric Nitisol	No Data	sub-Saharan Africa	Anjeni II	Ethiopia	12	1690	Conservation	Terracing (Stone and Soil Bunds)	2.125	2.428571429
238	Herweg and Ludi	9	Eutric Regosol	No Data	sub-Saharan Africa	Andit Tid	Ethiopia	24	1358	Conservation	Terracing (Stone and Soil Bunds)	1.8125	2.071428571
238	Herweg and Ludi	1	Eutric Nitisol	No Data	sub-Saharan Africa	Anjeni II	Ethiopia	12	1690	Conservation	Terracing (Fanya Juu Graded)	1.08875	1.221428571
238	Herweg and Ludi	5	Chromic Cambisol	No Data	sub-Saharan Africa	Afiteyu	Eritrea	31	382	Conservation	Contour Ridges (Stone and Soil)	0.8625	0.985714286
238	Herweg and Ludi	9	Eutric Regosol	No Data	sub-Saharan Africa	Andit Tid	Ethiopia	24	1358	Conservation	Strips (Lentil)	0.8125	0.928571429
238	Herweg and Ludi	18	Eutric Regosol	No Data	sub-Saharan Africa	Andit Tid	Ethiopia	24	1358	Conservation	Terracing (Fanya Juu Graded)	0.74375	0.85
238	Herweg and Ludi	5	Chromic Cambisol	No Data	sub-Saharan Africa	Afiteyu	Eritrea	31	382	Conservation	Strips (Lentil)	0.5	0.571428571
238	Herweg and Ludi	5	Chromic Cambisol	No Data	sub-Saharan Africa	Afiteyu	Eritrea	31	382	Conservation	Terracing (Fanya Juu Graded)	0.45	0.514285714
238	Herweg and Ludi	7	Haplic Phaeozem	No Data	sub-Saharan Africa	Maybar	Ethiopia	28	1211	Conservation	Terracing (Stone and Soil Bunds)	0.20625	0.235714286
238	Herweg and Ludi	7	Pellic Vertisol	No Data	sub-Saharan Africa	Hunde Lallo	Ethiopia	21	935	Conservation	Strips (Lentil)	0.18125	0.207142857
238	Herweg and Ludi	7	Pellic Vertisol	No Data	sub-Saharan Africa	Hunde Lallo	Ethiopia	21	935	Conservation	Terracing (Stone and Soil Bunds)	0.1125	0.1271428571
238	Herweg and Ludi	9	Pellic Vertisol	No Data	sub-Saharan Africa	Hunde Lallo	Ethiopia	21	935	Conservation	Contour Ridges (Stone and Soil)	0	0
238	Herweg and Ludi	10	Humic Nitisol	No Data	sub-Saharan Africa	Gununo	Ethiopia	14	1211	Conservation	Strips (Lentil)	0.11875	0.135714286
238	Herweg and Ludi	4	Haplic Luvisol	No Data	sub-Saharan Africa	Dizi	Ethiopia	18	1512	Conservation	Contour Ridges (Stone and Soil)	0.0125	0.014285714
238	Herweg and Ludi	14	Pellic Vertisol	No Data	sub-Saharan Africa	Hunde Lallo	Ethiopia	21	935	Conservation	Terracing (Fanya Juu Graded)	0.103125	0.117857143
238	Herweg and Ludi	4	Haplic Luvisol	No Data	sub-Saharan Africa	Dizi	Ethiopia	18	1512	Conservation	Strips (Lentil)	0.09375	0.107142857
238	Herweg and Ludi	10	Humic Nitisol	No Data	sub-Saharan Africa	Gununo	Ethiopia	14	1314	Conservation	Contour Ridges (Stone and Soil)	0.01875	0.021428571
238	Herweg and Ludi	10	Humic Nitisol	No Data	sub-Saharan Africa	Gununo	Ethiopia	14	1314	Conservation	Terracing (Stone and Soil Bunds)	0.03125	0.03257143
238	Herweg and Ludi	7	Haplic Phaeozem	No Data	sub-Saharan Africa	Maybar	Ethiopia	28	1211	Conservation	Contour Ridges (Stone and Soil)	0.075	0.085714286
238	Herweg and Ludi	14	Haplic Phaeozem	No Data	sub-Saharan Africa	Maybar	Ethiopia	28	1211	Conservation	Terracing (Fanya Juu Graded)	0.071875	0.082142857
238	Herweg and Ludi	20	Humic Nitisol	No Data	sub-Saharan Africa	Gununo	Ethiopia	14	1314	Conservation	Terracing (Fanya Juu Graded)	0.03125	0.035714286
238	Herweg and Ludi	7	Haplic Phaeozem	No Data	sub-Saharan Africa	Maybar	Ethiopia	28	1314	Conventional	Crop	0.11875	0.135714286
238	Herweg and Ludi	4	Haplic Luvisol	No Data	sub-Saharan Africa	Dizi	Ethiopia	18	1512	Conventional	Crop	0.31875	0.364285714
238	Herweg and Ludi	7	Pellic Vertisol	No Data	sub-Saharan Africa	Hunde Lallo	Ethiopia	21	382	Conventional	Crop	0.45	0.514285714
238	Herweg and Ludi	10	Humic Nitisol	No Data	sub-Saharan Africa	Gununo	Ethiopia	14	1314	Conventional	Crop	0.7125	0.814285714
238	Herweg and Ludi	5	Chromic Cambisol	No Data	sub-Saharan Africa	Afiteyu	Eritrea	31	382	Conventional	Crop	2.625	3
238	Herweg and Ludi	9	Eutric Regosol	No Data	sub-Saharan Africa	Andit Tid	Ethiopia	24	1358	Conventional	Crop	3	3.428571429
238	Herweg and Ludi	1	Eutric Nitisol	No Data	sub-Saharan Africa	Anjeni II	Ethiopia	12	1690	Conventional	Crop	5.625	6.428571429
238	Herweg and Ludi	5	Vertic Luvisol	No Data	sub-Saharan Africa	Anjeni I	Ethiopia	28	1690	Conventional	Crop	6.875	7.857142857
238	Herweg and Ludi	8	Haplic Luvisol	No Data	sub-Saharan Africa	Dizi	Ethiopia	18	1512	Conservation	Terracing (Fanya Juu Graded)	0.040625	0.046428571
239	Hashim	8	#N/A	No Data	Asia and Australia	Kemaman	Malaysia	17	3638	Conservation	Cover Crop	2.74109375	3.132878571
240	Coughlan and Rose	4.5	#N/A	Sandy Clay Loam	Asia and Australia	Kemaman	Malaysia	17	3638	Conservation	Grassland	1.0625	1.346206349
240	Coughlan and Rose	6	#N/A	Clay	Asia and Australia	Los Banos	Philippines	18	2037	Conservation	Mulching	0.431564676	0.48
240	Coughlan and Rose	2	#N/A	Clay	Asia and Australia	VISCA	Philippines	50	2800	Conservation	Mulching	0.215827338	0.24
240	Coughlan and Rose	3	#N/A	Loamy Sand	Asia and Australia	Goomboorian, Gympie	Australia	6	1045	Conservation	Mulching	0.181818182	0.20079021
240	Coughlan and Rose	3	#N/A	Loamy Sand	Asia and Australia	Khon Kaen	Thailand	4	913	Conservation	Contour Cultivation	0.060606061	0.0699307
240	Coughlan and Rose	1	#N/A	Clay	Asia and Australia	Khon Kaen	Thailand	4	913	Conventional	Cultivating Down slope	0.16969697	0.195804196
240	Coughlan and Rose	1	#N/A	Clay	Asia and Australia	Khon Kaen	Thailand	39	1886	Bare	Bare Soil	0.517985612	0.576
240	Coughlan and Rose	2	#N/A	Sandy Loam	Asia and Australia	Imbil, Gympie	Australia	38	1232	Conventional	Cultivating Down slope	1.875	2
240	Coughlan and Rose	2	#N/A	Clay	Asia and Australia	VISCA	Philippines	50	2800	Conventional	Cultivating Down slope	2.73381295	3.04
240	Coughlan and Rose	3	#N/A	Loamy Sand	Asia and Australia	Khon Kaen	Thailand	4	913	Bare	Bare Soil	2.909090909	3.35645357
240	Coughlan and Rose	3	#N/A	Loamy Sand	Asia and Australia	Goomboorian, Gympie	Australia	14	1045	Conventional	Conventional Tillage	3.090909091	3.56643566
240	Coughlan and Rose	2	#N/A	Clay	Asia and Australia	VISCA	Philippines	50	2800	Bare	Bare Soil	4.964028777	5.52
240	Coughlan and Rose	9	#N/A	Sandy Clay Loam	Asia and Australia	Kemaman	Malaysia	17	3638	Bare	Bare Soil	6.78125	8.611111111
240	Coughlan and Rose	6	#N/A	Clay	Asia and Australia	Los Banos	Philippines	18	2037	Conventional	Conventional Tillage	8.561151079	9.52
240	Coughlan and Rose	6	#N/A	Clay	Asia and Australia	Los Banos	Philippines	18	2037	Bare	Bare Soil	13.23741007	14.72
240	Coughlan and Rose	3	#N/A	Loamy Sand	Asia and Australia	Goomboorian, Gympie	Australia	14	1045	Bare	Bare Soil	13.09090909	15.1048951

Appendix 4.3: Definitions of Land Use and Management practices

Management Practice (Conventional)	
Conventional Tillage	Includes all ploughing, harrowing and discing operations that subject surface (0-0.3 m) soils to high invasive maximum disturbance, irrespective of the crop per se, tillage direction and frequency of passes.
Downslope Cultivation	Includes all ploughing, harrowing and discing operations that are conducted with passes up and down the maximum slope, irrespective of the crop per se or the frequency of passes. The operations, including the level of disturbance on surface soil, accord on the whole with those defined as conventional tillage (e.g: ploughing to 0.3 m, followed by seedbed harrowing).
Bare Soil	An experimental control plot, where weeds and other invasives are suppressed with regular herbicidal applications throughout the year.
Crop	Includes plots cultivating crops (such as potatoes or cereals), irrespective of ploughing, harrowing and discing operations, tillage direction and frequency of passes.
Management Practice (Conservation)	
Cover Crop	Includes plots that cultivate a vegetative cover during typical intercropping months, rather than practicing fallow management, irrespective of ploughing, harrowing and discing operations, tillage direction and frequency of passes. The cover crops per se are itemised in the supplementary data tables.
Conservation Tillage	Includes all ploughing, harrowing and discing operations that subject soils to low-invasive, shallow disturbance (0.05-0.08 m) whereby residues are typically not retained, irrespective of the crop per se, tillage direction and frequency of passes.
Contour Cultivation	Includes all ploughing, harrowing and discing operations that are conducted with passes either perpendicular to the maximum slope or along contours, irrespective of the crop per se or the frequency of passes. The operations, including the level of disturbance on surface soil, accord on the whole with those defined as conventional tillage (e.g: ploughing to 0.3 m, followed by seedbed harrowing).
Terracing	A terraced hillslope (of similar slope to partnering non-terraced plot), with risers 1-1.2 m in height, and 15-18 m between each terrace. These are subject to conventional tillage and hoeing throughout the year, irrespective of the crop per se, tillage direction and frequency of passes.
Contour Ridges	A ridged hillslope constructed with earth and/or stones. These are subject to conventional tillage and hoeing throughout the year, irrespective of the crop per se, tillage direction and frequency of passes.
Zero Tillage	Includes operations that subject soils to minimum disturbance, whereby residues are typically retained. In most cases, sowing takes place into dead mulch, irrespective of the crop per se, tillage direction and frequency of passes.
Grassland	A permanent grass cover throughout the year, irrespective of the grass species per se. Occasionally, this treatment is subject to a mower, which clips the grass and leaves the residues on the surface.
Forest	Typically, a permanent pine plantation or mixed forest, irrespective of the forest age.

Appendix 4.4: List of studies included in the Soil Lifespan Analysis

- 1 Liniger HP. 1992. Water and Soil Conservation in the Semi-arid Highlands Northwest of Mount Kenya. In *Erosion and small scale farming*, Hurni HaT, K. (ed). Geographica Bernensia: Marceline, Missouri; 483-504.
- 2 Basic, F., Kisic, I., Butorac, A., Nestroy, O. and Mesic, M. (2001) 'Runoff and Soil Loss under Different Tillage Methods on Stagnic Luvisols in Central Croatia', *Soil and Tillage Research*, 62, pp. 145-151.
- 3 Lundekvam, H. E. (2007) 'Plot studies and modelling of hydrology and erosion in southeast Norway', *Catena*, 71, pp. 200-209.
- 4 Gómez, J. A., Romero, P., Giráldez, J. V. and Fereres, E. (2004) 'Experimental assessment of runoff and soil erosion in an olive grove on a Vertic soil in southern Spain as affected by soil management', *Soil Use and Management*, 20, pp. 426-431.
- 5 Merten, G. H., Araújo, A. G., Biscaia, R. C. M., Barbosa, G. M. C. and Conte, O. (2015) 'No-till surface runoff and soil losses in southern Brazil', *Soil and Tillage Research*, 152, pp. 85-93.
- 6 Wang, Z., Gao, H., Tullberg, J. N., Hongwen, L., Kuhn, N., McHugh, A. D. and Li, Y. (2008) 'Traffic and Tillage Effects on Runoff and Soil Loss on the Loess Plateau of Northern China', *Australian Journal of Soil Research*, 46, pp. 667-675.
- 7 De Alba, S., Lacasta, C., Benito, G. and Pérez-González, A. (2001) 'Influence of soil management on water erosion in a Mediterranean semiarid environment in Central Spain', in García-Torres, L., Benitez, J. and Martinez-Vilela, A. (eds) *Conservation Agriculture: A Worldwide Challenge*. Códorba: European Conservation Agriculture Federation, pp. 173-177.
- 8 Chisci, G. and Zanchi, C. (1981) 'The influence of different tillage systems and different crops on soil losses on hilly silty-clayey soil', in Morgan, R. P. C. (ed.) *Soil Conservation: Problems and Prospects*. Chichester: Wiley, pp. 211-219.
- 9 Veihe, A. and Hasholt, B. (2006) 'Denmark', in Boardman, J. and Poesen, J. (eds) *Soil Erosion in Europe*. Chichester: John Wiley and Sons, pp. 33-42.
- 10 Skrodzki, M. (1972) 'Present-day water and wind erosion of soils in NE Poland', *Geographia Polonica*, 23, pp. 77-92.
- 11 De Alba, S. (1998) 'Redistribución y erosion del suelo por las prácticas agrícolas de laboreo en laderas cultivadas', in Gómez-Ortiz, A. and Salvador, F. F. (eds) *Investigaciones Rácientes de la Geomorfología Española*. Logroño: Geoforma, pp. 471-481.
- 12 USDA (2018) USLE Data. Available at: <https://www.ars.usda.gov/midwest-area/west-lafayette-in/national-soil-erosion-research/docs/usle-database/usle-data/> (Accessed: 22 June 2018).
- 13 Paningbatan, E. P., Ciesiolka, C. A., Coughlan, K. J. and Rose, C.W. (1995) 'Alley cropping for managing soil erosion of hilly lands in the Philippines', *Soil Technology*, 8, pp. 193-204.
- 14 Gómez, J. A., Guzmán, M. G., Giráldez, J. V. and Fereres, E. (2009) 'The influence of cover crops

- and tillage on water and sediment yield, and on nutrient, and organic matter losses in an olive orchard on a sandy loam soil', *Soil and Tillage Research*, 106, pp. 137-144.
- 15 Biddoccu, M., Ferraris, S., Pitacco, A. and Cavallo, E. (2017) 'Temporal variability of soil management effects on soil hydrological properties, runoff and erosion at the field scale in a hillslope vineyard, North-West Italy', *Soil and Tillage Research*, 165, pp. 46-58.
 - 16 Laloy, E. and Bielders, C. L. (2010) 'Effect of Intercropping Period Management on Runoff and Erosion in a Maize Cropping System', *Journal of Environmental Quality*, 39, pp. 1001-1008.
 - 17 Lanzanova, M. E., Eltz, F. L. F., Nicoloso, R. D. S., Cassol, E. A., Bertol, I., Amado, T. J. C. and Girardello, V. C. (2013) 'Residual Effect of Soil Tillage on Water Erosion from a Typic Paleudalf under Long-term No-Tillage and Cropping Systems', *Revista Brasileira de Ciência do Solo*, 37, pp. 1689-1698.
 - 18 Rejman, J., Turski, R. and Paluszek, J. (1998) 'Spatial and Temporal Variations in Erodibility of Loess Soil', *Soil and Tillage Research*, 46, pp. 61-68.
 - 19 Szpikowski, J. (1998) 'Magnitude and mechanics of water erosion of cultivated soils on moraine slopes (Chwalimski brook catchment, West Pomerania)', *Bibliotheca Fragmenta Agronomica*, 4B, pp. 113-124.
 - 20 Ionita, I., Radoane, M. and Mircea, S. (2006) 'Romania', in Boardman, J. and Poesen, J. (eds) *Soil Erosion in Europe*. Chichester: John Wiley and Sons, pp. 155-166.
 - 21 Horvat, A. and Zemljič, M. (1998) 'Protierozijska vloga gorskega gozda (Mountain forest as a countererosion factor)', in Diaci, J. (ed.) *Gorski gozd*. Ljubljana: Ljubljana Oddelek za gozdarstvo in obnovljive gozdne vire, Biotehniška fakulteta, pp. 411-424.
 - 22 Goeck, J. (1989) *Untersuchungen zur Wassererosion im Silomaisanbau mit und ohne Untersaat (Weißklee) bei variierten Saatterminen unter Berücksichtigung der Ertragsleistung*. PhD Thesis. University of Kiel.
 - 23 Richter, G. (1987) 'Investigation of Soil Erosion in Central Europe', *Seesoil*, 3, pp. 14-27.
 - 24 Jung, L. and Brechtel, R. (1980) *Messung von Oberflächenabfluß und Bodenabtrag auf verschiedenen Böden der BRD*. Hamburg: Parey.
 - 25 Martínez, J. R. F., Zuazo, V. H. D. and Raya, A. M. (2006) 'Environmental impact from mountainous olive orchards under different soil-management systems (SE Spain)', *Science of the Total Environment*, 358, pp. 46-60.
 - 26 Hudek, C. and Rey, F. (2009) 'Studying the Effects of Mahonia Aquifolium Populations on Small-Scale Mountain Agro-Ecosystems in Hungary with the View to Minimise Land Degradation', *Land Degradation and Development*, 20, pp. 252-260.
 - 27 Mitchell, D. J., Barton, A. P., Fullen, M. A., Hocking, T. J., Zhi, W. B. and Yi, Z. (2003) 'Field studies of the effects of jute geotextiles on runoff and erosion in Shropshire, UK', *Soil Use and Management*, 19, pp. 182-184.
 - 28 Gil, E. (1986) 'The role of land use in the processes of the surface runoff and wash-down on the flysch slopes', *Przegląd Geograficzny*, 58, pp. 51-65.
 - 29 Gil, E. (1999) 'Circulation of water and washing on flysch slopes under agricultural use in the years 1980-1990', *Zeszyty IGiPZ PAN*, 60, p. 77.

- 30 Oliveira, A. H., Silva, M. L. N., Curi, N., Avanzi, J. C., Neto, G. K. and Araújo, E. F. (2013) 'Water Erosion in Soils under Eucalyptus Forest as Affected by Development Stages and Management Systems', *Ciência e Agrotecnologia*, 37(2), pp. 159-169.
- 31 Silva, B. P. C., Silva, M. L. N., Batista, P. V. G., Pontes, L. M., Araújo, E. F. and Curi, N. (2016) 'Soil and water losses in eucalyptus plantation and natural forest and determination of the USLE factors at a pilot sub-basin in Rio Grande do Sul, Brazil', *Ciência e Agrotecnologia*, 40(4), pp. 432-442.
- 32 Hammad, A. A., Haugen, L. E. and Børresen, T. (2004) 'Effects of Stonewalled Terracing Techniques on Soil-Water Conservation and Wheat Production Under Mediterranean Conditions', *Environmental Management*, 34(5), pp. 701-710.
- 33 Rousseva, S., Lazarov, A., Tsvetkova, E., Marinov, I., Malinov, I., Kroumov, V. and Stefanova, V. (2006) 'Bulgaria', in Boardman, J. and Poesen, J. (eds) *Soil Erosion in Europe*. Chichester: John Wiley and Sons, pp. 167-181.
- 34 Voss, W. (1978) *Ermittlung der Nährstoffumlagerung durch Erosion und Charakterisierung der Erosionsfracht einiger Vorfluter in Hessischen Mittelgebirgs-Kleinlandschaften*. PhD Thesis. University of Gießen.
- 35 Aguiar, M.I., Maia, S.M.F., Oliveira, T.S., Mendonça, E.S., Araujo Filho, J.A., 2006. Perdas de solo, água e nutrientes em sistemas agroflorestais no município de Sobral, CE. *Revista Ciência Agron.* 37, 270–278.
- 36 Albuquerque, A.W., Lombardi-Neto, F., Srinivasan, V.S., Santos, J.R., 2002. Manejo da cobertura do solo e de práticas conservacionistas nas perdas de solo e água em Sumé, PB. *Revista Bras. de Eng. Agric. e Ambiental* 6, 136–141.
- 37 Amado, T.J.C., Prochnow, D., Eltz, F.L., 2002. Perdas de solo e água em períodos de anomalias climáticas: "El niño" e "La niña" no sul do Brasil. *Revista Bras. de Ciência do Solo* 26, 819–827
- 38 Amaral, A.J., Bertol, I., Cogo, N.P., Barbosa, F.T., 2008. Redução da erosão hídrica em três sistemas de manejo do solo em um Cambissolo Húmico da região do planalto sulcatarinense. *Revista Bras. de Ciência do Solo* 32, 2145–2155.
- 39 Baptista, J., Levien, R., 2010. Métodos de preparo de solo e sua influência na erosão hídrica e no acúmulo de biomassa da parte aérea de eucalyptus saligna em um CambissoloHáplico da depressão central do Rio Grande do Sul. *Revista Árvore* 34, 561–575.
- 40 Bertol, I., Miquelluti, D.J., 1993. Perdas de solo, água e nutrientes reduzidas pela cultura do milho. *Pesq. Agrop. Brasileira* 28, 1205–1213.
- 41 Bertol, I., Schick, J., Batistela, O., 2001. Razão de perdas de solo e fator C para as culturas de soja e trigo em três sistemas de preparo em um Cambissolo Húmico alumínico. *Revista Bras. de Ciência do Solo* 25, 451–461.
- 42 Bertol, I., Schick, J., Batistela, O., Leite, D., Amaral, A.J., 2002. Erodibilidade de um Cambissolo Húmico alumínico léptico, determinada sob chuva natural entre 1989 e 1998 em Lages (SC). *Revista Bras. de Ciência do Solo* 26, 465–471.
- 43 Bertol, I., Cogo, N.P., Schick, J., Guadagnin, J.C., Amaral, A.J., 2007. Aspectos financeiros relacionados às perdas de nutrientes por erosão hídrica em diferentes sistemas de manejo do solo. *Revista Bras. de Ciência do Solo* 31, 133–142.

- 44 Bertol et al. in Anache, J. A. A., Wendland, E. C., Oliveira, P. T. S., Flanagan, D. C. and Nearing, M. A. (2017) 'Runoff and soil erosion plot-scale studies under natural rainfall: A meta-analysis of the Brazilian experience', *Catena*, 152, pp. 29-39.
- 45 Bertol et al. in Anache, J. A. A., Wendland, E. C., Oliveira, P. T. S., Flanagan, D. C. and Nearing, M. A. (2017) 'Runoff and soil erosion plot-scale studies under natural rainfall: A meta-analysis of the Brazilian experience', *Catena*, 152, pp. 29-39.
- 46 Bertol et al. in Anache, J. A. A., Wendland, E. C., Oliveira, P. T. S., Flanagan, D. C. and Nearing, M. A. (2017) 'Runoff and soil erosion plot-scale studies under natural rainfall: A meta-analysis of the Brazilian experience', *Catena*, 152, pp. 29-39.
- 47 Bertolino, A.V.F.A., Soares, I.L.P., Cunha, L., 2015. Hydrological and erosive dynamics in traditional slash-and-burn farming methods in the Atlantic forest biome (RJ) – Brazil. *Territorium* 22, 65–75.
- 48 Bertoni, J., Lombardi-Neto, F., 2012. *Conservação do Solo*. eighth ed. Ícone, São Paulo, SP.
- 49 Cabral, C.E.A., Amorim, R.S.S., Dores, E.F.G.C., Bonfim-Silva, E.M., 2010. Estimativa de perda de solo em sistemas de cultivo em lavouras de algodão. *Enciclopédia Biosfera* 6, 1–8.
- 50 Campos Filho, O.R., Silva, I.F., Andrade, A.P., Leprun, J.C., 1992. Erosividade da chuva e erodibilidade do solo no agreste pernambucano. *Pesq. Agrop. Brasileira* 27, 1363–1370.
- 51 Cândido, B.M., Silva, M.L.N., Curi, N., Batista, P.V.G., 2014. Erosão hídrica pós-plantio em florestas de eucalipto na bacia do rio Paraná, no leste do Mato Grosso do Sul. *Revista Bras. de Ciência do Solo* 38, 1565–1575.
- 52 Cardoso, D.P., Silva, M.L.N., Carvalho, G.J., Freitas, D.A.F., Avanzi, J.C., 2012. Plantas de cobertura no controle das perdas de solo, água e nutrientes por erosão hídrica. *Revista Bras. de Eng. Agri. e Ambiental* 16, 632–638.
- 53 Carvalho, M.P., Hernani, L.C., 2001. Parâmetros de erosividade da chuva e da enxurrada correlacionados com perdas de solo e erodibilidade de um Latossolo Roxo de Dourados (MS). *Revista Bras. de Ciência do Solo* 25, 137–146.
- 54 Carvalho, R., Silva, M.L.N., Avanzi, J.C., Curi, N., Souza, F.S., 2007. Erosão hídrica em Latossolo Vermelho sob diversos sistemas de manejo do cafeeiro no sul de Minas Gerais. *Ciência e Agrotecnologia* 31, 1679–1687.
- 55 Cogo, N.P., Levien, R., Schwarz, R.A., 2003. Perdas de solo e água por erosão hídrica influenciadas por métodos de preparo, classes de declive e níveis de fertilidade do solo. *Revista Bras. de Ciência do Solo* 27, 743–753.
- 56 Correchel, V., Bacchi, O.O.S., DeMaria, I.C., Dechen, S.C.F., Reichardt, K., 2006. Erosion rates evaluated by the ¹³⁷Cs technique and direct measurements on long-term runoff plots under tropical conditions. *Soil Tillage Res.* 86, 199–208.
- 57 Cruz, E.S., 2006. *Influência do Preparo do Solo e de Plantas de Cobertura na Erosão Hídrica de um Argissolo Vermelho-Amarelo*. Universidade Federal Rural do Rio de Janeiro, Seropédica, RJ (58 pp. M.Sc. theses).
- 58 Debarba, L., Amado, T.J.C., 1997. Desenvolvimento de sistemas de produção de milho no sul do Brasil com características de sustentabilidade. *Revista Bras. de Ciência do Solo* 21, 473–480.

- 59 Dedecek, R., 1986. Erosão e Práticas Conservacionistas nos Cerrados. Embrapa, Planaltina, DF, p. 16.
- 60 Dedecek, R.A., 1989. Coberturas permanentes do solo na erosão sob condições de cerrados. *Pesq. Agrop. Brasileira* 24, 483–488.
- 61 Eduardo, E.N., Carvalho, D.F.D., Machado, R.L., Soares, P.F.C., Almeida, W.S.D., 2013. Erodibilidade, fatores cobertura e manejo e práticas conservacionistas em argissolo vermelho-amarelo, sob condições de chuva natural. *Revista Bras. de Ciência do Solo* 37, 796–803.
- 62 Encinas, O.C., 2010. Avaliação de Processos Erosivos na Base de operações Geólogo Pedro de Mora - Coari, AM. Instituto Nacional de Pesquisas da Amazônia, Manaus, AM (79 pp. M.Sc. theses).
- 63 Falcão Sobrinho, J., 2015. Precipitação e erosão do solo na Serra das Matas no ambiente do semiárido cearense. *Fórum Ambiental da Alta Paulista* 11.
- 64 Freire, R., Tavares, C.R.G., Soares, P.F., Abreu, M.H.M.D., 2014. Correlação entre condição da superfície do solo agrícola e o coeficiente de absorção acústica. *Revista Ambiente & Água* 9, 708–721.
- 65 Guadagnin, J.C., Bertol, I., Cassol, P.C., Amaral, A.J., 2005. Perdas de solo, água e nitrogênio por erosão hídrica em diferentes sistemas de manejo. *Revista Bras. de Ciência do Solo* 29, 277–286.
- 66 Guimarães, D.V., 2015. Erosão hídrica Em Sistemas Florestais No Extremo Sul Da Bahia Lavras. MG, Universidade Federal de Lavras (93 pp. M.Sc. theses).
- 67 Guimarães, G.P., Andrade, K.C., Mendonça, E.S., 2015. Rainfall erosion and compartments soil organic matter in coffee systems conservationist and conventional. *Coffee Science* 10, 365–374.
- 68 Hernani, L.C., Salton, J.C., Fabrício, A.C., Dedecek, R., Alves Júnior, M., 1997. Perdas por erosão e rendimentos de soja e de trigo em diferentes sistemas de preparo de um Latossolo Roxo de Dourados (MS). *Revista Bras. de Ciência do Solo* 21, 667–676.
- 69 Hernani, L.C., Kurihara, C.H., Silva, W.M., 1999. Sistemas de manejo de solo e perdas de nutrientes e matéria orgânica por erosão. *Revista Bras. de Ciência do Solo* 23, 145–154.
- 70 Lanzanova, M.E., Eltz, F.L.F., Nicoloso, R.D.S., Cassol, E.A., Bertol, I., Amado, T.J.C., Girardello, V.C., 2013. Residual effect of soil tillage on water erosion from a Typic Paleudalf under long-term no-tillage and cropping systems. *Revista Bras. de Ciência do Solo* 37, 1689–1698.
- 71 Leite, M.H.S., Couto, E.G., Amorim, R.S.S., Costa, E.L., Maraschin, L., 2009. Perdas de solo e nutrientes num Latossolo Vermelho-amarelo ácrico típico, com diferentes sistemas de preparo e sob chuva natural. *Revista Bras. de Ciência do Solo* 33, 689–699.
- 72 Lima, W.P., 1988. Escoamento superficial, perdas de solo e de nutriente em microparcelas reflorestadas com eucalipto em solos arenosos no município de São Simão, SP. *IPEF* 38, 5–16.
- 73 Marchioro, E., Augustin, C.H.R.R., 2007. Dimensão de parcelas experimentais: influência nas medidas de escoamento superficial e erosão do solo em Gouveia/MG. *Geografia* 3, 7–16.
- 74 Margolis, E., Galindo, I.C.L., Mello Netto, A.V., 1991. Comportamento de sistemas de cultivo da mandioca em relação à produção e às perdas por erosão. *Revista Bras. de Ciência do Solo* 15, 357–362.
- 75 Marques, S.R., Weill, M.A.M., Silva, L.F.S., 2010. Qualidade física de um latossolo vermelho, perdas

- por erosão e desenvolvimento domilho em dois sistemas de manejo. *Ciência e Agrotecnologia* 34, 967–974.
- 76 Martins, S.G., 2005. Erosão hídrica em povoamento de eucalipto sobre solos coesos no tabuleiros Costeiros, ES. Universidade Federal de Lavras, Lavras, MG (117 pp. Ph.D. dissertation).
- 77 Martins Filho, F.M., 2014. Balanço hídrico e erosão do solo em uma plantação de eucaliptos novos. Universidade de São Paulo, São Carlos, SP (138 pp. M.Sc. theses).
- 78 Merten, G.H., Araújo, A.G., Biscaia, R.C.M., Barbosa, G.M.C., Conte, O., 2015. No-till surface runoff and soil losses in southern Brazil. *Soil Tillage Res.* 152, 85–93.
- 79 Nacinovic, M.G.G., Mahler, C.F., Avelar, A.D.S., 2014. Soil erosion as a function of different agricultural land use in Rio de Janeiro. *Soil Tillage Res.* 144, 164–173.
- 80 Nagel, P.L., Panachuki, E., Bertol, I., Valim, W.C., Alves Sobrinho, T., 2016. Water erosion under rain in the ultison under conventional tillage. *Revista Bras. de Ciência do Solo.*
- 81 Nascimento, P.C., Lombardi-Neto, F., 1999. Razão de perdas de solo sob cultivo de três leguminosas. *Revista Bras. de Ciência do Solo* 23, 121–125.
- 82 Oliveira, L.C., 2012. Erosão hídrica e alguns processos hidrológicos em plantios de pinus, mata e campo nativos e estrada florestal. Universidade do Estado de Santa Catarina, Lages, SC (Ph.D. dissertation).
- 83 Oliveira, A.H., 2011. Erosão hídrica e seus componentes na sub-bacia hidrográfica do Horto Florestal Terra Dura, Eldorado do Sul (RS). Universidade Federal de Lavras, Lavras, MG (179 pp. Ph.D. dissertation).
- 84 Oliveira, S.P., Lacerda, N.B., Blum, S.C., Escobar, M.E.O., Oliveira, T.S., 2015a. Organic carbon and nitrogen stocks in soils of Northeastern Brazil converted to irrigated agriculture. *Land Degrad. Dev.* 26, 9–21.
- 85 Pereira, L.S., Rodrigues, A.M., Jorge, M.C.O., Guerra, A.J.T., Fullen, M.A., 2016. Hydro-erosive processes in degraded soils on gentle slope. *Revista Bras. de Geomorfologia* 17, 299–316.
- 86 Pinese Júnior, J.F., Cruz, L.M., Rodrigues, S.C., 2008. Monitoramento de erosão laminar em diferentes usos da terra, Uberlândia - MG. *Sociedade & Natureza* 20, 157–175.
- 87 Pires, L.S., Silva, M.L.N., Curi, N., Leite, F.P., Brito, L.F., 2006. Erosão hídrica pós-plantio em florestas de eucalipto na região centro-leste de Minas Gerais. *Pesq. Agrop. Brasileira* 41, 687–695.
- 88 Prochnow, D., 2003. Perdas de terra e água em sistemas de manejo na cultura do café no oeste do Estado de São Paulo. Instituto Agronômico de Campinas, Campinas, SP (133 pp. M.Sc. theses).
- 89 Prochnow, D., Dechen, S.C.F., De Maria, I.C., Castro, O.M.D., Vieira, S.R., 2005. Razão de perdas de terra e fator C da cultura do cafeeiro em cinco espaçamentos, em Pindorama (SP). *Revista Bras. de Ciência do Solo* 29, 91–98.
- 90 Rieger, F.A., Zolin, C.A., Magalhães, C.A.S., Paulino, J., Farias Neto, A.L., Meneguici, J.L.P. 2014. Perda de Água e Sedimentos em Diferentes Usos do Solo. *Proc. II Inovagri International Meeting, Fortaleza, CE*, pp. 5203–5211.
- 91 Santos, D., Curi, N., Ferreira, M.M., Evangelista, A.R., Cruz Filho, A.B., Teixeira, W.G., 1998. Perdas de solo e produtividade de pastagens nativas melhoradas sob diferentes práticas de manejo. *Pesq. Agrop. Brasileira* 33, 183–189.

- 92 Santos, C.A.G., Silva, R.M., Srinivasan, V.S., 2007. Análise das perdas de água e solo em diferentes coberturas superficiais no semi-árido da Paraíba. *Revista OKARA: Geografia em debate* 1, 1–152.
- 93 Santos, J.C.N.D., Palácio, H.A.D.Q., Andrade, E.M.D., Meireles, A.C.M., Araújo Neto, J.R.D., 2011. Runoff and soil and nutrient losses in semiarid uncultivated fields. *Revista Ciência Agron.* 42, 813–820.
- 94 Saraiva, O.F., Cogo, N.P., Mielniczuk, J., 1981. Erosividade das chuvas e perdas por erosão em diferentes manejos de solo e coberturas vegetais. *Pesq. Agrop. Brasileira* 16, 121–128.
- 95 Schick, J., Bertol, I., Balbinot Júnior, A.A., Batistela, O., 2000. Erosão hídrica em Cambissolo Húmico alumínico submetido a diferentes sistemas de preparo e cultivo do solo: II. Perdas de nutrientes e carbono orgânico. *Revista Bras. de Ciência do Solo* 24.
- 96 Schick, J., Bertol, I., Cogo, N.P., González, A.P., 2014. Erodibilidade de um Cambissolo Húmico sob chuva natural. *Revista Bras. de Ciência do Solo* 38, 1906–1917.
- 97 Silva, A.M., Silva, M.L.N., Curi, N., Lima, J.M., Avanzi, J.C., Ferreira, M.M., 2005. Perdas de solo, água, nutrientes e carbono orgânico em Cambissolo e Latossolo sob chuva natural. *Pesq. Agrop. Brasileira* 40, 1223–1230.
- 98 Silva, J.V., Alecrim, M.A.B., Silva, D.O., Costa, D.O., Costa, C.C., Oliveira, R.J., 2010. Perdas de solo e água por erosão hídrica em floresta equiânea em um Latossolo Vermelho-Amarelo. *Revista Bras. de Ciências Agrar.* 5, 579–584.
- 99 Silva, M.A., Silva, M.L.N., Curi, N., Avanzi, J.C., Leite, F.P., 2011. Sistemas de manejo em plantios florestais de eucalipto e perdas de solo e água na região do Vale do Rio Doce, MG. *Ciência Florestal* 21, 765–776.
- 100 Tenberg, A., Stocking, M., Dechen, S.C.F., 1997. The impact of erosion on soil productivity: an experimental design applied in São Paulo state. *Brazil. Geogr. Annaler* 79A, 95–107.
- 101 Thomaz, E.L., 2009. The influence of traditional steep land agricultural practices on runoff and soil loss. *Agric. Ecosyst. Environ.* 130, 23–30.
- 102 Wichert, M.C.P., 2005. Erosão hídrica e desenvolvimento inicial do *Eucalyptus grandis* em um Argissolo Vermelho-Amarelo submetido a diferentes métodos de preparo de solo no Vale do Paraíba-SP. Universidade de São Paulo, Piracicaba, SP (84 pp. M.Sc. theses).
- 103 Youlton, C., Wendland, C., Anache, J.A.A., Poblete-Echeverría, C., Dabney, S., 2016. Changes in erosion and runoff due to replacement of pasture land with sugarcane crops. *Sustainability* 8, 685–697.
- 104 Nearing, M. A., Govers, G. and Norton, L. D. (1999) 'Variability in Soil Erosion from Replicated Plots', *Soil Science Society of America Journal*, 63, pp. 1829-1835.
- 105 Prasuhn, V. (1992) 'A geoecological approach to soil erosion in Switzerland', in Hurni, H. and Tato, K. (eds) *Erosion, Conservation, and Small-Scale Farming*. Missouri: Walsworth Publishing Company, pp. 27-39.
- 106 Maass, J. M. (1992) 'The use of litter-mulch to reduce erosion on hilly land in Mexico', in Hurni, H. and Tato, K. (eds) *Erosion, Conservation, and Small-Scale Farming*. Missouri: Walsworth Publishing Company, pp. 383-393

- 107 Rodriguez, O. S. and De La Paz, N. F. (1992) 'Conservation practices for horticulture production in the mountainous regions of Venezuela', in Hurni, H. and Tato, K. (eds) *Erosion, Conservation, and Small-Scale Farming*. Missouri: Walsworth Publishing Company, pp. 393-407.
- 108 Bekele, M. W. and Thomas, D. B. (1992) 'The influence of surface residue on soil loss and runoff', in Hurni, H. and Tato, K. (eds) *Erosion, Conservation, and Small-Scale Farming*. Missouri: Walsworth Publishing Company, pp. 439-453.
- 109 Temple, P. H. (1972) 'Measurements of Runoff and Soil Erosion at an Erosion Plot Scale with Particular Reference to Tanzania', *Geografiska Annaler Series A Physical Geography*, 54, pp. 203-220.
- 110 Duran Zuazo, V. H., Rodriguez Pleguezuelo, C. R., Francia Martinez, J. R., Carceles Rodriguez, B., Martinez Raya, A. and Perez Galindo, P. (2008) 'Harvest intensity of aromatic shrubs vs. soil erosion: An equilibrium for sustainable agriculture (SE Spain)', *Catena*, 73(1), pp. 107-116.
- 111 Chirino, E., Bonet, A., Bellot, J. and Sanchez, J. R. (2006) 'Effects of 30-year-old Aleppo pine plantations on runoff, soil erosion, and plant diversity in a semi-arid landscape in south eastern Spain', *Catena*, 65, pp. 19-29.
- 112 Borst, H. L., McCall, A. G. and Bell, F. G. (1945) *Investigations in erosion control and reclamation of eroded land at the Northwest Appalachian Conservation Experiment Station, Zanesville, Ohio, 1934-42 Technical Bulletin 888*. Available at: <http://ageconsearch.umn.edu/record/169865?ln=en> (Accessed: 20 November 2018).
- 113 McGregor, K. C., Dabney, S. M. and Johnson, J. R. (1999) 'Runoff and soil loss from cotton plots with and without stiff-grass hedges', *Transactions of the American Society of Agricultural Engineers*, 42, pp. 361-368.
- 114 Kramer, L. A. (1986) 'Runoff and soil loss by cropstage from conventional and conservation tilled corn', *Transactions of the American Society of Agricultural Engineers*, 29, pp. 774-779.
- 115 McGregor, K. C., Greer, J. D. and Gurley, G. E. (1975) 'Erosion control with no-till cropping practices', *Transactions of the American Society of Agricultural Engineers*, 18, pp. 918-920.
- 116 McGregor, K. C. and Greer, J. D. (1982) 'Erosion control with no-till and reduced-till corn for silage and grain', *Transactions of the American Society of Agricultural Engineers*, 25, pp. 154-159.
- 117 Mutchler, C. K., McDowell, L. L. and Greer, J. D. (1985) 'Soil loss from cotton with conservation tillage', *Transactions of the American Society of Agricultural Engineers*, 28, pp. 160-163.
- 118 Bu (2008) cited in Zhao, J., Yang, Z. and Govers, G. (2019) 'Soil and water conservation measures reduce soil and water losses in China but not down to background levels: Evidence from erosion plot data', *Geoderma*, 337, pp. 729-741.
- 119 Cai, X. (2004) 'Benefits from soil and water conservation measures on reducing runoff and sediments in Shixia small watershed ', *Resources Science*, 26, pp. 144-150.
- 120 Chen, G., Fan, H., Chen, H. and Dong, G. (2006a) 'Benefits of sediment reduction of soil conservation practices in the black region of Northeast China', *Journal of Soil and Water Conservation*, 4, pp. 13-17.
- 121 Chen, S. (1999) 'Studies on soil and water conservation measurements on tea garden in eastern of Fujian', *Fujian Soil and Water Conservation*, 11, pp. 52-55.

- 122 Chen, Y. and Dai, X. (1996) 'Reduction of soil and water loss in a *Myrica rubra* garden', *Fujian Soil and Water Conservation*, 3, pp. 45-47.
- 123 Chen, R. (2005) 'Study on the rapid restoration of grass coverage and technique of controlling soil and water loss in eroded hilly land', *Subtropical Soil and Water Conservation*, 17, pp. 14-16.
- 124 Chen, Y., Zhang, X. and Li, S. (2011) 'Comparative study on conservational tillage in slope and flat farmland', *System Sciences and Comprehensive Studies in Agriculture*, 27, pp. 485-489.
- 125 Chen, Z., Tian, F. and Dong, J. (2015) 'The slope erosion sediment yield under different land use types in hilly area of Anhui province', *Journal of Arid Land Resources and Environment*, 29, pp. 186-191.
- 126 Chen, Q., Yuriy, S. K., Chen, Y., Li, X., Li, H., Song, C. and Zhang, X. (2014) 'Seasonal variations of soil structures and hydraulic conductivities and their effects on soil and water conservation under no-tillage and reduced tillage', *Acta Ecologica Sinica*, 51, pp. 11-21.
- 127 Chen, S., Hua, L., He, Z., Wei, D., Xia Hou, G. and Li, Y. (2002) 'Effect of soil erosion on soil properties in deep cultivated hill slope in loess plateau', *Agro-Environmental Protection*, 21, pp. 289-292.
- 128 Chen, S., Yang, Y., Lin, W. and Li, T. (2006b) 'Quantitative research on soil and water loss and countermeasures in man-made destroyed red soil region in subtropical region of Fujian Province', *Journal of Soil and Water Conservation*, 20, pp. 6-10.
- 129 Cui, Y., Han, Z., Cui, B., Liu, W. and Su, N. (1994) 'Effect of no-tillage with stalks mulching on controlling runoff and soil loss', *Journal of Shanxi Agricultural Sciences*, 22, pp. 20-21.
- 130 Fan, D., Yu, X., Jia, G., Wang, H. and Zhao, Y. (2015) 'Characteristics of soil erosion under different landuse types in upper area of miyun reservoir', *Bulletin of Soil and Water Conservation*, 35, pp. 5-8.
- 131 Fan, X., Ma, Z., Yang, Q., Han, Y., Mahmood, R. and Zheng, Z. (2014) 'Land use/land cover changes and regional climate over the Loess Plateau during 2001–2009. Part II: interrelationship from observations', *Climate Change*, doi: 10.1007/s10584-014-1068-5
- 132 Feng, Y., Meng, G., Yu, T. and Chu, Y. (2015) 'Characteristics of runoff and sediment production of runoff plot of Guanmaidai small watershed', *Journal of Chinese Soil and Water Conservation*, 9, pp. 42-45.
- 133 Fu, B. J., Meng, Q. H., Qiu, Y., Zhao, W. W., Zhang, Q. J. and Davidson, D. A. (2004) 'Effects of land use on soil erosion and nitrogen loss in the hilly area of the Loess Plateau, China', *Land Degradation and Development*, 15, pp. 87-96.
- 134 Fu, S., Liu, B., Lu, B., Yuan, A. and Wang, N. (2009) 'Effect of soil conservation practice on runoff and sediment in upper reach of Guanting Reservoir', *Journal of Soil and Water Conservation*, 7, pp. 18-23.
- 135 Fu, J., Jiang, Z., Yi, C., Zhang, W. and Wang, Y. (2000) 'Studies on soil and water conservation benefit of contour hedgerows in arid and hillside farmland', *Tillage Cultivation*, 14(1), pp. 38-40.
- 136 Gu, X., Yu, Z., Zhao, H., Ai, Z. and Guo, W. (1994) 'Assessment of the efficient of different soil and water control measurements', *Hebei Journal of Industrial Science and Technology*, 9, pp. 21-22.
- 137 Guan (1996) cited in Zhao, J., Yang, Z. and Govers, G. (2019) 'Soil and water conservation

- measures reduce soil and water losses in China but not down to background levels: Evidence from erosion plot data', *Geoderma*, 337, pp. 729-741.
- 138 Guo (2010) cited in Zhao, J., Yang, Z. and Govers, G. (2019) 'Soil and water conservation measures reduce soil and water losses in China but not down to background levels: Evidence from erosion plot data', *Geoderma*, 337, pp. 729-741.
- 139 Han, Y., Li, X., Duan, S., Yuan, A. and Lu, B. (2010) 'Influence of soil and water conservation measures to runoff sediment and nutrient loss', *Journal of Chinese Soil and Water Conservation*, 38(3) pp. 34-37.
- 140 He, J., Cai, Q., Fang, H. and Chen, X. (2009) 'Effect evaluation of spatial allocation of water and soil conservation measures in Zhangjiakou area', *Transactions of the Chinese Society of Agricultural Engineering*, 25(10), pp. 69-75.
- 141 Huang, Y., Luo, X., Zheng, Z., Zhang, W., Huang, X. and Zhan, J. (2009) 'Effects of different exploitation manners on soil and water losses in hilly orchard', *Journal of Soil and Water Conservation*, 7, pp. 30-34.
- 142 Huang, Y., Yang, X. and Jiang, F. (2007) 'Effects of different ways of sod in eroded slope orchard on soil and fruit tree growth', *Journal of Soil and Water Conservation*, 21, pp. 111-114.
- 143 Huang, C., Tan, W., Qin, W., Wei, G., Wu, M. and Wei, Y. (2012) 'Study on soil and water loss in Karst forest in Mulun', *Research of Soil and Water Conservation*, 19, pp. 34-37.
- 144 Huang, J. (2015) 'Benefits of soil and water conservation measures under different land-use patterns in Ninghua', *Journal of Agriculture and Forestry*, 5, pp. 57-61.
- 145 Huang, Z., Liu, L., Wu, C., and Yang, M. (2014) 'The efficacy of terrace on soil and water loss control on the loessal soil region of Guizhou', *Journal of Chinese Soil and Water Conservation*, pp. 55-57.
- 146 Jiang, N. and Shao, M. (2011) 'Characteristics of soil and water loss of different slope land uses in small watershed on the Loess Plateau', *Transactions of the Chinese Society of Agricultural Engineering*, 27, pp. 36-41
- 147 Jiang, B., Zhao, S., Wei, D., Jin, L., Li, Y., Guo, W., Xu, M. and Zhang, Z. (2015) 'Effect of slope and tillage measures on soil erosion and yield of soybean', *Soybean Science*, 34, pp. 238-242.
- 148 Jin, K., Cai, D., Lu, J., Zhang, J., Wu, H., Rong, X., Gabriels, D. and Schiettecatte, W. (2006) 'Effects of tillage practices on erosion and winter wheat yield on sloping dryland', *Journal of Soil and Water Conservation*, 20, pp. 1-5.
- 149 Lan, J., Fan, H., Chai, Y., Zhou, L. and Wu, M. (2009) 'Characteristics of soil erosion of different land use types in earth-rock low mountainous area in west of Liaoning', *Journal of Chinese Soil and Water Conservation*, 329, pp. 8-10.
- 150 Li, P., Peng, P., Hou, Y. and Xu, Z. (2006) 'Study of different replanting patterns to renovate sloping tea garden on effect of soil and water conservation', *Southwest China Journal of Agricultural Sciences*, 19, pp. 120-122.
- 151 Li, Y., Quine, T. A. A., Yu, H. Q. Q., Govers, G., Six, J. Gong, D. Z. Z., Wang, Z., Zhang, Y. Z. Z. and Van Oost, K. (2015) 'Sustained high magnitude erosional forcing generates an organic carbon sink: test and implications in the Loess Plateau, China', *Earth and Planetary Science Letters*, 411,

pp. 281-289.

- 152 Li, X., Zhang, X., Gao, Y., Chen, Y., Li, H., Tao, S. and Song, C. (2013) 'Benefits assessment for soil and water conservation projects in black soil region of Northeast China', *Bulletin of Soil and Water Conservation*, 33, pp. 43-47.
- 153 Liang (1999) cited in Zhao, J., Yang, Z. and Govers, G. (2019) 'Soil and water conservation measures reduce soil and water losses in China but not down to background levels: Evidence from erosion plot data', *Geoderma*, 337, pp. 729-741.
- 154 Lin, C., Tu, S., Huang, J. and Chen, Y. (2007) 'The effects of plant hedgerows on soil erosion and soil fertility on sloping farmland in the purple soil area', *Acta Ecologica Sinica*, 27, pp. 2191-2198.
- 155 Liu, L. (2007) 'Study on soil and water control measurements on the sloping orchard land', *International Journal of Hydrology Science and Technology*, pp. 16-17.
- 156 Liu, S. Y. (2006) 'Comparative study of effects of soil and water conservation on sloping land orchard of red soil', *Bulletin of Soil and Water Conservation*, 26, pp. 7-10.
- 157 Liu, G., Gao, M., Zhang, J., Li, Y. and Zhang, X. (2001) 'Soil erosion characteristics of slope land under alternative tillage systems in central hilly area of Sichuan, China', *Journal of Mountain Science*, 19, pp. 65-70.
- 158 Lu, G., Ban, X., Lei, Z. and Wu, X. (2009) 'Benefit of soil and water conservation in the process of harnessing a sloping farmland in the black soil region, Northeast China', *International Soil and Water Conservation Research*, 16, pp. 51-55.
- 159 Lu (2012) cited in Zhao, J., Yang, Z. and Govers, G. (2019) 'Soil and water conservation measures reduce soil and water losses in China but not down to background levels: Evidence from erosion plot data', *Geoderma*, 337, pp. 729-741.
- 160 Lv (1999) cited in Zhao, J., Yang, Z. and Govers, G. (2019) 'Soil and water conservation measures reduce soil and water losses in China but not down to background levels: Evidence from erosion plot data', *Geoderma*, 337, pp. 729-741.
- 161 Lv (1996) cited in Zhao, J., Yang, Z. and Govers, G. (2019) 'Soil and water conservation measures reduce soil and water losses in China but not down to background levels: Evidence from erosion plot data', *Geoderma*, 337, pp. 729-741.
- 162 Ma, J. and Wang, Z. (2009) 'Soil and water conservation benefits of artificial grassland in Yanggao County', *Soil and Water Conservation Science and Technology in Shanxi*, pp. 14-17.
- 163 Mao, F., Wan, J., Tan, D. (2010) 'Soil and water loss and its countermeasures in Zhangjiachong watershed', *Journal of Chinese Soil and Water Conservation*, pp. 59-61.
- 164 Meng, Q. H. and Yang, L. Z. (2001) 'Effects of land use on soil erosion and nutrient loss in the Three Gorges Reservoir Area, China', *Soil Use and Management*, 17, pp. 288-291.
- 165 Mi, Y., Pan, Y., Sha, L., Guo, Y., Li, J. and Zhang, X. (2006) 'Comprehensively harnessing measures to control soil, water and nutrients loss in slope cultivated land of red soil in Yunnan', *Journal of Soil Water Conservation*, 20, pp. 17-21.
- 166 NDSIESS (no date) cited in Zhao, J., Yang, Z. and Govers, G. (2019) 'Soil and water conservation measures reduce soil and water losses in China but not down to background levels: Evidence from erosion plot data', *Geoderma*, 337, pp. 729-741.

- 167 Ng, S. L., Cai, Q. G., Ding, S. W., Chau, K. C. and Qin, J. (2008) 'Effects of contour hedgerows on water and soil conservation, crop productivity and nutrient budget for slope farmland in the Three Gorges Region (TGR) of China', *Agroforestry System*, 74, pp. 279-291.
- 168 Ning (2006) cited in Zhao, J., Yang, Z. and Govers, G. (2019) 'Soil and water conservation measures reduce soil and water losses in China but not down to background levels: Evidence from erosion plot data', *Geoderma*, 337, pp. 729-741.
- 169 Qin, T., Jiang, X., Chen, Z. and Xiang, M. (1996) 'Experiment of soil and water benefit of ridge plantation in different angle', *Journal of Sichuan University*, 17, pp. 25-28.
- 170 Ruan, F. (1995) 'Influence of inclination and length of slope on soil erosion in granite area of Fujian', *Journal of Fujian Teachers University*, 11, pp. 100-106.
- 171 Shen, Z., Gong, Y., Li, Y. and Liu, R. (2010) 'Analysis and modeling of soil conservation measures in the Three Gorges Reservoir Area in China', *Catena*, 81, pp. 104-112.
- 172 Sheng (1999) cited in Zhao, J., Yang, Z. and Govers, G. (2019) 'Soil and water conservation measures reduce soil and water losses in China but not down to background levels: Evidence from erosion plot data', *Geoderma*, 337, pp. 729-741.
- 173 Shui, J., Ye, Y. and Liu, C. (2002) 'Regularity of erosion and soil loss tolerance in hilly red-earth region of China', *Agircultural Sciences in China*, 1, pp. 1232-1237.
- 174 Song (2014) cited in Zhao, J., Yang, Z. and Govers, G. (2019) 'Soil and water conservation measures reduce soil and water losses in China but not down to background levels: Evidence from erosion plot data', *Geoderma*, 337, pp. 729-741.
- 175 Su, B. and Liu, P. (2014) 'Characteristics of soil loss and runoff of runoff plot on Yizhe catchment', *Journal of Green Science and Technology*, 4, pp. 4-17.
- 176 Sun, J., Yang, Y., Zhang, B. and He, J. (1997) 'Hilly field erosion regulation in low mountain region of northern Liaoning', *International Soil and Water Conservation Research*, 4, pp. 65-74.
- 177 Sun (2004) cited in Zhao, J., Yang, Z. and Govers, G. (2019) 'Soil and water conservation measures reduce soil and water losses in China but not down to background levels: Evidence from erosion plot data', *Geoderma*, 337, pp. 729-741.
- 178 Sun (2005) cited in Zhao, J., Yang, Z. and Govers, G. (2019) 'Soil and water conservation measures reduce soil and water losses in China but not down to background levels: Evidence from erosion plot data', *Geoderma*, 337, pp. 729-741.
- 179 Sun (2000) cited in Zhao, J., Yang, Z. and Govers, G. (2019) 'Soil and water conservation measures reduce soil and water losses in China but not down to background levels: Evidence from erosion plot data', *Geoderma*, 337, pp. 729-741.
- 180 Sun (2006) cited in Zhao, J., Yang, Z. and Govers, G. (2019) 'Soil and water conservation measures reduce soil and water losses in China but not down to background levels: Evidence from erosion plot data', *Geoderma*, 337, pp. 729-741.
- 181 Sun (2001) cited in Zhao, J., Yang, Z. and Govers, G. (2019) 'Soil and water conservation measures reduce soil and water losses in China but not down to background levels: Evidence from erosion plot data', *Geoderma*, 337, pp. 729-741.
- 182 Sun (2002) cited in Zhao, J., Yang, Z. and Govers, G. (2019) 'Soil and water conservation

- measures reduce soil and water losses in China but not down to background levels: Evidence from erosion plot data', *Geoderma*, 337, pp. 729-741.
- 183 Sun (2003) cited in Zhao, J., Yang, Z. and Govers, G. (2019) 'Soil and water conservation measures reduce soil and water losses in China but not down to background levels: Evidence from erosion plot data', *Geoderma*, 337, pp. 729-741.
- 184 Sun, H., Tang, Y., Chen, K. and He, Y. (1999) 'Effect of contour hedgerow system on slope lands erosion control', *Bulletin of Soil and Water Conservation*, 19, pp. 1-5.
- 185 Tang, Y., Dai, S., Jiang, G., Shi, D. and Chen, Z. (2010) 'Calculation and analysis of the vegetation cover and management factor C value in slope farmland of Chongqing area', *Journal of Soil and Water Conservation*, 24, pp. 53-59.
- 186 Tang, Q. and Tian, Z. (2002) 'A preliminary report on the study of soil conservation technology of the new exploited orchard of red soil sloping fields', *Journal of Guangxi Agricultural and Biological Science*, pp. 44-49.
- 187 Tao, Y., Xiang, F., Ren, W., Lin, L. and Chen, J. (2015) 'Effect of engineering measures on soil and water conservation on granite red soil slope', *Journal of Soil and Water Conservation*, 29, pp. 34-39.
- 188 Tian, B., Chen, Q. and Wang, K. (2006) 'Study on runoff and sediment production on slopes treated by different measures in dry-hot valley of Jinshajiang River', *Journal of Southwest Forestry College*, 26, pp. 44-48.
- 189 Tian (2014) cited in Zhao, J., Yang, Z. and Govers, G. (2019) 'Soil and water conservation measures reduce soil and water losses in China but not down to background levels: Evidence from erosion plot data', *Geoderma*, 337, pp. 729-741.
- 190 Tian, F., Xie, Y., Chen, L., Suo, G. and Ding, Y. (2015) 'Sediment and water control effects by stone sill reverse-slope level terrace in slope farmland with thin soil layer', *Agricultural Research in the Arid Areas*, 33, pp. 247-253.
- 191 Wang, X., Gao, H., Tullberg, J. N., Li, H., Kuhn, N., McHugh, A. D. and Li, Y. (2008a) 'Traffic and tillage effects on runoff and soil loss on the loess', *Australian Journal of Soil Research*, 46, pp. 667-675.
- 192 Wang, J., Luo, S. and Ye, D. (2008b) 'Benefits of biological measures to the soil and water conservation in Gannan Mountain Area', *Journal of Soil and Water Conservation*, 6, pp. 37-43.
- 193 Wang, W. (2006) 'The relationship between rainfall and soil erosion under different land uses in slope land of northern Fujian', *Journal of Soil and Water Conservation*, 13, pp. 134-136.
- 194 Wang, J., Yin, W. and Liu, D. (2011) 'Influence of intercropping maize with alfalfa on runoff and sediment yield after rainfall on loess slope land', *Water Saving Irrigation*, 43-46, p. 54
- 195 Wang, X., Zhang, T. and Zhang, B. (1998) 'No-tillage and cover on sloping cropland on the red soil region', *Soil*, 2, pp. 84-88.
- 196 Wang (2012) cited in Zhao, J., Yang, Z. and Govers, G. (2019) 'Soil and water conservation measures reduce soil and water losses in China but not down to background levels: Evidence from erosion plot data', *Geoderma*, 337, pp. 729-741.
- 197 Wu, J. and Li, Y. (1998) 'Study on the relationship between different control measurement on runoff and sediment in a limestone watershed', *Beijing Water*, pp. 13-16.

- 198 Wu, F., Zhao, X., Liu, B. and Jia, R. (1998) 'Influence of cultivation activities on the runoff and Erosion on Slope land', *Journal of Northwest Forestry College*, 13, pp. 20-25.
- 199 Xiang, D., Yong, T., Yang, W., Yu, X. and Guo, K. (2010) 'Effects of planting system on soil and water conservation and crop output value in a sloping land of southwest China.', *Journal of Applied Ecology*, 21, pp. 1461-1467.
- 200 Xie, S., Zeng, J., Yang, J. and Yan, F. (2010) 'Effects of different tillage measures on soil and water conservation in slope farmland of red soil in Southern China', *Transactions of the Chinese Society of Agricultural Engineering*, 26, pp. 81-86.
- 201 Xie, T., Xie, S., Zhao, L. and Yang, A. (2015) 'Experiment of planting effect on ridge hayrick field in sloping farmland of red soil and low hilly land', *Journal of Water Resources Planning and Management*, 26, pp. 220-224.
- 202 Xu, Q., Wang, T., Li, Z., Cai, C., Shi, Z. and Jiang, C. (2010) 'Effect of soil conservation measurements on runoff, erosion and plant production: a case study on steep lands from the Three Gorges Area, China', *Journal of Food, Agriculture and Environment*, 8, pp. 980-984.
- 203 Xue, Y., Li, Y., Wang, Z. and Fan, M. (2011) 'Effect of straw mat mulch on soil and water loss of slope arable land and seed yield', *Chinese Agricultural Science Bulletin*, 27, pp. 192-198.
- 204 Yan, L., Hou, Q., Wang, F. and Mu, X. (2013) 'Effectiveness of soil and water conservation practices in runoff control on slope lands in loess plateau', *Bulletin of Soil and Water Conservation*, 33, pp. 213-217.
- 205 Yang, J., Mo, M., Song, Y. and Chen, X. (2012) 'Hydro-ecological effects of citrus land under vegetation measures of soil and water conservation in red-soil slope', *Resource and Environment in the Yangtze Basin*, 21, pp. 994-999.
- 206 Yao, Y., Wu, Q., Li, Z., Deng, Z., Jiang, M., Rang, Y., Meng, Y. and Wang, S. (2006) 'Study of the technical measures and ecological benefits of terracing sloping tea gardens', *Journal of Southwest University Natural Science*, 28, pp. 606-609.
- 207 Yin, D., Tang, H., Zhu, Q., Li, Y., Li, D. and Liang, D. (2001) 'Research on alley cropping technology integrated terracing slope land', *Journal of Soil and Water Conservation*, 15, pp. 84-87.
- 208 You, Z. (2003) 'The overland flow in different soil plough measures of *Dendrocalamus latiflorus* planted on hilly country', *Journal of Fujian College of Forestry*, 23, pp. 119-123.
- 209 Yu, D., Dai, Q., Wang, Q. and Xiao, B. (2010) 'Effects of contour grass hedges on soil and water losses of sloping cropland in Beijing', *Transactions of the Chinese Society of Agricultural Engineering*, 26(12), pp. 89-96.
- 210 Yuan, D., Wang, Z., Chen, X., Guo, X. and Zhang, R. (2001) 'Properties of soil and water loss from slope field in red soil in different farming systems', *Journal of Soil and Water Conservation*, 15, pp. 66-69.
- 211 Yue, H. (2008) 'Analysis on the impacts and the ecological benefits of different conservation measures to vegetation growth on the serious eroded mountain areas', *Subtropical Soil and Water Conservation*, 20, pp. 23-27.
- 212 Zhang, W., Zhang, X. and Zhidong, G. (2008a) 'Experimental study on the USLE model in granite gneiss region of Northern Jiangsu Province', *Subtropical Soil and Water Conservation*, 20, pp. 5-15.

- 213 Zhang, J. H., Su, Z. A. and Liu, G. C. (2008b) 'Effects of terracing and agroforestry on soil and water loss in hilly areas of the Sichuan Basin', *Journal of Mountain Science*, 5, pp. 241-248.
- 214 Zhang, P., Yan, L., Fan, J., Jiang, P., Wu, Y., Cai, L., Xu, H., Wang, X. and Wu, S. (2011) 'Effects of different patterns of contour grass hedgerow on soil erosion control', *Journal of Ecology and Rural Environment*, 27, pp. 29-34.
- 215 Zhang, S., Zhang, X., Liu, X., Liu, S. and Yu, T. (2009) 'Tillage effect on soil erosion in typical black soil region', *Journal of Soil and Water Conservation*, 33, pp. 11-15.
- 216 Zhang (2007) cited in Zhao, J., Yang, Z. and Govers, G. (2019) 'Soil and water conservation measures reduce soil and water losses in China but not down to background levels: Evidence from erosion plot data', *Geoderma*, 337, pp. 729-741.
- 217 Zhao, Y. and Wei, Y. (2009) 'Soil and water conservation effects of protective tillage measures on sloping farmland', *Journal of Soil and Water Conservation*, 7, pp. 86-90.
- 218 Zhao, T., Xie, Y., Jiang, Q., Zhang, H. and Zhou, W. (2011) 'Traditional control measures of soil erosion and their environmental effects on flow and sediment in the water source area of Beijing and Tianjin', *Journal of Soil and Water Conservation*, 9, pp. 32-37.
- 219 Zheng, W. and Zhang, C. (2006) 'Soil conservation benefit analysis for citrus orchard in the reservoir basin of three gorges', *Subtropical Soil and Water Conservation*, 18, pp. 15-18.
- 220 Zheng, H., Fang, S., Yang, J., Zhang, H., Wang, B. and Mo, M. (2012) 'Reduction effects of three garden types on runoff, sediment and nutrient loss in the red soil hilly region of China', *Journal of Food, Agriculture and Environment*, 3, pp. 1301-1307.
- 221 Zhou, J. (2007) 'Basic benefits from soil and water conservation in Sanchahe small watershed', *Bulletin of Soil and Water Conservation*, 27, p. 74.
- 222 Zhou, G., Tian, Y., Chen, G., Fu, Z. and Bao, W. (2009) 'Runoff and sediment yield on slope land in initial stages of conversion of cropland to forest in Northwestern Hunan Province', *Journal of Soil and Water Conservation*, 7, pp. 118-122.
- 223 Zhu (2010) cited in Zhao, J., Yang, Z. and Govers, G. (2019) 'Soil and water conservation measures reduce soil and water losses in China but not down to background levels: Evidence from erosion plot data', *Geoderma*, 337, pp. 729-741.
- 224 Zhuang, X. (2006) 'Analyzing the results of soil loss monitor of tea garden in Anxi county', *Subtropical Soil and Water Conservation*, 18, pp. 69-71.
- 225 Zuo, C., Hu, G. and Zhang, H. (2003) 'Study on soil and water erosion orderliness on sloping land of fourth century red soil', *Journal of Soil and Water Conservation*, 17, pp. 89-91.
- 226 Ciesiolka, C. A. A., Coughlan, K. J., Rose, C. W. and Smith, G. D. (1995) 'Erosion and hydrology of steeplands under commercial pineapple production', *Soil Technology*, 8, pp. 243-258.
- 227 Sombatpanit, S., Rose, C. W., Ciesiolka, C. A. and Coughlan, K. J. (1995) 'Soil and nutrient loss under Rozelle (*Hibiscus subdariffa* L. var. *altissima*) at Khon Kaen, Thailand', *Soil Technology*, 8, pp. 235-241.
- 228 Kothyari, B. P., Verma, P. K., Joshi, B. K. and Kothyari, U. C. (2004) 'Rainfall-runoff-soil and nutrient loss relationships for plot size areas of bhetagad watershed in Central Himalaya, India', *Journal of Hydrology*, 293, pp. 137-150.

- 229 Mitchell, H. W. (1965) 'Soil erosion losses in coffee', *Tanganyika coffee news*, pp. 135-155.
- 230 Roose, E. (1967) 'Importance relative de l'erosion, du drainage oblique et vertical dans la pedogenes actuelle d'un sol ferrallitique de Moyenne Cote D'Ivoire. Deux anneés de mesure sur parcelle experimentale', *Ser. pedol.*, 8(4), pp. 469-482.
- 231 Othieno, C. O. (1975) 'Surface run-off and soil erosion on fields of young tea', *Tropical Agriculture (Trinidad)*, 52(4), pp. 299-308.
- 232 Lal, R. (1976) 'Soil erosion on alfisols in Western Nigeria', *Geoderma*, 16, pp. 363-431.
- 233 Rhensburg, H. J. V. (1955) 'Runoff and soil erosion tests, Mpwapwa, central Tanganyika', *East African Agricultural Journal*, 20, pp. 228-231.
- 234 Hudson, N. W. and Jackson, D. C. (1959) 'Results achieved in the measurement of erosion and runoff in Southern Rhodesia', *Proceedings of the 3rd Inter-Afr. soil conference*. Dalaba, CCTA, pp. 573-583.
- 235 Haylett, D. G. (1960) 'Runoff and soil erosion studies at Pretoria', *South African Journal of Agricultural Science*, 3(3), pp. 379-394.
- 236 Rao, M. R., Ong, C. K., Pathak, P. and Sharma, M. M. (1991) 'Productivity of annual cropping and agroforestry systems on a shallow Alfisol in semi-arid India', *Agroforestry Systems*, 15, pp. 51-63.
- 237 Jirasuktaveekul, W., Sritulanon, C., Rungrojwanich, M. B. and Ploicharuen, P. (1998) *Soil and Water Losses in Reforestation Intercropped with Vetiver Strips at the Ping, Wang, Yom and Nan Sub-River Basins of Northern Thailand*. Bangkok, Thailand: Royal Forest Department.
- 238 Herweg, K. and Ludi, E. (1999) 'The performance of selected soil and water conservation measures- case studies from Ethiopia and Eritrea', *Catena*, 36, pp. 99-114.
- 239 Hashim, G. M. (2005) 'The influence of physical conditions on long-term soil productivity', in Teh, C., Zakaria, Z. Z., Ahmad, I., Ishak, C. F., Ahmed, O. H. and Daud, W. N. W. (2005) *Soils 2005 Conference: Advances in Soil System for Sustainable Food Production*. 12-13 April, Sg. Petani, Kedah, MSSS. pp. 121-124.
- 240 Coughlan, K. J. and Rose, C. W. (1997) 'Field Experimental Results- Runoff, Soil Loss and Crop Yield', in Coughlan, K. J. and Rose, C. W. (eds) *A New Soil Conservation Methodology and Application to Cropping Systems in Tropical Steeplands*. Canberra: Australian Centre for International Agricultural Research, pp. 9-23.

Appendix 5.1: Output from AMS for Rufford and Comer

Site	Catena Position	AMS ID	Latitude	Longitude	Elevation/p ressure. Meters or hPa	Shielding correction	¹⁰ Be concentration (atoms g ⁻¹)	Uncertainty in ¹⁰ Be concentration (atoms g ⁻¹)	Name of Be-10 standardization	²⁶ Al concentration (atoms g ⁻¹)	Uncertainty in ²⁶ Al concentration (atoms g ⁻¹)	Name of Al-26 standardization
Rufford	Summit	CNR01	53.1204	-1.0776693	98.692	0.9999999	35266	2364	NIST_27900	0	0	Z92-0222
Rufford	Summit	CNR02	53.1204	-1.0776693	98.692	0.9999999	22683	1586	NIST_27900	0	0	Z92-0222
Rufford	Shoulder	CNR03	53.11989	-1.0776654	99.275	0.9999991	54380	2030	NIST_27900	0	0	Z92-0222
Rufford	Shoulder	CNR04	53.11989	-1.0776654	99.275	0.9999991	30064	1850	NIST_27900	0	0	Z92-0222
Rufford	Backslope	CNR05	53.11954	-1.0776727	97.893	0.9999904	45603	1833	NIST_27900	0	0	Z92-0222
Rufford	Backslope	CNR06	53.11954	-1.0776727	97.893	0.9999904	28876	1661	NIST_27900	0	0	Z92-0222
Rufford	Toeslope	CNR07	53.11905	-1.0776833	95.707	0.99998338	32738	2006	NIST_27900	0	0	Z92-0222
Rufford	Toeslope	CNR08	53.11905	-1.0776833	95.707	0.99998338	25237	1562	NIST_27900	0	0	Z92-0222
Comer	Summit	CNR09	52.50954	-2.3789442	70.545	0.9999715	24507	1696	NIST_27900	0	0	Z92-0222
Comer	Shoulder	CNR10	52.50816	-2.3791828	65.318	0.9999713	24811	1333	NIST_27900	0	0	Z92-0222
Comer	Backslope	CNR11	52.50795	-2.3791515	58.93	0.996952	31263	2035	NIST_27900	0	0	Z92-0222
Comer	Toeslope	CNR12	52.50766	-2.3788101	50.099	0.99859266	41276	1522	NIST_27900	0	0	Z92-0222

C.2.1.1.3.I	Comer	10/08/2017	Summit	74881	90246	77	Soil	45	
C.2.1.1.3.J	Comer	10/08/2017	Summit	74881	90246	77	Soil	50	
C.2.1.1.3.K	Comer	10/08/2017	Summit	74881	90246	77	Soil	55	
C.2.1.1.3.L	Comer	10/08/2017	Summit	74881	90246	77	Soil	60	
C.2.1.1.3.M	Comer	10/08/2017	Summit	74881	90246	77	Soil	65	
C.2.1.1.3.N	Comer	10/08/2017	Summit	74881	90246	77	Soil	70	
C.2.1.1.3.O	Comer	10/08/2017	Summit	74881	90246	77	Soil	75	
C.2.1.1.3.P	Comer	10/08/2017	Summit	74881	90246	77	Soil	80	
C.2.1.1.3.Q	Comer	10/08/2017	Summit	74881	90246	77	Soil	85	
C.2.1.1.3.R	Comer	10/08/2017	Summit	74881	90246	77	Soil	90	
C.2.1.1.3.S	Comer	10/08/2017	Summit	74881	90246	77	Soil	95	
C.2.1.1.3.T	Comer	10/08/2017	Summit	74881	90246	77	Soil	100	
C.2.1.1.3.U	Comer	10/08/2017	Summit	74881	90246	77	Soil	105	
C.2.1.1.3.V	Comer	10/08/2017	Summit	74881	90246	77	Soil	110	
C.2.1.1.3.W	Comer	10/08/2017	Summit	74881	90246	77	Soil	115	
C.2.1.1.3.X	Comer	10/08/2017	Summit	74881	90246	77	Soil	120	
C.2.1.1.3.Y	Comer	10/08/2017	Summit	74881	90246	77	Soil	125	
C.2.1.1.3.Z	Comer	10/08/2017	Summit	74881	90246	77	Soil	130	
C.2.1.1.3.AA	Comer	10/08/2017	Summit	74881	90246	77	Soil	135	
C.2.1.1.3.AB	Comer	10/08/2017	Summit	74881	90246	77	Soil	140	
C.2.1.1.3.AC	Comer	10/08/2017	Summit	74881	90246	77	Soil	145	
C.2.1.1.3.AD	Comer	10/08/2017	Summit	74881	90246	77	Soil	150	
C.2.2.1.1.A	Comer	10/08/2017	Summit	74881	90246	77	Soil	20	1.35
C.2.2.1.1.B	Comer	10/08/2017	Summit	74881	90246	77	Soil	40	1.28
C.2.2.1.1.C	Comer	10/08/2017	Summit	74881	90246	77	Soil	60	1.56
C.2.2.1.1.D	Comer	10/08/2017	Summit	74881	90246	77	Soil	80	1.56
C.2.2.1.1.E	Comer	10/08/2017	Summit	74881	90246	77	Soil	100	1.55
C.1.1.1	Comer	10/08/2017	Summit	74881	90246	77	Saprolite	150	

Appendix 6.1: Output from AMS for Hilton and Woburn

Site	Catena Position	AMS ID	Latitude	Longitude	Shielding correction	¹⁰ Be concentration (atoms g ⁻¹)	Uncertainty in ¹⁰ Be concentration (atoms g ⁻¹)	Name of Be-10 standardization
Woburn	Summit	CRN_1	52.01265	-0.590347	0.999993	38324	2081	NIST_27900
Woburn	Summit	CRN_2	52.01265	-0.590347	0.999993			NIST_27900
Woburn	Shoulder	CRN_3	52.01249	-0.590342	0.999882	27931	2215	NIST_27900
Woburn	Shoulder	CRN_4	52.01249	-0.590342	0.999882	18129	1710	NIST_27900
Woburn	Backslope	CRN_5	52.01224	-0.590299	0.999952	21863	1553	NIST_27900
Woburn	Backslope	CRN_6	52.01224	-0.590299	0.999952	20488	1695	NIST_27900
Woburn	Toeslope	CRN_7	52.01182	-0.590253	1	49291	2592	NIST_27900
Woburn	Toeslope	CRN_8	52.01182	-0.590253	1	27384	4009	NIST_27900
Hilton	Summit	CRN_9	52.55159	-2.323442	0.999753	26958	1933	NIST_27900
Hilton	Summit	CRN_10	52.55159	-2.323442	0.999753	24110	2637	NIST_27900
Hilton	Shoulder	CRN_11	52.55156	-2.323781	0.998285	15983	1525	NIST_27900
Hilton	Shoulder	CRN_12	52.55156	-2.323781	0.998285	15878	1541	NIST_27900
Hilton	Backslope	CRN_13	52.55152	-2.324105	0.998391	32121	2373	NIST_27901
Hilton	Backslope	CRN_14	52.55152	-2.324105	0.998391	22656	1797	NIST_27902
Hilton	Toeslope	CRN_15	52.55147	-2.324557	0.999995	35605	5203	NIST_27903
Hilton	Toeslope	CRN_16	52.55147	-2.324557	0.999995	22512	1564	NIST_27904

Appendix 6.3: Soil Production Function analysis

Site / Paper	Mean Soil Formation Rate (mm/y)	Mean Depth (m)	Formation Rate at Zero Soil Thickness (mm/y)	Gamma
Hilton	0.128430138	0.89125	0.164	3.00142
Woburn	0.099671671	1.031429	0.229	1.14674
Comer	0.045917153	1	0.076	1.86897
Rufford	0.037194872	1.175	0.058	2.5039
Heimsath et al. 1997	0.034777778	0.393333	0.068	0.53654
Heimsath et al. 1999	0.117050667	0.565167	0.2	0.95969
Wilkinson et al. 2005	0.012233333	0.452222	0.02	1.53374

Appendix 6.4: Particle Size Analysis for Sapolite at Hilton and Woburn

Site	Catena Position	Sampling Position	Particle Bin Size (µm)	Run 1 (%)	Run 2 (%)	Run 3 (%)	Mean (%)	Std Dev (%)
Woburn	Summit	Soil-Sap Interface	0.375124	0.009521	0.00882	0.01009	0.00948	0.00063
Woburn	Summit	Soil-Sap Interface	0.411798	0.018164	0.01683	0.01926	0.01809	0.00121
Woburn	Summit	Soil-Sap Interface	0.452057	0.030576	0.02833	0.03243	0.03044	0.00205
Woburn	Summit	Soil-Sap Interface	0.496252	0.042254	0.03913	0.04483	0.04207	0.00285
Woburn	Summit	Soil-Sap Interface	0.544768	0.053286	0.04932	0.05657	0.05306	0.00363
Woburn	Summit	Soil-Sap Interface	0.598027	0.063501	0.05872	0.06746	0.06323	0.00437
Woburn	Summit	Soil-Sap Interface	0.656493	0.072715	0.06718	0.07731	0.0724	0.00507
Woburn	Summit	Soil-Sap Interface	0.720675	0.080703	0.07448	0.08589	0.08036	0.00571
Woburn	Summit	Soil-Sap Interface	0.791132	0.087238	0.08041	0.09295	0.08687	0.00628
Woburn	Summit	Soil-Sap Interface	0.868477	0.092084	0.08476	0.09823	0.09169	0.00675
Woburn	Summit	Soil-Sap Interface	0.953383	0.095014	0.08732	0.10149	0.09461	0.0071
Woburn	Summit	Soil-Sap Interface	1.04659	0.095833	0.08792	0.1025	0.09542	0.0073
Woburn	Summit	Soil-Sap Interface	1.14891	0.094576	0.08662	0.10129	0.09416	0.00734
Woburn	Summit	Soil-Sap Interface	1.26123	0.091379	0.08355	0.09799	0.09097	0.00723
Woburn	Summit	Soil-Sap Interface	1.38454	0.086486	0.07895	0.09284	0.08609	0.00695
Woburn	Summit	Soil-Sap Interface	1.5199	0.080271	0.07316	0.08622	0.07989	0.00654
Woburn	Summit	Soil-Sap Interface	1.66849	0.073236	0.06666	0.07869	0.07286	0.00602
Woburn	Summit	Soil-Sap Interface	1.83161	0.066005	0.06001	0.0709	0.06564	0.00546
Woburn	Summit	Soil-Sap Interface	2.01068	0.059279	0.05383	0.06363	0.05891	0.00491
Woburn	Summit	Soil-Sap Interface	2.20725	0.053776	0.04877	0.05767	0.0534	0.00446
Woburn	Summit	Soil-Sap Interface	2.42304	0.050137	0.04538	0.05373	0.04975	0.00419
Woburn	Summit	Soil-Sap Interface	2.65993	0.048826	0.04408	0.05235	0.04842	0.00415
Woburn	Summit	Soil-Sap Interface	2.91998	0.050058	0.04505	0.05376	0.04962	0.00437
Woburn	Summit	Soil-Sap Interface	3.20545	0.053746	0.0482	0.05786	0.05327	0.00485
Woburn	Summit	Soil-Sap Interface	3.51883	0.059492	0.0532	0.06423	0.05897	0.00553
Woburn	Summit	Soil-Sap Interface	3.86284	0.066625	0.05946	0.07209	0.06606	0.00633
Woburn	Summit	Soil-Sap Interface	4.24049	0.074321	0.06627	0.08052	0.0737	0.00714
Woburn	Summit	Soil-Sap Interface	4.65506	0.081757	0.07292	0.08859	0.08109	0.00786
Woburn	Summit	Soil-Sap Interface	5.11017	0.088274	0.07885	0.09558	0.08757	0.00838
Woburn	Summit	Soil-Sap Interface	5.60976	0.093492	0.08373	0.10104	0.09275	0.00868
Woburn	Summit	Soil-Sap Interface	6.1582	0.097354	0.08748	0.10494	0.09659	0.00876
Woburn	Summit	Soil-Sap Interface	6.76025	0.100114	0.09033	0.10757	0.09934	0.00864
Woburn	Summit	Soil-Sap Interface	7.42117	0.102227	0.09267	0.10943	0.10144	0.00841
Woburn	Summit	Soil-Sap Interface	8.14669	0.104378	0.09509	0.11128	0.10358	0.00813
Woburn	Summit	Soil-Sap Interface	8.94315	0.107474	0.09838	0.11413	0.10666	0.00791
Woburn	Summit	Soil-Sap Interface	9.81748	0.112562	0.10347	0.11912	0.11172	0.00786
Woburn	Summit	Soil-Sap Interface	10.7773	0.120724	0.11136	0.12743	0.11984	0.00807
Woburn	Summit	Soil-Sap Interface	11.8309	0.132782	0.12282	0.13994	0.13185	0.0086
Woburn	Summit	Soil-Sap Interface	12.9876	0.148993	0.13817	0.15691	0.14802	0.00941
Woburn	Summit	Soil-Sap Interface	14.2573	0.168709	0.15694	0.17759	0.16774	0.01036
Woburn	Summit	Soil-Sap Interface	15.6512	0.190306	0.17778	0.20013	0.18941	0.01121
Woburn	Summit	Soil-Sap Interface	17.1813	0.211326	0.19858	0.22176	0.21056	0.01161
Woburn	Summit	Soil-Sap Interface	18.861	0.229025	0.21688	0.23935	0.22842	0.01125
Woburn	Summit	Soil-Sap Interface	20.705	0.24149	0.23086	0.25073	0.24103	0.00994
Woburn	Summit	Soil-Sap Interface	22.7292	0.248409	0.24001	0.25557	0.248	0.00779
Woburn	Summit	Soil-Sap Interface	24.9513	0.251515	0.24565	0.25597	0.25104	0.00518
Woburn	Summit	Soil-Sap Interface	27.3906	0.254051	0.25061	0.25585	0.2535	0.00267
Woburn	Summit	Soil-Sap Interface	30.0685	0.2592	0.25783	0.25913	0.25872	0.00077
Woburn	Summit	Soil-Sap Interface	33.0081	0.267997	0.26845	0.26727	0.2679	0.0006
Woburn	Summit	Soil-Sap Interface	36.2352	0.27715	0.27961	0.27661	0.27779	0.0016
Woburn	Summit	Soil-Sap Interface	39.7777	0.280291	0.28532	0.27971	0.28177	0.00309
Woburn	Summit	Soil-Sap Interface	43.6665	0.273773	0.28159	0.27198	0.27578	0.00511
Woburn	Summit	Soil-Sap Interface	47.9356	0.260992	0.2707	0.25695	0.26288	0.00707
Woburn	Summit	Soil-Sap Interface	52.622	0.250922	0.26065	0.24472	0.2521	0.00803
Woburn	Summit	Soil-Sap Interface	57.7666	0.252911	0.2611	0.24565	0.25322	0.00773
Woburn	Summit	Soil-Sap Interface	63.4141	0.27004	0.27694	0.26248	0.26982	0.00723
Woburn	Summit	Soil-Sap Interface	69.6138	0.29736	0.30515	0.28875	0.29709	0.0082
Woburn	Summit	Soil-Sap Interface	76.4196	0.331351	0.34141	0.32065	0.33114	0.01038
Woburn	Summit	Soil-Sap Interface	83.8907	0.375704	0.38529	0.36422	0.37507	0.01055
Woburn	Summit	Soil-Sap Interface	92.0923	0.429863	0.43321	0.42122	0.4281	0.00619
Woburn	Summit	Soil-Sap Interface	101.096	0.487288	0.48141	0.48411	0.48427	0.00294
Woburn	Summit	Soil-Sap Interface	110.979	0.569273	0.5581	0.57015	0.56584	0.00672
Woburn	Summit	Soil-Sap Interface	121.829	0.763589	0.75495	0.7639	0.76081	0.00508
Woburn	Summit	Soil-Sap Interface	133.74	1.22707	1.22665	1.22219	1.2253	0.0027
Woburn	Summit	Soil-Sap Interface	146.815	2.13478	2.14099	2.12384	2.1332	0.00868
Woburn	Summit	Soil-Sap Interface	161.168	3.56234	3.56476	3.55028	3.55913	0.00776

Woburn	Summit	Soil-Sap Interface	176.925	5.38962	5.37568	5.3849	5.3834	0.00709
Woburn	Summit	Soil-Sap Interface	194.222	7.29704	7.26204	7.30576	7.28828	0.02314
Woburn	Summit	Soil-Sap Interface	213.21	8.84454	8.79711	8.86165	8.83443	0.03344
Woburn	Summit	Soil-Sap Interface	234.054	9.63717	9.59446	9.64461	9.62541	0.02706
Woburn	Summit	Soil-Sap Interface	256.936	9.5006	9.47777	9.47987	9.48608	0.01262
Woburn	Summit	Soil-Sap Interface	282.056	8.54624	8.54886	8.49581	8.5303	0.0299
Woburn	Summit	Soil-Sap Interface	309.631	7.10468	7.12826	7.04867	7.09387	0.04088
Woburn	Summit	Soil-Sap Interface	339.902	5.57852	5.61459	5.55877	5.58396	0.0283
Woburn	Summit	Soil-Sap Interface	373.132	4.28348	4.32765	4.33684	4.31599	0.02853
Woburn	Summit	Soil-Sap Interface	409.611	3.35367	3.40818	3.49042	3.41742	0.06884
Woburn	Summit	Soil-Sap Interface	449.657	2.75017	2.81742	2.94359	2.83706	0.09819
Woburn	Summit	Soil-Sap Interface	493.617	2.3392	2.41182	2.52756	2.42619	0.095
Woburn	Summit	Soil-Sap Interface	541.876	1.98502	2.04093	2.09173	2.03923	0.05338
Woburn	Summit	Soil-Sap Interface	594.852	1.61797	1.62843	1.59101	1.61247	0.01931
Woburn	Summit	Soil-Sap Interface	653.008	1.241	1.19103	1.09045	1.17416	0.07668
Woburn	Summit	Soil-Sap Interface	716.849	0.890234	0.79638	0.68904	0.79189	0.10067
Woburn	Summit	Soil-Sap Interface	786.932	0.606324	0.50795	0.44746	0.52058	0.08018
Woburn	Summit	Soil-Sap Interface	863.866	0.406798	0.33772	0.34938	0.36463	0.03698
Woburn	Summit	Soil-Sap Interface	948.322	0.264545	0.24649	0.30918	0.27341	0.03227
Woburn	Summit	Soil-Sap Interface	1041.03	0.157714	0.19281	0.25627	0.20226	0.04995
Woburn	Summit	Soil-Sap Interface	1142.81	0.107549	0.1758	0.20468	0.16268	0.04988
Woburn	Summit	Soil-Sap Interface	1254.54	0.108028	0.19486	0.15867	0.15385	0.04362
Woburn	Summit	Soil-Sap Interface	1377.19	0.119846	0.20906	0.09722	0.14204	0.05913
Woburn	Summit	Soil-Sap Interface	1511.83	0.141808	0.22015	0.04388	0.13528	0.08832
Woburn	Summit	Soil-Sap Interface	1659.63	0.166669	0.21285	0.01221	0.13058	0.10508
Woburn	Summit	Soil-Sap Interface	1821.88	0.155586	0.15865	0.00089	0.10504	0.09021
Woburn	Summit	~30 cm below interface	0.375124	0.022967	0.02893	0.03175	0.02788	0.00449
Woburn	Summit	~30 cm below interface	0.411798	0.043865	0.05532	0.06076	0.05332	0.00863
Woburn	Summit	~30 cm below interface	0.452057	0.074012	0.09365	0.10297	0.09021	0.01478
Woburn	Summit	~30 cm below interface	0.496252	0.102646	0.1305	0.14374	0.12563	0.02098
Woburn	Summit	~30 cm below interface	0.544768	0.130067	0.16641	0.18371	0.16006	0.02738
Woburn	Summit	~30 cm below interface	0.598027	0.155948	0.2011	0.2226	0.19321	0.03402
Woburn	Summit	~30 cm below interface	0.656493	0.179917	0.23418	0.26004	0.22471	0.04089
Woburn	Summit	~30 cm below interface	0.720675	0.20147	0.26505	0.29537	0.25396	0.04792
Woburn	Summit	~30 cm below interface	0.791132	0.22007	0.293	0.32777	0.28028	0.05497
Woburn	Summit	~30 cm below interface	0.868477	0.235098	0.31709	0.35616	0.30278	0.06179
Woburn	Summit	~30 cm below interface	0.953383	0.245905	0.33622	0.37921	0.32044	0.06804
Woburn	Summit	~30 cm below interface	1.04659	0.25184	0.34915	0.39533	0.33211	0.07325
Woburn	Summit	~30 cm below interface	1.14891	0.252722	0.35509	0.40348	0.33709	0.07697
Woburn	Summit	~30 cm below interface	1.26123	0.248601	0.35353	0.40283	0.33499	0.07877
Woburn	Summit	~30 cm below interface	1.38454	0.239778	0.3443	0.393	0.32569	0.07829
Woburn	Summit	~30 cm below interface	1.5199	0.226937	0.32786	0.37434	0.30971	0.07536
Woburn	Summit	~30 cm below interface	1.66849	0.211159	0.30542	0.34815	0.28824	0.07009
Woburn	Summit	~30 cm below interface	1.83161	0.193988	0.27916	0.31697	0.26337	0.06299
Woburn	Summit	~30 cm below interface	2.01068	0.177339	0.25217	0.28454	0.23802	0.05498
Woburn	Summit	~30 cm below interface	2.20725	0.163368	0.22832	0.25559	0.21576	0.04737
Woburn	Summit	~30 cm below interface	2.42304	0.154168	0.21164	0.23519	0.20033	0.04168
Woburn	Summit	~30 cm below interface	2.65993	0.151421	0.20566	0.22775	0.19495	0.03928
Woburn	Summit	~30 cm below interface	2.91998	0.15606	0.21259	0.23602	0.20156	0.04111
Woburn	Summit	~30 cm below interface	3.20545	0.167968	0.23258	0.26015	0.22023	0.04732
Woburn	Summit	~30 cm below interface	3.51883	0.185916	0.26349	0.29729	0.2489	0.0571
Woburn	Summit	~30 cm below interface	3.86284	0.207656	0.30085	0.34165	0.28338	0.06868
Woburn	Summit	~30 cm below interface	4.24049	0.230402	0.33896	0.38588	0.31841	0.07975
Woburn	Summit	~30 cm below interface	4.65506	0.251513	0.37235	0.42315	0.349	0.08817
Woburn	Summit	~30 cm below interface	5.11017	0.269118	0.39738	0.44922	0.3719	0.09271
Woburn	Summit	~30 cm below interface	5.60976	0.282642	0.41326	0.46372	0.38654	0.09345
Woburn	Summit	~30 cm below interface	6.1582	0.292764	0.42206	0.47	0.39494	0.09168
Woburn	Summit	~30 cm below interface	6.76025	0.301326	0.42798	0.47403	0.40111	0.08943
Woburn	Summit	~30 cm below interface	7.42117	0.310726	0.43596	0.48227	0.40965	0.08874
Woburn	Summit	~30 cm below interface	8.14669	0.324012	0.45123	0.50082	0.42535	0.0912
Woburn	Summit	~30 cm below interface	8.94315	0.344467	0.47827	0.53369	0.45214	0.09728
Woburn	Summit	~30 cm below interface	9.81748	0.375339	0.52059	0.58271	0.49288	0.10643
Woburn	Summit	~30 cm below interface	10.7773	0.419648	0.58068	0.64815	0.54949	0.1174
Woburn	Summit	~30 cm below interface	11.8309	0.478575	0.65847	0.72783	0.62163	0.12865
Woburn	Summit	~30 cm below interface	12.9876	0.55138	0.75176	0.81935	0.7075	0.13936
Woburn	Summit	~30 cm below interface	14.2573	0.635037	0.8566	0.92117	0.80427	0.15007
Woburn	Summit	~30 cm below interface	15.6512	0.725859	0.97019	1.03545	0.9105	0.1632
Woburn	Summit	~30 cm below interface	17.1813	0.819397	1.08776	1.16016	1.02244	0.17953
Woburn	Summit	~30 cm below interface	18.861	0.91061	1.20051	1.28274	1.13129	0.19548
Woburn	Summit	~30 cm below interface	20.705	0.997526	1.30188	1.38828	1.22923	0.20526

Woburn	Summit	~30 cm below interface	22.7292	1.08022	1.39008	1.46793	1.31274	0.2051
Woburn	Summit	~30 cm below interface	24.9513	1.16452	1.4759	1.53622	1.39221	0.19948
Woburn	Summit	~30 cm below interface	27.3906	1.26206	1.57657	1.61996	1.4862	0.19532
Woburn	Summit	~30 cm below interface	30.0685	1.38371	1.71081	1.74375	1.61276	0.19904
Woburn	Summit	~30 cm below interface	33.0081	1.53055	1.88697	1.91634	1.77795	0.21476
Woburn	Summit	~30 cm below interface	36.2352	1.67717	2.05188	2.07218	1.93374	0.22243
Woburn	Summit	~30 cm below interface	39.7777	1.78473	2.12406	2.11534	2.00804	0.19344
Woburn	Summit	~30 cm below interface	43.6665	1.83942	2.09889	2.04714	1.99515	0.13733
Woburn	Summit	~30 cm below interface	47.9356	1.85473	2.03446	1.94056	1.94325	0.0899
Woburn	Summit	~30 cm below interface	52.622	1.85684	1.98897	1.86452	1.90344	0.07417
Woburn	Summit	~30 cm below interface	57.7666	1.87462	1.9997	1.86502	1.91311	0.07514
Woburn	Summit	~30 cm below interface	63.4141	1.89993	2.03439	1.89299	1.94244	0.07971
Woburn	Summit	~30 cm below interface	69.6138	1.89668	1.9781	1.78707	1.88728	0.09586
Woburn	Summit	~30 cm below interface	76.4196	1.88983	1.86192	1.59891	1.78355	0.16051
Woburn	Summit	~30 cm below interface	83.8907	1.94768	1.92519	1.65337	1.84208	0.16381
Woburn	Summit	~30 cm below interface	92.0923	2.01325	2.14898	1.97637	2.0462	0.0909
Woburn	Summit	~30 cm below interface	101.096	1.86862	2.08713	2.06627	2.00734	0.12059
Woburn	Summit	~30 cm below interface	110.979	1.39988	1.74129	1.72696	1.62271	0.19311
Woburn	Summit	~30 cm below interface	121.829	1.17467	1.95571	1.72689	1.61909	0.40152
Woburn	Summit	~30 cm below interface	133.74	2.23612	3.94548	3.44245	3.20802	0.87846
Woburn	Summit	~30 cm below interface	146.815	5.71874	9.01639	8.70317	7.81277	1.82023
Woburn	Summit	~30 cm below interface	161.168	11.1653	14.6436	14.9137	13.5742	2.09054
Woburn	Summit	~30 cm below interface	176.925	15.8169	13.1944	13.3834	14.1316	1.4626
Woburn	Summit	~30 cm below interface	194.222	14.4317	4.77136	4.7182	7.97375	5.59281
Woburn	Summit	~30 cm below interface	213.21	5.66392	0.34866	0.33629	2.11629	3.07234
Woburn	Summit	~30 cm below interface	234.054	0.447004	0	0	0.149	0.25808
Woburn	Summit	~30 cm below interface	256.936	0	0	0	0	0
Woburn	Summit	~30 cm below interface	282.056	0	0	0	0	0
Woburn	Summit	~30 cm below interface	309.631	0	0	0	0	0
Woburn	Summit	~30 cm below interface	339.902	0	0	0	0	0
Woburn	Summit	~30 cm below interface	373.132	0	0	0	0	0
Woburn	Summit	~30 cm below interface	409.611	0	0	0	0	0
Woburn	Summit	~30 cm below interface	449.657	0	0	0	0	0
Woburn	Summit	~30 cm below interface	493.617	0	0	0	0	0
Woburn	Summit	~30 cm below interface	541.876	0	0	0	0	0
Woburn	Summit	~30 cm below interface	594.852	0	0	0	0	0
Woburn	Summit	~30 cm below interface	653.008	0	0	0	0	0
Woburn	Summit	~30 cm below interface	716.849	0	0	0	0	0
Woburn	Summit	~30 cm below interface	786.932	0	0	0	0	0
Woburn	Summit	~30 cm below interface	863.866	0	0	0	0	0
Woburn	Summit	~30 cm below interface	948.322	0	0	0	0	0
Woburn	Summit	~30 cm below interface	1041.03	0	0	0	0	0
Woburn	Summit	~30 cm below interface	1142.81	0	0	0	0	0
Woburn	Summit	~30 cm below interface	1254.54	0	0	0	0	0
Woburn	Summit	~30 cm below interface	1377.19	0	0	0	0	0
Woburn	Summit	~30 cm below interface	1511.83	0	0	0	0	0
Woburn	Summit	~30 cm below interface	1659.63	0	0	0	0	0
Woburn	Summit	~30 cm below interface	1821.88	0	0	0	0	0
Woburn	Shoulder	Soil-Sap Interface	0.375124	0.009019	0.00822	0.00894	0.00872	0.00044
Woburn	Shoulder	Soil-Sap Interface	0.411798	0.017217	0.01477	0.01606	0.01602	0.00122
Woburn	Shoulder	Soil-Sap Interface	0.452057	0.029017	0.02205	0.02397	0.02501	0.0036
Woburn	Shoulder	Soil-Sap Interface	0.496252	0.040175	0.03175	0.0345	0.03548	0.0043
Woburn	Shoulder	Soil-Sap Interface	0.544768	0.050793	0.03977	0.04322	0.0446	0.00564
Woburn	Shoulder	Soil-Sap Interface	0.598027	0.060727	0.04727	0.05137	0.05312	0.0069
Woburn	Shoulder	Soil-Sap Interface	0.656493	0.06982	0.05447	0.05918	0.06116	0.00786
Woburn	Shoulder	Soil-Sap Interface	0.720675	0.077869	0.06182	0.06714	0.06894	0.00818
Woburn	Shoulder	Soil-Sap Interface	0.791132	0.084667	0.06791	0.07376	0.07545	0.0085
Woburn	Shoulder	Soil-Sap Interface	0.868477	0.089986	0.07325	0.07954	0.08093	0.00845
Woburn	Shoulder	Soil-Sap Interface	0.953383	0.0936	0.07787	0.08453	0.08533	0.0079
Woburn	Shoulder	Soil-Sap Interface	1.04659	0.0953	0.08192	0.08889	0.0887	0.00669
Woburn	Shoulder	Soil-Sap Interface	1.14891	0.095076	0.08492	0.09213	0.09071	0.00523
Woburn	Shoulder	Soil-Sap Interface	1.26123	0.093013	0.087	0.09438	0.09146	0.00392
Woburn	Shoulder	Soil-Sap Interface	1.38454	0.089298	0.08836	0.09584	0.09116	0.00407
Woburn	Shoulder	Soil-Sap Interface	1.5199	0.08425	0.08916	0.09669	0.09003	0.00627
Woburn	Shoulder	Soil-Sap Interface	1.66849	0.078325	0.0895	0.09708	0.0883	0.00944
Woburn	Shoulder	Soil-Sap Interface	1.83161	0.07212	0.08937	0.09698	0.08616	0.01274
Woburn	Shoulder	Soil-Sap Interface	2.01068	0.06633	0.08899	0.09663	0.08398	0.01576
Woburn	Shoulder	Soil-Sap Interface	2.20725	0.061698	0.08853	0.09621	0.08215	0.01812
Woburn	Shoulder	Soil-Sap Interface	2.42304	0.058902	0.08831	0.09608	0.0811	0.01961
Woburn	Shoulder	Soil-Sap Interface	2.65993	0.058465	0.08833	0.09624	0.08101	0.01992

Woburn	Shoulder	Soil-Sap Interface	2.91998	0.060639	0.08872	0.09683	0.08206	0.01899
Woburn	Shoulder	Soil-Sap Interface	3.20545	0.065345	0.08959	0.09793	0.08429	0.01693
Woburn	Shoulder	Soil-Sap Interface	3.51883	0.072144	0.09111	0.09976	0.08767	0.01412
Woburn	Shoulder	Soil-Sap Interface	3.86284	0.080282	0.09328	0.10227	0.09194	0.01105
Woburn	Shoulder	Soil-Sap Interface	4.24049	0.088826	0.09611	0.10548	0.09681	0.00835
Woburn	Shoulder	Soil-Sap Interface	4.65506	0.096846	0.09961	0.10938	0.10195	0.00659
Woburn	Shoulder	Soil-Sap Interface	5.11017	0.103615	0.10383	0.114	0.10715	0.00593
Woburn	Shoulder	Soil-Sap Interface	5.60976	0.108741	0.10875	0.11931	0.11227	0.0061
Woburn	Shoulder	Soil-Sap Interface	6.1582	0.112231	0.11444	0.12539	0.11735	0.00705
Woburn	Shoulder	Soil-Sap Interface	6.76025	0.114463	0.12092	0.13227	0.12255	0.00901
Woburn	Shoulder	Soil-Sap Interface	7.42117	0.11607	0.12832	0.14005	0.12815	0.01199
Woburn	Shoulder	Soil-Sap Interface	8.14669	0.117971	0.13682	0.1489	0.13456	0.01559
Woburn	Shoulder	Soil-Sap Interface	8.94315	0.121364	0.14673	0.15917	0.14242	0.01927
Woburn	Shoulder	Soil-Sap Interface	9.81748	0.127635	0.15839	0.17122	0.15241	0.0224
Woburn	Shoulder	Soil-Sap Interface	10.7773	0.138246	0.17219	0.18542	0.16528	0.02433
Woburn	Shoulder	Soil-Sap Interface	11.8309	0.154397	0.18848	0.20216	0.18168	0.0246
Woburn	Shoulder	Soil-Sap Interface	12.9876	0.176645	0.20762	0.22178	0.20201	0.02308
Woburn	Shoulder	Soil-Sap Interface	14.2573	0.204522	0.22992	0.24463	0.22636	0.02029
Woburn	Shoulder	Soil-Sap Interface	15.6512	0.236445	0.25554	0.27086	0.25428	0.01724
Woburn	Shoulder	Soil-Sap Interface	17.1813	0.269953	0.28449	0.30046	0.28497	0.01526
Woburn	Shoulder	Soil-Sap Interface	18.861	0.302477	0.31634	0.3329	0.31724	0.01523
Woburn	Shoulder	Soil-Sap Interface	20.705	0.332717	0.35053	0.3675	0.35025	0.01739
Woburn	Shoulder	Soil-Sap Interface	22.7292	0.361444	0.38637	0.40346	0.38376	0.02113
Woburn	Shoulder	Soil-Sap Interface	24.9513	0.391689	0.42356	0.44039	0.41855	0.02473
Woburn	Shoulder	Soil-Sap Interface	27.3906	0.428	0.46234	0.47835	0.45623	0.02573
Woburn	Shoulder	Soil-Sap Interface	30.0685	0.474421	0.5034	0.51782	0.49855	0.0221
Woburn	Shoulder	Soil-Sap Interface	33.0081	0.531772	0.54758	0.55936	0.54624	0.01384
Woburn	Shoulder	Soil-Sap Interface	36.2352	0.594846	0.59509	0.603	0.59765	0.00464
Woburn	Shoulder	Soil-Sap Interface	39.7777	0.653855	0.64554	0.64841	0.64927	0.00422
Woburn	Shoulder	Soil-Sap Interface	43.6665	0.701969	0.69778	0.69491	0.69822	0.00355
Woburn	Shoulder	Soil-Sap Interface	47.9356	0.740927	0.74946	0.74102	0.7438	0.0049
Woburn	Shoulder	Soil-Sap Interface	52.622	0.779168	0.79555	0.78271	0.78581	0.00862
Woburn	Shoulder	Soil-Sap Interface	57.7666	0.825443	0.82716	0.81183	0.82148	0.0084
Woburn	Shoulder	Soil-Sap Interface	63.4141	0.879361	0.8335	0.81761	0.84349	0.03207
Woburn	Shoulder	Soil-Sap Interface	69.6138	0.929073	0.80748	0.792	0.84285	0.07507
Woburn	Shoulder	Soil-Sap Interface	76.4196	0.968194	0.75474	0.73909	0.82067	0.128
Woburn	Shoulder	Soil-Sap Interface	83.8907	1.00674	0.70012	0.68223	0.79636	0.18241
Woburn	Shoulder	Soil-Sap Interface	92.0923	1.05293	0.6856	0.6627	0.80041	0.21899
Woburn	Shoulder	Soil-Sap Interface	101.096	1.10339	0.76359	0.73278	0.86659	0.20565
Woburn	Shoulder	Soil-Sap Interface	110.979	1.17545	0.99415	0.95302	1.04087	0.11835
Woburn	Shoulder	Soil-Sap Interface	121.829	1.34694	1.44385	1.39215	1.39431	0.04849
Woburn	Shoulder	Soil-Sap Interface	133.74	1.7522	2.1624	2.10414	2.00625	0.22193
Woburn	Shoulder	Soil-Sap Interface	146.815	2.52863	3.15283	3.09645	2.92597	0.34526
Woburn	Shoulder	Soil-Sap Interface	161.168	3.73267	4.34945	4.30512	4.12908	0.34402
Woburn	Shoulder	Soil-Sap Interface	176.925	5.27406	5.62509	5.60071	5.49995	0.19601
Woburn	Shoulder	Soil-Sap Interface	194.222	6.90228	6.81	6.8078	6.84003	0.05392
Woburn	Shoulder	Soil-Sap Interface	213.21	8.24877	7.72985	7.74478	7.9078	0.29538
Woburn	Shoulder	Soil-Sap Interface	234.054	8.9607	8.24417	8.2661	8.49032	0.40751
Woburn	Shoulder	Soil-Sap Interface	256.936	8.86409	8.27694	8.29454	8.47852	0.33403
Woburn	Shoulder	Soil-Sap Interface	282.056	8.02757	7.83295	7.8381	7.89954	0.11091
Woburn	Shoulder	Soil-Sap Interface	309.631	6.70984	6.99141	6.9817	6.89432	0.15984
Woburn	Shoulder	Soil-Sap Interface	339.902	5.25149	5.88784	5.86654	5.66862	0.36141
Woburn	Shoulder	Soil-Sap Interface	373.132	3.95193	4.68042	4.65408	4.42881	0.4132
Woburn	Shoulder	Soil-Sap Interface	409.611	2.9711	3.51553	3.49056	3.32573	0.30737
Woburn	Shoulder	Soil-Sap Interface	449.657	2.30506	2.49398	2.47518	2.42474	0.10407
Woburn	Shoulder	Soil-Sap Interface	493.617	1.83159	1.66392	1.65281	1.71611	0.10017
Woburn	Shoulder	Soil-Sap Interface	541.876	1.40514	1.02848	1.02424	1.15262	0.2187
Woburn	Shoulder	Soil-Sap Interface	594.852	0.961757	0.56232	0.5656	0.69656	0.22967
Woburn	Shoulder	Soil-Sap Interface	653.008	0.527041	0.24495	0.25059	0.34086	0.16126
Woburn	Shoulder	Soil-Sap Interface	716.849	0.159761	0.07329	0.07776	0.1036	0.04869
Woburn	Shoulder	Soil-Sap Interface	786.932	0.01148	0.0114	0.01257	0.01182	0.00065
Woburn	Shoulder	Soil-Sap Interface	863.866	0	0.00065	0.00079	0.00048	0.00042
Woburn	Shoulder	Soil-Sap Interface	948.322	0	0	0	0	0
Woburn	Shoulder	Soil-Sap Interface	1041.03	0	0	0	0	0
Woburn	Shoulder	Soil-Sap Interface	1142.81	0	0	0	0	0
Woburn	Shoulder	Soil-Sap Interface	1254.54	0	0	0	0	0
Woburn	Shoulder	Soil-Sap Interface	1377.19	0	0	0	0	0
Woburn	Shoulder	Soil-Sap Interface	1511.83	0	0	0	0	0
Woburn	Shoulder	Soil-Sap Interface	1659.63	0	0	0	0	0
Woburn	Shoulder	Soil-Sap Interface	1821.88	0	0	0	0	0

Woburn	Shoulder	~30 cm below interface	0.375124	0.00758	0.0069	0.00768	0.00739	0.00042
Woburn	Shoulder	~30 cm below interface	0.411798	0.014474	0.01241	0.0138	0.01356	0.00105
Woburn	Shoulder	~30 cm below interface	0.452057	0.024409	0.01852	0.02059	0.02117	0.00299
Woburn	Shoulder	~30 cm below interface	0.496252	0.033825	0.02668	0.02966	0.03005	0.00359
Woburn	Shoulder	~30 cm below interface	0.544768	0.042817	0.03345	0.03719	0.03782	0.00472
Woburn	Shoulder	~30 cm below interface	0.598027	0.051269	0.0398	0.04426	0.04511	0.00578
Woburn	Shoulder	~30 cm below interface	0.656493	0.059056	0.04592	0.05107	0.05201	0.00662
Woburn	Shoulder	~30 cm below interface	0.720675	0.066011	0.05219	0.05805	0.05875	0.00693
Woburn	Shoulder	~30 cm below interface	0.791132	0.071959	0.05746	0.06393	0.06445	0.00726
Woburn	Shoulder	~30 cm below interface	0.868477	0.076704	0.06213	0.06915	0.06933	0.00729
Woburn	Shoulder	~30 cm below interface	0.953383	0.08005	0.06624	0.07376	0.07335	0.00691
Woburn	Shoulder	~30 cm below interface	1.04659	0.081807	0.06994	0.0779	0.07655	0.00605
Woburn	Shoulder	~30 cm below interface	1.14891	0.081951	0.07282	0.08117	0.07864	0.00506
Woburn	Shoulder	~30 cm below interface	1.26123	0.080534	0.07499	0.08366	0.07973	0.00439
Woburn	Shoulder	~30 cm below interface	1.38454	0.077697	0.0766	0.08555	0.07995	0.00488
Woburn	Shoulder	~30 cm below interface	1.5199	0.073699	0.07781	0.08699	0.0795	0.00681
Woburn	Shoulder	~30 cm below interface	1.66849	0.068922	0.07868	0.0881	0.07857	0.00959
Woburn	Shoulder	~30 cm below interface	1.83161	0.063876	0.07923	0.08887	0.07732	0.0126
Woburn	Shoulder	~30 cm below interface	2.01068	0.059166	0.0796	0.08946	0.07608	0.01545
Woburn	Shoulder	~30 cm below interface	2.20725	0.055446	0.07996	0.09006	0.07515	0.0178
Woburn	Shoulder	~30 cm below interface	2.42304	0.053323	0.08055	0.09093	0.07494	0.01942
Woburn	Shoulder	~30 cm below interface	2.65993	0.053268	0.08138	0.09209	0.07558	0.02005
Woburn	Shoulder	~30 cm below interface	2.91998	0.055524	0.08254	0.09364	0.07724	0.01961
Woburn	Shoulder	~30 cm below interface	3.20545	0.060045	0.08412	0.09564	0.07994	0.01816
Woburn	Shoulder	~30 cm below interface	3.51883	0.066465	0.08625	0.09825	0.08366	0.01605
Woburn	Shoulder	~30 cm below interface	3.86284	0.074139	0.08892	0.10142	0.08816	0.01366
Woburn	Shoulder	~30 cm below interface	4.24049	0.082251	0.09213	0.10518	0.09319	0.0115
Woburn	Shoulder	~30 cm below interface	4.65506	0.089973	0.09587	0.10948	0.09844	0.01
Woburn	Shoulder	~30 cm below interface	5.11017	0.096636	0.10018	0.11434	0.10372	0.00937
Woburn	Shoulder	~30 cm below interface	5.60976	0.101846	0.10503	0.11974	0.10887	0.00955
Woburn	Shoulder	~30 cm below interface	6.1582	0.10555	0.11049	0.12574	0.11393	0.01053
Woburn	Shoulder	~30 cm below interface	6.76025	0.108018	0.11657	0.13238	0.11899	0.01236
Woburn	Shoulder	~30 cm below interface	7.42117	0.109746	0.1234	0.13975	0.1243	0.01502
Woburn	Shoulder	~30 cm below interface	8.14669	0.111497	0.13111	0.14802	0.13021	0.01828
Woburn	Shoulder	~30 cm below interface	8.94315	0.114324	0.14002	0.15753	0.13729	0.02173
Woburn	Shoulder	~30 cm below interface	9.81748	0.119516	0.15049	0.16866	0.14622	0.02485
Woburn	Shoulder	~30 cm below interface	10.7773	0.128533	0.16293	0.18187	0.15778	0.02704
Woburn	Shoulder	~30 cm below interface	11.8309	0.142732	0.17782	0.19767	0.17274	0.02782
Woburn	Shoulder	~30 cm below interface	12.9876	0.163	0.19567	0.21662	0.19176	0.02702
Woburn	Shoulder	~30 cm below interface	14.2573	0.189358	0.21711	0.23936	0.21528	0.02505
Woburn	Shoulder	~30 cm below interface	15.6512	0.220744	0.24267	0.26647	0.2433	0.02287
Woburn	Shoulder	~30 cm below interface	17.1813	0.255232	0.27291	0.29842	0.27552	0.02171
Woburn	Shoulder	~30 cm below interface	18.861	0.290801	0.30797	0.33523	0.31133	0.02241
Woburn	Shoulder	~30 cm below interface	20.705	0.326623	0.34784	0.37672	0.35039	0.02514
Woburn	Shoulder	~30 cm below interface	22.7292	0.363744	0.3922	0.42233	0.39276	0.0293
Woburn	Shoulder	~30 cm below interface	24.9513	0.404909	0.44072	0.4715	0.43904	0.03333
Woburn	Shoulder	~30 cm below interface	27.3906	0.453813	0.493	0.52354	0.49012	0.03495
Woburn	Shoulder	~30 cm below interface	30.0685	0.513222	0.54846	0.5776	0.54643	0.03224
Woburn	Shoulder	~30 cm below interface	33.0081	0.582229	0.60617	0.63249	0.60696	0.02514
Woburn	Shoulder	~30 cm below interface	36.2352	0.653916	0.66437	0.68635	0.66821	0.01655
Woburn	Shoulder	~30 cm below interface	39.7777	0.717189	0.7207	0.73711	0.725	0.01063
Woburn	Shoulder	~30 cm below interface	43.6665	0.764402	0.7724	0.78274	0.77318	0.00919
Woburn	Shoulder	~30 cm below interface	47.9356	0.797403	0.81631	0.82111	0.81161	0.01253
Woburn	Shoulder	~30 cm below interface	52.622	0.825706	0.84802	0.84885	0.84086	0.01313
Woburn	Shoulder	~30 cm below interface	57.7666	0.858701	0.86138	0.86034	0.86014	0.00135
Woburn	Shoulder	~30 cm below interface	63.4141	0.895448	0.85022	0.84912	0.86493	0.02643
Woburn	Shoulder	~30 cm below interface	69.6138	0.92402	0.81267	0.81218	0.84962	0.06443
Woburn	Shoulder	~30 cm below interface	76.4196	0.93962	0.7573	0.7566	0.81784	0.10547
Woburn	Shoulder	~30 cm below interface	83.8907	0.955166	0.70691	0.70412	0.78873	0.14414
Woburn	Shoulder	~30 cm below interface	92.0923	0.983291	0.69639	0.6895	0.78973	0.16767
Woburn	Shoulder	~30 cm below interface	101.096	1.02567	0.76813	0.75567	0.84982	0.15242
Woburn	Shoulder	~30 cm below interface	110.979	1.1004	0.96922	0.9508	1.00681	0.08158
Woburn	Shoulder	~30 cm below interface	121.829	1.27624	1.34962	1.32686	1.31757	0.03756
Woburn	Shoulder	~30 cm below interface	133.74	1.66566	1.94495	1.92247	1.84436	0.15517
Woburn	Shoulder	~30 cm below interface	146.815	2.37027	2.75656	2.74141	2.62275	0.21878
Woburn	Shoulder	~30 cm below interface	161.168	3.40578	3.73551	3.73469	3.62533	0.19013
Woburn	Shoulder	~30 cm below interface	176.925	4.66741	4.78855	4.80578	4.75391	0.07541
Woburn	Shoulder	~30 cm below interface	194.222	5.95379	5.79195	5.82542	5.85705	0.08543
Woburn	Shoulder	~30 cm below interface	213.21	7.0134	6.61842	6.66081	6.76421	0.21684
Woburn	Shoulder	~30 cm below interface	234.054	7.62868	7.16334	7.20447	7.33216	0.25761

Woburn	Shoulder	~30 cm below interface	256.936	7.71227	7.36446	7.39505	7.49059	0.19259
Woburn	Shoulder	~30 cm below interface	282.056	7.32611	7.21243	7.22735	7.2553	0.06178
Woburn	Shoulder	~30 cm below interface	309.631	6.62177	6.74591	6.74487	6.70418	0.07137
Woburn	Shoulder	~30 cm below interface	339.902	5.76867	6.04193	6.02813	5.94624	0.15394
Woburn	Shoulder	~30 cm below interface	373.132	4.90459	5.19571	5.1727	5.091	0.16185
Woburn	Shoulder	~30 cm below interface	409.611	4.11181	4.30167	4.27125	4.22824	0.10197
Woburn	Shoulder	~30 cm below interface	449.657	3.40899	3.43656	3.39795	3.4145	0.01989
Woburn	Shoulder	~30 cm below interface	493.617	2.75847	2.65148	2.60158	2.67051	0.08016
Woburn	Shoulder	~30 cm below interface	541.876	2.10781	1.97305	1.90554	1.99547	0.10298
Woburn	Shoulder	~30 cm below interface	594.852	1.45205	1.40805	1.31715	1.39242	0.0688
Woburn	Shoulder	~30 cm below interface	653.008	0.856358	0.95245	0.83811	0.8823	0.06143
Woburn	Shoulder	~30 cm below interface	716.849	0.413532	0.59809	0.46848	0.49337	0.09476
Woburn	Shoulder	~30 cm below interface	786.932	0.176161	0.33425	0.20734	0.23925	0.08374
Woburn	Shoulder	~30 cm below interface	863.866	0.110688	0.14977	0.0638	0.10809	0.04305
Woburn	Shoulder	~30 cm below interface	948.322	0.120573	0.04718	0.01021	0.05932	0.05618
Woburn	Shoulder	~30 cm below interface	1041.03	0.092429	0.00774	0.00063	0.0336	0.05107
Woburn	Shoulder	~30 cm below interface	1142.81	0.025828	0.0005	0	0.00878	0.01477
Woburn	Shoulder	~30 cm below interface	1254.54	0.001416	0	0	0.00047	0.00082
Woburn	Shoulder	~30 cm below interface	1377.19	0	0	0	0	0
Woburn	Shoulder	~30 cm below interface	1511.83	0	0	0	0	0
Woburn	Shoulder	~30 cm below interface	1659.63	0	0	0	0	0
Woburn	Shoulder	~30 cm below interface	1821.88	0	0	0	0	0
Woburn	Backslope	Soil-Sap Interface	0.375124	0.008129	0.00884	0.00957	0.00885	0.00072
Woburn	Backslope	Soil-Sap Interface	0.411798	0.015513	0.01688	0.01829	0.01689	0.00139
Woburn	Backslope	Soil-Sap Interface	0.452057	0.026128	0.02846	0.03085	0.02848	0.00236
Woburn	Backslope	Soil-Sap Interface	0.496252	0.036138	0.03943	0.04277	0.03945	0.00332
Woburn	Backslope	Soil-Sap Interface	0.544768	0.045628	0.04988	0.05419	0.0499	0.00428
Woburn	Backslope	Soil-Sap Interface	0.598027	0.054457	0.05969	0.06494	0.0597	0.00524
Woburn	Backslope	Soil-Sap Interface	0.656493	0.06248	0.06869	0.07489	0.06869	0.00621
Woburn	Backslope	Soil-Sap Interface	0.720675	0.069508	0.0767	0.08381	0.07667	0.00715
Woburn	Backslope	Soil-Sap Interface	0.791132	0.075353	0.0835	0.09148	0.08344	0.00806
Woburn	Backslope	Soil-Sap Interface	0.868477	0.079814	0.08887	0.09764	0.08877	0.00892
Woburn	Backslope	Soil-Sap Interface	0.953383	0.082696	0.09257	0.10204	0.09243	0.00967
Woburn	Backslope	Soil-Sap Interface	1.04659	0.083826	0.09439	0.10439	0.0942	0.01028
Woburn	Backslope	Soil-Sap Interface	1.14891	0.083218	0.09429	0.10466	0.09406	0.01072
Woburn	Backslope	Soil-Sap Interface	1.26123	0.080971	0.09236	0.10288	0.09207	0.01096
Woburn	Backslope	Soil-Sap Interface	1.38454	0.077273	0.08875	0.09922	0.08842	0.01098
Woburn	Backslope	Soil-Sap Interface	1.5199	0.072425	0.08377	0.09399	0.0834	0.01079
Woburn	Backslope	Soil-Sap Interface	1.66849	0.066837	0.07786	0.08768	0.07746	0.01043
Woburn	Backslope	Soil-Sap Interface	1.83161	0.061031	0.07161	0.08095	0.0712	0.00997
Woburn	Backslope	Soil-Sap Interface	2.01068	0.055598	0.06571	0.07458	0.0653	0.0095
Woburn	Backslope	Soil-Sap Interface	2.20725	0.051156	0.0609	0.06944	0.0605	0.00915
Woburn	Backslope	Soil-Sap Interface	2.42304	0.048261	0.05786	0.06632	0.05748	0.00904
Woburn	Backslope	Soil-Sap Interface	2.65993	0.047332	0.05711	0.06583	0.05676	0.00925
Woburn	Backslope	Soil-Sap Interface	2.91998	0.048575	0.05894	0.06828	0.0586	0.00986
Woburn	Backslope	Soil-Sap Interface	3.20545	0.051939	0.06328	0.07359	0.06294	0.01083
Woburn	Backslope	Soil-Sap Interface	3.51883	0.057105	0.06977	0.08128	0.06938	0.01209
Woburn	Backslope	Soil-Sap Interface	3.86284	0.063517	0.07769	0.09048	0.07723	0.01348
Woburn	Backslope	Soil-Sap Interface	4.24049	0.070478	0.08618	0.10012	0.08559	0.01483
Woburn	Backslope	Soil-Sap Interface	4.65506	0.077278	0.09434	0.10915	0.09359	0.01595
Woburn	Backslope	Soil-Sap Interface	5.11017	0.083337	0.10144	0.11671	0.1005	0.01671
Woburn	Backslope	Soil-Sap Interface	5.60976	0.0883	0.10703	0.12232	0.10588	0.01704
Woburn	Backslope	Soil-Sap Interface	6.1582	0.092095	0.11102	0.12595	0.10969	0.01697
Woburn	Backslope	Soil-Sap Interface	6.76025	0.094922	0.11368	0.12801	0.1122	0.01659
Woburn	Backslope	Soil-Sap Interface	7.42117	0.097199	0.11552	0.12919	0.11397	0.01605
Woburn	Backslope	Soil-Sap Interface	8.14669	0.099589	0.11736	0.13056	0.11584	0.01554
Woburn	Backslope	Soil-Sap Interface	8.94315	0.103033	0.12036	0.13352	0.11897	0.01529
Woburn	Backslope	Soil-Sap Interface	9.81748	0.108667	0.12589	0.13965	0.12474	0.01552
Woburn	Backslope	Soil-Sap Interface	10.7773	0.117743	0.13548	0.15057	0.1346	0.01643
Woburn	Backslope	Soil-Sap Interface	11.8309	0.131367	0.15039	0.16754	0.14976	0.01809
Woburn	Backslope	Soil-Sap Interface	12.9876	0.150222	0.17134	0.19108	0.17088	0.02043
Woburn	Backslope	Soil-Sap Interface	14.2573	0.17433	0.19815	0.22069	0.19772	0.02318
Woburn	Backslope	Soil-Sap Interface	15.6512	0.202878	0.22956	0.25466	0.22903	0.0259
Woburn	Backslope	Soil-Sap Interface	17.1813	0.234304	0.26329	0.29013	0.26258	0.02792
Woburn	Backslope	Soil-Sap Interface	18.861	0.266476	0.29641	0.32346	0.29545	0.02851
Woburn	Backslope	Soil-Sap Interface	20.705	0.297484	0.32643	0.35183	0.32525	0.02719
Woburn	Backslope	Soil-Sap Interface	22.7292	0.326513	0.35247	0.37489	0.35129	0.02421
Woburn	Backslope	Soil-Sap Interface	24.9513	0.354562	0.37616	0.39565	0.37546	0.02055
Woburn	Backslope	Soil-Sap Interface	27.3906	0.384728	0.40168	0.41964	0.40202	0.01746
Woburn	Backslope	Soil-Sap Interface	30.0685	0.420389	0.43324	0.45144	0.43502	0.0156

Woburn	Backslope	Soil-Sap Interface	33.0081	0.462369	0.47145	0.49036	0.47473	0.01428
Woburn	Backslope	Soil-Sap Interface	36.2352	0.506253	0.51019	0.52749	0.51464	0.0113
Woburn	Backslope	Soil-Sap Interface	39.7777	0.543052	0.53806	0.54942	0.54351	0.0057
Woburn	Backslope	Soil-Sap Interface	43.6665	0.565832	0.54725	0.54946	0.55418	0.01015
Woburn	Backslope	Soil-Sap Interface	47.9356	0.574784	0.53954	0.53259	0.54897	0.02262
Woburn	Backslope	Soil-Sap Interface	52.622	0.57666	0.52469	0.5108	0.53738	0.03472
Woburn	Backslope	Soil-Sap Interface	57.7666	0.582268	0.5163	0.49816	0.53224	0.04426
Woburn	Backslope	Soil-Sap Interface	63.4141	0.599515	0.52316	0.50244	0.5417	0.05113
Woburn	Backslope	Soil-Sap Interface	69.6138	0.626887	0.54289	0.51975	0.56318	0.05637
Woburn	Backslope	Soil-Sap Interface	76.4196	0.658753	0.57101	0.54616	0.59198	0.05915
Woburn	Backslope	Soil-Sap Interface	83.8907	0.69263	0.60913	0.58649	0.62942	0.0559
Woburn	Backslope	Soil-Sap Interface	92.0923	0.728001	0.65765	0.64279	0.67614	0.04552
Woburn	Backslope	Soil-Sap Interface	101.096	0.778927	0.72333	0.71831	0.74019	0.03364
Woburn	Backslope	Soil-Sap Interface	110.979	0.910171	0.86033	0.86122	0.87724	0.02852
Woburn	Backslope	Soil-Sap Interface	121.829	1.26011	1.20258	1.20381	1.22217	0.03287
Woburn	Backslope	Soil-Sap Interface	133.74	2.01993	1.94647	1.94845	1.97162	0.04185
Woburn	Backslope	Soil-Sap Interface	146.815	3.33664	3.25141	3.26528	3.28444	0.04573
Woburn	Backslope	Soil-Sap Interface	161.168	5.16779	5.08498	5.12898	5.12725	0.04143
Woburn	Backslope	Soil-Sap Interface	176.925	7.22888	7.16169	7.25124	7.21394	0.04661
Woburn	Backslope	Soil-Sap Interface	194.222	9.06262	9.01225	9.14989	9.07492	0.06964
Woburn	Backslope	Soil-Sap Interface	213.21	10.183	10.1334	10.304	10.2068	0.08775
Woburn	Backslope	Soil-Sap Interface	234.054	10.2719	10.1987	10.3722	10.2809	0.0871
Woburn	Backslope	Soil-Sap Interface	256.936	9.32488	9.2185	9.36055	9.30131	0.0739
Woburn	Backslope	Soil-Sap Interface	282.056	7.64136	7.52142	7.609	7.59059	0.06205
Woburn	Backslope	Soil-Sap Interface	309.631	5.68402	5.59163	5.61691	5.63085	0.04775
Woburn	Backslope	Soil-Sap Interface	339.902	3.90732	3.88058	3.85073	3.87954	0.02831
Woburn	Backslope	Soil-Sap Interface	373.132	2.6152	2.65805	2.59436	2.62254	0.03247
Woburn	Backslope	Soil-Sap Interface	409.611	1.87423	1.95109	1.88077	1.90203	0.04261
Woburn	Backslope	Soil-Sap Interface	449.657	1.55122	1.60356	1.55846	1.57108	0.02836
Woburn	Backslope	Soil-Sap Interface	493.617	1.42596	1.39154	1.39846	1.40532	0.01821
Woburn	Backslope	Soil-Sap Interface	541.876	1.27673	1.13047	1.19329	1.20016	0.07337
Woburn	Backslope	Soil-Sap Interface	594.852	0.994812	0.77146	0.87408	0.88012	0.1118
Woburn	Backslope	Soil-Sap Interface	653.008	0.616645	0.41121	0.48924	0.5057	0.1037
Woburn	Backslope	Soil-Sap Interface	716.849	0.235471	0.18046	0.14417	0.1867	0.04597
Woburn	Backslope	Soil-Sap Interface	786.932	0.033602	0.11785	0.00985	0.05377	0.05675
Woburn	Backslope	Soil-Sap Interface	863.866	0.000771	0.18536	0	0.06204	0.1068
Woburn	Backslope	Soil-Sap Interface	948.322	0	0.30507	0	0.10169	0.17613
Woburn	Backslope	Soil-Sap Interface	1041.03	0	0.32297	0	0.10766	0.18646
Woburn	Backslope	Soil-Sap Interface	1142.81	0	0.23554	0	0.07851	0.13599
Woburn	Backslope	Soil-Sap Interface	1254.54	0	0.14458	0	0.04819	0.08347
Woburn	Backslope	Soil-Sap Interface	1377.19	0	0.07464	0	0.02488	0.0431
Woburn	Backslope	Soil-Sap Interface	1511.83	0	0.02102	0	0.00701	0.01214
Woburn	Backslope	Soil-Sap Interface	1659.63	0	0.00138	0	0.00046	0.00079
Woburn	Backslope	Soil-Sap Interface	1821.88	0	0	0	0	0
Woburn	Backslope	~30 cm below interface	0.375124	0	0.00576	0.00618	0.00398	0.00345
Woburn	Backslope	~30 cm below interface	0.411798	0	0.01099	0.01178	0.00759	0.00659
Woburn	Backslope	~30 cm below interface	0.452057	0	0.0185	0.01984	0.01278	0.01109
Woburn	Backslope	~30 cm below interface	0.496252	0.000356	0.02557	0.02744	0.01779	0.01513
Woburn	Backslope	~30 cm below interface	0.544768	0.004787	0.03226	0.03463	0.02389	0.01659
Woburn	Backslope	~30 cm below interface	0.598027	0.014707	0.03846	0.04132	0.0315	0.01461
Woburn	Backslope	~30 cm below interface	0.656493	0.02446	0.04408	0.04739	0.03864	0.0124
Woburn	Backslope	~30 cm below interface	0.720675	0.033179	0.04898	0.05271	0.04496	0.01037
Woburn	Backslope	~30 cm below interface	0.791132	0.040792	0.05304	0.05714	0.05032	0.0085
Woburn	Backslope	~30 cm below interface	0.868477	0.047032	0.05612	0.06054	0.05456	0.00689
Woburn	Backslope	~30 cm below interface	0.953383	0.051664	0.05811	0.06277	0.05751	0.00557
Woburn	Backslope	~30 cm below interface	1.04659	0.054473	0.05889	0.06372	0.05903	0.00462
Woburn	Backslope	~30 cm below interface	1.14891	0.055472	0.0585	0.06341	0.05913	0.00401
Woburn	Backslope	~30 cm below interface	1.26123	0.05477	0.05701	0.06193	0.0579	0.00366
Woburn	Backslope	~30 cm below interface	1.38454	0.052572	0.05457	0.05942	0.05552	0.00352
Woburn	Backslope	~30 cm below interface	1.5199	0.049175	0.05137	0.0561	0.05222	0.00354
Woburn	Backslope	~30 cm below interface	1.66849	0.044954	0.04769	0.05226	0.0483	0.00369
Woburn	Backslope	~30 cm below interface	1.83161	0.040334	0.04383	0.04825	0.04414	0.00397
Woburn	Backslope	~30 cm below interface	2.01068	0.035766	0.04017	0.04446	0.04013	0.00435
Woburn	Backslope	~30 cm below interface	2.20725	0.03168	0.03706	0.04129	0.03668	0.00482
Woburn	Backslope	~30 cm below interface	2.42304	0.028442	0.03482	0.0391	0.03412	0.00536
Woburn	Backslope	~30 cm below interface	2.65993	0.026318	0.0337	0.03815	0.03272	0.00598
Woburn	Backslope	~30 cm below interface	2.91998	0.025444	0.03382	0.03858	0.03261	0.00665
Woburn	Backslope	~30 cm below interface	3.20545	0.025822	0.03516	0.04034	0.03377	0.00736
Woburn	Backslope	~30 cm below interface	3.51883	0.027323	0.03756	0.04325	0.03605	0.00807
Woburn	Backslope	~30 cm below interface	3.86284	0.029712	0.04075	0.04697	0.03914	0.00874

Woburn	Backslope	~30 cm below interface	4.24049	0.032681	0.04435	0.05109	0.04271	0.00931
Woburn	Backslope	~30 cm below interface	4.65506	0.035907	0.04801	0.05517	0.04636	0.00974
Woburn	Backslope	~30 cm below interface	5.11017	0.039096	0.0514	0.05886	0.04978	0.00998
Woburn	Backslope	~30 cm below interface	5.60976	0.042031	0.05429	0.0619	0.05274	0.01002
Woburn	Backslope	~30 cm below interface	6.1582	0.04459	0.05658	0.0642	0.05512	0.00989
Woburn	Backslope	~30 cm below interface	6.76025	0.046751	0.05832	0.06583	0.05697	0.00961
Woburn	Backslope	~30 cm below interface	7.42117	0.048566	0.05962	0.06697	0.05839	0.00927
Woburn	Backslope	~30 cm below interface	8.14669	0.050175	0.06075	0.06793	0.05962	0.00893
Woburn	Backslope	~30 cm below interface	8.94315	0.051836	0.0621	0.06917	0.06104	0.00872
Woburn	Backslope	~30 cm below interface	9.81748	0.05391	0.06419	0.07128	0.06313	0.00873
Woburn	Backslope	~30 cm below interface	10.7773	0.056867	0.06762	0.07491	0.06647	0.00908
Woburn	Backslope	~30 cm below interface	11.8309	0.061203	0.07294	0.0806	0.07158	0.00977
Woburn	Backslope	~30 cm below interface	12.9876	0.067356	0.0805	0.08865	0.07884	0.01075
Woburn	Backslope	~30 cm below interface	14.2573	0.075579	0.09032	0.09896	0.08829	0.01182
Woburn	Backslope	~30 cm below interface	15.6512	0.085765	0.10191	0.11092	0.09953	0.01275
Woburn	Backslope	~30 cm below interface	17.1813	0.097374	0.11434	0.12353	0.11175	0.01327
Woburn	Backslope	~30 cm below interface	18.861	0.109409	0.12639	0.13547	0.12376	0.01323
Woburn	Backslope	~30 cm below interface	20.705	0.120791	0.13698	0.14568	0.13448	0.01263
Woburn	Backslope	~30 cm below interface	22.7292	0.130871	0.14564	0.15371	0.14341	0.01158
Woburn	Backslope	~30 cm below interface	24.9513	0.139833	0.15282	0.16018	0.15094	0.0103
Woburn	Backslope	~30 cm below interface	27.3906	0.148836	0.15998	0.16666	0.15849	0.00901
Woburn	Backslope	~30 cm below interface	30.0685	0.159244	0.16869	0.17476	0.16757	0.00782
Woburn	Backslope	~30 cm below interface	33.0081	0.17164	0.17942	0.18479	0.17862	0.00661
Woburn	Backslope	~30 cm below interface	36.2352	0.184881	0.19028	0.19464	0.18993	0.00489
Woburn	Backslope	~30 cm below interface	39.7777	0.196223	0.19745	0.20028	0.19799	0.00208
Woburn	Backslope	~30 cm below interface	43.6665	0.203752	0.19812	0.19901	0.20029	0.00303
Woburn	Backslope	~30 cm below interface	47.9356	0.208632	0.19321	0.19201	0.19795	0.00927
Woburn	Backslope	~30 cm below interface	52.622	0.21547	0.18802	0.18463	0.19604	0.01691
Woburn	Backslope	~30 cm below interface	57.7666	0.231278	0.19125	0.18551	0.20268	0.02493
Woburn	Backslope	~30 cm below interface	63.4141	0.261285	0.21049	0.2024	0.22472	0.03192
Woburn	Backslope	~30 cm below interface	69.6138	0.302966	0.2461	0.23626	0.26178	0.03601
Woburn	Backslope	~30 cm below interface	76.4196	0.344585	0.2894	0.27959	0.30453	0.03504
Woburn	Backslope	~30 cm below interface	83.8907	0.370184	0.32598	0.3191	0.33842	0.02772
Woburn	Backslope	~30 cm below interface	92.0923	0.37055	0.34371	0.34221	0.35216	0.01595
Woburn	Backslope	~30 cm below interface	101.096	0.3647	0.3535	0.35681	0.35834	0.00575
Woburn	Backslope	~30 cm below interface	110.979	0.420186	0.4149	0.41909	0.41806	0.00279
Woburn	Backslope	~30 cm below interface	121.829	0.656891	0.64513	0.64524	0.64909	0.00676
Woburn	Backslope	~30 cm below interface	133.74	1.24364	1.21606	1.20915	1.22295	0.01825
Woburn	Backslope	~30 cm below interface	146.815	2.32759	2.28739	2.27724	2.29741	0.02663
Woburn	Backslope	~30 cm below interface	161.168	3.91815	3.88509	3.8833	3.89551	0.01962
Woburn	Backslope	~30 cm below interface	176.925	5.83835	5.8405	5.86094	5.8466	0.01247
Woburn	Backslope	~30 cm below interface	194.222	7.75362	7.81197	7.8624	7.80933	0.05444
Woburn	Backslope	~30 cm below interface	213.21	9.26608	9.37833	9.45426	9.36622	0.09467
Woburn	Backslope	~30 cm below interface	234.054	10.051	10.1847	10.2699	10.1685	0.11034
Woburn	Backslope	~30 cm below interface	256.936	9.97222	10.0745	10.1489	10.0652	0.08871
Woburn	Backslope	~30 cm below interface	282.056	9.11715	9.1372	9.18689	9.14708	0.0359
Woburn	Backslope	~30 cm below interface	309.631	7.74787	7.6615	7.68258	7.69732	0.04503
Woburn	Backslope	~30 cm below interface	339.902	6.20246	6.02722	6.02471	6.0848	0.10191
Woburn	Backslope	~30 cm below interface	373.132	4.78091	4.57176	4.55551	4.63606	0.12571
Woburn	Backslope	~30 cm below interface	409.611	3.65643	3.481	3.46038	3.5326	0.10773
Woburn	Backslope	~30 cm below interface	449.657	2.85174	2.75898	2.73788	2.78287	0.06057
Woburn	Backslope	~30 cm below interface	493.617	2.28137	2.28389	2.25824	2.2745	0.01414
Woburn	Backslope	~30 cm below interface	541.876	1.82884	1.90496	1.86386	1.86589	0.0381
Woburn	Backslope	~30 cm below interface	594.852	1.41605	1.52464	1.45599	1.46556	0.05492
Woburn	Backslope	~30 cm below interface	653.008	1.02881	1.12955	1.03264	1.06367	0.05709
Woburn	Backslope	~30 cm below interface	716.849	0.693071	0.75695	0.64679	0.69894	0.05531
Woburn	Backslope	~30 cm below interface	786.932	0.438712	0.4507	0.35253	0.41398	0.05356
Woburn	Backslope	~30 cm below interface	863.866	0.278775	0.24851	0.18431	0.2372	0.04824
Woburn	Backslope	~30 cm below interface	948.322	0.183171	0.13348	0.1035	0.14005	0.04024
Woburn	Backslope	~30 cm below interface	1041.03	0.096914	0.04588	0.03794	0.06024	0.032
Woburn	Backslope	~30 cm below interface	1142.81	0.024542	0.00371	0.00315	0.01047	0.01219
Woburn	Backslope	~30 cm below interface	1254.54	0.001355	0	0	0.00045	0.00078
Woburn	Backslope	~30 cm below interface	1377.19	0	0	0	0	0
Woburn	Backslope	~30 cm below interface	1511.83	0	0	0	0	0
Woburn	Backslope	~30 cm below interface	1659.63	0	0	0	0	0
Woburn	Backslope	~30 cm below interface	1821.88	0	0	0	0	0
Woburn	Toeslope	Soil-Sap Interface	0.375124	0.02173	0.02249	0.02356	0.02259	0.00092
Woburn	Toeslope	Soil-Sap Interface	0.411798	0.038975	0.04034	0.04225	0.04052	0.00164
Woburn	Toeslope	Soil-Sap Interface	0.452057	0.05801	0.06004	0.06287	0.0603	0.00244
Woburn	Toeslope	Soil-Sap Interface	0.496252	0.083302	0.08621	0.09026	0.08659	0.0035

Woburn	Toeslope	Soil-Sap Interface	0.544768	0.104155	0.10779	0.11286	0.10827	0.00437
Woburn	Toeslope	Soil-Sap Interface	0.598027	0.123197	0.12749	0.13347	0.12805	0.00516
Woburn	Toeslope	Soil-Sap Interface	0.656493	0.141023	0.14592	0.15273	0.14656	0.00588
Woburn	Toeslope	Soil-Sap Interface	0.720675	0.158768	0.16425	0.17188	0.16497	0.00658
Woburn	Toeslope	Soil-Sap Interface	0.791132	0.173117	0.17908	0.18736	0.17985	0.00715
Woburn	Toeslope	Soil-Sap Interface	0.868477	0.184725	0.19105	0.19984	0.19187	0.00759
Woburn	Toeslope	Soil-Sap Interface	0.953383	0.19371	0.20029	0.20943	0.20114	0.00789
Woburn	Toeslope	Soil-Sap Interface	1.04659	0.200429	0.20717	0.21651	0.20804	0.00807
Woburn	Toeslope	Soil-Sap Interface	1.14891	0.204174	0.21097	0.22037	0.21184	0.00813
Woburn	Toeslope	Soil-Sap Interface	1.26123	0.204919	0.21166	0.22096	0.21251	0.00805
Woburn	Toeslope	Soil-Sap Interface	1.38454	0.203298	0.20988	0.21896	0.21072	0.00787
Woburn	Toeslope	Soil-Sap Interface	1.5199	0.199858	0.20622	0.21498	0.20702	0.00759
Woburn	Toeslope	Soil-Sap Interface	1.66849	0.1954	0.20151	0.2099	0.20227	0.00728
Woburn	Toeslope	Soil-Sap Interface	1.83161	0.189978	0.19581	0.20381	0.19653	0.00694
Woburn	Toeslope	Soil-Sap Interface	2.01068	0.184308	0.18988	0.1975	0.19056	0.00662
Woburn	Toeslope	Soil-Sap Interface	2.20725	0.179061	0.1844	0.1917	0.18505	0.00634
Woburn	Toeslope	Soil-Sap Interface	2.42304	0.175293	0.18048	0.18757	0.18111	0.00616
Woburn	Toeslope	Soil-Sap Interface	2.65993	0.173311	0.17844	0.18545	0.17907	0.00609
Woburn	Toeslope	Soil-Sap Interface	2.91998	0.173389	0.17857	0.18564	0.1792	0.00615
Woburn	Toeslope	Soil-Sap Interface	3.20545	0.17568	0.18102	0.1883	0.18166	0.00633
Woburn	Toeslope	Soil-Sap Interface	3.51883	0.180364	0.18596	0.19357	0.18663	0.00663
Woburn	Toeslope	Soil-Sap Interface	3.86284	0.187412	0.19334	0.20139	0.19405	0.00701
Woburn	Toeslope	Soil-Sap Interface	4.24049	0.196483	0.20281	0.21134	0.20354	0.00746
Woburn	Toeslope	Soil-Sap Interface	4.65506	0.207219	0.21397	0.22301	0.21473	0.00792
Woburn	Toeslope	Soil-Sap Interface	5.11017	0.219269	0.22644	0.23597	0.22723	0.00838
Woburn	Toeslope	Soil-Sap Interface	5.60976	0.232603	0.24018	0.25016	0.24098	0.00881
Woburn	Toeslope	Soil-Sap Interface	6.1582	0.247198	0.25514	0.26554	0.25596	0.0092
Woburn	Toeslope	Soil-Sap Interface	6.76025	0.263029	0.27129	0.28206	0.27213	0.00954
Woburn	Toeslope	Soil-Sap Interface	7.42117	0.280112	0.28864	0.29974	0.2895	0.00984
Woburn	Toeslope	Soil-Sap Interface	8.14669	0.29884	0.30759	0.31902	0.30848	0.01012
Woburn	Toeslope	Soil-Sap Interface	8.94315	0.32001	0.32893	0.34076	0.3299	0.01041
Woburn	Toeslope	Soil-Sap Interface	9.81748	0.344366	0.3534	0.36575	0.3545	0.01073
Woburn	Toeslope	Soil-Sap Interface	10.7773	0.372412	0.3815	0.39453	0.38281	0.01112
Woburn	Toeslope	Soil-Sap Interface	11.8309	0.404512	0.4136	0.42756	0.41522	0.01161
Woburn	Toeslope	Soil-Sap Interface	12.9876	0.44124	0.45033	0.46549	0.45235	0.01225
Woburn	Toeslope	Soil-Sap Interface	14.2573	0.483041	0.49213	0.50874	0.49464	0.01303
Woburn	Toeslope	Soil-Sap Interface	15.6512	0.529425	0.53842	0.55661	0.54149	0.01385
Woburn	Toeslope	Soil-Sap Interface	17.1813	0.57861	0.58733	0.60686	0.59093	0.01447
Woburn	Toeslope	Soil-Sap Interface	18.861	0.627982	0.63619	0.65644	0.64021	0.01465
Woburn	Toeslope	Soil-Sap Interface	20.705	0.675773	0.68328	0.70329	0.68745	0.01422
Woburn	Toeslope	Soil-Sap Interface	22.7292	0.721955	0.7286	0.74733	0.73263	0.01316
Woburn	Toeslope	Soil-Sap Interface	24.9513	0.767781	0.77324	0.78985	0.77696	0.0115
Woburn	Toeslope	Soil-Sap Interface	27.3906	0.813529	0.81713	0.83107	0.82058	0.00926
Woburn	Toeslope	Soil-Sap Interface	30.0685	0.856233	0.85675	0.86763	0.8602	0.00643
Woburn	Toeslope	Soil-Sap Interface	33.0081	0.889031	0.88479	0.89222	0.88868	0.00373
Woburn	Toeslope	Soil-Sap Interface	36.2352	0.902605	0.89176	0.89524	0.89653	0.00554
Woburn	Toeslope	Soil-Sap Interface	39.7777	0.889281	0.87041	0.86929	0.87633	0.01123
Woburn	Toeslope	Soil-Sap Interface	43.6665	0.847468	0.82003	0.81388	0.82713	0.01788
Woburn	Toeslope	Soil-Sap Interface	47.9356	0.783437	0.74812	0.73713	0.75623	0.02419
Woburn	Toeslope	Soil-Sap Interface	52.622	0.708642	0.6673	0.65261	0.67618	0.02905
Woburn	Toeslope	Soil-Sap Interface	57.7666	0.633686	0.58894	0.57259	0.5984	0.03163
Woburn	Toeslope	Soil-Sap Interface	63.4141	0.56375	0.51842	0.50287	0.52835	0.03163
Woburn	Toeslope	Soil-Sap Interface	69.6138	0.4979	0.45445	0.44201	0.46479	0.02934
Woburn	Toeslope	Soil-Sap Interface	76.4196	0.434045	0.39408	0.38618	0.40477	0.02566
Woburn	Toeslope	Soil-Sap Interface	83.8907	0.376507	0.34046	0.33708	0.35135	0.02185
Woburn	Toeslope	Soil-Sap Interface	92.0923	0.341412	0.30849	0.30816	0.31935	0.01911
Woburn	Toeslope	Soil-Sap Interface	101.096	0.356583	0.32489	0.3254	0.33563	0.01815
Woburn	Toeslope	Soil-Sap Interface	110.979	0.462314	0.42964	0.4286	0.44018	0.01917
Woburn	Toeslope	Soil-Sap Interface	121.829	0.719556	0.68483	0.67993	0.69477	0.0216
Woburn	Toeslope	Soil-Sap Interface	133.74	1.20043	1.16509	1.15519	1.17357	0.02378
Woburn	Toeslope	Soil-Sap Interface	146.815	1.95557	1.92356	1.91029	1.92981	0.02328
Woburn	Toeslope	Soil-Sap Interface	161.168	2.96974	2.9463	2.93393	2.94999	0.01819
Woburn	Toeslope	Soil-Sap Interface	176.925	4.14684	4.13669	4.12937	4.13763	0.00877
Woburn	Toeslope	Soil-Sap Interface	194.222	5.31985	5.32525	5.32369	5.32293	0.00278
Woburn	Toeslope	Soil-Sap Interface	213.21	6.2964	6.31572	6.31567	6.30926	0.01114
Woburn	Toeslope	Soil-Sap Interface	234.054	6.91668	6.94443	6.93826	6.93312	0.01457
Woburn	Toeslope	Soil-Sap Interface	256.936	7.09961	7.12782	7.10852	7.11198	0.01442
Woburn	Toeslope	Soil-Sap Interface	282.056	6.86152	6.88191	6.84738	6.8636	0.01736
Woburn	Toeslope	Soil-Sap Interface	309.631	6.29651	6.30293	6.25729	6.28558	0.02471
Woburn	Toeslope	Soil-Sap Interface	339.902	5.53962	5.53035	5.48167	5.51721	0.03113

Woburn	Toeslope	Soil-Sap Interface	373.132	4.72244	4.7013	4.65623	4.69332	0.03382
Woburn	Toeslope	Soil-Sap Interface	409.611	3.94181	3.91751	3.87679	3.91204	0.03285
Woburn	Toeslope	Soil-Sap Interface	449.657	3.24698	3.23041	3.18806	3.22182	0.03039
Woburn	Toeslope	Soil-Sap Interface	493.617	2.64541	2.64556	2.59311	2.62803	0.03024
Woburn	Toeslope	Soil-Sap Interface	541.876	2.12162	2.14173	2.07516	2.11284	0.03414
Woburn	Toeslope	Soil-Sap Interface	594.852	1.65656	1.69183	1.6179	1.65543	0.03698
Woburn	Toeslope	Soil-Sap Interface	653.008	1.24262	1.28155	1.21846	1.24754	0.03183
Woburn	Toeslope	Soil-Sap Interface	716.849	0.886526	0.9161	0.88601	0.89621	0.01723
Woburn	Toeslope	Soil-Sap Interface	786.932	0.602013	0.61464	0.62907	0.61524	0.01354
Woburn	Toeslope	Soil-Sap Interface	863.866	0.393488	0.38989	0.44212	0.4085	0.02917
Woburn	Toeslope	Soil-Sap Interface	948.322	0.251864	0.23933	0.30763	0.26627	0.03636
Woburn	Toeslope	Soil-Sap Interface	1041.03	0.157727	0.14523	0.20563	0.16953	0.03188
Woburn	Toeslope	Soil-Sap Interface	1142.81	0.086603	0.08464	0.12047	0.09724	0.02014
Woburn	Toeslope	Soil-Sap Interface	1254.54	0.036541	0.04874	0.06255	0.04928	0.01301
Woburn	Toeslope	Soil-Sap Interface	1377.19	0.008612	0.031	0.03281	0.02414	0.01348
Woburn	Toeslope	Soil-Sap Interface	1511.83	0.000965	0.02906	0.02463	0.01822	0.0151
Woburn	Toeslope	Soil-Sap Interface	1659.63	1.03E-05	0.03486	0.02621	0.02036	0.01814
Woburn	Toeslope	Soil-Sap Interface	1821.88	0	0.04285	0.0209	0.02125	0.02143
Woburn	Toeslope	~30 cm below interface	0.375124	0.012497	0.01378	0.01451	0.0136	0.00102
Woburn	Toeslope	~30 cm below interface	0.411798	0.023869	0.02634	0.02773	0.02598	0.00196
Woburn	Toeslope	~30 cm below interface	0.452057	0.040274	0.0445	0.04687	0.04388	0.00334
Woburn	Toeslope	~30 cm below interface	0.496252	0.055853	0.06183	0.06519	0.06096	0.00473
Woburn	Toeslope	~30 cm below interface	0.544768	0.070766	0.07852	0.08289	0.07739	0.00614
Woburn	Toeslope	~30 cm below interface	0.598027	0.084824	0.0944	0.09981	0.09301	0.00759
Woburn	Toeslope	~30 cm below interface	0.656493	0.097813	0.10923	0.11571	0.10758	0.00906
Woburn	Toeslope	~30 cm below interface	0.720675	0.109438	0.12271	0.13026	0.1208	0.01054
Woburn	Toeslope	~30 cm below interface	0.791132	0.119384	0.13446	0.14307	0.1323	0.01199
Woburn	Toeslope	~30 cm below interface	0.868477	0.127284	0.14406	0.15367	0.14167	0.01335
Woburn	Toeslope	~30 cm below interface	0.953383	0.132748	0.15103	0.16152	0.14843	0.01456
Woburn	Toeslope	~30 cm below interface	1.04659	0.135383	0.15486	0.16605	0.1521	0.01552
Woburn	Toeslope	~30 cm below interface	1.14891	0.135072	0.15534	0.16697	0.15246	0.01614
Woburn	Toeslope	~30 cm below interface	1.26123	0.131836	0.15239	0.16416	0.14946	0.01636
Woburn	Toeslope	~30 cm below interface	1.38454	0.125852	0.14614	0.15771	0.14323	0.01612
Woburn	Toeslope	~30 cm below interface	1.5199	0.117528	0.13699	0.14799	0.13417	0.01542
Woburn	Toeslope	~30 cm below interface	1.66849	0.107516	0.12565	0.13575	0.12297	0.01431
Woburn	Toeslope	~30 cm below interface	1.83161	0.096736	0.11319	0.12216	0.1107	0.01289
Woburn	Toeslope	~30 cm below interface	2.01068	0.086318	0.10097	0.1087	0.09866	0.01137
Woburn	Toeslope	~30 cm below interface	2.20725	0.077508	0.09052	0.09709	0.08837	0.00997
Woburn	Toeslope	~30 cm below interface	2.42304	0.071472	0.0833	0.089	0.08125	0.00894
Woburn	Toeslope	~30 cm below interface	2.65993	0.06911	0.08046	0.08573	0.07843	0.00849
Woburn	Toeslope	~30 cm below interface	2.91998	0.070863	0.08258	0.08797	0.08047	0.00875
Woburn	Toeslope	~30 cm below interface	3.20545	0.0766	0.08954	0.09561	0.08725	0.00971
Woburn	Toeslope	~30 cm below interface	3.51883	0.085566	0.10041	0.10763	0.09787	0.01125
Woburn	Toeslope	~30 cm below interface	3.86284	0.096448	0.11354	0.12218	0.11072	0.01309
Woburn	Toeslope	~30 cm below interface	4.24049	0.10761	0.12689	0.13694	0.12381	0.01491
Woburn	Toeslope	~30 cm below interface	4.65506	0.117439	0.13844	0.14962	0.13517	0.01634
Woburn	Toeslope	~30 cm below interface	5.11017	0.124701	0.14666	0.15849	0.14328	0.01714
Woburn	Toeslope	~30 cm below interface	5.60976	0.128787	0.15085	0.16275	0.14746	0.01723
Woburn	Toeslope	~30 cm below interface	6.1582	0.129818	0.15122	0.16266	0.1479	0.01667
Woburn	Toeslope	~30 cm below interface	6.76025	0.12857	0.14885	0.15942	0.14561	0.01568
Woburn	Toeslope	~30 cm below interface	7.42117	0.126249	0.14528	0.1548	0.14211	0.01454
Woburn	Toeslope	~30 cm below interface	8.14669	0.124503	0.14258	0.15107	0.13938	0.01357
Woburn	Toeslope	~30 cm below interface	8.94315	0.12531	0.14307	0.15079	0.13972	0.01306
Woburn	Toeslope	~30 cm below interface	9.81748	0.130698	0.14901	0.15641	0.14537	0.01323
Woburn	Toeslope	~30 cm below interface	10.7773	0.142461	0.16227	0.16992	0.15822	0.01417
Woburn	Toeslope	~30 cm below interface	11.8309	0.161563	0.18368	0.19219	0.17914	0.01581
Woburn	Toeslope	~30 cm below interface	12.9876	0.187672	0.21255	0.22244	0.20755	0.01791
Woburn	Toeslope	~30 cm below interface	14.2573	0.218836	0.2464	0.25793	0.24105	0.02009
Woburn	Toeslope	~30 cm below interface	15.6512	0.251665	0.28115	0.2942	0.27567	0.02179
Woburn	Toeslope	~30 cm below interface	17.1813	0.28159	0.31134	0.32523	0.30605	0.02229
Woburn	Toeslope	~30 cm below interface	18.861	0.303895	0.33146	0.34473	0.3267	0.02083
Woburn	Toeslope	~30 cm below interface	20.705	0.316231	0.33926	0.34987	0.33512	0.0172
Woburn	Toeslope	~30 cm below interface	22.7292	0.32048	0.33786	0.34371	0.33402	0.01208
Woburn	Toeslope	~30 cm below interface	24.9513	0.322862	0.33528	0.33498	0.33104	0.00708
Woburn	Toeslope	~30 cm below interface	27.3906	0.330984	0.34042	0.33394	0.33512	0.00483
Woburn	Toeslope	~30 cm below interface	30.0685	0.349662	0.35803	0.34693	0.35154	0.00578
Woburn	Toeslope	~30 cm below interface	33.0081	0.377412	0.38469	0.37174	0.37795	0.00649
Woburn	Toeslope	~30 cm below interface	36.2352	0.404423	0.4071	0.39467	0.40206	0.00654
Woburn	Toeslope	~30 cm below interface	39.7777	0.41833	0.41029	0.39838	0.409	0.01004
Woburn	Toeslope	~30 cm below interface	43.6665	0.416669	0.39298	0.37924	0.3963	0.01893

Woburn	Toeslope	~30 cm below interface	47.9356	0.410032	0.36971	0.35187	0.37721	0.02979
Woburn	Toeslope	~30 cm below interface	52.622	0.412498	0.35799	0.33679	0.36909	0.03906
Woburn	Toeslope	~30 cm below interface	57.7666	0.431984	0.36718	0.34742	0.38219	0.04424
Woburn	Toeslope	~30 cm below interface	63.4141	0.461739	0.38978	0.37669	0.4094	0.04579
Woburn	Toeslope	~30 cm below interface	69.6138	0.482807	0.4046	0.39725	0.42822	0.04742
Woburn	Toeslope	~30 cm below interface	76.4196	0.49332	0.41127	0.40273	0.43577	0.05002
Woburn	Toeslope	~30 cm below interface	83.8907	0.520985	0.44461	0.43063	0.46541	0.04863
Woburn	Toeslope	~30 cm below interface	92.0923	0.583415	0.52728	0.51014	0.54028	0.03833
Woburn	Toeslope	~30 cm below interface	101.096	0.658601	0.63055	0.61595	0.63503	0.02168
Woburn	Toeslope	~30 cm below interface	110.979	0.728121	0.71778	0.70959	0.7185	0.00929
Woburn	Toeslope	~30 cm below interface	121.829	0.860153	0.84665	0.8441	0.8503	0.00863
Woburn	Toeslope	~30 cm below interface	133.74	1.22398	1.19476	1.19285	1.20386	0.01745
Woburn	Toeslope	~30 cm below interface	146.815	2.02199	1.98673	1.97796	1.99556	0.02331
Woburn	Toeslope	~30 cm below interface	161.168	3.36674	3.36421	3.34402	3.35832	0.01245
Woburn	Toeslope	~30 cm below interface	176.925	5.17647	5.26202	5.2355	5.22466	0.04379
Woburn	Toeslope	~30 cm below interface	194.222	7.15153	7.36583	7.34425	7.2872	0.11799
Woburn	Toeslope	~30 cm below interface	213.21	8.80455	9.13223	9.1211	9.01929	0.18606
Woburn	Toeslope	~30 cm below interface	234.054	9.63907	9.99175	9.9849	9.87191	0.20167
Woburn	Toeslope	~30 cm below interface	256.936	9.4142	9.6747	9.65857	9.58249	0.14597
Woburn	Toeslope	~30 cm below interface	282.056	8.2585	8.35512	8.31611	8.30991	0.04861
Woburn	Toeslope	~30 cm below interface	309.631	6.58759	6.52483	6.45745	6.52329	0.06508
Woburn	Toeslope	~30 cm below interface	339.902	4.91434	4.74325	4.65613	4.77124	0.13136
Woburn	Toeslope	~30 cm below interface	373.132	3.62415	3.40395	3.31203	3.44671	0.16039
Woburn	Toeslope	~30 cm below interface	409.611	2.82793	2.61569	2.52541	2.65634	0.1553
Woburn	Toeslope	~30 cm below interface	449.657	2.39152	2.24397	2.14984	2.26178	0.12182
Woburn	Toeslope	~30 cm below interface	493.617	2.08445	2.04292	1.93659	2.02132	0.07626
Woburn	Toeslope	~30 cm below interface	541.876	1.73561	1.78895	1.6758	1.73345	0.05661
Woburn	Toeslope	~30 cm below interface	594.852	1.32086	1.39026	1.30329	1.33814	0.04599
Woburn	Toeslope	~30 cm below interface	653.008	0.918101	0.90792	0.89056	0.90553	0.01393
Woburn	Toeslope	~30 cm below interface	716.849	0.602632	0.4805	0.54847	0.54387	0.0612
Woburn	Toeslope	~30 cm below interface	786.932	0.404445	0.25003	0.37313	0.34254	0.08163
Woburn	Toeslope	~30 cm below interface	863.866	0.310507	0.23901	0.38464	0.31138	0.07282
Woburn	Toeslope	~30 cm below interface	948.322	0.261363	0.36804	0.48181	0.3704	0.11024
Woburn	Toeslope	~30 cm below interface	1041.03	0.200803	0.47068	0.47178	0.38109	0.15613
Woburn	Toeslope	~30 cm below interface	1142.81	0.169655	0.47426	0.36744	0.33712	0.15455
Woburn	Toeslope	~30 cm below interface	1254.54	0.222308	0.43667	0.31231	0.32376	0.10764
Woburn	Toeslope	~30 cm below interface	1377.19	0.327433	0.34596	0.29808	0.32382	0.02414
Woburn	Toeslope	~30 cm below interface	1511.83	0.442678	0.21292	0.29559	0.31706	0.11638
Woburn	Toeslope	~30 cm below interface	1659.63	0.553177	0.07484	0.29517	0.30773	0.23942
Woburn	Toeslope	~30 cm below interface	1821.88	0.592768	0.00628	0.26712	0.28872	0.29384
Hilton	Summit	Soil-Sap Interface	0.375124	0	0	0	0	0
Hilton	Summit	Soil-Sap Interface	0.411798	0	0	0	0	0
Hilton	Summit	Soil-Sap Interface	0.452057	0	0	0	0	0
Hilton	Summit	Soil-Sap Interface	0.496252	0.000291	0.00031	0.00033	0.00031	2.1E-05
Hilton	Summit	Soil-Sap Interface	0.544768	0.003907	0.00414	0.00446	0.00417	0.00028
Hilton	Summit	Soil-Sap Interface	0.598027	0.011997	0.01272	0.01371	0.01281	0.00086
Hilton	Summit	Soil-Sap Interface	0.656493	0.019926	0.02113	0.0228	0.02129	0.00144
Hilton	Summit	Soil-Sap Interface	0.720675	0.026975	0.02864	0.03092	0.02884	0.00198
Hilton	Summit	Soil-Sap Interface	0.791132	0.033081	0.03517	0.03799	0.03541	0.00246
Hilton	Summit	Soil-Sap Interface	0.868477	0.038024	0.0405	0.04378	0.04077	0.00289
Hilton	Summit	Soil-Sap Interface	0.953383	0.041621	0.04442	0.04807	0.0447	0.00323
Hilton	Summit	Soil-Sap Interface	1.04659	0.043719	0.04677	0.05067	0.04706	0.00349
Hilton	Summit	Soil-Sap Interface	1.14891	0.044369	0.0476	0.05164	0.04787	0.00364
Hilton	Summit	Soil-Sap Interface	1.26123	0.043709	0.04703	0.0511	0.04728	0.0037
Hilton	Summit	Soil-Sap Interface	1.38454	0.041973	0.04531	0.0493	0.04553	0.00367
Hilton	Summit	Soil-Sap Interface	1.5199	0.039477	0.04275	0.04659	0.04294	0.00356
Hilton	Summit	Soil-Sap Interface	1.66849	0.03661	0.03976	0.0434	0.03993	0.0034
Hilton	Summit	Soil-Sap Interface	1.83161	0.033808	0.03681	0.04024	0.03695	0.00322
Hilton	Summit	Soil-Sap Interface	2.01068	0.031515	0.03436	0.03763	0.0345	0.00306
Hilton	Summit	Soil-Sap Interface	2.20725	0.030142	0.03288	0.03606	0.03303	0.00296
Hilton	Summit	Soil-Sap Interface	2.42304	0.030019	0.03274	0.03596	0.03291	0.00297
Hilton	Summit	Soil-Sap Interface	2.65993	0.03136	0.03418	0.03759	0.03438	0.00312
Hilton	Summit	Soil-Sap Interface	2.91998	0.034221	0.03728	0.04104	0.03751	0.00341
Hilton	Summit	Soil-Sap Interface	3.20545	0.038486	0.04193	0.04617	0.04219	0.00385
Hilton	Summit	Soil-Sap Interface	3.51883	0.043854	0.04779	0.05262	0.04809	0.00439
Hilton	Summit	Soil-Sap Interface	3.86284	0.049878	0.05438	0.05981	0.05469	0.00497
Hilton	Summit	Soil-Sap Interface	4.24049	0.056037	0.0611	0.06709	0.06141	0.00553
Hilton	Summit	Soil-Sap Interface	4.65506	0.061825	0.06738	0.0738	0.06767	0.00599
Hilton	Summit	Soil-Sap Interface	5.11017	0.066845	0.07278	0.07946	0.07303	0.00631
Hilton	Summit	Soil-Sap Interface	5.60976	0.070868	0.07702	0.08378	0.07722	0.00646

Hilton	Summit	Soil-Sap Interface	6.1582	0.073873	0.08009	0.08676	0.08024	0.00645
Hilton	Summit	Soil-Sap Interface	6.76025	0.076036	0.08219	0.08867	0.0823	0.00632
Hilton	Summit	Soil-Sap Interface	7.42117	0.077685	0.08368	0.08995	0.08377	0.00613
Hilton	Summit	Soil-Sap Interface	8.14669	0.079329	0.08515	0.09128	0.08525	0.00598
Hilton	Summit	Soil-Sap Interface	8.94315	0.081677	0.08739	0.09357	0.08755	0.00595
Hilton	Summit	Soil-Sap Interface	9.81748	0.085572	0.09135	0.09788	0.0916	0.00616
Hilton	Summit	Soil-Sap Interface	10.7773	0.091881	0.09802	0.10525	0.09838	0.00669
Hilton	Summit	Soil-Sap Interface	11.8309	0.101284	0.10815	0.11644	0.10862	0.00759
Hilton	Summit	Soil-Sap Interface	12.9876	0.114003	0.12194	0.13159	0.12251	0.00881
Hilton	Summit	Soil-Sap Interface	14.2573	0.12961	0.13884	0.14995	0.13947	0.01019
Hilton	Summit	Soil-Sap Interface	15.6512	0.146952	0.15739	0.16985	0.15806	0.01147
Hilton	Summit	Soil-Sap Interface	17.1813	0.164364	0.17549	0.18888	0.17625	0.01228
Hilton	Summit	Soil-Sap Interface	18.861	0.1802	0.19111	0.20461	0.19197	0.01223
Hilton	Summit	Soil-Sap Interface	20.705	0.193691	0.2033	0.21591	0.2043	0.01114
Hilton	Summit	Soil-Sap Interface	22.7292	0.205662	0.21315	0.22416	0.21432	0.0093
Hilton	Summit	Soil-Sap Interface	24.9513	0.218414	0.22364	0.23312	0.22506	0.00745
Hilton	Summit	Soil-Sap Interface	27.3906	0.234785	0.23836	0.24723	0.24013	0.00641
Hilton	Summit	Soil-Sap Interface	30.0685	0.256394	0.25922	0.2687	0.26144	0.00645
Hilton	Summit	Soil-Sap Interface	33.0081	0.281991	0.28434	0.29501	0.28711	0.00694
Hilton	Summit	Soil-Sap Interface	36.2352	0.307245	0.30793	0.31876	0.31131	0.00646
Hilton	Summit	Soil-Sap Interface	39.7777	0.326813	0.32313	0.33158	0.32718	0.00423
Hilton	Summit	Soil-Sap Interface	43.6665	0.338303	0.3272	0.33056	0.33202	0.0057
Hilton	Summit	Soil-Sap Interface	47.9356	0.344144	0.32356	0.32041	0.32937	0.01289
Hilton	Summit	Soil-Sap Interface	52.622	0.349048	0.31856	0.30909	0.32557	0.02088
Hilton	Summit	Soil-Sap Interface	57.7666	0.355859	0.31656	0.30229	0.3249	0.02774
Hilton	Summit	Soil-Sap Interface	63.4141	0.36221	0.31568	0.29839	0.32543	0.03301
Hilton	Summit	Soil-Sap Interface	69.6138	0.362786	0.30969	0.28989	0.32079	0.03769
Hilton	Summit	Soil-Sap Interface	76.4196	0.359376	0.2998	0.27688	0.31202	0.04258
Hilton	Summit	Soil-Sap Interface	83.8907	0.364026	0.29929	0.27327	0.3122	0.04673
Hilton	Summit	Soil-Sap Interface	92.0923	0.386552	0.31971	0.29172	0.33266	0.04872
Hilton	Summit	Soil-Sap Interface	101.096	0.425698	0.36027	0.33177	0.37258	0.04816
Hilton	Summit	Soil-Sap Interface	110.979	0.479196	0.4173	0.38997	0.42882	0.04572
Hilton	Summit	Soil-Sap Interface	121.829	0.558937	0.50029	0.47674	0.51199	0.04233
Hilton	Summit	Soil-Sap Interface	133.74	0.687204	0.62932	0.61275	0.64309	0.03909
Hilton	Summit	Soil-Sap Interface	146.815	0.876669	0.81581	0.8078	0.83343	0.03766
Hilton	Summit	Soil-Sap Interface	161.168	1.12333	1.05708	1.05547	1.07863	0.03872
Hilton	Summit	Soil-Sap Interface	176.925	1.42803	1.35815	1.35791	1.38136	0.04041
Hilton	Summit	Soil-Sap Interface	194.222	1.81546	1.74693	1.74327	1.76855	0.04066
Hilton	Summit	Soil-Sap Interface	213.21	2.32318	2.25883	2.24954	2.27718	0.0401
Hilton	Summit	Soil-Sap Interface	234.054	2.98546	2.92094	2.908	2.93813	0.04149
Hilton	Summit	Soil-Sap Interface	256.936	3.82246	3.7464	3.73672	3.76853	0.04696
Hilton	Summit	Soil-Sap Interface	282.056	4.81477	4.7145	4.7184	4.74922	0.0568
Hilton	Summit	Soil-Sap Interface	309.631	5.87723	5.74772	5.77504	5.8	0.06827
Hilton	Summit	Soil-Sap Interface	339.902	6.86596	6.71669	6.77247	6.78504	0.07542
Hilton	Summit	Soil-Sap Interface	373.132	7.61506	7.4692	7.55208	7.54545	0.07316
Hilton	Summit	Soil-Sap Interface	409.611	7.98008	7.86472	7.97221	7.939	0.06445
Hilton	Summit	Soil-Sap Interface	449.657	7.87494	7.81024	7.945	7.87673	0.0674
Hilton	Summit	Soil-Sap Interface	493.617	7.29603	7.28857	7.45446	7.34635	0.0937
Hilton	Summit	Soil-Sap Interface	541.876	6.32636	6.36974	6.55858	6.41823	0.12347
Hilton	Summit	Soil-Sap Interface	594.852	5.12461	5.20306	5.38388	5.23718	0.13296
Hilton	Summit	Soil-Sap Interface	653.008	3.88678	3.97988	4.10307	3.98991	0.10849
Hilton	Summit	Soil-Sap Interface	716.849	2.79138	2.88698	2.90609	2.86148	0.06146
Hilton	Summit	Soil-Sap Interface	786.932	1.95182	2.05522	1.95438	1.98714	0.05897
Hilton	Summit	Soil-Sap Interface	863.866	1.39022	1.51822	1.32588	1.41144	0.09791
Hilton	Summit	Soil-Sap Interface	948.322	1.05255	1.22089	0.99439	1.08928	0.11763
Hilton	Summit	Soil-Sap Interface	1041.03	0.859136	1.0626	0.85947	0.92707	0.11737
Hilton	Summit	Soil-Sap Interface	1142.81	0.757011	0.97407	0.83289	0.85465	0.11015
Hilton	Summit	Soil-Sap Interface	1254.54	0.715156	0.92343	0.8484	0.829	0.10548
Hilton	Summit	Soil-Sap Interface	1377.19	0.687148	0.8545	0.81442	0.78536	0.08738
Hilton	Summit	Soil-Sap Interface	1511.83	0.669975	0.78353	0.74909	0.7342	0.05822
Hilton	Summit	Soil-Sap Interface	1659.63	0.660151	0.69884	0.65798	0.67233	0.02299
Hilton	Summit	Soil-Sap Interface	1821.88	0.623716	0.57534	0.52421	0.57442	0.04976
Hilton	Summit	~30 cm below interface	0.375124	0.00548	0.0057	0.00459	0.00525	0.00059
Hilton	Summit	~30 cm below interface	0.411798	0.010456	0.01087	0.00825	0.00986	0.00141
Hilton	Summit	~30 cm below interface	0.452057	0.017606	0.01832	0.01233	0.01608	0.00327
Hilton	Summit	~30 cm below interface	0.496252	0.024344	0.02535	0.01778	0.02249	0.00411
Hilton	Summit	~30 cm below interface	0.544768	0.030725	0.03203	0.02233	0.02836	0.00527
Hilton	Summit	~30 cm below interface	0.598027	0.036658	0.03828	0.02665	0.03386	0.0063
Hilton	Summit	~30 cm below interface	0.656493	0.042045	0.04399	0.03085	0.03896	0.00709
Hilton	Summit	~30 cm below interface	0.720675	0.046766	0.04904	0.03522	0.04368	0.00741

Hilton	Summit	~30 cm below interface	0.791132	0.050703	0.05332	0.03897	0.04766	0.00764
Hilton	Summit	~30 cm below interface	0.868477	0.053735	0.05668	0.04241	0.05094	0.00754
Hilton	Summit	~30 cm below interface	0.953383	0.055752	0.05901	0.04556	0.05344	0.00702
Hilton	Summit	~30 cm below interface	1.04659	0.056663	0.06021	0.04855	0.05514	0.00598
Hilton	Summit	~30 cm below interface	1.14891	0.056508	0.0603	0.05108	0.05596	0.00463
Hilton	Summit	~30 cm below interface	1.26123	0.055382	0.05937	0.05326	0.056	0.0031
Hilton	Summit	~30 cm below interface	1.38454	0.053445	0.05758	0.05517	0.0554	0.00208
Hilton	Summit	~30 cm below interface	1.5199	0.050928	0.05516	0.0569	0.05433	0.00307
Hilton	Summit	~30 cm below interface	1.66849	0.048132	0.05243	0.0585	0.05302	0.00521
Hilton	Summit	~30 cm below interface	1.83161	0.045425	0.04978	0.05995	0.05172	0.00746
Hilton	Summit	~30 cm below interface	2.01068	0.043208	0.04765	0.06137	0.05074	0.00947
Hilton	Summit	~30 cm below interface	2.20725	0.041883	0.04648	0.06283	0.0504	0.01101
Hilton	Summit	~30 cm below interface	2.42304	0.041799	0.04667	0.0645	0.05099	0.01195
Hilton	Summit	~30 cm below interface	2.65993	0.043202	0.0485	0.06634	0.05268	0.01212
Hilton	Summit	~30 cm below interface	2.91998	0.046179	0.05205	0.06844	0.05556	0.01154
Hilton	Summit	~30 cm below interface	3.20545	0.050632	0.0572	0.07082	0.05955	0.0103
Hilton	Summit	~30 cm below interface	3.51883	0.056263	0.06361	0.07359	0.06449	0.0087
Hilton	Summit	~30 cm below interface	3.86284	0.062612	0.07075	0.07671	0.07003	0.00708
Hilton	Summit	~30 cm below interface	4.24049	0.069129	0.07799	0.0802	0.07577	0.00586
Hilton	Summit	~30 cm below interface	4.65506	0.07527	0.08471	0.08404	0.08134	0.00527
Hilton	Summit	~30 cm below interface	5.11017	0.080596	0.09043	0.08827	0.08643	0.00517
Hilton	Summit	~30 cm below interface	5.60976	0.084841	0.09488	0.09285	0.09086	0.00531
Hilton	Summit	~30 cm below interface	6.1582	0.087963	0.09804	0.09783	0.09461	0.00576
Hilton	Summit	~30 cm below interface	6.76025	0.090126	0.10017	0.10322	0.09784	0.00685
Hilton	Summit	~30 cm below interface	7.42117	0.091662	0.10166	0.10907	0.1008	0.00874
Hilton	Summit	~30 cm below interface	8.14669	0.093105	0.10318	0.11545	0.10391	0.01119
Hilton	Summit	~30 cm below interface	8.94315	0.095229	0.10558	0.12255	0.10778	0.01379
Hilton	Summit	~30 cm below interface	9.81748	0.098988	0.10988	0.13053	0.11313	0.01602
Hilton	Summit	~30 cm below interface	10.7773	0.10541	0.11713	0.13958	0.12071	0.01737
Hilton	Summit	~30 cm below interface	11.8309	0.11538	0.12813	0.14987	0.13113	0.01744
Hilton	Summit	~30 cm below interface	12.9876	0.129315	0.14317	0.16155	0.14468	0.01617
Hilton	Summit	~30 cm below interface	14.2573	0.146938	0.16178	0.17479	0.16117	0.01394
Hilton	Summit	~30 cm below interface	15.6512	0.16705	0.18261	0.18965	0.17977	0.01156
Hilton	Summit	~30 cm below interface	17.1813	0.187674	0.2035	0.20617	0.19911	0.01
Hilton	Summit	~30 cm below interface	18.861	0.206534	0.22201	0.22408	0.21754	0.00959
Hilton	Summit	~30 cm below interface	20.705	0.222076	0.23661	0.24312	0.23394	0.01077
Hilton	Summit	~30 cm below interface	22.7292	0.234685	0.24803	0.26291	0.24854	0.01412
Hilton	Summit	~30 cm below interface	24.9513	0.247008	0.25938	0.28331	0.26323	0.01845
Hilton	Summit	~30 cm below interface	27.3906	0.26342	0.27516	0.30424	0.28094	0.02101
Hilton	Summit	~30 cm below interface	30.0685	0.287662	0.29857	0.32554	0.30392	0.0195
Hilton	Summit	~30 cm below interface	33.0081	0.319718	0.32831	0.3466	0.33154	0.01373
Hilton	Summit	~30 cm below interface	36.2352	0.354471	0.35759	0.366	0.35935	0.00596
Hilton	Summit	~30 cm below interface	39.7777	0.383968	0.37752	0.38184	0.38111	0.00329
Hilton	Summit	~30 cm below interface	43.6665	0.403777	0.38445	0.39228	0.3935	0.00972
Hilton	Summit	~30 cm below interface	47.9356	0.416574	0.38303	0.39628	0.39863	0.01689
Hilton	Summit	~30 cm below interface	52.622	0.429339	0.38189	0.39387	0.4017	0.02467
Hilton	Summit	~30 cm below interface	57.7666	0.449667	0.38929	0.38654	0.4085	0.03568
Hilton	Summit	~30 cm below interface	63.4141	0.481567	0.40931	0.3785	0.42312	0.05291
Hilton	Summit	~30 cm below interface	69.6138	0.524089	0.44136	0.37789	0.44778	0.07331
Hilton	Summit	~30 cm below interface	76.4196	0.579841	0.48936	0.39787	0.48902	0.09099
Hilton	Summit	~30 cm below interface	83.8907	0.661821	0.56796	0.45662	0.56213	0.10273
Hilton	Summit	~30 cm below interface	92.0923	0.786422	0.69373	0.57717	0.68577	0.10485
Hilton	Summit	~30 cm below interface	101.096	0.967713	0.87807	0.78684	0.87754	0.09044
Hilton	Summit	~30 cm below interface	110.979	1.22571	1.13674	1.11196	1.15814	0.05982
Hilton	Summit	~30 cm below interface	121.829	1.59549	1.50276	1.57178	1.55668	0.04817
Hilton	Summit	~30 cm below interface	133.74	2.118	2.01875	2.16951	2.10209	0.07663
Hilton	Summit	~30 cm below interface	146.815	2.81178	2.70652	2.89048	2.80293	0.0923
Hilton	Summit	~30 cm below interface	161.168	3.65031	3.54231	3.69847	3.63036	0.07997
Hilton	Summit	~30 cm below interface	176.925	4.56711	4.46228	4.54024	4.52321	0.05445
Hilton	Summit	~30 cm below interface	194.222	5.46744	5.37334	5.34928	5.39669	0.06244
Hilton	Summit	~30 cm below interface	213.21	6.23486	6.15569	6.05625	6.14893	0.0895
Hilton	Summit	~30 cm below interface	234.054	6.76466	6.69807	6.5989	6.68721	0.08341
Hilton	Summit	~30 cm below interface	256.936	7.01012	6.94829	6.92998	6.9628	0.04199
Hilton	Summit	~30 cm below interface	282.056	6.9874	6.92037	7.02474	6.9775	0.05288
Hilton	Summit	~30 cm below interface	309.631	6.74614	6.66665	6.8805	6.76443	0.10809
Hilton	Summit	~30 cm below interface	339.902	6.34179	6.25159	6.51706	6.37015	0.13499
Hilton	Summit	~30 cm below interface	373.132	5.81948	5.72825	5.9705	5.83941	0.12235
Hilton	Summit	~30 cm below interface	409.611	5.2055	5.12223	5.2873	5.20501	0.08254
Hilton	Summit	~30 cm below interface	449.657	4.50977	4.43544	4.51773	4.48765	0.04539
Hilton	Summit	~30 cm below interface	493.617	3.74156	3.66832	3.71274	3.70754	0.0369

Hilton	Summit	~30 cm below interface	541.876	2.92769	2.8449	2.92175	2.89811	0.04618
Hilton	Summit	~30 cm below interface	594.852	2.12896	2.02939	2.18789	2.11541	0.08011
Hilton	Summit	~30 cm below interface	653.008	1.42167	1.31168	1.54341	1.42559	0.11591
Hilton	Summit	~30 cm below interface	716.849	0.864173	0.76936	1.00837	0.88063	0.12035
Hilton	Summit	~30 cm below interface	786.932	0.479997	0.43246	0.58813	0.5002	0.07978
Hilton	Summit	~30 cm below interface	863.866	0.237151	0.2594	0.27529	0.25728	0.01916
Hilton	Summit	~30 cm below interface	948.322	0.072263	0.16498	0.09107	0.10944	0.04901
Hilton	Summit	~30 cm below interface	1041.03	0.005431	0.11013	0.01557	0.04371	0.05774
Hilton	Summit	~30 cm below interface	1142.81	0	0.10211	0.00107	0.03439	0.05865
Hilton	Summit	~30 cm below interface	1254.54	0	0.14449	0	0.04816	0.08342
Hilton	Summit	~30 cm below interface	1377.19	0	0.23773	0	0.07924	0.13725
Hilton	Summit	~30 cm below interface	1511.83	0	0.37512	0	0.12504	0.21657
Hilton	Summit	~30 cm below interface	1659.63	0	0.52234	0	0.17411	0.30157
Hilton	Summit	~30 cm below interface	1821.88	0	0.61355	0	0.20452	0.35423
Hilton	Shoulder	Soil-Sap Interface	0.375124	0	0.00493	0.00511	0.00335	0.0029
Hilton	Shoulder	Soil-Sap Interface	0.411798	0	0.00943	0.00978	0.0064	0.00555
Hilton	Shoulder	Soil-Sap Interface	0.452057	0	0.01593	0.01655	0.01083	0.00938
Hilton	Shoulder	Soil-Sap Interface	0.496252	0.000366	0.02214	0.02305	0.01518	0.01284
Hilton	Shoulder	Soil-Sap Interface	0.544768	0.004915	0.02813	0.02936	0.0208	0.01377
Hilton	Shoulder	Soil-Sap Interface	0.598027	0.015091	0.03384	0.03543	0.02812	0.01131
Hilton	Shoulder	Soil-Sap Interface	0.656493	0.02506	0.0392	0.04118	0.03514	0.00879
Hilton	Shoulder	Soil-Sap Interface	0.720675	0.03391	0.04408	0.0465	0.0415	0.00668
Hilton	Shoulder	Soil-Sap Interface	0.791132	0.041547	0.04837	0.05126	0.04706	0.00499
Hilton	Shoulder	Soil-Sap Interface	0.868477	0.047681	0.05191	0.0553	0.05163	0.00382
Hilton	Shoulder	Soil-Sap Interface	0.953383	0.05206	0.05454	0.05842	0.055	0.0032
Hilton	Shoulder	Soil-Sap Interface	1.04659	0.054465	0.05608	0.06041	0.05698	0.00307
Hilton	Shoulder	Soil-Sap Interface	1.14891	0.054933	0.05647	0.06118	0.05753	0.00326
Hilton	Shoulder	Soil-Sap Interface	1.26123	0.05362	0.0557	0.06069	0.05667	0.00363
Hilton	Shoulder	Soil-Sap Interface	1.38454	0.050802	0.05383	0.05897	0.05454	0.00413
Hilton	Shoulder	Soil-Sap Interface	1.5199	0.046876	0.05105	0.0562	0.05138	0.00467
Hilton	Shoulder	Soil-Sap Interface	1.66849	0.042344	0.04766	0.05269	0.04756	0.00517
Hilton	Shoulder	Soil-Sap Interface	1.83161	0.037785	0.04409	0.0489	0.04359	0.00558
Hilton	Shoulder	Soil-Sap Interface	2.01068	0.033818	0.0409	0.04546	0.04006	0.00587
Hilton	Shoulder	Soil-Sap Interface	2.20725	0.031034	0.0387	0.04306	0.0376	0.00609
Hilton	Shoulder	Soil-Sap Interface	2.42304	0.029929	0.03809	0.04239	0.0368	0.00633
Hilton	Shoulder	Soil-Sap Interface	2.65993	0.030851	0.03953	0.04401	0.03813	0.00669
Hilton	Shoulder	Soil-Sap Interface	2.91998	0.033943	0.0433	0.04822	0.04182	0.00725
Hilton	Shoulder	Soil-Sap Interface	3.20545	0.039108	0.04935	0.05501	0.04782	0.00806
Hilton	Shoulder	Soil-Sap Interface	3.51883	0.045975	0.05733	0.06398	0.05576	0.0091
Hilton	Shoulder	Soil-Sap Interface	3.86284	0.053937	0.06656	0.07435	0.06495	0.0103
Hilton	Shoulder	Soil-Sap Interface	4.24049	0.062251	0.07618	0.08512	0.07452	0.01152
Hilton	Shoulder	Soil-Sap Interface	4.65506	0.070172	0.08528	0.09527	0.08357	0.01263
Hilton	Shoulder	Soil-Sap Interface	5.11017	0.077095	0.09315	0.10394	0.0914	0.01351
Hilton	Shoulder	Soil-Sap Interface	5.60976	0.082644	0.09934	0.11064	0.09754	0.01408
Hilton	Shoulder	Soil-Sap Interface	6.1582	0.086729	0.10375	0.11528	0.10192	0.01436
Hilton	Shoulder	Soil-Sap Interface	6.76025	0.089527	0.10666	0.11817	0.10478	0.01441
Hilton	Shoulder	Soil-Sap Interface	7.42117	0.091395	0.10853	0.11988	0.1066	0.01434
Hilton	Shoulder	Soil-Sap Interface	8.14669	0.092901	0.11012	0.12128	0.1081	0.0143
Hilton	Shoulder	Soil-Sap Interface	8.94315	0.094853	0.11241	0.12351	0.11026	0.01445
Hilton	Shoulder	Soil-Sap Interface	9.81748	0.098217	0.11653	0.12786	0.1142	0.01496
Hilton	Shoulder	Soil-Sap Interface	10.7773	0.104004	0.12361	0.13557	0.12106	0.01593
Hilton	Shoulder	Soil-Sap Interface	11.8309	0.112991	0.13441	0.14746	0.13162	0.0174
Hilton	Shoulder	Soil-Sap Interface	12.9876	0.1254	0.14905	0.16354	0.146	0.01925
Hilton	Shoulder	Soil-Sap Interface	14.2573	0.140615	0.16672	0.18273	0.16336	0.02126
Hilton	Shoulder	Soil-Sap Interface	15.6512	0.157085	0.18556	0.20278	0.18181	0.02308
Hilton	Shoulder	Soil-Sap Interface	17.1813	0.172499	0.20273	0.22038	0.19854	0.02422
Hilton	Shoulder	Soil-Sap Interface	18.861	0.184429	0.21506	0.23201	0.2105	0.02412
Hilton	Shoulder	Soil-Sap Interface	20.705	0.191601	0.22071	0.23598	0.2161	0.02254
Hilton	Shoulder	Soil-Sap Interface	22.7292	0.195013	0.221	0.23426	0.21676	0.01996
Hilton	Shoulder	Soil-Sap Interface	24.9513	0.198283	0.22075	0.2326	0.21721	0.01743
Hilton	Shoulder	Soil-Sap Interface	27.3906	0.20666	0.22663	0.23819	0.22383	0.01595
Hilton	Shoulder	Soil-Sap Interface	30.0685	0.224518	0.24382	0.25597	0.24144	0.01586
Hilton	Shoulder	Soil-Sap Interface	33.0081	0.252577	0.27238	0.28507	0.27001	0.01638
Hilton	Shoulder	Soil-Sap Interface	36.2352	0.286487	0.30536	0.31741	0.30309	0.01559
Hilton	Shoulder	Soil-Sap Interface	39.7777	0.319843	0.33337	0.34299	0.33207	0.01163
Hilton	Shoulder	Soil-Sap Interface	43.6665	0.35128	0.3546	0.36053	0.35547	0.00469
Hilton	Shoulder	Soil-Sap Interface	47.9356	0.386933	0.37796	0.38022	0.38171	0.00467
Hilton	Shoulder	Soil-Sap Interface	52.622	0.435333	0.4159	0.41594	0.42239	0.01121
Hilton	Shoulder	Soil-Sap Interface	57.7666	0.500941	0.47556	0.47572	0.48408	0.01461
Hilton	Shoulder	Soil-Sap Interface	63.4141	0.578427	0.55054	0.55212	0.56036	0.01567

Hilton	Shoulder	Soil-Sap Interface	69.6138	0.654154	0.62248	0.62384	0.63349	0.01791
Hilton	Shoulder	Soil-Sap Interface	76.4196	0.721868	0.68342	0.68142	0.69557	0.0228
Hilton	Shoulder	Soil-Sap Interface	83.8907	0.790393	0.74731	0.74154	0.75975	0.0267
Hilton	Shoulder	Soil-Sap Interface	92.0923	0.865688	0.82511	0.81878	0.83652	0.02545
Hilton	Shoulder	Soil-Sap Interface	101.096	0.937086	0.90342	0.89963	0.91338	0.02062
Hilton	Shoulder	Soil-Sap Interface	110.979	0.993794	0.96462	0.96291	0.97378	0.01736
Hilton	Shoulder	Soil-Sap Interface	121.829	1.04925	1.02102	1.01922	1.02983	0.01684
Hilton	Shoulder	Soil-Sap Interface	133.74	1.13534	1.10925	1.10693	1.11717	0.01578
Hilton	Shoulder	Soil-Sap Interface	146.815	1.27012	1.249	1.24609	1.25507	0.01311
Hilton	Shoulder	Soil-Sap Interface	161.168	1.44262	1.4255	1.41948	1.4292	0.01201
Hilton	Shoulder	Soil-Sap Interface	176.925	1.63436	1.61841	1.60757	1.62011	0.01348
Hilton	Shoulder	Soil-Sap Interface	194.222	1.83808	1.82241	1.81147	1.82399	0.01337
Hilton	Shoulder	Soil-Sap Interface	213.21	2.05177	2.03358	2.03118	2.03884	0.01126
Hilton	Shoulder	Soil-Sap Interface	234.054	2.29384	2.26423	2.27541	2.27783	0.01495
Hilton	Shoulder	Soil-Sap Interface	256.936	2.63419	2.58542	2.60927	2.60963	0.02439
Hilton	Shoulder	Soil-Sap Interface	282.056	3.17648	3.1136	3.14277	3.14428	0.03147
Hilton	Shoulder	Soil-Sap Interface	309.631	3.99615	3.93905	3.95779	3.96433	0.02911
Hilton	Shoulder	Soil-Sap Interface	339.902	5.08597	5.0616	5.05096	5.06618	0.01795
Hilton	Shoulder	Soil-Sap Interface	373.132	6.33037	6.36219	6.31374	6.33543	0.02462
Hilton	Shoulder	Soil-Sap Interface	409.611	7.51218	7.60775	7.53342	7.55112	0.05018
Hilton	Shoulder	Soil-Sap Interface	449.657	8.36002	8.50176	8.42779	8.42986	0.07089
Hilton	Shoulder	Soil-Sap Interface	493.617	8.63583	8.78009	8.72646	8.71413	0.07292
Hilton	Shoulder	Soil-Sap Interface	541.876	8.2224	8.3087	8.27206	8.26772	0.04331
Hilton	Shoulder	Soil-Sap Interface	594.852	7.18134	7.16261	7.11555	7.15317	0.0339
Hilton	Shoulder	Soil-Sap Interface	653.008	5.73349	5.61047	5.52697	5.62364	0.10389
Hilton	Shoulder	Soil-Sap Interface	716.849	4.13966	3.96059	3.85516	3.98514	0.14383
Hilton	Shoulder	Soil-Sap Interface	786.932	2.63312	2.47729	2.393	2.50114	0.12182
Hilton	Shoulder	Soil-Sap Interface	863.866	1.38929	1.30534	1.28841	1.32768	0.05402
Hilton	Shoulder	Soil-Sap Interface	948.322	0.428291	0.40463	0.51517	0.44936	0.0582
Hilton	Shoulder	Soil-Sap Interface	1041.03	0.032084	0.03035	0.10158	0.05467	0.04063
Hilton	Shoulder	Soil-Sap Interface	1142.81	0	0	0.00456	0.00152	0.00263
Hilton	Shoulder	Soil-Sap Interface	1254.54	0	0	0	0	0
Hilton	Shoulder	Soil-Sap Interface	1377.19	0	0	0	0	0
Hilton	Shoulder	Soil-Sap Interface	1511.83	0	0	0	0	0
Hilton	Shoulder	Soil-Sap Interface	1659.63	0	0	0	0	0
Hilton	Shoulder	Soil-Sap Interface	1821.88	0	0	0	0	0
Hilton	Shoulder	~30 cm below interface	0.375124	0.011611	0.0134	0.01438	0.01313	0.0014
Hilton	Shoulder	~30 cm below interface	0.411798	0.02082	0.02401	0.02576	0.02353	0.0025
Hilton	Shoulder	~30 cm below interface	0.452057	0.031023	0.03577	0.03836	0.03505	0.00372
Hilton	Shoulder	~30 cm below interface	0.496252	0.044619	0.05144	0.05517	0.05041	0.00535
Hilton	Shoulder	~30 cm below interface	0.544768	0.055978	0.06459	0.06928	0.06328	0.00675
Hilton	Shoulder	~30 cm below interface	0.598027	0.066512	0.07677	0.08237	0.07522	0.00804
Hilton	Shoulder	~30 cm below interface	0.656493	0.0766	0.08845	0.0949	0.08665	0.00928
Hilton	Shoulder	~30 cm below interface	0.720675	0.086835	0.1003	0.10763	0.09826	0.01055
Hilton	Shoulder	~30 cm below interface	0.791132	0.095545	0.11047	0.11859	0.1082	0.01169
Hilton	Shoulder	~30 cm below interface	0.868477	0.103133	0.11936	0.12817	0.11689	0.0127
Hilton	Shoulder	~30 cm below interface	0.953383	0.109766	0.12717	0.13661	0.12451	0.01362
Hilton	Shoulder	~30 cm below interface	1.04659	0.115639	0.13413	0.14415	0.1313	0.01446
Hilton	Shoulder	~30 cm below interface	1.14891	0.120427	0.13992	0.15047	0.13694	0.01524
Hilton	Shoulder	~30 cm below interface	1.26123	0.124155	0.14454	0.15557	0.14142	0.01594
Hilton	Shoulder	~30 cm below interface	1.38454	0.127186	0.14841	0.15989	0.14516	0.01659
Hilton	Shoulder	~30 cm below interface	1.5199	0.129779	0.15182	0.16374	0.14845	0.01723
Hilton	Shoulder	~30 cm below interface	1.66849	0.132343	0.15529	0.16772	0.15178	0.01795
Hilton	Shoulder	~30 cm below interface	1.83161	0.134923	0.15887	0.17187	0.15522	0.01874
Hilton	Shoulder	~30 cm below interface	2.01068	0.13786	0.16298	0.17666	0.15917	0.01968
Hilton	Shoulder	~30 cm below interface	2.20725	0.14149	0.16799	0.18249	0.16399	0.02079
Hilton	Shoulder	~30 cm below interface	2.42304	0.146271	0.17446	0.18993	0.17022	0.02214
Hilton	Shoulder	~30 cm below interface	2.65993	0.152347	0.18255	0.19919	0.17803	0.02375
Hilton	Shoulder	~30 cm below interface	2.91998	0.15979	0.19231	0.21031	0.18747	0.0256
Hilton	Shoulder	~30 cm below interface	3.20545	0.16873	0.20388	0.22338	0.19866	0.0277
Hilton	Shoulder	~30 cm below interface	3.51883	0.179171	0.21717	0.2383	0.21155	0.02996
Hilton	Shoulder	~30 cm below interface	3.86284	0.191064	0.2321	0.25493	0.22603	0.03236
Hilton	Shoulder	~30 cm below interface	4.24049	0.204199	0.24831	0.27283	0.24178	0.03478
Hilton	Shoulder	~30 cm below interface	4.65506	0.218453	0.26562	0.29178	0.25862	0.03716
Hilton	Shoulder	~30 cm below interface	5.11017	0.233779	0.28389	0.3116	0.27642	0.03944
Hilton	Shoulder	~30 cm below interface	5.60976	0.25015	0.30312	0.33229	0.29518	0.04164
Hilton	Shoulder	~30 cm below interface	6.1582	0.267753	0.3235	0.35404	0.3151	0.04375
Hilton	Shoulder	~30 cm below interface	6.76025	0.286553	0.34504	0.37688	0.33616	0.04581
Hilton	Shoulder	~30 cm below interface	7.42117	0.307196	0.36848	0.40163	0.3591	0.04791
Hilton	Shoulder	~30 cm below interface	8.14669	0.330154	0.39448	0.42904	0.38456	0.05019

Hilton	Shoulder	~30 cm below interface	8.94315	0.356727	0.42466	0.46089	0.41409	0.05288
Hilton	Shoulder	~30 cm below interface	9.81748	0.387682	0.46006	0.49828	0.44867	0.05617
Hilton	Shoulder	~30 cm below interface	10.7773	0.4247	0.50264	0.5433	0.49021	0.06027
Hilton	Shoulder	~30 cm below interface	11.8309	0.469022	0.55392	0.59752	0.54015	0.06534
Hilton	Shoulder	~30 cm below interface	12.9876	0.522181	0.61577	0.66289	0.60028	0.07162
Hilton	Shoulder	~30 cm below interface	14.2573	0.585005	0.68908	0.74022	0.67143	0.0791
Hilton	Shoulder	~30 cm below interface	15.6512	0.657253	0.77311	0.82846	0.75294	0.08737
Hilton	Shoulder	~30 cm below interface	17.1813	0.738018	0.8658	0.92505	0.84296	0.09559
Hilton	Shoulder	~30 cm below interface	18.861	0.824571	0.96291	1.02522	0.93757	0.1027
Hilton	Shoulder	~30 cm below interface	20.705	0.914869	1.06139	1.12572	1.03399	0.10806
Hilton	Shoulder	~30 cm below interface	22.7292	1.00669	1.15881	1.22427	1.12992	0.11163
Hilton	Shoulder	~30 cm below interface	24.9513	1.09999	1.25567	1.32167	1.22578	0.11382
Hilton	Shoulder	~30 cm below interface	27.3906	1.1961	1.35375	1.41989	1.32325	0.11497
Hilton	Shoulder	~30 cm below interface	30.0685	1.29774	1.45531	1.52097	1.42467	0.11473
Hilton	Shoulder	~30 cm below interface	33.0081	1.40926	1.56335	1.62737	1.53333	0.11211
Hilton	Shoulder	~30 cm below interface	36.2352	1.53618	1.68169	1.74234	1.6534	0.10595
Hilton	Shoulder	~30 cm below interface	39.7777	1.6868	1.81778	1.8731	1.79256	0.09568
Hilton	Shoulder	~30 cm below interface	43.6665	1.87073	1.98201	2.03057	1.9611	0.08195
Hilton	Shoulder	~30 cm below interface	47.9356	2.09654	2.1855	2.22675	2.1696	0.06655
Hilton	Shoulder	~30 cm below interface	52.622	2.36652	2.43415	2.46886	2.42318	0.05204
Hilton	Shoulder	~30 cm below interface	57.7666	2.67134	2.72203	2.75189	2.71509	0.04072
Hilton	Shoulder	~30 cm below interface	63.4141	2.9885	3.02874	3.05557	3.02427	0.03376
Hilton	Shoulder	~30 cm below interface	69.6138	3.28591	3.32219	3.34677	3.31829	0.03062
Hilton	Shoulder	~30 cm below interface	76.4196	3.53145	3.56829	3.58934	3.56303	0.0293
Hilton	Shoulder	~30 cm below interface	83.8907	3.70368	3.74271	3.75652	3.7343	0.0274
Hilton	Shoulder	~30 cm below interface	92.0923	3.79962	3.83952	3.84069	3.82661	0.02338
Hilton	Shoulder	~30 cm below interface	101.096	3.83645	3.87353	3.85701	3.85566	0.01858
Hilton	Shoulder	~30 cm below interface	110.979	3.84534	3.87495	3.83854	3.85294	0.01936
Hilton	Shoulder	~30 cm below interface	121.829	3.86106	3.87915	3.82553	3.85525	0.02728
Hilton	Shoulder	~30 cm below interface	133.74	3.90527	3.90998	3.84674	3.88733	0.03523
Hilton	Shoulder	~30 cm below interface	146.815	3.97552	3.96742	3.90455	3.94916	0.03885
Hilton	Shoulder	~30 cm below interface	161.168	4.03752	4.01747	3.96325	4.00608	0.03842
Hilton	Shoulder	~30 cm below interface	176.925	4.03533	4.00011	3.9568	3.99741	0.03933
Hilton	Shoulder	~30 cm below interface	194.222	3.91139	3.84876	3.81065	3.85693	0.05086
Hilton	Shoulder	~30 cm below interface	213.21	3.63434	3.52154	3.47685	3.54424	0.08116
Hilton	Shoulder	~30 cm below interface	234.054	3.21843	3.02718	2.96295	3.06952	0.1329
Hilton	Shoulder	~30 cm below interface	256.936	2.721	2.42891	2.33673	2.49555	0.20061
Hilton	Shoulder	~30 cm below interface	282.056	2.2235	1.82834	1.7077	1.91985	0.2698
Hilton	Shoulder	~30 cm below interface	309.631	1.79837	1.32575	1.18459	1.43624	0.32146
Hilton	Shoulder	~30 cm below interface	339.902	1.48574	0.98122	0.83164	1.09954	0.34272
Hilton	Shoulder	~30 cm below interface	373.132	1.28565	0.79839	0.65003	0.91136	0.33253
Hilton	Shoulder	~30 cm below interface	409.611	1.16694	0.73979	0.59857	0.8351	0.29593
Hilton	Shoulder	~30 cm below interface	449.657	1.08311	0.74855	0.6202	0.81728	0.23899
Hilton	Shoulder	~30 cm below interface	493.617	0.988951	0.76053	0.65168	0.80039	0.17213
Hilton	Shoulder	~30 cm below interface	541.876	0.857837	0.72568	0.64144	0.74165	0.10908
Hilton	Shoulder	~30 cm below interface	594.852	0.687552	0.62784	0.56999	0.62846	0.05879
Hilton	Shoulder	~30 cm below interface	653.008	0.49893	0.48698	0.45354	0.47982	0.02353
Hilton	Shoulder	~30 cm below interface	716.849	0.319353	0.33936	0.32445	0.32772	0.0104
Hilton	Shoulder	~30 cm below interface	786.932	0.162577	0.20922	0.20487	0.19222	0.02576
Hilton	Shoulder	~30 cm below interface	863.866	0.059098	0.10424	0.10386	0.08906	0.02595
Hilton	Shoulder	~30 cm below interface	948.322	0.010957	0.03663	0.03673	0.02811	0.01485
Hilton	Shoulder	~30 cm below interface	1041.03	0.000853	0.00663	0.00665	0.00471	0.00334
Hilton	Shoulder	~30 cm below interface	1142.81	0	0.00047	0.00046	0.00031	0.00027
Hilton	Shoulder	~30 cm below interface	1254.54	0	0	0	0	0
Hilton	Shoulder	~30 cm below interface	1377.19	0	0	0	0	0
Hilton	Shoulder	~30 cm below interface	1511.83	0	0	0	0	0
Hilton	Shoulder	~30 cm below interface	1659.63	0	0	0	0	0
Hilton	Shoulder	~30 cm below interface	1821.88	0	0	0	0	0
Hilton	Backslope	Soil-Sap Interface	0.375124	0	0.00543	0.0058	0.00374	0.00325
Hilton	Backslope	Soil-Sap Interface	0.411798	0	0.01037	0.01107	0.00714	0.0062
Hilton	Backslope	Soil-Sap Interface	0.452057	0	0.01747	0.01867	0.01205	0.01045
Hilton	Backslope	Soil-Sap Interface	0.496252	0.000341	0.02419	0.02587	0.0168	0.01428
Hilton	Backslope	Soil-Sap Interface	0.544768	0.004581	0.03058	0.03276	0.02264	0.01568
Hilton	Backslope	Soil-Sap Interface	0.598027	0.014067	0.03657	0.03925	0.02996	0.01383
Hilton	Backslope	Soil-Sap Interface	0.656493	0.023375	0.04207	0.04526	0.0369	0.01182
Hilton	Backslope	Soil-Sap Interface	0.720675	0.031673	0.04696	0.05067	0.0431	0.01007
Hilton	Backslope	Soil-Sap Interface	0.791132	0.038891	0.05115	0.05536	0.04847	0.00856
Hilton	Backslope	Soil-Sap Interface	0.868477	0.044786	0.05452	0.05923	0.05285	0.00737
Hilton	Backslope	Soil-Sap Interface	0.953383	0.049156	0.05697	0.06215	0.05609	0.00654
Hilton	Backslope	Soil-Sap Interface	1.04659	0.051834	0.05842	0.06404	0.0581	0.00611

Hilton	Backslope	Soil-Sap Interface	1.14891	0.052884	0.05891	0.06491	0.0589	0.00601
Hilton	Backslope	Soil-Sap Interface	1.26123	0.052472	0.05853	0.06485	0.05862	0.00619
Hilton	Backslope	Soil-Sap Interface	1.38454	0.050868	0.05744	0.06404	0.05745	0.00658
Hilton	Backslope	Soil-Sap Interface	1.5199	0.04843	0.05589	0.0627	0.05567	0.00714
Hilton	Backslope	Soil-Sap Interface	1.66849	0.045596	0.05418	0.06118	0.05365	0.0078
Hilton	Backslope	Soil-Sap Interface	1.83161	0.042844	0.05269	0.05988	0.05181	0.00855
Hilton	Backslope	Soil-Sap Interface	2.01068	0.040657	0.05185	0.05928	0.05059	0.00937
Hilton	Backslope	Soil-Sap Interface	2.20725	0.039474	0.05208	0.05985	0.05047	0.01028
Hilton	Backslope	Soil-Sap Interface	2.42304	0.039645	0.05375	0.06201	0.0518	0.01131
Hilton	Backslope	Soil-Sap Interface	2.65993	0.041388	0.05711	0.06605	0.05485	0.01249
Hilton	Backslope	Soil-Sap Interface	2.91998	0.044759	0.06224	0.07206	0.05969	0.01383
Hilton	Backslope	Soil-Sap Interface	3.20545	0.04963	0.069	0.07985	0.06616	0.01531
Hilton	Backslope	Soil-Sap Interface	3.51883	0.055689	0.077	0.08898	0.07389	0.01686
Hilton	Backslope	Soil-Sap Interface	3.86284	0.062484	0.08568	0.09879	0.08232	0.01838
Hilton	Backslope	Soil-Sap Interface	4.24049	0.069488	0.09436	0.10848	0.09078	0.01974
Hilton	Backslope	Soil-Sap Interface	4.65506	0.076188	0.10241	0.1173	0.09863	0.02082
Hilton	Backslope	Soil-Sap Interface	5.11017	0.08217	0.10929	0.12467	0.10538	0.02152
Hilton	Backslope	Soil-Sap Interface	5.60976	0.087179	0.11472	0.13025	0.11072	0.02181
Hilton	Backslope	Soil-Sap Interface	6.1582	0.091148	0.11867	0.13405	0.11462	0.02174
Hilton	Backslope	Soil-Sap Interface	6.76025	0.094209	0.12138	0.1364	0.11733	0.02138
Hilton	Backslope	Soil-Sap Interface	7.42117	0.096624	0.12328	0.13781	0.11924	0.02089
Hilton	Backslope	Soil-Sap Interface	8.14669	0.098838	0.12502	0.13909	0.12098	0.02043
Hilton	Backslope	Soil-Sap Interface	8.94315	0.101496	0.12752	0.1413	0.12344	0.02021
Hilton	Backslope	Soil-Sap Interface	9.81748	0.105385	0.13182	0.14563	0.12761	0.02045
Hilton	Backslope	Soil-Sap Interface	10.7773	0.111329	0.13894	0.15321	0.13449	0.02129
Hilton	Backslope	Soil-Sap Interface	11.8309	0.119943	0.14958	0.16475	0.14476	0.02279
Hilton	Backslope	Soil-Sap Interface	12.9876	0.131382	0.16374	0.18013	0.15842	0.02481
Hilton	Backslope	Soil-Sap Interface	14.2573	0.145041	0.18044	0.19809	0.17452	0.02701
Hilton	Backslope	Soil-Sap Interface	15.6512	0.159498	0.19759	0.2161	0.19106	0.02886
Hilton	Backslope	Soil-Sap Interface	17.1813	0.172641	0.2122	0.23062	0.20515	0.02962
Hilton	Backslope	Soil-Sap Interface	18.861	0.182315	0.22123	0.23826	0.21394	0.02868
Hilton	Backslope	Soil-Sap Interface	20.705	0.187405	0.22328	0.23779	0.21616	0.02593
Hilton	Backslope	Soil-Sap Interface	22.7292	0.188751	0.22002	0.23176	0.21351	0.02223
Hilton	Backslope	Soil-Sap Interface	24.9513	0.189478	0.21644	0.22624	0.21072	0.01904
Hilton	Backslope	Soil-Sap Interface	27.3906	0.19379	0.21853	0.22791	0.21341	0.01763
Hilton	Backslope	Soil-Sap Interface	30.0685	0.204938	0.23018	0.24045	0.22519	0.01827
Hilton	Backslope	Soil-Sap Interface	33.0081	0.223036	0.25021	0.26159	0.24494	0.01981
Hilton	Backslope	Soil-Sap Interface	36.2352	0.2441	0.27159	0.28301	0.26623	0.02
Hilton	Backslope	Soil-Sap Interface	39.7777	0.262185	0.28563	0.29518	0.281	0.01698
Hilton	Backslope	Soil-Sap Interface	43.6665	0.273725	0.2888	0.29468	0.28574	0.01081
Hilton	Backslope	Soil-Sap Interface	47.9356	0.280697	0.2861	0.28762	0.2848	0.00364
Hilton	Backslope	Soil-Sap Interface	52.622	0.288945	0.28673	0.28487	0.28685	0.00204
Hilton	Backslope	Soil-Sap Interface	57.7666	0.303444	0.29699	0.29374	0.29806	0.00494
Hilton	Backslope	Soil-Sap Interface	63.4141	0.324516	0.31532	0.3118	0.31721	0.00657
Hilton	Backslope	Soil-Sap Interface	69.6138	0.349004	0.33464	0.32975	0.3378	0.01001
Hilton	Backslope	Soil-Sap Interface	76.4196	0.378401	0.35577	0.3475	0.36056	0.016
Hilton	Backslope	Soil-Sap Interface	83.8907	0.420613	0.39219	0.38038	0.39773	0.02068
Hilton	Backslope	Soil-Sap Interface	92.0923	0.476145	0.45105	0.43807	0.45509	0.01936
Hilton	Backslope	Soil-Sap Interface	101.096	0.528602	0.5172	0.506	0.51727	0.0113
Hilton	Backslope	Soil-Sap Interface	110.979	0.561283	0.56933	0.56143	0.56401	0.0046
Hilton	Backslope	Soil-Sap Interface	121.829	0.590838	0.61857	0.61412	0.60784	0.01489
Hilton	Backslope	Soil-Sap Interface	133.74	0.68615	0.73082	0.72924	0.7154	0.02535
Hilton	Backslope	Soil-Sap Interface	146.815	0.963119	1.02126	1.02143	1.00194	0.03362
Hilton	Backslope	Soil-Sap Interface	161.168	1.57175	1.64081	1.64384	1.6188	0.04077
Hilton	Backslope	Soil-Sap Interface	176.925	2.65291	2.73802	2.75223	2.71439	0.05371
Hilton	Backslope	Soil-Sap Interface	194.222	4.24801	4.36754	4.40977	4.34177	0.0839
Hilton	Backslope	Soil-Sap Interface	213.21	6.21168	6.38333	6.46996	6.35499	0.13145
Hilton	Backslope	Soil-Sap Interface	234.054	8.21025	8.42734	8.55753	8.39837	0.17544
Hilton	Backslope	Soil-Sap Interface	256.936	9.82557	10.0476	10.1976	10.0236	0.18717
Hilton	Backslope	Soil-Sap Interface	282.056	10.6932	10.8544	10.9849	10.8442	0.14612
Hilton	Backslope	Soil-Sap Interface	309.631	10.6222	10.6533	10.7257	10.6671	0.05311
Hilton	Backslope	Soil-Sap Interface	339.902	9.65811	9.51593	9.51542	9.56315	0.08224
Hilton	Backslope	Soil-Sap Interface	373.132	8.06008	7.75373	7.69334	7.83572	0.19664
Hilton	Backslope	Soil-Sap Interface	409.611	6.19735	5.78917	5.70114	5.89589	0.26476
Hilton	Backslope	Soil-Sap Interface	449.657	4.41257	3.99509	3.90728	4.10498	0.26997
Hilton	Backslope	Soil-Sap Interface	493.617	2.92734	2.58722	2.48821	2.66759	0.23033
Hilton	Backslope	Soil-Sap Interface	541.876	1.81297	1.58817	1.45774	1.61963	0.17969
Hilton	Backslope	Soil-Sap Interface	594.852	1.04023	0.92003	0.73062	0.89696	0.15609
Hilton	Backslope	Soil-Sap Interface	653.008	0.540283	0.47995	0.2143	0.41151	0.17344
Hilton	Backslope	Soil-Sap Interface	716.849	0.237752	0.15283	0.01527	0.13528	0.11228

Hilton	Backslope	Soil-Sap Interface	786.932	0.085353	0.01177	0	0.03237	0.04626
Hilton	Backslope	Soil-Sap Interface	863.866	0.021237	0	0	0.00708	0.01226
Hilton	Backslope	Soil-Sap Interface	948.322	0.001578	0	0	0.00053	0.00091
Hilton	Backslope	Soil-Sap Interface	1041.03	0	0	0	0	0
Hilton	Backslope	Soil-Sap Interface	1142.81	0	0	0	0	0
Hilton	Backslope	Soil-Sap Interface	1254.54	0	0	0	0	0
Hilton	Backslope	Soil-Sap Interface	1377.19	0	0	0	0	0
Hilton	Backslope	Soil-Sap Interface	1511.83	0	0	0	0	0
Hilton	Backslope	Soil-Sap Interface	1659.63	0	0	0	0	0
Hilton	Backslope	Soil-Sap Interface	1821.88	0	0	0	0	0
Hilton	Backslope	~30 cm below interface	0.375124	0.006163	0.0064	0.0066	0.00639	0.00022
Hilton	Backslope	~30 cm below interface	0.411798	0.011763	0.01222	0.01261	0.0122	0.00042
Hilton	Backslope	~30 cm below interface	0.452057	0.019821	0.02062	0.02131	0.02058	0.00075
Hilton	Backslope	~30 cm below interface	0.496252	0.027435	0.02861	0.02962	0.02855	0.00109
Hilton	Backslope	~30 cm below interface	0.544768	0.034673	0.03628	0.03764	0.0362	0.00149
Hilton	Backslope	~30 cm below interface	0.598027	0.041436	0.04354	0.0453	0.04342	0.00193
Hilton	Backslope	~30 cm below interface	0.656493	0.04762	0.05029	0.05249	0.05013	0.00244
Hilton	Backslope	~30 cm below interface	0.720675	0.053091	0.05639	0.0591	0.05619	0.00301
Hilton	Backslope	~30 cm below interface	0.791132	0.057713	0.06172	0.06496	0.06146	0.00363
Hilton	Backslope	~30 cm below interface	0.868477	0.061344	0.06609	0.06991	0.06578	0.00429
Hilton	Backslope	~30 cm below interface	0.953383	0.06385	0.06937	0.07377	0.06899	0.00497
Hilton	Backslope	~30 cm below interface	1.04659	0.065115	0.07138	0.07634	0.07095	0.00562
Hilton	Backslope	~30 cm below interface	1.14891	0.065167	0.07212	0.07758	0.07162	0.00622
Hilton	Backslope	~30 cm below interface	1.26123	0.0641	0.07163	0.07751	0.07108	0.00672
Hilton	Backslope	~30 cm below interface	1.38454	0.06209	0.07007	0.07625	0.06947	0.0071
Hilton	Backslope	~30 cm below interface	1.5199	0.059407	0.0677	0.07407	0.06706	0.00735
Hilton	Backslope	~30 cm below interface	1.66849	0.056418	0.06491	0.07135	0.06423	0.00749
Hilton	Backslope	~30 cm below interface	1.83161	0.053588	0.06223	0.06866	0.06149	0.00756
Hilton	Backslope	~30 cm below interface	2.01068	0.051447	0.06028	0.06669	0.05947	0.00765
Hilton	Backslope	~30 cm below interface	2.20725	0.05055	0.05974	0.0662	0.05883	0.00786
Hilton	Backslope	~30 cm below interface	2.42304	0.051403	0.06125	0.06792	0.06019	0.00831
Hilton	Backslope	~30 cm below interface	2.65993	0.054394	0.0653	0.07244	0.06405	0.00909
Hilton	Backslope	~30 cm below interface	2.91998	0.059716	0.07215	0.08006	0.07064	0.01026
Hilton	Backslope	~30 cm below interface	3.20545	0.067302	0.08172	0.09072	0.07991	0.01181
Hilton	Backslope	~30 cm below interface	3.51883	0.076803	0.09354	0.10389	0.09141	0.01367
Hilton	Backslope	~30 cm below interface	3.86284	0.087611	0.10681	0.11866	0.10436	0.01567
Hilton	Backslope	~30 cm below interface	4.24049	0.098956	0.1205	0.13387	0.11777	0.01761
Hilton	Backslope	~30 cm below interface	4.65506	0.110035	0.13354	0.14825	0.13061	0.01928
Hilton	Backslope	~30 cm below interface	5.11017	0.120157	0.14502	0.16076	0.14198	0.02047
Hilton	Backslope	~30 cm below interface	5.60976	0.128848	0.15433	0.17067	0.15128	0.02108
Hilton	Backslope	~30 cm below interface	6.1582	0.135919	0.16125	0.17772	0.15829	0.02105
Hilton	Backslope	~30 cm below interface	6.76025	0.141467	0.16598	0.18212	0.16319	0.02047
Hilton	Backslope	~30 cm below interface	7.42117	0.145796	0.16902	0.18442	0.16641	0.01944
Hilton	Backslope	~30 cm below interface	8.14669	0.149466	0.17124	0.18561	0.16877	0.0182
Hilton	Backslope	~30 cm below interface	8.94315	0.153361	0.17397	0.18719	0.17151	0.01705
Hilton	Backslope	~30 cm below interface	9.81748	0.15862	0.17888	0.19107	0.17619	0.01639
Hilton	Backslope	~30 cm below interface	10.7773	0.166519	0.18771	0.19931	0.18451	0.01663
Hilton	Backslope	~30 cm below interface	11.8309	0.178124	0.20174	0.21355	0.19781	0.01804
Hilton	Backslope	~30 cm below interface	12.9876	0.193862	0.22116	0.23426	0.21643	0.02061
Hilton	Backslope	~30 cm below interface	14.2573	0.21301	0.24444	0.25995	0.23913	0.02391
Hilton	Backslope	~30 cm below interface	15.6512	0.233417	0.26819	0.2869	0.26284	0.02714
Hilton	Backslope	~30 cm below interface	17.1813	0.251652	0.28776	0.30963	0.28301	0.02928
Hilton	Backslope	~30 cm below interface	18.861	0.264123	0.29897	0.32265	0.29525	0.02944
Hilton	Backslope	~30 cm below interface	20.705	0.269231	0.30062	0.32346	0.29777	0.02723
Hilton	Backslope	~30 cm below interface	22.7292	0.269092	0.2959	0.31464	0.29321	0.02289
Hilton	Backslope	~30 cm below interface	24.9513	0.269385	0.29166	0.30384	0.2883	0.01747
Hilton	Backslope	~30 cm below interface	27.3906	0.276918	0.29545	0.30099	0.29112	0.0126
Hilton	Backslope	~30 cm below interface	30.0685	0.295984	0.3116	0.31342	0.307	0.00959
Hilton	Backslope	~30 cm below interface	33.0081	0.325145	0.33744	0.34018	0.33426	0.00801
Hilton	Backslope	~30 cm below interface	36.2352	0.357207	0.36268	0.36942	0.3631	0.00612
Hilton	Backslope	~30 cm below interface	39.7777	0.384318	0.37596	0.38503	0.38177	0.00504
Hilton	Backslope	~30 cm below interface	43.6665	0.405724	0.37554	0.38133	0.38753	0.01602
Hilton	Backslope	~30 cm below interface	47.9356	0.43171	0.37483	0.3732	0.39325	0.03332
Hilton	Backslope	~30 cm below interface	52.622	0.479816	0.39745	0.38966	0.42231	0.04996
Hilton	Backslope	~30 cm below interface	57.7666	0.567446	0.46691	0.45762	0.49733	0.0609
Hilton	Backslope	~30 cm below interface	63.4141	0.703116	0.59517	0.58724	0.62851	0.06474
Hilton	Backslope	~30 cm below interface	69.6138	0.883016	0.77762	0.76937	0.81	0.06337
Hilton	Backslope	~30 cm below interface	76.4196	1.10452	1.00958	0.99774	1.03728	0.05853
Hilton	Backslope	~30 cm below interface	83.8907	1.37485	1.29901	1.28376	1.31921	0.04879
Hilton	Backslope	~30 cm below interface	92.0923	1.68964	1.64134	1.62718	1.65272	0.03275

Hilton	Backslope	~30 cm below interface	101.096	2.01768	1.99849	1.99023	2.00213	0.01408
Hilton	Backslope	~30 cm below interface	110.979	2.32841	2.32969	2.32941	2.32917	0.00067
Hilton	Backslope	~30 cm below interface	121.829	2.63222	2.64157	2.64942	2.64107	0.00861
Hilton	Backslope	~30 cm below interface	133.74	2.9865	2.99752	3.01275	2.99892	0.01318
Hilton	Backslope	~30 cm below interface	146.815	3.46227	3.47694	3.49691	3.47871	0.01739
Hilton	Backslope	~30 cm below interface	161.168	4.10515	4.13025	4.15039	4.1286	0.02267
Hilton	Backslope	~30 cm below interface	176.925	4.91736	4.96411	4.98186	4.95444	0.03332
Hilton	Backslope	~30 cm below interface	194.222	5.83835	5.9213	5.94117	5.90027	0.05454
Hilton	Backslope	~30 cm below interface	213.21	6.72163	6.8466	6.87616	6.8148	0.08203
Hilton	Backslope	~30 cm below interface	234.054	7.37236	7.52186	7.56065	7.48496	0.09942
Hilton	Backslope	~30 cm below interface	256.936	7.63508	7.7691	7.80755	7.73724	0.09054
Hilton	Backslope	~30 cm below interface	282.056	7.44196	7.51154	7.53913	7.49754	0.05007
Hilton	Backslope	~30 cm below interface	309.631	6.82329	6.78451	6.79516	6.80099	0.02004
Hilton	Backslope	~30 cm below interface	339.902	5.90083	5.73219	5.72964	5.78755	0.09811
Hilton	Backslope	~30 cm below interface	373.132	4.8411	4.55688	4.55581	4.65126	0.1644
Hilton	Backslope	~30 cm below interface	409.611	3.79328	3.43696	3.45246	3.5609	0.2014
Hilton	Backslope	~30 cm below interface	449.657	2.84052	2.47865	2.5116	2.61026	0.20009
Hilton	Backslope	~30 cm below interface	493.617	1.99873	1.70786	1.73702	1.81454	0.16018
Hilton	Backslope	~30 cm below interface	541.876	1.25758	1.09905	1.08912	1.14858	0.09452
Hilton	Backslope	~30 cm below interface	594.852	0.624748	0.63889	0.56192	0.60852	0.04097
Hilton	Backslope	~30 cm below interface	653.008	0.169407	0.34624	0.19878	0.23814	0.09476
Hilton	Backslope	~30 cm below interface	716.849	0.011069	0.20932	0.04346	0.08795	0.10635
Hilton	Backslope	~30 cm below interface	786.932	0	0.17681	0.02623	0.06768	0.09542
Hilton	Backslope	~30 cm below interface	863.866	0	0.18705	0.07371	0.08692	0.09422
Hilton	Backslope	~30 cm below interface	948.322	0	0.15318	0.10836	0.08718	0.07875
Hilton	Backslope	~30 cm below interface	1041.03	0	0.05473	0.04941	0.03471	0.03018
Hilton	Backslope	~30 cm below interface	1142.81	0	0.00395	0.00408	0.00268	0.00232
Hilton	Backslope	~30 cm below interface	1254.54	0	0	0	0	0
Hilton	Backslope	~30 cm below interface	1377.19	0	0	0	0	0
Hilton	Backslope	~30 cm below interface	1511.83	0	0	0	0	0
Hilton	Backslope	~30 cm below interface	1659.63	0	0	0	0	0
Hilton	Backslope	~30 cm below interface	1821.88	0	0	0	0	0
Hilton	Toeslope	Soil-Sap Interface	0.375124	0.005527	0.00669	0.00777	0.00666	0.00112
Hilton	Toeslope	Soil-Sap Interface	0.411798	0.009913	0.01199	0.01393	0.01194	0.00201
Hilton	Toeslope	Soil-Sap Interface	0.452057	0.014773	0.01786	0.02074	0.01779	0.00298
Hilton	Toeslope	Soil-Sap Interface	0.496252	0.021255	0.02569	0.02982	0.02559	0.00428
Hilton	Toeslope	Soil-Sap Interface	0.544768	0.026668	0.03225	0.03743	0.03212	0.00538
Hilton	Toeslope	Soil-Sap Interface	0.598027	0.0317	0.03834	0.04448	0.03817	0.00639
Hilton	Toeslope	Soil-Sap Interface	0.656493	0.036525	0.04417	0.05122	0.04397	0.00735
Hilton	Toeslope	Soil-Sap Interface	0.720675	0.041448	0.05012	0.05808	0.04988	0.00832
Hilton	Toeslope	Soil-Sap Interface	0.791132	0.045646	0.05523	0.06395	0.05494	0.00916
Hilton	Toeslope	Soil-Sap Interface	0.868477	0.049339	0.05972	0.0691	0.05939	0.00988
Hilton	Toeslope	Soil-Sap Interface	0.953383	0.052601	0.0637	0.07362	0.06331	0.01051
Hilton	Toeslope	Soil-Sap Interface	1.04659	0.055559	0.06732	0.07769	0.06686	0.01108
Hilton	Toeslope	Soil-Sap Interface	1.14891	0.058037	0.0704	0.08116	0.06986	0.01157
Hilton	Toeslope	Soil-Sap Interface	1.26123	0.060063	0.07296	0.084	0.07234	0.01198
Hilton	Toeslope	Soil-Sap Interface	1.38454	0.061799	0.0752	0.08649	0.07449	0.01236
Hilton	Toeslope	Soil-Sap Interface	1.5199	0.063393	0.0773	0.08881	0.0765	0.01273
Hilton	Toeslope	Soil-Sap Interface	1.66849	0.06503	0.07951	0.0913	0.07861	0.01316
Hilton	Toeslope	Soil-Sap Interface	1.83161	0.066722	0.08185	0.09399	0.08085	0.01366
Hilton	Toeslope	Soil-Sap Interface	2.01068	0.068611	0.0845	0.0971	0.0834	0.01428
Hilton	Toeslope	Soil-Sap Interface	2.20725	0.07083	0.08762	0.10084	0.08643	0.01504
Hilton	Toeslope	Soil-Sap Interface	2.42304	0.073595	0.09147	0.1055	0.09019	0.01599
Hilton	Toeslope	Soil-Sap Interface	2.65993	0.076935	0.09609	0.11115	0.09473	0.01715
Hilton	Toeslope	Soil-Sap Interface	2.91998	0.080852	0.10146	0.11776	0.10003	0.0185
Hilton	Toeslope	Soil-Sap Interface	3.20545	0.085329	0.10755	0.12526	0.10604	0.02001
Hilton	Toeslope	Soil-Sap Interface	3.51883	0.09035	0.11428	0.13354	0.11272	0.02164
Hilton	Toeslope	Soil-Sap Interface	3.86284	0.095854	0.12156	0.14246	0.11996	0.02335
Hilton	Toeslope	Soil-Sap Interface	4.24049	0.10172	0.12919	0.15173	0.12755	0.02504
Hilton	Toeslope	Soil-Sap Interface	4.65506	0.107815	0.13698	0.16107	0.13529	0.02667
Hilton	Toeslope	Soil-Sap Interface	5.11017	0.114043	0.14478	0.1703	0.14304	0.02817
Hilton	Toeslope	Soil-Sap Interface	5.60976	0.12036	0.15256	0.17936	0.15076	0.02954
Hilton	Toeslope	Soil-Sap Interface	6.1582	0.126816	0.16037	0.18829	0.15849	0.03078
Hilton	Toeslope	Soil-Sap Interface	6.76025	0.13338	0.1682	0.19707	0.16622	0.03189
Hilton	Toeslope	Soil-Sap Interface	7.42117	0.140168	0.17618	0.20587	0.17407	0.0329
Hilton	Toeslope	Soil-Sap Interface	8.14669	0.147247	0.18447	0.21491	0.18221	0.03389
Hilton	Toeslope	Soil-Sap Interface	8.94315	0.154971	0.19355	0.22477	0.1911	0.03497
Hilton	Toeslope	Soil-Sap Interface	9.81748	0.163605	0.20379	0.2359	0.2011	0.03622
Hilton	Toeslope	Soil-Sap Interface	10.7773	0.173617	0.21571	0.2489	0.21274	0.03773
Hilton	Toeslope	Soil-Sap Interface	11.8309	0.185289	0.22964	0.26418	0.22637	0.03955

Hilton	Toeslope	Soil-Sap Interface	12.9876	0.199003	0.24606	0.28236	0.24247	0.04179
Hilton	Toeslope	Soil-Sap Interface	14.2573	0.21511	0.26533	0.3038	0.26141	0.04448
Hilton	Toeslope	Soil-Sap Interface	15.6512	0.233745	0.28733	0.32823	0.2831	0.04738
Hilton	Toeslope	Soil-Sap Interface	17.1813	0.254878	0.31153	0.35469	0.30703	0.05006
Hilton	Toeslope	Soil-Sap Interface	18.861	0.277953	0.33679	0.38163	0.33212	0.052
Hilton	Toeslope	Soil-Sap Interface	20.705	0.302847	0.36274	0.40856	0.35805	0.05301
Hilton	Toeslope	Soil-Sap Interface	22.7292	0.329882	0.3899	0.43631	0.38537	0.05336
Hilton	Toeslope	Soil-Sap Interface	24.9513	0.360533	0.42022	0.46731	0.41602	0.05351
Hilton	Toeslope	Soil-Sap Interface	27.3906	0.396811	0.45587	0.50402	0.45223	0.0537
Hilton	Toeslope	Soil-Sap Interface	30.0685	0.440385	0.49796	0.5473	0.49522	0.05351
Hilton	Toeslope	Soil-Sap Interface	33.0081	0.491883	0.54585	0.59569	0.54447	0.05192
Hilton	Toeslope	Soil-Sap Interface	36.2352	0.550232	0.59681	0.64539	0.59748	0.04758
Hilton	Toeslope	Soil-Sap Interface	39.7777	0.613274	0.64745	0.69216	0.65096	0.03956
Hilton	Toeslope	Soil-Sap Interface	43.6665	0.678216	0.69478	0.73273	0.70191	0.02795
Hilton	Toeslope	Soil-Sap Interface	47.9356	0.742318	0.73706	0.76582	0.7484	0.01531
Hilton	Toeslope	Soil-Sap Interface	52.622	0.803257	0.7739	0.79188	0.78968	0.0148
Hilton	Toeslope	Soil-Sap Interface	57.7666	0.859178	0.80554	0.81204	0.82559	0.02927
Hilton	Toeslope	Soil-Sap Interface	63.4141	0.909306	0.8328	0.82783	0.85664	0.04567
Hilton	Toeslope	Soil-Sap Interface	69.6138	0.954441	0.85731	0.84136	0.88437	0.06121
Hilton	Toeslope	Soil-Sap Interface	76.4196	0.9973	0.88196	0.85591	0.91172	0.07525
Hilton	Toeslope	Soil-Sap Interface	83.8907	1.042	0.91087	0.87613	0.943	0.08748
Hilton	Toeslope	Soil-Sap Interface	92.0923	1.09265	0.94856	0.90712	0.98277	0.09739
Hilton	Toeslope	Soil-Sap Interface	101.096	1.15246	0.99936	0.95402	1.03528	0.10398
Hilton	Toeslope	Soil-Sap Interface	110.979	1.22224	1.06607	1.02072	1.10301	0.10572
Hilton	Toeslope	Soil-Sap Interface	121.829	1.29973	1.14874	1.10849	1.18565	0.10082
Hilton	Toeslope	Soil-Sap Interface	133.74	1.37796	1.24188	1.21253	1.27746	0.08827
Hilton	Toeslope	Soil-Sap Interface	146.815	1.44683	1.33451	1.32082	1.36739	0.06914
Hilton	Toeslope	Soil-Sap Interface	161.168	1.49755	1.41351	1.41627	1.44244	0.04774
Hilton	Toeslope	Soil-Sap Interface	176.925	1.53236	1.4738	1.48746	1.49787	0.03064
Hilton	Toeslope	Soil-Sap Interface	194.222	1.57257	1.52908	1.54207	1.54791	0.02232
Hilton	Toeslope	Soil-Sap Interface	213.21	1.66035	1.61692	1.61559	1.63095	0.02547
Hilton	Toeslope	Soil-Sap Interface	234.054	1.85182	1.79348	1.76742	1.80424	0.04322
Hilton	Toeslope	Soil-Sap Interface	256.936	2.20416	2.12057	2.06636	2.13036	0.06942
Hilton	Toeslope	Soil-Sap Interface	282.056	2.75995	2.64965	2.57271	2.66077	0.09411
Hilton	Toeslope	Soil-Sap Interface	309.631	3.52475	3.39862	3.31225	3.41187	0.10687
Hilton	Toeslope	Soil-Sap Interface	339.902	4.44885	4.3301	4.25024	4.34306	0.09994
Hilton	Toeslope	Soil-Sap Interface	373.132	5.42295	5.34147	5.27822	5.34755	0.07256
Hilton	Toeslope	Soil-Sap Interface	409.611	6.29648	6.27928	6.23067	6.26881	0.03413
Hilton	Toeslope	Soil-Sap Interface	449.657	6.91256	6.97348	6.92605	6.93736	0.032
Hilton	Toeslope	Soil-Sap Interface	493.617	7.14731	7.28076	7.21674	7.21494	0.06674
Hilton	Toeslope	Soil-Sap Interface	541.876	6.94334	7.12456	7.03231	7.0334	0.09061
Hilton	Toeslope	Soil-Sap Interface	594.852	6.32857	6.51952	6.40179	6.41663	0.09634
Hilton	Toeslope	Soil-Sap Interface	653.008	5.40772	5.5691	5.44404	5.47362	0.08466
Hilton	Toeslope	Soil-Sap Interface	716.849	4.32959	4.43203	4.32588	4.3625	0.06024
Hilton	Toeslope	Soil-Sap Interface	786.932	3.23515	3.26944	3.20271	3.23577	0.03337
Hilton	Toeslope	Soil-Sap Interface	863.866	2.23363	2.21197	2.19037	2.21199	0.02163
Hilton	Toeslope	Soil-Sap Interface	948.322	1.38482	1.33413	1.3465	1.35515	0.02643
Hilton	Toeslope	Soil-Sap Interface	1041.03	0.690504	0.64606	0.6675	0.66802	0.02223
Hilton	Toeslope	Soil-Sap Interface	1142.81	0.245357	0.22274	0.23635	0.23481	0.01139
Hilton	Toeslope	Soil-Sap Interface	1254.54	0.044564	0.03952	0.04288	0.04232	0.00257
Hilton	Toeslope	Soil-Sap Interface	1377.19	0.003336	0.00287	0.00321	0.00314	0.00024
Hilton	Toeslope	Soil-Sap Interface	1511.83	0	0	0	0	0
Hilton	Toeslope	Soil-Sap Interface	1659.63	0	0	0	0	0
Hilton	Toeslope	Soil-Sap Interface	1821.88	0	0	0	0	0
Hilton	Toeslope	~30 cm below interface	0.375124	0.005472	0.00632	0.00679	0.00619	0.00067
Hilton	Toeslope	~30 cm below interface	0.411798	0.009824	0.01134	0.01217	0.01111	0.00119
Hilton	Toeslope	~30 cm below interface	0.452057	0.014656	0.01691	0.01815	0.01657	0.00177
Hilton	Toeslope	~30 cm below interface	0.496252	0.021113	0.02437	0.02615	0.02388	0.00255
Hilton	Toeslope	~30 cm below interface	0.544768	0.026514	0.03063	0.03286	0.03	0.00322
Hilton	Toeslope	~30 cm below interface	0.598027	0.031587	0.0365	0.03917	0.03575	0.00384
Hilton	Toeslope	~30 cm below interface	0.656493	0.036496	0.04219	0.04527	0.04132	0.00445
Hilton	Toeslope	~30 cm below interface	0.720675	0.041561	0.04807	0.05158	0.04707	0.00508
Hilton	Toeslope	~30 cm below interface	0.791132	0.045917	0.05317	0.05706	0.05205	0.00566
Hilton	Toeslope	~30 cm below interface	0.868477	0.049854	0.0578	0.06203	0.05656	0.00618
Hilton	Toeslope	~30 cm below interface	0.953383	0.053433	0.06203	0.06658	0.06068	0.00668
Hilton	Toeslope	~30 cm below interface	1.04659	0.056798	0.06604	0.07089	0.06457	0.00716
Hilton	Toeslope	~30 cm below interface	1.14891	0.059702	0.06957	0.0747	0.06799	0.00762
Hilton	Toeslope	~30 cm below interface	1.26123	0.062222	0.07268	0.07808	0.07099	0.00806
Hilton	Toeslope	~30 cm below interface	1.38454	0.064495	0.07555	0.08119	0.07375	0.00849
Hilton	Toeslope	~30 cm below interface	1.5199	0.066668	0.07833	0.08423	0.07641	0.00894

Hilton	Toeslope	~30 cm below interface	1.66849	0.068872	0.0812	0.08739	0.07916	0.00943
Hilton	Toeslope	~30 cm below interface	1.83161	0.071121	0.08417	0.09068	0.08199	0.00996
Hilton	Toeslope	~30 cm below interface	2.01068	0.073552	0.0874	0.09426	0.08507	0.01055
Hilton	Toeslope	~30 cm below interface	2.20725	0.076294	0.09101	0.09828	0.08853	0.0112
Hilton	Toeslope	~30 cm below interface	2.42304	0.079568	0.09528	0.10303	0.09263	0.01195
Hilton	Toeslope	~30 cm below interface	2.65993	0.08339	0.10022	0.10851	0.09737	0.0128
Hilton	Toeslope	~30 cm below interface	2.91998	0.087809	0.10586	0.11476	0.10281	0.01373
Hilton	Toeslope	~30 cm below interface	3.20545	0.092834	0.1122	0.12175	0.10893	0.01473
Hilton	Toeslope	~30 cm below interface	3.51883	0.09853	0.11928	0.12952	0.11578	0.01579
Hilton	Toeslope	~30 cm below interface	3.86284	0.104853	0.12704	0.13801	0.1233	0.01689
Hilton	Toeslope	~30 cm below interface	4.24049	0.111756	0.13541	0.14709	0.13142	0.018
Hilton	Toeslope	~30 cm below interface	4.65506	0.119146	0.14425	0.15663	0.14001	0.0191
Hilton	Toeslope	~30 cm below interface	5.11017	0.126988	0.1535	0.16652	0.149	0.02015
Hilton	Toeslope	~30 cm below interface	5.60976	0.135234	0.16312	0.17673	0.15836	0.02115
Hilton	Toeslope	~30 cm below interface	6.1582	0.143927	0.17314	0.1873	0.16812	0.02212
Hilton	Toeslope	~30 cm below interface	6.76025	0.153037	0.18355	0.1982	0.17826	0.02304
Hilton	Toeslope	~30 cm below interface	7.42117	0.162633	0.19441	0.20949	0.18884	0.02392
Hilton	Toeslope	~30 cm below interface	8.14669	0.17278	0.20581	0.22125	0.19995	0.02476
Hilton	Toeslope	~30 cm below interface	8.94315	0.183749	0.21807	0.23386	0.21189	0.02562
Hilton	Toeslope	~30 cm below interface	9.81748	0.19576	0.23148	0.24759	0.22494	0.02653
Hilton	Toeslope	~30 cm below interface	10.7773	0.209085	0.24632	0.26276	0.23939	0.0275
Hilton	Toeslope	~30 cm below interface	11.8309	0.223896	0.26277	0.27953	0.2554	0.02854
Hilton	Toeslope	~30 cm below interface	12.9876	0.240404	0.28105	0.29814	0.2732	0.02966
Hilton	Toeslope	~30 cm below interface	14.2573	0.258822	0.30137	0.31879	0.293	0.03085
Hilton	Toeslope	~30 cm below interface	15.6512	0.279186	0.32364	0.34132	0.31472	0.03202
Hilton	Toeslope	~30 cm below interface	17.1813	0.301381	0.34745	0.36517	0.338	0.03293
Hilton	Toeslope	~30 cm below interface	18.861	0.324897	0.37191	0.38922	0.36201	0.03328
Hilton	Toeslope	~30 cm below interface	20.705	0.349433	0.39642	0.41268	0.38618	0.03284
Hilton	Toeslope	~30 cm below interface	22.7292	0.374933	0.42079	0.43526	0.41033	0.03149
Hilton	Toeslope	~30 cm below interface	24.9513	0.40198	0.44559	0.45743	0.435	0.0292
Hilton	Toeslope	~30 cm below interface	27.3906	0.431334	0.4714	0.47974	0.46082	0.02588
Hilton	Toeslope	~30 cm below interface	30.0685	0.463359	0.49811	0.50192	0.48779	0.02125
Hilton	Toeslope	~30 cm below interface	33.0081	0.497606	0.52446	0.52257	0.51488	0.01499
Hilton	Toeslope	~30 cm below interface	36.2352	0.532544	0.54809	0.53923	0.53996	0.0078
Hilton	Toeslope	~30 cm below interface	39.7777	0.566341	0.56671	0.54981	0.56096	0.00965
Hilton	Toeslope	~30 cm below interface	43.6665	0.597464	0.57915	0.55366	0.57676	0.022
Hilton	Toeslope	~30 cm below interface	47.9356	0.625237	0.58597	0.55217	0.58779	0.03657
Hilton	Toeslope	~30 cm below interface	52.622	0.649568	0.58905	0.54816	0.59559	0.05102
Hilton	Toeslope	~30 cm below interface	57.7666	0.670413	0.59058	0.54457	0.60186	0.06367
Hilton	Toeslope	~30 cm below interface	63.4141	0.688246	0.59302	0.54432	0.60853	0.07321
Hilton	Toeslope	~30 cm below interface	69.6138	0.704972	0.59972	0.5508	0.6185	0.07878
Hilton	Toeslope	~30 cm below interface	76.4196	0.725689	0.61641	0.56943	0.63718	0.08017
Hilton	Toeslope	~30 cm below interface	83.8907	0.759312	0.65195	0.60855	0.67327	0.07761
Hilton	Toeslope	~30 cm below interface	92.0923	0.818213	0.71823	0.67945	0.73863	0.07159
Hilton	Toeslope	~30 cm below interface	101.096	0.917281	0.82969	0.796	0.84766	0.0626
Hilton	Toeslope	~30 cm below interface	110.979	1.0715	1.00116	0.97243	1.01503	0.05097
Hilton	Toeslope	~30 cm below interface	121.829	1.29443	1.24614	1.22136	1.25398	0.03716
Hilton	Toeslope	~30 cm below interface	133.74	1.59422	1.57191	1.5491	1.57174	0.02256
Hilton	Toeslope	~30 cm below interface	146.815	1.97316	1.97848	1.95488	1.96884	0.01238
Hilton	Toeslope	~30 cm below interface	161.168	2.42574	2.45658	2.42939	2.43724	0.01685
Hilton	Toeslope	~30 cm below interface	176.925	2.94232	2.99218	2.95974	2.96475	0.0253
Hilton	Toeslope	~30 cm below interface	194.222	3.50987	3.56899	3.53189	3.53692	0.02988
Hilton	Toeslope	~30 cm below interface	213.21	4.11417	4.17194	4.13378	4.13996	0.02938
Hilton	Toeslope	~30 cm below interface	234.054	4.73726	4.78501	4.7522	4.75816	0.02443
Hilton	Toeslope	~30 cm below interface	256.936	5.35163	5.38434	5.36515	5.36704	0.01644
Hilton	Toeslope	~30 cm below interface	282.056	5.91608	5.93227	5.93515	5.92783	0.01028
Hilton	Toeslope	~30 cm below interface	309.631	6.37138	6.37192	6.40296	6.38209	0.01808
Hilton	Toeslope	~30 cm below interface	339.902	6.64864	6.63467	6.69549	6.6596	0.03186
Hilton	Toeslope	~30 cm below interface	373.132	6.68212	6.65372	6.73969	6.69184	0.0438
Hilton	Toeslope	~30 cm below interface	409.611	6.43	6.386	6.48628	6.43409	0.05027
Hilton	Toeslope	~30 cm below interface	449.657	5.8929	5.83062	5.93078	5.88477	0.05057
Hilton	Toeslope	~30 cm below interface	493.617	5.1192	5.03687	5.12206	5.09271	0.04838
Hilton	Toeslope	~30 cm below interface	541.876	4.19945	4.0975	4.15703	4.15133	0.05121
Hilton	Toeslope	~30 cm below interface	594.852	3.22728	3.11878	3.14307	3.16304	0.05694
Hilton	Toeslope	~30 cm below interface	653.008	2.29433	2.19962	2.18654	2.22683	0.05882
Hilton	Toeslope	~30 cm below interface	716.849	1.46755	1.41109	1.36373	1.41412	0.05198
Hilton	Toeslope	~30 cm below interface	786.932	0.769394	0.78687	0.69949	0.75192	0.04624
Hilton	Toeslope	~30 cm below interface	863.866	0.296428	0.34519	0.26537	0.30233	0.04023
Hilton	Toeslope	~30 cm below interface	948.322	0.064522	0.10339	0.05789	0.07527	0.02458
Hilton	Toeslope	~30 cm below interface	1041.03	0.006611	0.01607	0.00602	0.00957	0.00564

Hilton	Toeslope	~30 cm below interface	1142.81	7.46E-05	0.00092	8.07E-05	0.00036	0.00049
Hilton	Toeslope	~30 cm below interface	1254.54	0	0	0	0	0
Hilton	Toeslope	~30 cm below interface	1377.19	0	0	0	0	0
Hilton	Toeslope	~30 cm below interface	1511.83	0	0	0	0	0
Hilton	Toeslope	~30 cm below interface	1659.63	0	0	0	0	0
Hilton	Toeslope	~30 cm below interface	1821.88	0	0	0	0	0
